ДОКЛАДЫ
АКАДЕМИИ НАУК СССР

Volume 124, Nos. 1 – 6

January-February 1959

PROCEEDINGS OF THE ACADEMY OF SCIENCES

OF THE USSR

(DOKLADY AKADEMII NAUK SSSR)

Physical Chemistry Section

IN ENGLISH TRANSLATION

M. I. T. Linguistics Laboratory
FEB 11 1960
Received - Library

CONSULTANTS BUREAU, INC.

DENDRITIC CRYSTALLIZATION

by **D. D. SARATOVKIN**

2nd Edition,
Revised and Enlarged

Translated from Russian

THIS SIGNIFICANT volume has been extensively revised by the author from the 1953 edition; in particular with *fresh material derived from observations under the stereoscopic microscope.*

The first section deals briefly with some general concepts on crystallization, drawing an important distinction between *genetic* and *structural* types of crystals, including some aspects of the *defect crystal state.* The second section covers at length the illuminating ideas and observations of the 19th-century Russian metallurgist D. K. Chernov, who proposed many of the basic ideas of dendritic crystallization. The third section is an extended survey of current views on dendritic crystallization, in which the ideas of many Soviet and other scientists are briefly summarized and criticized. Section four presents the growth forms of real crystals; all types are reviewed, but only dendritic or closely related forms are selected for subsequent investigation.

Following sections discuss the causes and forms of crystal growth, with *detailed applications* to certain substances that have been extensively studied *(particularly the ammonium halides),* and to eutectics in metal and organic systems; an extensively revised presentation on steel castings which provides a lucid explanation of how the various structures found in real castings can be fitted into the author's theory of dendritic crystallization. Nearly all the concepts developed earlier in the book are utilized in this final section.

The main bulk of the volume contains many *original* and *unpublished* ideas and observations, and is an excellent example of the modern macroscopic approach to the crystalline state by an experienced worker concerned with the infinite variety of real crystals—all of which is enhanced by a *profusion of explanatory line diagrams and sets of stereoscopic photographs.*

CB translations are by bilingual scientists, and include all photographic, diagrammatic and tabular material integral with the text.

CONTENTS

Foreword . . . .
Introduction . . . .
The famous Russian metallurgist D.K. Chernov, founder of the modern theory of metal crystallization. . . . .
A brief review of the existing views on dendritic crystal growth. . . . .
The growth forms of real crystals . . . .
Methods of studying the growth of real crystals . . . .
Some essential aspects of the optics of stereoscopy. . . . .
The causes of skeletal and dendritic growth. . . . .
The dendrite formation process . . . .
Feathered crystals . . . .
Crystals with sector structures . . . .
The difference between skeletal and dendritic forms of crystals. . . . .
Growth of ammonium chloride dendrites from a supersaturated solution as a typical example of dendritic crystallization . . . .
Effects of surface-active impurities on crystallization. . . . .
The cubic form of dendritic crystallization produced in ammonium chloride by surface-active impurities . . . .
Formation of cellular dendrites of cubic form . . . .
Dendritic growth of ammonium chloride in the presence of diammonium hydrogen phosphate . . . .
Break-up of dendritic crystals as a transition from a nonequilibrium form to an equilibrium form . . . .
Dendritic growth of solid-solution crystals . . . .
Some brief notes on spiral growth as an example of antiskeletal growth . . . .
Dendritic forms of crystals produced in antiskeletal growth
Eutectics and dendritic structures in alloys . . . .
Eutectic crystallization . . . .
Contact fusion as the cause of eutectic fusion . . . .
Experimental study of contact fusion for crystals of fusible organic compounds and metals. . . . .
Capillary phenomena in contact fusion. . . . .
The fusion of an alloy. . . . .
Use of contact fusion in physicochemical analysis, or as a method of producing high-melting compounds . . . .
The solidification of bubble-free steel in a metal mold. . . . .
Conclusion . . . .
Literature cited . . . .

Cloth-bound; 126 pp., illustrated; $6.00

CONSULTANTS BUREAU, INC.
227 WEST 17TH STREET, NEW YORK 11, N. Y

Volume 124, Nos. 1 – 6

January-February 1959

PROCEEDINGS OF THE ACADEMY OF SCIENCES

OF THE USSR

(DOKLADY AKADEMII NAUK SSSR)

Physical Chemistry Section

A publication of the Academy of Sciences of the USSR

IN ENGLISH TRANSLATION

Year and issue of first translation:
Vol. 112, Nos. 1-6 Jan.-Feb. 1957

Annual subscription	*$160.00*
Single issue	*35.00*

Copyright 1959

CONSULTANTS BUREAU INC.
227 W. 17th ST., NEW YORK 11, N. Y.

A complete copy of any paper in this issue may be purchased from the publisher for $5.00

Note: The sale of photostatic copies of any portion of this copyright translation is expressly prohibited by the copyright owners.

Printed in the United States of America

PROCEEDINGS OF THE ACADEMY OF SCIENCES OF THE USSR

Physical Chemistry Section

Volume 124, Numbers 1-6 January-February 1959

CONTENTS

	PAGE	RUSS. ISSUE	RUSS. PAGE
The Hydrogen Bond and Proton Magnetic Resonance. I. V. Aleksandrov and N. D. Sokolov	1	1	115
Paths for the Formation of Methyl Hydroperoxide and Formaldehyde in the Low-Temperature Oxidation of Methane. N. A. Kleimenov and A. B. Nalbandyan	5	1	119
Theory of Radiationless Electron Transitions Between Ions in Solutions. V. G. Levich and R. R. Doganadre	9	1	123
Study of the Free Radicals Formed in the Irradiation of Oxalic Acid by the Method of Electron Paramagnetic Resonance. Yu. N. Molin, A. T. Koritskii, N. Ya. Buben and V. V. Voevodskii	15	1	127
The Relationship Between the Energetic, Electrophysical and Mechanical Properties of Semiconductors. B. F. Ormont	17	1	129
Effect of Annealing on the Packing Density of Polystyrene. A. A. Tager, M. V. Tsilipotkina and A. L. Suvorova	23	1	133
Determination of the Adsorption Coefficients of Ether, Water and Ethylene by the Kinetic Method. K. V. Topchieva and B. V. Romanovskii	25	1	135
Determination of the True Rate Constants in the Decomposition of Aliphatic Alcohols. V. L. Tsvetkova, A. P. Firsov and N. M. Chirkov	29	1	139
Formation of Vibrations in the Passage of a Current in Electrolytic Systems with a Falling Polarization Characteristic. Yu. A. Chizmadzhev	33	1	142
The Salt Effect at the Exchange of Deuterium in Liquid Ammonia. A. I. Shatenshtein, Yu. P. Vyrskii and E. A. Rabinovich	37	1	146
Measurement of the Rate of Combustion of a Powder under Detonation Wave Conditions. A. Ya. Apin and L. G. Bolkhovitinov	41	2	338
The Isotope Effect in the Cracking of Ethane. A. M. Brodskii, R. A. Kalinenko, and K. P. Lavrovskii	43	2	340
Use of the Dropping Mercury Electrode for the Determination of Diffusion Coefficients. Evgenii Budevskii	45	2	342
The Effect of Crystallographic Orientation of the Reaction of Isotopic Exchange at a Metallic surface. B. N. Bushmanov and G. S. Vozdvizhenskii	49	2	346
Voltage-Current Characteristics of an Electrolyte–N-Type Semiconductor Contact. Yu. A. Vdovin, V. G. Levich, and V. A. Myamlin	53	2	353

CONTENTS (continued)

	PAGE	RUSS. ISSUE	RUSS. PAGE
Application of the Emanation Method to the Investigation of Catalysts. Study of the Emanating Power During the Preparation of Oxidation Catalysts. G. M. Zhabrova, M. D. Sinitsyna and S. Z. Roginskii	57	2	354
The Emulsifying Action of Highly Dispersed Solids. A. F. Koretskii and A. B. Taubman	61	2	358
The Theory of Thermal Detonation of Condensed Explosives. A. G. Merzhanov and F. I. Dubovitskii	65	2	362
The Relationship Between the Thermal Dissociation Rate Constants of Diatomic Molecules in the Presence and Absence of Equilibrium. E. E. Nikitin and N. D. Sokolov	69	2	366
The Behavior of Sulfate Ion in the Electrolytic Preparation of Magnesium. S. A. Pushkareva and E. A. Ukshe	73	2	370
The Infrared Spectra of Water, Ethanol, and Methanol Adsorbed on Chromic Oxide. L. M. Roev and A. N. Terenin	77	2	373
The Migration Current on a Rotating Disc Electrode. V. D. Yukhtanova	81	2	377
The Surface Charges of Semiconducting Oxides in the Adsorption of Gases and Vapors. E. Kh. Enikeev, L. Ya. Margolis and S. Z. Roginskii	85	3	606
An Investigation of the Electrode Reactions on the Silicon Cathode. E. A. Efimov and I. G. Erusalimchik	89	3	609
Resistance of Some Deformed Materials to Corrosion Cracking. Yu. S. Zuev and A. Z. Borshchevskaya	93	3	613
The Chemical Modification of Adsorbent Surfaces and Its Effect on the Adsorptional Characteristics. A. V. Kiselev, N. V. Kovaleva, A. Ya. Korolev and K. D. Shcherbakova	97	3	617
A Polarization Mechanism of the Suppression of Structural Etching During Electrochemical Polishing. S. I. Krichmar	103	3	621
The Effect of Various Factors aon the Magnitude of the Specific Surface and the Porosity of Chromate Catalysts. T. V. Rode and A. E. Agronomov	109	3	625
The Isotopic Exchange Between CO and CO_2 on Various Surfaces. S. S. Stroeva, N. V. Kul'kova and M. I. Temkin	113	3	628
The Mechanism of the Low Temperature Polymerization of Monomers Under the Action of Gamma Radiation. A. P. Sheinker, M. K. Yakovleva, E. V. Kristal'nyi and A. D. Abkin	117	3	632
The Formation and Properties of Metal Soaps in Dilute Aqueous Solutions. N. A. Aleinikov and A. M. Makarova	121	4	852
The Anodic Passivation of Silver in Alkaline Solutions. G. I. Vidovich, D. I. Leikis, and B. N. Kabanov	125	4	855
Phase Composition Study of the Copper Catalyst Used in the Oxidation of Propylene to Acrolein. O. V. Isaev and M. Ya. Kushnerev	129	4	858
The Gas-Crystalline State of Matter in Polymers. A. I. Kitaigorodskii	133	4	861

CONTENTS (continued)

	PAGE	RUSS. ISSUE	RUSS. PAGE
The Ultraviolet and Visible Absorption Spectra of Aromatic Amines Adsorbed on Specific Centers of Aluminosilicate Catalysts. E. L. Kotov and A. N. Terenin	137	4	865
Theory of the Nonequilibrium Electrical Double Layer. V. G. Levich	141	4	869
Infrared Absorption Spectra of Ethyllithium Dissolved in Benzene, Hexane and Diethyl Ether. V. N. Nikitin, G. V. Rabova, and N. V. Mikhailova	145	4	873
Causes for the Decreased Stability of the Crystalline Structure of Monocalcium Aluminate Formed at Elevated Temperatures. E. E. Segalova, Z. D. Tulovskaya, E. A. Amelina, and P. A. Rebinder	149	4	876
The Effect of Alkali Metal Halides on the Mechanism of the Catalytic Hydrogenation of Cyclohexene. D. V. Sokol'skii and G. D. Zakumbaeva	153	4	880
Determination of the Elementary Constants in the Oxidation of Ethylbenzene by the Method of Interrupted Illumination. V. F. Tsepalov and V. Ya. Shlyapintokh	157	4	883
The Vibrational Relaxation of Diatomic Molecules. E. E. Nikitin	161	5	1085
The Isotopic Exchange of Nitrogen Between Amino Compounds and Liquid Ammonia. L. L. Strizhak, S. G. Demidenko and A. L. Brodskii	165	5	1089
The Surface Tension of Metallic Indium. O. A. Timofeevicheva and P. P. Pugachevich	171	5	1093
The Calculation of the Acidity Function and Molecular Composition of Hydrofluoric Acid From the Nuclear Magnetic Resonance Data for F^{19}. E. Z. Utyanskaya, A. U. Stepanyants, M. I. Vinnik and N. M. Chirkov	173	5	1095
The Influence of Added Alkali Metal Compounds on the Kinetics of the Reduction of Zinc Silicate by Carbon Monoxide. D. M. Chizhikov and L. G. Berezkina	179	5	1099
The Determination of the Internal Stresses Produced When Solid Surfaces are Glued to One Another. S. A. Shreiner and P. I. Zubov	183	5	1102
Gaseous Initiation with Ozone in the Oxidation of Isodecane and Its Associated Chemiluminescence. R. F. Vasil'ev, O. N. Karpukhin, V. Ya. Shlyapintokh and N. M. Émanuél'	187	6	1258
Role of the Tunnel Effect in the Kinetics of Chemical Reactions at Low Temperatures. V. I. Gol'danskii	191	6	1261
Effective Radius of the Electron in Crystal Lattices. A. F. Kapustinskii	195	6	1265
Theory of Strain in Organic Molecules. A. I. Kitaigorodskii	197	6	1267
Theory of the Heat-Chain Propagation of a Flame with Two Active Centers. L. A. Lovachev	201	6	1271
Kinetic Isotopic Effect in the Oxidation of Hydrogen on Platinum. V. I. Popov and S. Z. Roginskii	205	6	1275
The Character and Role of Intermediate Products in the Radiolytic Reduction of Nitrate. V. A. Sharpatyi, V. D. Orekhov and M. A. Proskurnin	209	6	1279

THE HYDROGEN BOND AND PROTON MAGNETIC RESONANCE

I. V. Aleksandrov and N. D. Sokolov

Institute of Chemical Physics, Academy of Sciences of the USSR

(Presented by Academician V. N. Kondrat'ev, July 28, 1958)

As one of us had shown [1], the concept of a simple electrostatic nature for the hydrogen bond (H-bond, A — H . . . B) is inadequate to explain its main spectroscopic characteristics, namely a shift of the vibration frequency of the group A — H toward longer waves. To explain satisfactorily both the sign and the magnitude of this shift it is necessary to assume that the H-bridge is due partially to a donor-acceptor interaction of the proton of bond A — H and atom B by means of the unshared pair of electrons of the latter.

However, to accomplish such interaction it is necessary that the bond A — H (for example, O — H) be sufficiently polar and that atom H have a sufficiently large effective positive charge. On the other hand, calculations [2] reveal that in such molecules as, for example, the water molecule, the polarity of the O — H bonds is very small due to the presence of a large atomic dipole moment for the O atom. As a result of this it could be expected that if the H atoms in such molecules do have an effective positive charge, still it is probably so small that it can hardly assure a donor-acceptor interaction with other molecules.

In order for the condition of a donor-acceptor interaction in the H-bridge to be at all capable of realization there remains the assumption that the center of gravity of the electron cloud should shift from atom H to atom A during the very process of forming the H-bond. Such a shift in itself does not necessarily mean that the H atom in the H-bridge has a greater positive charge, since due to its donor-acceptor interaction with atom B the center of gravity of the cloud of the unshared pair of electrons of the latter is shifted toward the H atom and may partially neutralize this charge. In order to answer the question of the final distribution of the electron density in the H-bridge it is necessary to turn to experimental facts.

A number of attempts to determine the electron density near the hydrogen atom in complexes containing the H-bond by means of x-ray and electronographic methods are described in the literature [3]. However, because of their insufficient accuracy, the obtained results cannot be considered as being well-defined. In addition, the results obtained by different authors prove to be contradictory.

The data on the intensity of the infrared spectra testify to the increase of the absolute value of the derivative of the dipole moment with respect to the vibration coordinate of the bond A — H in the formation of the H-bridge [4]. However, without additional assumptions, it is impossible to extract from these data any reliable information regarding the change in the electron density near the H atom.

The data on the spectra of the proton magnetic resonance offer somewhat better possibilities. The absorption frequency in proton magnetic resonance is extremely sensitive to H-bond formation [5-7]. The position of the signal from the proton in the magnetic spectrum during H-bridge formation is shifted toward smaller values of the magnetic field strength, which corresponds to a reduction in the constant σ of the magnetic shielding of the proton to a value of the order $\Delta\sigma = 5 \times 10^{-6}$. In many cases $\Delta\sigma$ exceeds the value of the chemical shift of the proton. According to some authors [6, 7], such a great reduction in σ is evidence that the hydrogen bond is pure electrostatic in nature. Schneider, Bernstein and Pople [8] expressed the opinion that the indicated shift of the signal is due to the simple action of the electric field of neighboring molecules, which hinders the precession of the electrons in the external magnetic field. This viewpoint in essence is also applied to the electrostatic concept of the H-bond and is in agreement with the opinions of Pople himself as to its nature [9].

However, it is obvious that without an actual theoretical evaluation of all of the effects, exerting an influence on the magnetic shielding of the proton in the H-bridge, it is still impossible to make any basic conclusions regarding the electron distribution and the nature of the H-bond. It could be expected that in the formation of the complex RA — H . . . BR' the following effects contribute to changing the value of the proton shielding: 1) a change in the polarity of the bond A — H (a shift of the center of gravity of the electron cloud of this bond toward atom A); 2) a stretching of the A — H bond; 3) the formation of a donor-acceptor bond H . . . B, leading to some shift of the center of gravity of the cloud of the unshared pair of electrons of B toward atom H; 4) the action of the electric field of the dipole of molecule BR'; and 5) the effect of the unshared pair of p-electrons of atom B (or of the π-bond B = R').

Strictly speaking, to answer the question as to the nature of the shift of the signal in the formation of the H-bond should require the solving of not less than a six-electron problem. However, considering the complexity of such a calculation, to obtain semiquantitative results it is sufficient to study each of these effects separately, solving only the proper two-electron problem each time. The results of such an operational procedure for the case of O — H . . . O are given below.

1. The relationship between proton shielding and the polarity of the bond A — H can be estimated using the method proposed by one of us [10, 11]. If the molecular orbit, composed of the 1s-function of the H atom and the 2s- and 2p-functions of the Slater O atom in the form

$$\psi^0 = N\,[\varphi_{1s} + \lambda\,(a\varphi^0_{2s} + b\varphi^0_{2p})], \qquad (1)$$

is taken as the wave function of the bond, then the parameter will characterize the polarity of the O — H bond. Based on calculating the dipole moment of the free H_2O molecule it follows [2] that λ is close to one. As calculation shows a change in the hybridization parameters a and b exerts little influence on the value of the shielding constant: if λ lies between 0 and 1.5, then changing a from 0 to $1/\sqrt{2}$ causes σ to change by less than 6%.

Using equation (6) in [10] and function (1) makes it possible to determine σ as a function of λ. If λ is close to one ($\lambda \approx 1.0 \pm 0.4$), then with the internuclear distance R = 1 A it is possible to write with a sufficient degree of accuracy

$$\Delta\sigma_1 = -1{,}5 \cdot 10^{-5}\,\Delta\lambda.$$

If it is assumed that under the influence of the H-bond λ increases by $\Delta\lambda = 0.3$, then we find that $\Delta\sigma_1 \approx \approx -4.5 \cdot 10^{-6}$.

2. The effect of stretching the O — H bond, caused by the formation of the H-bridge, can be estimated using the same equations that were used in estimating the effect of polarity. For small changes in R with $\lambda = 1$ calculation gives

$$\Delta\sigma_2 = -k \cdot 10^{-5}\,\Delta R,$$

where the numerical factor k changes from 0.9 for a = 0 to 1.3 for a = 1. At $\Delta R = 0.05$ A we find $\Delta\sigma_2 \approx \approx -0.5 \cdot 10^{-6}$.

3. The effect of the donor-acceptor bond H^+. . . O can be calculated approximately if the molecular orbit of this bond is written in the form

$$\psi' = N'\,(\varphi_{2p} + \beta\varphi_{1s}),$$

where parameter β characterizes the extent to which the 1s orbit of the H atom participates in the bond. At sufficiently small values of β ($\beta \approx 0.1 - 0.3$), with the interatomic distance H . . . O equal to 1.7 A, the contribution of this bond to the magnetic shielding of the proton is equal to

$$\Delta\sigma_3 = (-0{,}08 + \beta + 3{,}6\,\beta^2) \cdot 10^{-5}.$$

If it is assumed that $\beta \approx 0.2$, then we find that $\Delta\sigma_3 \approx +2.5 \cdot 10^{-6}$.

4. For the free hydrogen atom a calculation of the effect of a constant electric field E on the shielding of the proton can be made if it is assumed that the interaction of the electron with field E, directed along the z axis, is considerably greater than its interaction with the magnetic field, and that the wave function of the electron in the electric field has the form

$$\psi_E = \psi_{1s}(1 + \xi z),$$

where ξ is the variation parameter. Using the virial theorem it follows here that the change in σ when an electric field is applied is equal to [11]

$$\Delta\sigma_4 = -\frac{5a_0^3}{mc^2}E^2, \qquad (2)$$

where a_0 is the Bohr radius.

The effect of an electric field on the shielding of the nucleus of a bound H atom can be estimated using the same equation,* since the structure of the electron cloud in the vicinity of the proton is apparently not very different from the 1s state of the H atom (see, for example, [3]). Assuming that the z axis coincides with the direction of H . . . O, for the dipole μ = 1.6 D, with the distance between it and the proton equal to 1.7 A, by means of equation (2) we find that $\Delta\sigma_4 \approx 0.5 \cdot 10^{-6}$. In particular, it follows from this that in contrast to the opinion of Schneider, Bernstein and Pople [3], it is impossible to explain the observed shift of the signal in the formation of the H-bond only by the influence of the electric field.

5. The calculate the effect of the second unshared pair of electrons of the O atom, whose cloud has an axis perpendicular to the line H . . . O, it proves possible to make use of the fact that these electrons are localized at a considerably greater distance from the proton. Then to calculate the contribution of these electrons to the shielding it proves possible to use the equation [11]

$$\Delta\sigma_5 = \frac{\chi - \chi_{zz}}{R^3},$$

where χ_{zz} is a tensor component of the diamagnetic susceptibility χ. Calculation reveals that when R = 1.7 A, $\Delta\sigma_5$ lies between $+0.2 \times 10^{-6}$ and $-0.2 \cdot 10^{-6}$, i.e., negligibly small.

Consequently we see that all of the components of $\Delta\sigma$, with the exception of $\Delta\sigma_5$ have the same order of magnitude and coincide with the experimental. However, the principal role is apparently played by the change in σ due to an increase in the polarity of the bond A — H and the formation of the donor-acceptor bond H. . . B. From the given calculations it follows that with some intelligent assumptions regarding the parameters $\Delta\lambda$ and $\beta(\Delta\lambda \simeq 0.3 > \beta = 0.2)$ the resulting values of $\Delta\lambda$ prove to be of both the right sign and the right order of magnitude. The values assumed for $\Delta\lambda$ and β corresponds to a reduction of approximately only 15% in the electron density at the point of proton location.

As a result, it can be stated that the data on the magnetic shielding of the proton in the H-bond support first the hypothesis that there is a substantial increase in the polarity of the A — H bond when the H-bridge is formed, and second, that they are in harmony with the hypothesis that the donor-acceptor bond AH . . . B is formed.

LITERATURE CITED

[1] N. D. Sokolov, J. Exptl. Theor. Physics (USSR) 23, 392 (1952); Advances in Physical Sciences (USSR) 107, 205 (1955).

[2] A. Duncan and J. Pople, Trans. Farad. Soc. 49, 217 (1953); F. O. Ellison and H. Shull, J. Chem. Phys. 23, 2348 (1955); L. Burnelle and C. A. Coulson, Trans. Farad. Soc., 53, 403(1957).

[3] R. Pepinsky, International Symposium on Hydrogen Bonding, London, 1958; S. Darlow, ibid.

[4] H. Tsubomura, J. Chem. Phys. 24, 927 (1956).

*For bound atoms, in addition to the quadratic effect of the influence of the electric field, described approximately by equation (2), there also exists a linear effect [11], which is automatically discounted when the influence of the polarity of the bond A — H is calculated.

[5] M. Packard and J. Arnold, Phys. Rev, 83, 210 (1951); J. Arnold and M. P. Packard, J. Chem. Phys. 19, 1608 (1951); U. Liddel and N. Ramsey, J. Chem. Phys. 19, 1608 (1951).

[6] R. Ogg, J. Chem. Phys. 22, 560 (1954); Helv. Phys. Acta 30, 89 (1957).

[7] P. Diehl, Helv. Phys. Acta 30, 91 (1957).

[8] W. Schneider, H. Bernstein, and J. Pople, J. Chem. Phys. 28, 601 (1958).

[9] J. Pople, Proc. Roy. Soc., A, 205, 163 (1951).

[10] L. V. Aleksandrov, Proc. Acad. Sci. USSR 121, No. 5 (1958).*

[11] L. V. Aleksandrov, Dissertation. Inst. Chem. Phys., Acad. Sci. USSR, 1958.**

Received July 23, 1958

*Original Russian pagination. See C.B. Translation.

**In Russian.

PATHS FOR THE FORMATION OF METHYL HYDROPEROXIDE AND FORMALDEHYDE IN THE LOW-TEMPERATURE OXIDATION OF METHANE

N. A. Kleimenov and A. B. Nalbandyan

Institute of Chemical Physics, Academy of Sciences of the USSR

(Presented by Academician V. N. Kondrat'ev, July 28, 1958)

It is known [1] that hydroperoxides and aldehydes are the primary reaction products when gaseous hydrocarbons are subjected to low-temperature oxidation. In particular, in the oxidation of methane, initiated by the oxygen atoms that arise in the thermal decomposition of ozone [2], or under the influence of the light from the Schumann spectral region [3], the principal reaction products are methyl hydroperoxide and formaldehyde. It was established that the rate of formaldehyde formation increases with increase in the temperature, whereas the formation rate of the peroxide begins to fall when a certain temperature is reached, approaching zero at a temperature close to 400°.

In designing a mechanism for the oxidation of hydrocarbons it is important to answer the question of the manner in which the aldehydes are formed — do they arise as a result of the further oxidation or decomposition of organic peroxides or can they be formed by independent paths.

According to the opinions of N. N. Semenov [4], expounded by him in recent years, both aldehydes and peroxides arise in parallel reactions from peroxide radicals of the type $ROO\dot{}$. At low temperatures the peroxide radicals react with the original hydrocarbon, forming hydroperoxide and a new chain carrier

$$ROO\dot{} + RH \rightarrow ROOH + \dot{R}. \qquad (I)$$

On raising the temperature, together with reaction (I), the peroxide radical can decompose with the formation of aldehydes. For example, the peroxide radical $CH_3O\dot{O}$ can decompose into formaldehyde and hydroxyl; for the propyl peroxide radical $C_3H_7O\dot{O}$ such decomposition can proceed with the formation, for example, of acetaldehyde and alcohol radicals. In all cases the peroxide radicals first suffer isomerization [5]. Since the isomerization process requires a certain, quite large, energy of activation (20 kcal / mole), then the probability of decomposition will increase with increase in the temperature. Consequently, the fraction of aldehydes, arising directly from the peroxide radicals, will also increase. As regards the peroxides, then their fraction in the reaction products will decrease due to an increase in the decomposition rate of the peroxide radicals.

The validity of these assumptions is supported, for example, by the studies made by one of us [1] on the photochemical sensitization of the oxidation of a number of saturated hydrocarbons using mercury. However, these experimental data can serve only as a qualitative proof of the indicated hypotheses and do not permit solving the problem of the formation rates of each of the products separately. It should be mentioned that up to now there has been no direct proof given in the literature that these processes are parallel.

In this paper, on the example of the oxidation of methane, we are the first to offer quantitative proof that parallel processes are present, leading to the formation of both aldehydes and peroxides, and in addition, we have determined the formation rate of each of these substances. We used the method of labeled atoms to solve the present problem.

EXPERIMENTAL RESULTS AND THEIR DISCUSSION

The photochemical method described in [6] was used to initiate the low-temperature reaction. A PRK-2 mercury-quartz lamp served as the light source. For maximum utilization of the radiation energy a special quartz apparatus was constructed, making it possible to illuminate the reactor from within. The experiments were run under flow conditions. To make it possible to follow the behavior of the methyl hydroperoxide formed during reaction, the starting mixture fed into the reactor was mixed with about 0.003% of methyl peroxide, labeled with radioactive carbon C^{14}. The latter was obtained by the method given in the literature for the synthesis of unlabeled methyl peroxide [7]. By means of preliminary experiments, run at 360°, it was established that in the investigated interval of time of contact the only products formed are peroxide and formaldehyde. To trap these substances the gasses escaping from the reactor were passed through water scrubbers. The concentration of peroxide in the solution was determined iodometrically. We ran into considerable difficulties when we attempted to determine the concentration of formaldehyde in the presence of methyl hydroperoxide by conventional methods. It was also discovered that the use of 2,4-dinitrophenylhydrazine to precipitate only the formaldehyde in the condensate failed to achieve the desired purpose. Due to the indicated difficulties we worked out a new method, which made it possible to solve the raised problems in an accurate manner. Together with determining separately the concentration of each product, we determined the total amount of carbon-containing products present in the condensate by combustion. Within the limits of experimental error, the sum of aldehydes and peroxides, determined separately, coincided with their sum, determined by combustion.

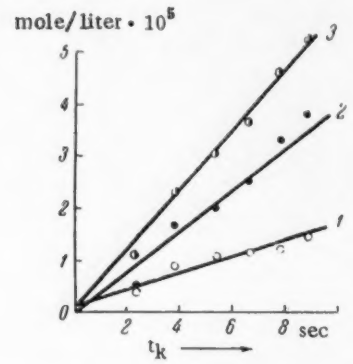

Fig. 1. Yield of methyl hydroperoxide (1) and of formaldehyde (2) as a function of the time the methane-oxygen mixture remains in the reactor. (3) total yield of products (experimental points obtained by the combustion of the products with potassium dichromate). Mixture composed of 90% CH_4 and 10% O_2; furnace temperature 360°.

Having determined the specific activity of the carbon dioxide obtained after combustion, and knowing its concentration, it was a simple matter to calculate the specific activity of the peroxide, making use of the equation for the activity balance:

$$\alpha_{CO_2}[CO_2] = \alpha_f [CH_2O] + \alpha_p[CH_3OOH],$$

where α_{CO_2}, α_f and α_p are respectively the specific activities of carbon dioxide, formaldehyde and peroxide; $[CO_2]$, $[CH_2O]$ and $[CH_3OOH]$ are respectively their concentrations at a given moment.

The kinetic curves for the formation of CH_3OOH and CH_2O at 360°. are shown in Fig. 1. As can be seen from the plot, in the studied interval of time of contact the yield of these products is a linear function of t_K.

The changes in the specific activities of peroxide and aldehydes are shown in Fig. 2. The presence of activity in the formaldehyde indicates that a certain fraction of the peroxide either decomposes or oxidizes to formaldehyde. Characteristic of the obtained results is the fact that the curve for the change in the specific activity of the peroxide remains above that for the change in the specific activity of the formaldehyde over the entire range studied. As is known [9], such a behavior for the specific activity is characteristic for parallel reactions. It is obvious that in the given case a part of the formaldehyde is formed apart from the peroxide, while another part originates as the result of the decomposition or further oxidation of the peroxide — a fact that possesses independent interest.

The question as to the fraction of aldehyde that originates apart from the peroxide can be answered by resort to the kinetic method of utilizing labeled atoms [10]. According to this method the rate W_p for the formation of peroxide from methane is equal to

$$W_p = -\frac{d \ln \alpha_p}{dt}[CH_3OOH]. \qquad (1)$$

On the other hand, the rate with which methane is consumed to form formaldehyde and peroxide is obviously equal to:

$$\frac{d[CH_4]}{dt} = W_f + W_p, \qquad (2)$$

where W_f is the rate of formaldehyde formation. Consequently, we have two equations for determining the two values W_p and W_f.

By graphical differentiation of the curve $\ln\alpha_p$ vs t it is a simple matter to determine the value of $d\ln\alpha_p / dt$ for each contact time. The values of W_p, calculated for different contact times, are given in Table 1.

TABLE 1

t_k, sec	$[CH_3OOH]$, 10^{-6} mole/liter	$\frac{d\ln\alpha_p}{dt}$, $\frac{1}{sec}$	W_p 10^{-6} mole/liter
2	4	0,495	2
3	6	0,33	2
4	8	0,25	2
6	12	0,17	1,9
9	18	0,125	2

$W_{p\,av} \cong 2 \cdot 10^{-6}$

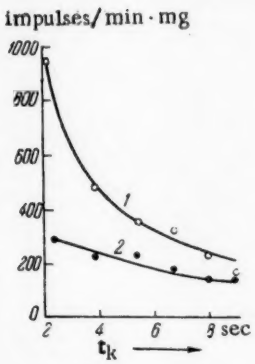

Fig. 2. Specific activity of methyl hydroperoxide (1) and of formaldehyde (2) as a function of the time the methane-oxygen mixture remains in the reactor.

As can be seen from the table, for the investigated interval of mixture remaining in the reaction zone the rate of peroxide formation remains constant and equal to 2×10^{-6} mole/liter · sec.

The rate of formaldehyde formation we find from equation (2). From the slope of straight line 1 in Fig. 1, we determine $d[CH_4]/dt = 5.5 \times 10^{-6}$ mole/liter · sec. From this for W_f we have $W_f = d[CH_4]/dt - W_p = 3.5 \times 10^{-6}$ mole/liter · sec. Consequently for the proportion W_f / W_p we have:

$$\frac{W_f}{W_p} = \frac{3{,}5 \cdot 10^{-6}}{2 \cdot 10^{-6}} = 1{,}75.$$

As a result, at the given temperature about 64% of the reacted methane goes to formaldehyde due to direct decomposition of the peroxide radical, and only 36% of it is converted to hydroperoxide due to reaction of the peroxide radical with methane.

It is essential to find the values of W_f / W_p for several temperatures. Knowing the relationship that exists between W_f / W_p and the temperature permits calculating the difference between the energies of activation for the processes of isomerization and decomposition of the peroxide radical and its reaction with methane. Knowing that $W_f / W_p = 1.75$, it becomes possible to calculate this difference at 360°. Assuming that the pre-exponential factors for the monomolecular decomposition of the peroxide radical and for its bimolecular reaction with methane have respectively the normal values $10^{+13}\ \frac{1}{sec}$ and $10^{-10}\ \frac{cu\ cm}{sec}$, we obtain $\Delta E \cong 9600$ cal/mole. Consequently, the postulation of N. N. Semenov [4] that ΔE should be of the order of 10,000 cal/mole is fully justified.

LITERATURE CITED

[1] N. V. Fok and A. B. Nalbandyan, Monograph "Problems of Chemical Kinetics, Catalysis and Reactivity" [in Russian] (Izd. AN SSSR, 1955), p. 219.

[2] N. A. Kleimenov, I. N. Antonova, A. M. Markevich and A. B. Nalbandyan, J. Phys. Chem. (USSR), 30, 794 (1956); J. Chem. Phys. 54, No. 4, 321 (1957).

[3] N. A. Kleimenov and A. B. Nalbandyan, Proc. Acad. Sci. USSR 122, No. 1 (1958).*

[4] N. N. Semenov, Prog. Chem. 20, 706 (1951); Some Problem of Chemical Kinetics and Reactivity [in Russian] (Izd. An SSSR, 1954), p. 87.

[5] N. N. Semenov, Prog. Chem. 20, 687 (1951); N. Ya. Chernyak and V. Ya. Shtern, Proc. Acad. Sci. USSR 78, 91 (1951); N. Ya. Chernyak, V. A. Antonovskii, A. F. Revzin and V. Ya. Shtern, J. Phys. Chem. (USSR) 28, 240 (1954).

[6] A. B. Nalbandyan, Proc. Acad. Sci. Armenian SSR 7, 109 (1947); 9, 101 (1948); J. Phys. Chem. (USSR) 22, 1443 (1948); Proc. Acad. Sci. USSR 66, 2468 (1949).

[7] A. Rieche and F. Hitz, Ber. 62, 2468 (1929).

[8] A. L Gulyaeva, et al., Analysis of the Products Obtained in the Production of Divinyl from Ethyl Alcohol by the S. V. Lebedev Method [in Russian], 1950.

[9] L. N. Antonova, R. L. Moshkina, et al., Monograph "Problems of Kinetics and Catalysis, Vol. 9, Isotopes in Catalysis" [in Russian] (Izd. AN SSSR, 1957), p. 97; L. N. Antonova, V. A. Kuz'min, et al., Bull. Acad. Sci. USSR, Div. Chem. Sci., No. 5, 789 (1955).*

[10] M. B. Neiman, J. Phys. Chem. (USSR) 28, 1235 (1954).

Received July 24, 1958

*Original Russian pagination. See C.B. Translation.

THEORY OF RADIATIONLESS ELECTRON TRANSITIONS BETWEEN IONS IN SOLUTIONS

Acad. Sci. USSR Corresponding Member V. G. Levich and

R. R. Dogonadze

Institute of Electrochemistry, Academy of Sciences of the USSR

The reactions between similarly charged ions in solutions play an important role in the elementary act of chemical oxidation-reduction reactions. A distinguishing trait of reactions of this type is the fact that the reacting ions, due to the presence of a strong electrostatic repulsion, cannot approach each other very closely. The reaction of electron exchange in the system

$$Fe^{2+} - Fe^{3+}. \tag{1a}$$

has been studied in some detail experimentally. Both spectrophotometric and potentiometric experiment [1] have shown that together with the direct reaction (1a), reactions also progress in solution between Fe^{2+} and the complexes formed by Fe^{3+} with the anions present in solution:

$$Fe^{2+} - FeOH^{2+}, \tag{1b}$$

$$Fe^{2+} - FeCl^{2+}, \tag{1c}$$

$$Fe^{3+} - FeF^{2+} \tag{1d}$$

etc. Attempts have been made in a number of papers [2-4] to calculate theoretically the probability of electron transition in reaction of Type (1). In particular, the hypothesis of a tunnel transition of the electron was expressed in [3]. In view of the fact that tunnel transitions can occur only under the conditions of the energies of the initial and final states being equal, the authors made the assumption that the transition occurs at the moment when the solvate shells of the ions are rebuilt in such manner that the initial and final state of the electron proves to be the same. Here the term ΔF_r^* was introduced into the free energy of activation, which theoretically could not be calculated.

An important fault of all of the theoretical studies here was the fact that improper consideration was given to the role played by the solvent. In reactions of Type (1) the role played by the solvent is especially important, and taking it into consideration only by introducing the macroscopic dielectric constant ϵ is quite inadequate; these viewpoints are also supported by a number of experimental studies [5-7].

In this paper the solvent is considered to be a collection of atoms, showing small vibrations around fixed equilibrium positions. During electron transition, which is regarded as a radiationless transition of the whole electron-solvent system, a certain number of vibrational quanta (phonons) is absorbed (or emitted). The calculation was made in adiabatic approximation, in which connection the solvent was taken as the slow subsystem, and the electron as the rapid. The Hamiltonian of the complete system

$$H(x, q) = H(x) + H(q) + V(x, q) \tag{2}$$

consists of the electron portion

$$H(x) = -\frac{\hbar^2}{2m}\nabla^2 + U(x, R), \tag{3}$$

the Hamiltonian of the vibrating atoms (reduced to the normal form)

$$H(q) = \frac{1}{2}\sum_{\varkappa}\hbar\omega_{\varkappa}\left(q_{\varkappa}^2 - \frac{\partial^2}{\partial q_{\varkappa}^2}\right) \tag{4}$$

and the energy of interaction between electron and phonons. The coordinates $\underline{x}$ and $\underline{q}$ refer to the electron and phonons, respectively. The potential U(x, R), entering in (3), describes the interaction of the electron with the ions, separated from each other by the distance R, and with the static portion of the solvent polarized by them. V(x, q) can be broken down into a stepwise series of small deviations of the solvent atoms from the equilibrium positions

$$V(x, q) = V_0(x) + \sum_{\varkappa} V_{\varkappa}(x)(q_{\varkappa} - q_{\varkappa s}) +$$

$$+ \sum_{\varkappa\varkappa'} V_{\varkappa\varkappa'}(x)(q_{\varkappa} - q_{\varkappa s})(q_{\varkappa'} - q_{\varkappa' s}) + \ldots \approx V_0 + V_1 + V_2, \tag{5}$$

where the equilibrium configurations (at a given electron state s) are determined by the equality $q_{\varkappa s} = -V_{\varkappa}^{ss}/\hbar\omega_{\varkappa}$, in which connection the matrix elements $V_{\varkappa}^{ss'}$ are taken with respect to the electron wave functions $\psi_s(x, q_s)$ and $\psi_{s'}(x, q_{s'})$. In (5) V_0 corresponds to the interaction of the electron with the solvent polarized by it; V_1 represents the electron–phonon interaction, while V_2 originates in calculating the anharmonicity of the vibrations of the solvent atoms and appears as a small correction of the harmonic potential. As a result, in theory there are two small values: the parameter of adiabaticity

$$\frac{x_{\varkappa}^{ss'}}{\hbar\omega_{\varkappa}} = \int \psi_s^*(x, q)\frac{\partial}{\partial q_{\varkappa}}\psi_{s'}(x, q)\,dx, \quad q \to q_s,$$

and the small interaction of the electron with the anharmonic portion of vibration V_2, which in various cases can play the role of disturbances. The selection of the proper approximation is tied up essentially with the selection of the frequency spectrum $\omega_{\varkappa}$.

The energy of the complete system E_{sn} is given by the expression

$$E_{sn} = E_s(q_s) + {}^1/_2\sum_{\varkappa}\hbar\omega_{\varkappa}q_{\varkappa s}^2 + \sum_{\varkappa}\hbar\omega_{\varkappa}(n_{\varkappa} + {}^1/_2) = J_s + \sum_{\varkappa}\hbar\omega_{\varkappa}(n_{\varkappa} + {}^1/_2),$$

where $E_s(q_s)$ is the natural value of the operator $H(x) + V_0(x)$, and is the energy of the electron in the field of two ions and the polarized (by the ions and the electron) static solvent. In the adiabatic theory of disturbances the value J_s plays the role of the "complete" energy of the electron. The term ${}^1/_2\sum_{\varkappa}\hbar\omega_{\varkappa}q_{\varkappa s}^2$ entering into it has the meaning of the energy of the solvent polarized by the electron and in order of magnitude is equal to the energy of electronic polarization.

Optical branch. If the optical branch plays the principal role in electron–phonon interaction, then the dispersion of the frequencies can be neglected and the substitution $\omega_{\varkappa} \equiv \omega_0$ can be made. Physically the frequency ω_0 can correspond to the vibrations of different bonds, both intramolecular and intermolecular (for example, the hydrogen bond). In such case the anharmonicity can be neglected, and for the probability of transition (more accurately, the number of transitions per unit of time), we obtain the formula

$$W_{12} = \frac{2\pi}{\hbar^2\omega_0}\exp\left\{-\sigma(\bar{n} + {}^1/_2) - \frac{m\hbar\omega_0}{kT}\right\}\left(\frac{\bar{n}+1}{\bar{n}}\right)^{m/2} \times$$

$$\times\left\{(\bar{n} + {}^1/_2)^2B^2I_m(z) + \left[\frac{z}{2\sigma}C - \frac{z}{\sigma}(\bar{n} + {}^1/_2)B^2\right][I_{m+1}(z) + I_{m-1}(z)]\right. +$$

$$+\frac{z^2}{4\sigma^2}B^2[I_{m+2}(z)+2I_m(z)+I_{m-2}(z)]\Big\}; \tag{6}$$

$$\sigma=\sum_{\varkappa}{}'(q_{\varkappa s_1}-q_{\varkappa s_2})^2=\sum_{\varkappa}{}'(\Delta q_{\varkappa})^2;\quad B=\sum_{\varkappa}{}'\Delta q_{\varkappa}x_{\varkappa}^{s_1s_2};\quad C=\sum_{\varkappa}{}'(x_{\varkappa}^{s_1s_2});$$

$$z=\sigma\sqrt{\bar{n}(\bar{n}+1)};\qquad m=\frac{J_{s_2}-J_{s_1}}{\hbar\omega_0};\qquad \bar{n}=\left[\exp\left\{\frac{\hbar\omega_0}{kT}\right\}-1\right]^{-1}$$

$I_m(z)$ is the Bessel function of the mth order from the imaginary argument. Using the asymptotic expression $I_m(z)$, equation (6) can be substantially simplified for several limiting cases:

$$W_{12}\simeq\frac{2\pi}{\hbar^2\omega_0}\frac{\sigma^{m-1}\exp(-1/2\sigma)}{2^m(m-1)!}\left[C+\left(\frac{m}{\sigma}-\frac{1}{2}\right)B^2\right]\exp\left\{\frac{J_{s_1}-J_{s_2}}{kT}\right\},$$
$$m\gg z,\quad kT\ll\hbar\omega_0; \tag{7}$$

$$W_{12}\simeq\frac{C\exp(-1/2\sigma)}{2\hbar^2\omega_0}\sqrt{\frac{2\pi}{\sigma}}\exp\left\{\frac{J_{s_1}-J_{s_2}}{2kT}+\sigma\exp\left(-\frac{\hbar\omega_0}{2kT}\right)\right\},$$
$$m\ll z,\quad kT\ll\hbar\omega_0; \tag{8}$$

$$W_{12}\simeq\frac{2\pi}{\hbar^2\omega_0}\frac{\sigma^{m-1}\exp(-1/2\sigma)}{2^m(m-1)!}\left[C+\frac{m}{\sigma}B^2\right]\left(\frac{kT}{\hbar\omega_0}\right)^m\exp\left\{-\sigma\frac{kT}{\hbar\omega_0}\right\},$$
$$m\gg z,\quad kT\gg\hbar\omega_0; \tag{9}$$

$$W_{12}\simeq\left(\frac{2\pi C^2kT}{\sigma\omega_0^3\hbar^5}\right)^{1/2}\exp\left\{-\frac{\hbar\omega_0(\sigma+2m)^2}{8\sigma}\frac{1}{kT}\right\},\quad m\ll z,\quad kT\gg\hbar\omega_0. \tag{10}$$

Acoustical branch. Apparently, a consideration of the anharmonicity is more important for the liquid. In this case it can be assumed that adiabaticity is achieved with a greater degree of accuracy and, substituting $x_K^{SS'}=0$, take V_3 as the disturbance. Regarding the frequency spectrum we will only postulate that it is cut at a certain maximum frequency ω_D (by analogy with the Debye spectrum). Omitting the bulky calculations, we give the general equation for W_{12}:

$$W_{12}=\frac{1}{2\hbar^2}\int_{-\infty}^{+\infty}P(t)\,e^{Q(t)}\,dt; \tag{11}$$

$$P(t)=\sum_{\sigma\sigma'\rho\rho'}{}'V_{\sigma\sigma'}^{s_1s_2}V_{\rho\rho'}^{s_1s_2}\{[(1+4\bar{n}_\rho\cos\omega_\rho t)\delta_{\sigma\rho}+\Delta q_\sigma\Delta q_\rho f_\sigma f_\rho]\times$$
$$\times(1+4\bar{n}_{\rho'}\cos\omega_{\rho'}t)\delta_{\sigma'\rho'}+1/8[2(2\bar{n}_\rho+e^{i\omega_\rho t})\delta_{\rho\rho'}+\Delta q_\rho\Delta q_{\rho'}f_\rho f_{\rho'}]\times$$
$$\times[2(\bar{n}_\sigma+1)\delta_{\sigma\sigma'}+\Delta q_\sigma\Delta q_{\sigma'}f_\sigma f_{\sigma'}]\};$$

$$Q(t)=\frac{i}{\hbar}(J_{s_2}-J_{s_1})t+\frac{1}{2}\sum_{\varkappa}{}'(\Delta q_\varkappa)^2g_\varkappa;$$

$$f_\varkappa(t)=(\cos\omega_\varkappa t-1)+i(2\bar{n}_\varkappa+1)\sin\omega_\varkappa t;$$

$$g_\varkappa(t)=(2\bar{n}_\varkappa+1)(\cos\omega_\varkappa t-1)+i\sin\omega_\varkappa t.$$

The integral in (11) can be taken on the assumption that $|J_{s_2}-J_{s_1}|\gg\hbar\omega_D$, and in the case of high temperatures ($kT\gg\hbar\omega_D$) W_{12} assumes the form

$$W_{12} \simeq \left[\frac{2\pi (kT)^3}{\hbar^7 \sum_{\varkappa}' (\Delta q_\varkappa)^2 \omega_\varkappa} \right]^{1/2} \sum_{\alpha\rho}' \frac{(V_{\alpha\rho}^{s_1 s_2})^2 (8 + \delta_{\alpha\rho})}{\omega_\alpha \omega_\rho} \times$$

$$\times \exp \left\{ - \frac{\left[J_{s_2} - J_{s_1} + \frac{1}{2} \sum_{\varkappa}' (\Delta q_\varkappa)^2 \hbar\omega_\varkappa \right]^2}{2 \sum_{\varkappa}' (\Delta q_\varkappa)^2 \hbar\omega_\varkappa} \frac{1}{kT} \right\}. \qquad (12)$$

Equations (10) and (12) have the same form as in the theory of absolute reaction rates: $W_{12} = A \exp \{ - Q/kT \}$, whence

$$Q = \frac{\left[J_{s_2} - J_{s_1} + \frac{1}{2} \sum_{\varkappa}' (\Delta q_\varkappa)^2 \hbar\omega_\varkappa \right]^2}{2 \sum_{\varkappa}' (\Delta q_\varkappa)^2 \hbar\omega_\varkappa}.$$

We will oberve that if we substitute $\omega_K \equiv \omega_0$ here, then we will immediately obtain the energy of activation, coinciding with Q in (10). Analysis of the obtained equations reveals that a deviation from the Arrhenius curves occurs when the temperature is lowered, and specifically toward a more rapid drop in ln W_{12}, with increase in 1/T. This is the essential conclusion of the theory, associated with the fact that in the theory of the transitional state equations are used that have been introduced through methods of statistical physics, according to which the probability depends on the temperature as $e^{-Q/kT}$. However, as had been already indicated many times [8-9], the application of the equilibrium equations of statistical physics to the essentially nonequilibrium process being discussed is not justified. From what has been said it is obvious that the theory of the transitional state is applicable at high temperatures.

In order to estimate theoretically the temperature T^*, at which the deviation from linearity begins, it is necessary to known the characteristic frequencies ω_0 and ω_D, entering into the theory. If physically ω_0 corresponds to the vibrations of hydrogen bond, then for T^* we obtain a temperature of about 280° K. A rough estimate of the Debye temperature for H_2O reveals that in the case where the acoustical branch plays the essential role, $T^* \simeq 240°$ K. It should be mentioned that the experiments are usually run in a fairly narrow temperature range (280-330° K), where the obtained equation can be approximated quite well by the linear function.

A calculation of the energy of activation requires knowing the concrete wave functions of the electron, but still it can be estimated fairly well. It proved that all reactions of Type (1) $Q \cong 8$ kcal/mole, which agrees very well with experiment. Still another essential conclusion ensues from the theory: the energy of activation depends on the electron energies of solvation of the initial and final states $S_1^{(e)}$ and $S_2^{(e)}$ and, on the other hand, on $\Delta E_{el} \equiv E_{s_2}(q_{s_2}) - E_{s_2}(q_{s_1})$. With increase in $S_2^{(e)}$ in energy of activation at small ΔE_{el} increases, while at large ΔE_{el} it falls. For reactions of Type (1), ΔE_{el} is small, for which reason the energy of activation should increase in succession for reactions (1b), (1c) and (1d). The conclusion is also found to be in good agreement with experiment [10].

From the very manner in which the problem is set up it is clear that in the given theory the energy of activation can only increase when the mass of the solvent atoms is increased, which is in agreement with the experiments [6-7] in which D_2O served as the solvent.

LITERATURE CITED

[1] G. C. Laurence, Trans. Farad. Soc. 53, 1326 (1957).

[2] W. F. Libby, J. Phys. Chem. 56, 863 (1952).

[3] R. J. Marcus, B. J. Zwolinski, and H. Eyring, J. Phys. Chem. 58, 432 (1954).

[4] J. Weiss, Proc. Roy. Soc. A, 222, 128 (1954).

[5] W. L. Reynolds and R. W. Lumry, J. Chem. Phys. 23, 2460 (1955).

[6] J. Hudis and R. W. Dodson, J. Am. Chem. Soc. 78, 911 (1956).

[7] J. C. Sullivan, D. Cohen and C. Hindman, J. Am. Chem. Soc. 79, 3672 (1957).

[8] R. H. Fowler and E. A. Guggenheim, Statistical Thermodynamics [Russian Translation] (IL, 1949).

[9] S. Glasstone, K. J. Laidler and H. Eyring, Theory of the Absolute Rates of Chemical Reactions [Russian translation] (IL, 1948).

[10] J. Hudis and A. C. Wahl, J. Am. Chem. Soc. 75, 4153 (1953).

Received August 29, 1958

STUDY OF THE FREE RADICALS FORMED IN THE IRRADIATION OF OXALIC ACID BY THE METHOD OF ELECTRON PARAMAGNETIC RESONANCE

Yu. N. Molin, A. T. Koritskii, N. Ya. Buben and Corresponding Member Acad. Sci. USSR V. V. Voevodskii

Institute of Chemical Physics, Academy of Sciences of the USSR

The method of electron paramagnetic resonance (e. p. r.) developed by us for observing free radicals in the action of fast electrons on a substance [1] also permits making kinetic studies of the formation and destruction of radicals in solids. Some preliminary data on the properties of the radicals arising in oxalic acid when the latter is bombarded with electrons having an energy of 1.6 mev are given below. The signal of paramagnetic absorption in oxalic acid represents a single line with a width (determined by the distance between the points of the extremal values of the derivative) of about 4.5 oersteds and a g-factor close to the g-factor of the diphenylpicrylhydrazyl radical (2.0036). On terminating the irradiation the signal falls at a rate that is essentially dependent on the temperature.

One of the curves for the change in the concentration of the radical, taken at room temperature, is shown in Fig. 1. The amplitude h of the first derivative of the absorption line was taken as a measure of the intensity of the e. p. r. signal, since neither the shape of the signal nor its width changed during measurement. Analysis of that portion of the curve corresponding to a drop in the signal revealed that in the temperature range between +10 and +40° the recombination of the radicals is described by the equation

$$\frac{dn}{dt} = -kn^2, \tag{1}$$

where n is the concentration of the radicals, and k is a constant dependent on the temperature. By the usual methods it was found that $k \cong 9 \cdot 10^{-22}$ cu cm/sec for a temperature of +25° (see Fig. 2).*

TABLE 1

j, μa/sq cm	$[n]_{stationary}$ (arbitrary units)	$\frac{[n]_{stationary}}{\sqrt{j}}$
0.143	0.074	0.195
0.276	0.105	0.200
0.610	0.139	0.178

*The absolute values of the concentration of the radical were obtained by comparing the area of the absorption line of the investigated signal with that of the signal from a diphenylpicrylhydrazyl specimen of known concentration.

In accordance with the quadratic recombination rule (1) it could be expected that at a constant temperature the stationary concentration of the radicals after saturation had been achieved will be proportional to the square root of the irradiation dosage.

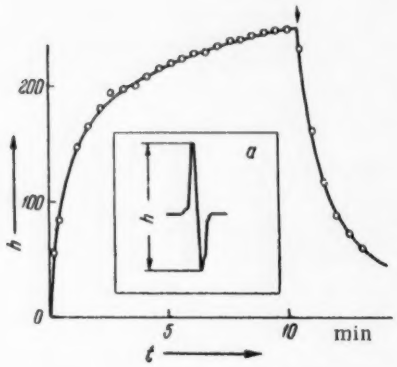

Fig. 1. Change in the intensity h of the e.p.r. signal of oxalic acid during irradiation and after termination of irradiation (the arrow denotes the point at which irradiation was terminated). The first derivative of the absorption line is shown by a.

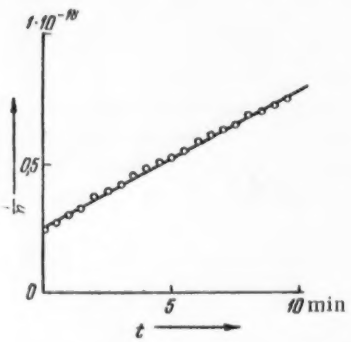

Fig. 2. Linear anamorphosis for the relationship between the concentration of radicals and the time: $\frac{1}{n} = \frac{1}{n_0} + kt$.

Some data on the relationship between the stationary concentration of the radical and the current density of the electrons are given in Table 1. A constancy of the proportion $[n]_{stationary}/\sqrt{j}$ when the current density is increased by approximately 4 times supports the postulation that recombination at small dosages has a quadratic mechanism.

However, it should be mentioned that an accumulation of radicals is not described by the simple kinetic equation

$$\frac{dn}{dt} = w_0 - kn^2, \qquad (2)$$

but instead bears a more complex nature, since the time required to establish a stationary concentration greatly exceeds the recombination time (see Fig. 1).

To answer the question of the nature of the radical in oxalic acid we made a comparison of the e.p.r. spectra of irradiated oxalic, succinic and stearic acids and of some of their salts. It was established that paramagnetic absorption signals, similar to the signal in oxalic acid, are also present in the quite complex spectra of succinic and stearic acids. In the spectra of the salts these signals either have a weaker intensity (Li, Na, NH_4, and Ca oxalates) or are completely absent (sodium succinate). Apparently, the only radical to which the appearance of this signal in the spectra of all three acids can be attributed is the radical of type $R-C\overset{O}{\underset{O\cdot}{<}}$, formed as a result of the hydrogen atom cleaving from the carboxyl group. The conditions for the formation of such a radical in the salts and in the acids are essentially different due to the greater mobility of the free hydrogen atom. Herein apparently lies the reason for the difference in the e. p. r. spectra of the acids and the corresponding salts.

The experimentally found quadratic recombination rule (1) indicates that destruction of the radicals occurs in the interaction of two radicals with each other. As possible mechanisms here it could be postulated that either the radical diffuses through the substance by the mechanism of a hydrogen atom migrating from a neighboring molecule to the radical, or else that the mechanism involves a delocalization of a free electron along a system of conjugated hydrogen bonds, similar to the theory that has been advanced by L. A. Blyumenfel'd for protein molecules [2].

To establish the true mechanism it is necessary to run additional experiments. The results obtained in the chemical analysis of the radiolysis products of oxalic acid could have great importance here, as could also an accurate measurement of the pre-exponential factor of the recombination rate constant.

LITERATURE CITED

[1] Yu. N. Molin, A. T. Koritskii, et al., Proc. Acad. Sci. USSR 123, No. 5 (1958).*

[2] L. A. Blyumenfel'd and A. É. Kalmanson, Biophysics (USSR) 3, 87 (1958).

Received August 11, 1958

*Original Russian pagination. See C.B. Translation.

THE RELATIONSHIP BETWEEN THE ENERGETIC, ELECTROPHYSICAL AND MECHANICAL PROPERTIES OF SEMICONDUCTORS

B. F. Ormont

L. Ya. Karpov Institute of Physical Chemistry

(Presented by Academician P. A. Rebinder, June 18, 1958)

The very important problem of the relationship between the energetic, electrophysical and mechanical properties of semiconductors, despite a number of published papers on the subject, still remains one of the least developed [1]. In recent years we undertook a new approach to the problem.

1. Relationship between the atomization energy of a compound, the lattice energy, and the enthalpy (corresponding to the heat effect) of formation. As had been discussed by us [2, 3], between the energy of atomization Ω of a solid AB (with the atomic lattice and bonds quite removed from the ionic) and the enthalpy, corresponding to the heat effect of formation according to the equation [A] + [B] = [AB] + Q, where the brackets designate the solid aggregate state, there exists the relationship:

$$\Omega = Q + S_A + S_B, \tag{1}$$

where S_A and S_B is the energy of sublimation of A and B, respectively, with the formation of a monatomic pair (i.e., the energy of their atomization).

The energy of atomization of substance AB is linked to the lattice energy by the equation:

$$\Omega = U - \sum_n I - \sum_n E + \alpha, \tag{2}$$

where $\Sigma_n I$ is the total ionization potential of A, $\Sigma_n E$ is the energy of adding n electrons to B, and U is the energy of the ionic lattice in the Born concept, the α-energy of transition from the ideal Born state of the lattice to the real [2,3]. The energetic (thermodynamic) strength of the lattice is described more accurately by the atomization energy value Ω, if the lattice is mainly atomic, and by the lattice energy U, if the bonds are close to ionic.

2. Relationship between the total specific surface energy ϵ_{hkl} and the atomization energy Ω. If the bonds are mainly covalent, then, as had been shown by us in [2], the specific surface energy is linked to the atomization energy in the following manner:

$$\varepsilon_{hkl} = \frac{\Omega}{a^2} M_{\varepsilon(hkl)} \text{ erg/cm}^2, \tag{3}$$

where $M_{\epsilon(hkl)}$ is the structural constant of the surface energy. The values of M_ϵ were calculated by us [2, 7] for a number of structures and planes (hkl). Thus, for the diamond type $M_{\epsilon(100)} = 694.34$; $M_{\epsilon(111)} = 401.33$. For the zinc blend type $M_{\epsilon(100)} = 347.17$; $M_{\epsilon(110)} = 244.8$; $M_{\epsilon(111)} = 200.66$. For the rock salt type $M_{\epsilon(100)} = 231.45$. The specific free surface energy σ_{hkl} is easily calculated from ϵ_{hkl}, taking into consideration that $\sigma_{hkl} = \epsilon_{hkl} + T\,\partial\sigma/\partial T$.

As is known, an experimental varification of the calculated values of σ_{hkl} for solids is a difficult problem. In [4] we have developed jointly with V. L. Smirnova a method for determining the surface energy of solids at the melting point. Included in the substances examined we determined that for β-Sn, σ = 610 ergs/ /sq cm. Taking into account the values of $d\epsilon/dT$ [5], we find for β-Sn ϵ_{111}^{298} = 630 − 640 ergs/sq cm. The calculation for α-Sn ϵ_{111}^{298} gives 670 ergs /sq cm. Taking into consideration that tin has bonds that are close to metallic (and here the applicability of equation (3) runs into limitations), it must be acknowledged that the agreement is good.

At this time we have set ourselves the task of measuring ϵ for Ge and Si using the same method.

We also used an indirect approach. Employing equation (3), we calculated ϵ_{hkl} for a series of brittle solids (carbides, nitrides, etc.) [2]. The relative values ϵ and σ for substances with a similar structure and type of chemical bond form the thermodynamic hardness scale. (For $H_1 : H_2 : H_3 \ldots = \sigma_1 : \sigma_2 : \sigma_3 \ldots$ [11].) When the ϵ_{hkl} series were compared with the literature values for the microhardness H of the same carbides it was found that the carbides of tantalum and vanadium should be much harder than is indicated in the literature on the basis of experimental data. A verification of the microhardness of TaC_x and VC_x, made by us jointly with other authors, revealed the validity of the series ensuing from our calculations [6].

3. Calculated values of the specific surface energies of some semiconductors and their microhardness. In [7] and in this paper we have calculated the values of ϵ_{hkl} for some semiconductors with a diamond and a zinc blend structure and compared them with the experimental values of the microhardness H from [8, 9]. From Table 1, in which the values of ϵ_{hkl}, H, etc., are compared, it can be seen that a valid correlation exists between these series of values.

4. Dependence of the width of the forbidden zone of some semiconductors on the strength and character of the chemical bond. The width of the forbidden zone ΔE should be directly dependent on the strength of the chemical bonds, but not on the heat effect of formation of the semiconductor, as is frequently postulated (cf., for example [10]) (the heat effect of formation is a characteristic of the system, and not of the phase), and on the atomization energy (corresponding to the lattice energy) of the semiconductor [7]. Consequently, in the same series of simple substances, for example, $A^{IV}A^{IV}$, or compounds, for example $A^{III}B^{V}$ (of type GeGe and GaAs, respectively), a direct relationship between ΔE and ϵ_{hkl} (characterizing the mechanical strenght of the lattice) could be expected, and likewise between ΔE and Ω (characterizing the energetic strength of the latter), i.e., a relationship of the type $\Delta E = k\epsilon_{hkl}$ or $\Delta E = q\Omega$. However, ΔE is not only a structure-sensitive, but also a bond-sensitive [7] property. Consequently, with increase in the total atomic number (ΣZ), calculated on the basis of 2 atomic pairs*, the coefficients $\underline{k}$ and $\underline{q}$, due to a strengthening of the metallic component of the bond, should decrease. It is expedient to depict $\underline{k}$ and $\underline{q}$ as a number of terms: $k = C - M + P$ and $q = c - m + p$, respectively. Conditionally it can be assumed that terms C and $\underline{c}$ express the influence of the covalent, terms M and $\underline{m}$ (decreasing with decrease in ΔZ) the metallic, and terms P and $\underline{p}$ the ionic component of the chemical bond. With some reservations it can be assumed that P and $\underline{p}$ are proportional (as a first approximation) to the difference in the electronegativity Δx of the atoms forming the substance.

Analysis of the values of the $\underline{k}$ and $\underline{q}$ factors, increasing sharply in going from types $A^{IV}A^{IV}$ or $A^{IV}B^{IV}$ to types $A^{III}B^{V}$ and $A^{II}B^{VI}$, reveals that the difference in the electronegativity Δx cannot be responsible for the large increase in ΔE with transition from $A^{IV}A^{IV}$ to $A^{III}B^{V}$ or, correspondingly, to $A^{II}B^{VI}$, contrary to the widely held opinion in the literature. An increase in ΔE (and correspondingly of $\underline{k}$ and $\underline{q}$) corresponds to a principle, which we will formulate in the following manner:

With other conditions equal, the width of the forbidden zone of the semiconductor should be proportional to the ratio of the effective charges of the nuclei (atomic fragments), corresponding to the number of valence electrons of the atomic pairs raised to some power $\underline{n}$, i.e., $(V_B/V_A)^n$, where V_A and V_B are the effective charges of the atomic fragments of atoms A and B.

As a result, ΔE should be described by equations of the type:

*For binary compounds, and for purposes of comparison, for simple substances.

$$\Delta E = \left(\frac{V_B}{V_A}\right)^n [C - M + P]\varepsilon_{hhl}, \tag{4}$$

$$\Delta E = \left(\frac{V_B}{V_A}\right)^n [c - m + p]\Omega. \tag{5}$$

Mathematical analysis brings us to the conclusion that in a series of semiconductors of type $A^{IV}{}_A{}^{IV}$ the dependence of the terms M and m on (ΣZ) can be expressed by both exponential (which is more accurate in a number of cases) and linear functions. If the coefficients of the equations describing the behavior of the series $A^{IV}{}_A{}^{IV}$ and $A^{IV}{}_B{}^{IV}$ are found, then using these same coefficients it is possible to extend equation (4)-(9) to the $A^{III}{}_B{}^{V}$ series, and even (better than could have been expected due to the sharp increase in the strength of the ionic component of the chemical bond), with some reservations, to the $A^{III}{}_B{}^{VI}$ series (zinc blend type of structure), and to some compounds of the $A^{IV}{}_B{}^{VI}$ series (NaCl type of structure). Equations (6)-(9) have the following form:

$$\Delta E = \left(\frac{V_B}{V_A}\right)^n [1{,}093 - 0{,}087\, e^{0{,}0235\,(\Sigma Z)} + 0{,}2\,(\Delta x)]\, 10^{-3}\varepsilon_{111}, \tag{6}$$

$$\Delta E = \left(\frac{V_B}{V_A}\right)^n [1{,}093 - 0{,}0076\,(\Sigma Z) + 0{,}2\,(\Delta x)]\, 10^{-3}\varepsilon_{111}, \tag{7}$$

$$\Delta E = \left(\frac{V_B}{V_A}\right)^n [0{,}860 - 0{,}217\, e^{0{,}0129\,(\Sigma Z)} + 0{,}2\,(\Delta x)]\cdot 10^{-2}\Omega, \tag{8}$$

$$\Delta E = \left(\frac{V_B}{V_A}\right)^n [0{,}860 - 0{,}0076\,(\Sigma Z) + 0{,}2\,(\Delta x)]\cdot 10^{-2}\Omega. \tag{9}$$

Here n = 1.2. For the series $A^{IV}{}_A{}^{IV}$ and $A^{IV}{}_B{}^{IV}$ $(V_B/V_A)^n = (4/4)^{1.2} = 1$, for the series $A^{III}{}_B{}^{V}$ $(V_B/V_A)^n = (5/3)^{1.2} = 1.85$, for the series $A^{II}{}_B{}^{VI}$ $(V_B/V_A)^n = (6/2)^{1.2} = 3.72$, etc. The results of calculating calculating ΔE are given in Table.

A comparison of the experimental and calculated data also permits formulating a second principle, embracing general theoretical considerations:

Of the analogs with the same total atomic number and the same V_B/V_A ratio, i.e., belonging to the same structural and chemical type of substance (compound), the greatest width of the forbidden zone at constant Δx is possessed by the analog with the smallest "cation" and the largest "anion" and, consequently, with the maximum polarization of the electron cloud of the latter.

As a result, ΔE for AlSb is greater than for GaAs and InP, while ΔE for GaSb is greater than for InAs. In connection with this it should be mentioned that the generally held opinion in the literature that ΔE always increases with increases in Δx is incorrect. A weakening of the metallic and a growth of the ionic (or covalent) component of the bond induce an increase in ΔE. But also a weakening of the ionic component with an increase in the strength of the covalent component, customary in the polarization of the electron cloud of a large anion by a small cation, can cause an increase in ΔE. In calculating ΔE for compounds of type $A^{II}{}_B{}^{VI}$, and especially of type $A^{IV}{}_B{}^{VI}$ (with a type of structure different from that of zinc blend), it is necessary to exercise some caution due to the substantial strengthening for them of the ionic component of the chemical bond. (For this reason the lower portion of Table 1 is separated by a line.) And still calculation using equations (4)-(9) and the same coefficients does not lead to any serious differences between the experimental and the calculated data. And thus it is quite obvious that both of the above formulated principles are justified. In particular, ΔE for ZnSe is greater than for CdS, and ΔE for ZnTe is greater than for CdSe.

It is important that in the case of diamond and silicon carbide the calculation of ΔE via ϵ_{hkl} gives good results, whereas calculation via Ω gives sharply lower results due to the extremely high mechanical strength of these substances. As a result, the correlation between ΔE and the mechanical strength proves in the given case to be better than between ΔE and the energetic strength of the lattice.

TABLE 1

Substance	Σz	Δx	H, kg/sq mm	ϵ_{111}, ergs/sq cm	Ω, kcal/mole	ΔE, ev	Calculated ΔE from (5)	from (6)	from (7)	from (8)
				Type $A^{IV}A^{IV}$						
Cdiamond	12	0	—	5380	340	5,3	5,26	5,38	(2,06)*	(2,61)*
SiSi	28	0	1050	1230	204	1,12	1,28	1,37	1,12	1,32
GeGe	64	0	992	1120	178	0,75	0,79	0,70	0,65	0,66
SnSn	100	0	—	670	139	0,10	0,12	0,22	0,12	0,16
				Type $A^{IV}B^{IV}$						
CSi	20	0,7	—	3150	300	3,50	3,45	3,41	(2,79)*	(2,57)*
				Type $A^{III}B^{V}$						
GaP	46	0,5	—	1150	170	2,25	2,00	1,80	1,77	1,91
AlSb	64	0,5	—	850	160	1,60	1,25	1,10	1,37	1,39
GaAs	64	0,4	721	920	146	1,40	1,32	1,15	1,21	1,23
InP	64	0,5	—	930	159	1,30	1,38	1,20	1,36	1,38
average						1,43	1,32	1,14	1,31	1,33
GaSb	82	0,4	—	730	134	0,70	0,78	0,74	0,77	0,77
InAs	82	0,4	—	720	130	0,40	0,77	0,73	0,75	0,75
average	—	—	—	—	—	0,55	0,78	0,74	0,76	0,76
InSb	100	0,4	225	580	121	0,20	0,28	0,44	0,33	0,39
				Type $A^{II}B^{VI}$						
ZnS	46	1,0	—	1000	146	3,7	3,85	3,50	3,62	3,85
ZnSe	64	0,8	—	710	114	2,8	2,28	2,03	2,20	2,27
CdS	64	1,0	—	750	127	2,4	2,55	2,28	2,59	2,61
average	—	—	—	—	—	2,6	2,42	2,16	2,40	2,44
ZnTe	82	0,8	—	590	109	2,2	1,44	1,38	1,57	1,59
CdSe	82	0,8	—	550	101	1,8	1,34	1,28	1,46	1,48
average						2,0	1,39	1,33	1,53	1,53
				Type $A^{IV}B^{VI}$						
SnS	66	0,8	—		154	1,26	(=)	(=)	1,30	1,32
PbS	98	0,9	—	890**	135	0,7	0,59	0,62	0,59	0,62

(=) The calculation was not made since here it is necessary to calculate previously the structure constant of the surface energy for the SnS structure.

*The sharply lower results obtained when ΔE was calculated from the Ω data using equations (7) and (8) (when compared with equations (5) and (6) and experimental ΔE) are due to the high hardness of diamond and silicon carbide (small periods of identity a).

** ϵ_{100} of the NaCl type.

LITERATURE CITED

[1] A. F. Ioffe, Physics of Semiconductors [in Russian], p. 178 (1957).

[2] B. F. Ormont, Proc. Acad. Sci. USSR 106 No. 4, 687 (1956).

[3] B. F. Ormont, J. Phys. Chem. (USSR) 31, No. 2, 509 (1957).

[4] V. I. Smirnova and B. F. Ormont, Proc. Acad. Sci. USSR 82, No. 5, 751 (1952).

[5] R. A. Orlani, J. Chem. Phys. 18, 575 (1950).

[6] M. A. Gurevich and B. F. Ormont, J. Inorg. Chem. (USSR) 2, No. 7, 1578 (1957).

[7] B. F. Ormont, J. Tech. Phys. (USSR), 1959 (in press).

[8] A. S. Borshchevskii, N. A. Goryunova and N. K. Takhtarova, J. Tech. Phys. (USSR) 27, 1408 (1957).

[9] E. M. Onitsch-Modl, Chem. Abstr. 48, 4886 (1954).

[10] V. P. Zhuze, J. Tech. Phys. (USSR) 25, 2079 (1955).

[11] P. A. Rebinder, and co-workers, Investigations in the Domain of Applied Physical Chemistry of Surface Phenomena [In Russian] (Moscow, 1936); Bull. Acad. Sci. USSR 1936, 369.

Received June 18, 1958

EFFECT OF ANNEALING ON THE PACKING DENSITY OF POLYSTYRENE

A. A. Tager, M. V. Tsilipotkina and A. I. Suvorova

A. M. Gor'kii, Ural State University

(Presented by Academician V. A. Kargin, August 7, 1958)

The properties of polymeric materials (mechanical properties, gas permeability, etc.) are determined by the packing density of their macromolecules, which depends on the branching and regularity of the chains, their degree of brittleness, the molecular weight of the polymer, and its physical state. It was shown in a number of studies that the linear flexible chains of a polymer, found in a highly elastic state, due to the mobility of the links, show close packing [1]. A loose type of packing is usually observed for some glasslike polymer [1, 2]. A loose or crumbly packing has the character of ultramicropores, i.e., pores of molecular size, and for this reason such polymers in their behavior should resemble the ordinary microporous solid sorbents typified by fine-pored charcoals and silica gels [3]. Such an analogy proved to be valid, and it was shown by us that in the sorption of vapors by liquids, inert toward the given polymer, it is possible to determine quantitatively both the specific surface and the pore volume of the latter [4]. From the shape of the sorption isotherm of methanol on polystyrene, and also from the calculations made by us, it follows that glasslike high-molecular polystyrene is a very fine-pored sorbent.

It is obvious that the loose packing of glasslike polymers has a relaxation nature, determined by the fact that on cooling below the glass transition temperature the relaxation time increases greatly, and the chain during cooling does not succeed in reaching the equilibrium position for the given temperature. The relaxation nature of a loose packing appears in its dependence on the molecular weight of the polymer: low-molecular polystyrenes and poly(methylmethacrylates) are packed tightly, while increasing the molecular weight causes the looseness of the packing to increase [3]. That the loose packing of high-molecular glasses has a relaxation nature also follows from the studies made on the relationship between the value of the polystyrene volume and the temperature [5, 6]. Employing the method of slowly heating and cooling (annealing) polystyrene, Spencer and Boyer [6] determined the equilibrium values of the polystyrene volume at various temperatures and showed that the polystyrene volume is a linear function of the temperature in a broad temperature range (from +20 to +140°), and that the curve $V = f(T)$ does not have an inflection point. The time required to obtain the equilibrium volume becomes greater the lower the temperature. At 60° it is 17 hours.

From a recently published paper by V. A. Kargin and Yu. S. Lipatov [7] it follows that rapidly cooled (tempered) poly(methylmethacrylate) specimens sorb the vapors of methyl isobutyrate (hydrogenated monomer) and water in greater amount than do the annealed specimens, i.e., the latter are more densely packed than the former.

We studied the effect of long annealing on the sorption capacity of polystyrene. The annealing was accomplished by continuously cooling the polystyrene specimens, previously heated to +140°, in a very slow and gradual manner. The experiments were run in an air thermostat, fitted with a relay and a contact thermometer. In the temperature region from +140° to +95° the cooling rate on the average was 0.5°/hr, and at lower temperature at therate of 0.1°/hour. Thus, for example, the specimen was kept for 152 hours at 55-65°, which is several times greater than the time required, according to Boyer and Spencer, to reach equilibrium in the given temperature region. Consequently, the rate of cooling used by us was considerably slower than in all the previous studies. The total time of cooling from +140° to +20° was one month.

TABLE 1

Specific Surface and Pore Volume of Annealed and Unannealed Polystyrene Specimens

Polymer (polystyrene)	Mol. wt.	S_{sp}, sq m/g	W_0, cu cm/g
Unannealed	133000	30.0	0.015
Annealed	110000	14.0	0.007

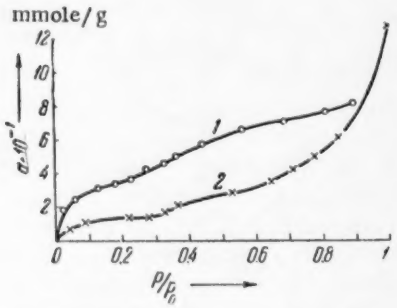

Fig. 1. Sorption isotherms of methanol on polystyrene. 1) Unannealed specimen, 2) annealed specimen.

Keeping the polystyrene for a long time at comparatively high temperatures (above 100°) could cause the specimens to decompose. Actually, the molecular weight of the annealed specimens, determined viscosimetrically, decreased to approximately 1/4 of its original value (from 456,000 to 110,000). Since the packing density of polystyrene strongly depends on the molecular weight [3], then a direct comparison of the annealed specimen with the original would have been incorrect. For this reason we took for testing an annealed polystyrene specimen and an unannealed polystyrene fraction of close molecular weight. Both specimens were tested for the sorption of methyl alcohol vapors, i.e., a compound that is inert to polystyrene. From Fig. 1, it follows that the sorption isotherm of methanol on the unannealed specimen has a shape that, according to the classification of A. V. Kiselev is characteristic for homogeneous fine-pored sorbents [8]. The sorption isotherm for the annealed specimen resembles the sorption isotherms of nonporous sorbents [3]. The values of the specific surface, calculated by the B. E. T. method, are given in Table 1, as are also the values of the pore volumes, determined by the method of M. M. Dubinin and L. V. Radushkevich [9]. From Table 1 it follows that substantial contraction of the molecule occurs under very long annealing, which is characterized by a reduction in both the pore volume and the specific surface to 1/2 the original. Since for the investigation we used the vapors of an inert solvent and since the structure of the specimens during sorption hardly changed, the given result is proof that the loose packing of high-molecular polystyrene has a relaxation nature.

LITERATURE CITED

[1] A. A. Tager and V. A. Kargin, Colloid J. (USSR) 14, 367 (1952).*

[2] A. A. Tager and Zh. S. Dombek, Colloid J. (USSR) 15, 69 (1953);* Kh. U. Usmanov and V. A. Kargin, J. Phys. Chem. (USSR) 28, 224 (1954); T. V. Gatovskaya, V. I. Kargin and A. A. Tager, J. Phys. Chem. (USSR) 29, 883 (1955).

[3] A. A. Tager, Doctoral Dissertation, L. Ya. Karpov Institute of Physical Chemistry, Moscow, 1956;** A.A. Tager, R. V. Krivokorytova and P. M. Khodorov, Proc. Acad. Sci. (USSR) 100, 741 (1955).

[4] A. A. Tager, M. V. Tsilipotkina and A. I. Suvorova, Proc. Acad. Sci. USSR 120, No. 3 (1958).*

[5] T. Alfrey, G. Goldfinger and H. Mark, J. Appl. Phys. 14, 700 (1943).

[6] R. S. Spencer and R. F. Boyer, J. Appl. Phys. 17, 398 (1946).

[7] V. A. Kargin and Yu. S. Lipatov, J. Phys. Chem. (USSR) 32, 326 (1958).

[8] A. V. Kiselev, J. Phys. Chem. (USSR) 23, 452 (1949).

[9] S. Brunauer, P. H. Emmett and E. Teller, J. Am. Chem. Soc. 60, 309 (1938); M. M. Dubinin and L. V. Radushkevich, Proc. Acad. Sci. USSR 55, 331 (1947); L. V. Radushkevich, J. Phys. Chem. (USSR) 23, 1410 (1949).

Received August 6, 1958

*Original Russian pagination. See C.B. Translation.

**In Russian.

DETERMINATION OF THE ADSORPTION COEFFICIENTS OF ETHER WATER AND ETHYLENE BY THE KINETIC METHOD

K. V. Topchieva and B. V. Romanovskii

M. V. Lomonosov State University (Moscow)

(Presented by Academician A. N. Frumkin, August 28, 1958)

The most important characteristic of any heterogeneous catalytic process is the rate constant, which fully defines the operational efficiency of a catalytic setup. In those cases where the catalytic reaction proceeds in the kinetic region, the rate constant and the dependence on it of the temperature of the activation energy are a direct measure of the catalyst activity. From this it is clear that the problem of determining the rate constant assumes great importance.

A direct determination of the true rate constant is impossible in the majority of cases for reactions proceeding in the kinetic region, since the current method of studying heterogeneous catalytic reactions, developed from the research of Langmuir and Schwab, permits finding from the experimental data even at best only the apparent rate constant and energy of activation. The apparent rate constant is always proportional to the true rate constant of a surface catalytic reaction, but it also includes still other parameters of the catalytic process. Adsorption coefficients are usually such parameters, i.e., the constants of the adsorption equilibrium established between the gas phase and the active surface of the catalyst. As a rule, the presence of such an equilibrium is always postulated in the kinetic method, and the apparent rate constant, determined using various kinetic equations, in the general case includes the adsorption coefficients of all of the components of the gas phase, both of the starting materials and of the reaction products.

In principle two different methods exist for determining adsorption coefficients — kinetic and adsorption sorption. However, numerous experimental facts indicate that the adsorption and catalytic portions of a catalyst surface are essentially different in their properties. For this reason, adsorption coefficients found by the purely adsorption method are, generally speaking, unsuitable for calculating the true rate constant, and only the kinetic method gives the proper way of determining adsorption coefficients.

The kinetic method is based on studying the hindering effect of the reaction products (or of foreign substances). Based on the experimentally observed decrease in the rate constant when the reaction is run at different dilutions, kinetic equations permit calculating the adsorption coefficients. To be sure, up to now only the adsorption coefficients of the reaction products were determined using the kinetic method. Only in recent years did a number of American authors [1-3] develop and successfully apply the differential kinetic method, which permits determining also the adsorption coefficients of the starting materials. Consequently, we feel that at the present time we have in principle the possibility of fully calculating the true rate constants of catalytic reactions.

In this paper, we used the kinetic method of A. V. Frost [4] to determine the adsorption coefficients. For a reaction progressing in a flow system according to the scheme

$$A_1 \rightarrow \nu_2 A_2 + \nu_3 A_3 + \ldots + \nu_i A_i$$

he proposed the equation

$$v_0 \ln \frac{1}{1-y} = \alpha + \beta v_0 y, \tag{1}$$

where v_0 is the rate of addition of starting material to the reactor in moles per unit of time per unit weight of catalyst, y is the degree of conversion, and α and β are constants, not depending on either the addition rate or the degree of conversion.

Plotting equation (1) in the coordinates $v_0 \ln \frac{1}{1-y}$ vs $v_0 y$ gives a straight line that intersects the ordinate at a distance equal to α. In developed form α has the form

$$\alpha = \frac{kB_0 S_g b_1}{1 + \delta(1 + b_i/\nu_i) + n + \sum_2^i b_i}, \tag{2}$$

where k is the rate constant of the surface reaction, b_0 is the concentration of active centers on the surface of the catalyst in moles/sq cm, S_g is the specific surface of the catalyst, b_1 is the adsorption coefficient of the starting material, δ is the dilution, i.e., the ratio of the number of moles of reaction product or foreign substance to the number of moles of starting material in the mixture fed into the reactor, b_i is the adsorption coefficient of the reaction product or foreign substance, and n is the increase in the number of moles per mole of starting material as a result of reaction.

The value $1/\alpha$ can be depicted as a linear function of the dilution δ:

$$\frac{1}{\alpha} = \frac{1}{\alpha_0} + D_i \delta, \tag{3}$$

where

$$D_i = \frac{1 + b_i/\nu_i}{kB_0 S_g b_1}. \tag{4}$$

When plotted in the coordinates $1/\alpha$ vs δ the slope of the straight line gives D_i.

If only an inert diluent, practically not adsorbed on the active centers (i.e., its adsorption coefficient can be set equal to zero), is added to the starting material, then equation (4) is transformed to

$$D_0 = \frac{1}{kB_0 S_g b_1}. \tag{5}$$

From Equations (4) and (5) we easily find

$$b_i = \nu_i \frac{D_i - D_0}{D_0}. \tag{6}$$

As a result, to determine the adsorption coefficient of a substance that hinders catalytic reaction it is necessary to run two series of experiments: one in which dilution is made with the substance whose adsorption coefficient is being determined, and the other with dilution by an inert diluent. These two series of experiments give D_i and D_0 respectively.

In this paper we investigated the hindering effect exerted by the addition of ether, water or ethylene on the dehydration rate of ethyl alcohol over aluminum oxide for the purpose of determining the adsorption coefficients of these substances. We used argon as the inert diluent.

A determination of the adsorption coefficients of water and ethylene, besides of purely theoretical interest, is a very actual problem at the present time due to the great importance assumed currently by the reverse reaction, namely the hydration of the ethylene obtained from natural and petroleum gases. Although data are given

in the literature for the adsorption coefficients of water and ethylene [5-8], still we feel that the numerical values given in the indicated papers are much to high and require correction.

We determined the adsorption coefficients of water and ether at 250°, and of water and ethylene at 430°. At 250° ethyl alcohol decomposes only to ether and water [9]; when the temperature is increased the reaction is complicated by the further dehydration of the either to ethylene, while lowering the temperature causes the degree of conversion to drop, which leads to a reduction in the accuracy of the kinetic equation employed. At 430° ethyl alcohol is dehydrated to ethylene and water, and here the amount of ether in the catalyzate is very small (the conversion of alcohol to ether under these conditions is less than 3-5% [10]).

All of the experiments were run at atmospheric pressure, using the conventional laboratory flow setup, with automatic addition of the starting materials. The gases (ethylene, argon) before entering the apparatus were dried with especial care. The water—alcohol mixtures were prepared from rectified alcohol by accurate weighing on an analytical balance; the ether—alcohol mixtures were prepared from absolute alcohol and ether in a similar manner. The liquid catalyzate was analyzed by the method given in [11]. The degree of conversion was determined as the ratio of the number of moles of reacted alcohol to the number of moles of alcohol fed into the reactor.

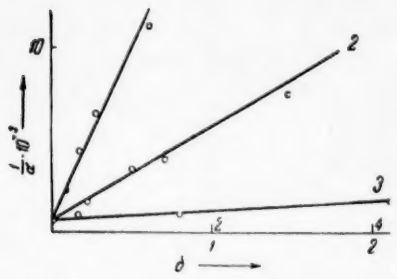

Fig. 1. $1/\alpha$ as a function of δ at 250° (the argon scale along the abscissa was reduced in half). 1) water, 2) ether, 3) argon.

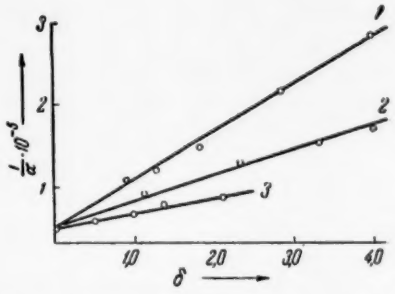

Fig. 2. $1/\alpha$ as a function of δ at 430°. 1) water, 2) ethylene, 3) argon.

We ran two series of experiments: in one series the dilution was made with water, ether or argon at 250°, and in the other with dilution by water, ethylene or argon at 430°. In all cases β has a constant value, approximately equal to one (within the limits of experimental error), which serves as evidence that the rate is retained in the selected dilution range. Using the experimentally found values of α, we plotted $1/\alpha$ as a function of

TABLE 1

Temperature in °C	D_{H_2O}	D_{ether}	$D_{C_2H_4}$	D_{Ar}	b_{H_2O} in atm^{-1}	b_{ether} in atm^{-1}	$b_{C_2H_4}$ in atm^{-1}
250	$12.7 \cdot 10^3$	$3.4 \cdot 10^5$	—	$0.14 \cdot 10^3$	90	22	—
430	$0.54 \cdot 10^5$	—	$0.31 \cdot 10^5$	$0.17 \cdot 10^5$	2.00	—	0.83

the dilution δ (Figs. 1 and 2). From the slopes of the graphs we calculated the values of D_{H_2O}, D_{ether} and D_{Ar} at 250° and of D_{H_2O}, $D_{C_2H_4}$ and D_{Ar} at 430°, and using equation (6) we found the numerical values of the adsorption coefficeints. The values of the adsorption coefficients found by us are given in Table 1.

As can be seen from Table 1, the value of the adsorption coefficient for water at 250° is more than 4 times that of the adsorption coefficient for ether, and at 430° is more than twice that of the adsorption coefficient for ethylene, which is proof that water exerts a much greater hindering effect on the dehydration of ethyl alcohol than does either ether or ethylene. This result differs from the data given in [8], where it was found that the adsorption coefficients of water and ethylene have approximately the same values. We believe that the values given in [8] for the adsorption coefficient of ethylene is too high, due to an insufficiently careful drying of the ethylene.

LITERATURE CITED

[1] P. B. Weisz and C. D. Prater, Adv. Catal. 6, 144 (1954).

[2] C. D. Prater and R. M. Lago, Adv. Catal. 8, 293 (1956).

[3] R. W. Maatman, R. M. Lago and C. D. Prater, Paper delivered at the Congress on Catalysis, 1956.

[4] A. V. Frost, Bull. Moscow State Univ. No. 3, 111 (1946).

[5] A. V. Frost and T. V. Antipina, J. Phys. Chem. (USSR) 24, 860 (1950).

[6] A. V. Frost and T. V. Antipina, Bull. Moscow State Univ. No. 3, 81 (1950).

[7] A. V. Frost and T. V. Antipina, Bull. Moscow State Univ. No. 8, 69 (1951).

[8] A. V. Frost and T. V. Antipina, Bull. Moscow State Univ. No. 10, 79 (1951).

[9] K. V. Topchieva and K. Yung-Ping, Bull. Moscow State Univ. No. 12, 39 (1952).

[10] K. V. Topchieva and K. Yung-Ping, J. Phys. Chem. (USSR) 29, 1678 (1955).

[11] A. N. Pudovik and G. M. Sinaiskii, J. Appl. Chem. (USSR) 21, 862 (1948).

Received August 27, 1958

DETERMINATION OF THE TRUE RATE CONSTANTS IN THE DECOMPOSITION OF ALIPHATIC ALCOHOLS

V. I. Tsvetkova, A. P. Firsov and N. M. Chirkov

Institute of Chemical Physics, Academy of Sciences of the USSR

(Presented by Academician V. N. Kondrat'ev, August 14, 1958)

According to the most widely accepted theory, supported by a series of experimental results, the catalytic action of acids is due to the ability of acids to release protons to the reacting molecules with the formation of reactive ions, the transformation rate of which determines the reaction rate [1, 2]. As a result, in acid catalyzed transformations the principal factors influencing the rate of reaction are the basicity of the reactant molecule, giving the concentration of the protonized forms, and the reactivity of the latter. A study of these factors constitutes one of the main problems of the theory of acid catalysis.

This problem is solved relatively simply for the case of comparatively complex molecules, where the use of spectroscopic methods permits showing immediately the formation of protonized forms of the reagent in acid media. Thus, spectroscopic study of the reaction for the decarboxylation of benzoylformic acid [3] made it possible to determine the concentration of the protonized molecules of the reagent, and in this way find the values of both the basicity constants of the starting materials and the rate constant of the elementary act.

Up to now the formation of ions has not been shown by direct methods for a number of very important reactions, such as hydration, hydrochlorination, polymerization of the lower olefins and the dehydration of alcohols. However, the nature of the dependence of the rate of these processes on the acidity of the medium indicates that these reactions also proceed with involvement of the protonized molecules of the reagent [4] (for example, the alkoxonium ions in the dehydration of alcohols).

All of the above indicated processes were studied in aqueous media, for which reason the concentration of the reacting particles remained unknown, and from the experimental data only the effective rate constants could be found, including, besides the true rate constant of the limiting act, the thermodynamic value -- the basicity constant of the starting reagent [4].

The sharp difference observed in the dehydration rate of a number of alcohols can obviously be due not only to a different decomposition rate of the corresponding alkoxonium ions, but also to a different concentration of these ions. For example, in the presence of phosphoric acid, with the acidity of the medium, temperature and pressure kept constant, the decomposition rate of tertiary butyl alcohol exceeds that of isopropyl alcohol by approximately 500 times [5].

A sharp difference in the dehydration rates of alcohols was also observed when heterogeneous catalysts, such as $Ca_3(PO_4)_2$, Al_2O_3, etc. [6, 7] were used, which apparently also function as acid catalysts.

A fault of the researches devoted to a study of the reactivity of alcohols was the fact that in them the reaction rates were compared at different concentrations of the reacting particles. In order to remove this falt we selected as study subjects solutions of HCl in anhydrous alcohols, in which, naturally, only the alcohol molecules are protonized.

With sufficiently great dilution the HCl molecules show almost complete dissociation [10, 11], and consequently the concentration of alkoxonium ions will be practically equal to the stoichiometric concentration

of the acid. Here, as experiment reveals, the dehydration of alcohols under the studied conditions yields only alkyl halides as the final products.

The reactions that take place in the studied systems can be described by the following scheme:

$$ROH + HCl \rightleftarrows ROH_2^+Cl^- \rightleftarrows ROH_2^+ + Cl^- \quad (1)$$

(in dilute solutions the equilibrium is shifted to the right):

$$ROH_2^+ \xrightarrow{k_1} R^+ + H_2O \text{ (slow)} \quad (2)$$

$$R^+ + Cl^- \rightarrow RCl \text{ (rapid)} \quad (3)$$

$$ROH_2^+ + Cl^- \xrightarrow{k_2} RCl + H_2O. \quad (4)$$

If the formation of the alkyl chloride goes according to reactions (1), (2) and (3), then knowing the concentration of the reacting particles makes it possible to find the value of the true monomolecular rate constant of the limiting act (2).

We will mention that under our experimental conditions, we failed to observe the measurable formation of either olefin or ether.

As study subjects, we took the aliphatic alcohols: ethyl, n-propyl, isopropyl, n-butyl, isobutyl and tert-butyl. The experiments were run at 65-95° and with different initial HCl concentrations (from 0.03 to 1.5 N), using the conventional ampule technique. The alcohols were made thoroughly absolute employing the method of Lund and Bjerrum [9].

TABLE 1

n-Butyl Alcohol

Temp. °C	N_0 = 0,03110 N	N_0 = 0,06220 N	N_0 = 0,09344 N	N_0 = 0,2129 N	N_0 = 0,4486 N	N_0 = 0,6982 N	N_0 = 1,079 N	N_0 = 1,547 N
			$k_1 \cdot 10^4$, min^{-1}					
65,0		1,57	1,62	1,45	2,38	2,36	2,64	2,70
70,0	2,87	2,76	2,89	2,99	3,87	3,83	4,09	4,22
77,1	6,39	6,39	6,50	6,17	7,51	7,87	8,14	8,43
85,0	15,2	15,2	15,6	15,2	17,51	17,92	17,91	18,8
92,8	35,8	35,3	35,4	34,3	39,5	37,3	38,7	38,9
			E, kcal/mole					
	28,5	27,6	27,5	28,0	25,7	24,5	23,5	23,3
			k_0, sec^{-1}					
	$2,8 \cdot 10^{12}$	$2,8 \cdot 10^{12}$	$2,9 \cdot 10^{12}$	$3,35 \cdot 10^{12}$	$1,5 \cdot 10^{11}$	$2,67 \cdot 10^{10}$	$7,2 \cdot 10^{9}$	$5,3 \cdot 10^{9}$

As an example, we give in Table 1 the results obtained using n-butyl alcohol (k_1 is the monomolecular constant, E is the activation energy, k_0 is the pre-exponent, and N_0 is the initial HCl concentration). As can be seen from the table, the reaction is excellently monomolecular with respect to HCl in dilute solutions (from 0.03 to 0.2 N). The deviations from a first-order reaction observed at lower temperatures and higher HCl concentrations are probably due to the parallel progress of the bimolecular reaction (4). The statements in the literature that this reaction is bimolecular in nature is explained by the fact that in the indicated studies the experiments were run either at lower temperatures [8] or at higher HCl concentrations [12, 13].

Analogous results were also obtained for the other alcohols studied by us.

As a result, under our experimental conditions it is the monomolecular mechanism that predominates (reactions (1), (2) and (3)). Obviously, the values of the monomolecular constants characterize the decomposition rate of the alkoxonium ions, which appears as the limiting act also in the dehydration of alcohols using aqueous acid solutions.

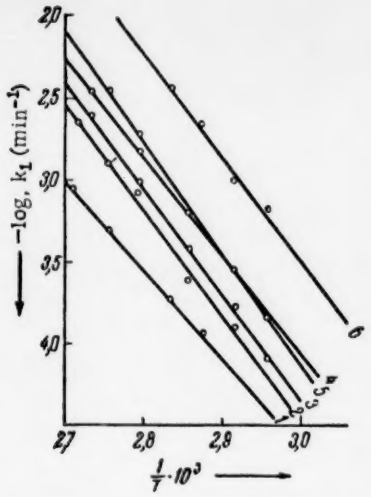

Fig. 1. 1) i-C_4H_9OH; 2) i-C_3H_7OH; 3) n-C_3H_7OH; 4) n-C_4H_9OH; 5) C_2H_5OH; 6) tert-C_4H_9OH.

TABLE 2

Alcohol	E, $\frac{cal}{mole}$	k_0, sec^{-1}
C_2H_5OH	31000	$2.54 \cdot 10^{14}$
n-C_3H_7OH	29700	$2.12 \cdot 10^{13}$
n-C_4H_9OH	28500	$6.35 \cdot 10^{12}$
i-C_3H_7OH	29600	$2.50 \cdot 10^{13}$
i-C_4H_9OH	24500	$4.94 \cdot 10^{9}$
tert-C_4H_9OH	28200	$1.96 \cdot 10^{13}$

The dependence of the found constants on the temperature, at an initial HCl concentration of approximately 0.03 N for various alcohols is plotted in Fig. 1.

The values of the energies of activation and of the pre-exponents, calculated from the obtained data, are given in Table 2 (at a HCl concentration approximately equal to 0.03 N). From Table 2 it follows that the energies of activation are essentially the same for most of the studied alcohols, while the pre-exponential factors are close to normal.• Isobutyl alcohol is an exception, for which both the energy of activation and the pre-exponent are substantially lower. It is possible that in this case the reaction goes by a different, more complex mechanism, and the found values of the constants do not correspond to the true ones.

The close values of the monomolecular constants for most of the studied alcohols indicate that the greater difference observed for the dehydration rates of alcohols in aqueous acid solutions is mainly due to a difference in the degree of protonization shown by the alcohols, i.e., to a difference in the concentration of the reacting ions, and only in comparatively slight degree to a difference in the transformation rate of these ions.

LITERATURE CITED

[1] L. P. Hammett, Physical Organic Chemistry, London, 1940.

[2] A. I. Shatenshtein, Theory of Acids and Bases [in Russian], 1949.

[3] M. I. Vinnik and R. S. Ryabova, Proc. Acad. Sci. USSR 117, No. 6 (1957).••

[4] N. M. Chirkov, M. I. Vinnik, S. G. Éntelis and V. I. Tsvetkova, Trans. All-Union Conference on Kinetics and Catalysis, 1955.

[5] V. I. Tsvetkova, Candidate's Dissertation, Inst. Chem. Phys., Acad. Sci. USSR, 1956. [In Russian].

[6] L. Kh. Freidlin and A. M. Levit, Bull. Acad. Sci. USSR, Div. Chem. Sci., 1952, 163.••

[7] A. Kh. Bork and A. A. Tolstopyakova, J. Phys. Chem. (USSR) 12, 224 (1938).

[8] E. Grunwalds and S. Winstein, J. Am. Chem. Soc. 69, 2051 (1947).

[9] H. Lund, and J. Bjerrum, Ber. 64, 210 (1931).

[10] I. Bezman and F. Verhoek, J. Am. Chem. Soc. 67, 1330 (1945).

[11] E. Braude, J. Chem. Soc. 1948, 1971.

•In the case of ethyl alcohol the monomolecular constants could not be determined accurately due to the substantial increase in the proportion of bimolecular reaction when the temperature was lowered.

••Original Russian pagination. See C.B. Translation.

[12] G. Bennett and F. Reynolds, J. Chem. Soc. 1935, 131.

[13] S. Kilpi, Zs. Phys. Chem. 141 A, 424 (1929); 166 A, 285 (1933).

Received August 9, 1958

FORMATION OF VIBRATIONS IN THE PASSAGE OF A CURRENT IN ELECTROLYTIC SYSTEMS WITH A FALLING POLARIZATION CHARACTERISTIC

Yu. A. Chizmadzhev

Institute of Electrochemistry, Academy of Sciences of USSR

(Presented by Academician A. N. Frumkin, July 30, 1958)

Processes are known in electrochemistry that lead to the formation of polarization characteristics with descending portions, for example, the N-type of characteristic (Fig. 1, a). Equipotential systems with such a characteristic were discussed by Franck [1], who showed that the stationary states on a descending branch could be unstable. This result follows directly from the theory for the vibrations of systems with one degree of freedom [2]. However, the characteristic traits of the phenomena arising in such systems were linked with a definite mechanism for the formation of the descending portions of the polarization curve, and specifically with the mechanism of passive film growth.

A. N. Frumkin expressed the theory that the phenomenon of instability in equipotential and distributed systems with falling polarization characteristics bears a general character and permits a purely phenomenological treatment. A discussion of extended systems, where the different points of the electrode surface correspond to different portions of the polarization characteristic, is of special interest. This last circumstance, as will be shown below, leads to a number of important features that are not present in the equipotential case. Systems with distributed parameters have been discussed in the literature [4], but here the nonlinear element was considered as being centralized. The present paper is devoted to a discussion of the phenomena occurring in distributed electrochemical systems, possessing a polarization curve with descending portions.

As the model of a distributed system, we will consider a tube having a length of $2\,l$, filled with an electrolyte and showing symmetrical polarization at both ends (Fig. 2):

$$\varphi = \varphi_1 \text{ at } x = 0 \text{ and } x = 2l; \qquad \frac{d\varphi}{dx} = 0 \text{ at } x = l.$$

The equation for the stationary distribution of the potential in the cylindrical coordinate system has the form

$$\frac{\partial^2\varphi}{\partial x^2} + \frac{\partial^2\varphi}{\partial r^2} + \frac{1}{r}\frac{\partial\varphi}{\partial r} = 0. \tag{1}$$

The anodic process takes place on the tube surface at $r = r_0$, i.e., the limiting condition holds

$$-\varkappa\left(\frac{\partial\varphi}{\partial r}\right)_{r=r_0} = j(\varphi),$$

where $j(\varphi)$ is the polarization characteristic of the electrode reaction. Following V. G. Levich [5], we will employ the concept of the chemical resistance $R_{chem} = d\varphi/dj$. We will examine the case where the potential drop due to chemical resistance is considerably greater than the potential drop due to the transverse ohmic

resistance $R_{ohm}^{transverse} = r_0/\kappa$. It is easy to show that when the inequality $R_{ohm}^{transverse}/R_{chem} \ll 1$ is fulfilled equation (1) changes to the equation

$$\kappa r_0 \frac{d^2\varphi}{dx^2} - j(\varphi) = 0,$$

first derived by A. N. Frumkin [3] directly for the one-dimensional case.

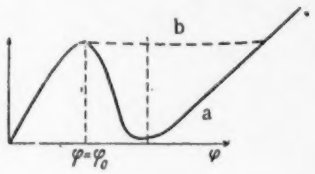

Fig. 1.

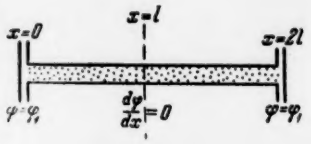

Fig. 2.

The equation can be used to investigate different forms of the $j(\varphi)$ function.

1) The linear ascending characteristic $j = K\varphi$, when discussing an infinite tube polarized at one end (A. N. Frumkin), leads to the following distribution of the potential and the current:

$$\varphi = \varphi_1 e^{-\alpha' x}, \quad I = \alpha' \varphi_1 e^{-\alpha' x}, \quad \alpha' = \sqrt{\frac{K}{\kappa r_0}}.$$

2) The linear descending characteristic $j = K(\varphi_0 - \varphi)$ for a finite tube, under the conditions $\varphi_{x=0} = \varphi_1$, $\left.\frac{d\varphi}{dx}\right|_{x=l} = 0$, leads to the following distribution of the potential:

$$\varphi = \varphi_0 - (\varphi_0 - \varphi_1)[\operatorname{tg}\alpha' l \cdot \sin\alpha' x + \cos\alpha' x],$$

having, generally speaking, an oscillating character. Setting $d\varphi/dx = 0$, we have $\tan \alpha^* l = \tan \alpha x$, from which it is directly obvious that the solution of $\varphi(x)$ is monotonic, if $\sqrt{K/\kappa r_0} < \pi/2$. Actually, $d\varphi/dx = -(\varphi_0 - \varphi_1)\alpha^* \tan \alpha^* l < 0$, if $\alpha^* l < \pi/2$.

3) The region of weak anodic polarization (up to the point of inflection on the descending branch of the curve, Fig. 1, a) can be approximated using the function $j(\varphi) = -K(\varphi - \varphi_0)^2 + K\varphi_0^2$.

Replacing the variable $\varphi - \varphi_0 = u$ and introducing the terms $K\kappa r_0 = \alpha$, $K\varphi_0^2 \kappa r_0 = \beta$, $u_{x=l} = u_l$, we come to the equation $d^2u/dx^2 = -\alpha u^2 + \beta$ and the limiting conditions $u = u^*$, $du/dx = 0$, $x = l$. Here u^* designates the given potential at the point $x = 0$. The solution has the form

$$u = u_1 - (u_1 - u_l)\frac{1 - \operatorname{sn}^2 Z}{1 - k^2 \operatorname{sn}^2 Z}, \qquad Z = \left[\frac{\alpha}{6}(u_1 - u_3)\right]^{1/2}(l - x),$$

where sn Z is the elliptic sine, k is its modulus, and u_1 and u_3 are the roots of some equation, having the form

$$u_1 = -\frac{u_l}{2} + \sqrt{3\varphi_0^2 - {}^3/_4 u_l^2}, \quad u_3 = -\frac{u_l}{2} - \sqrt{3\varphi_0^2 - {}^3/_4 u_l^2}.$$

The solution has an arbitrary constant which can be determined from the limiting condition $u_{x=0} = u^*$:

$$u^* = u_1 - (u_1 - u_l)\frac{1 - \operatorname{sn}^2 Z^*}{1 - k^2 \operatorname{sn}^2 Z^*} = \Psi(u_l).$$

At $u_l \to -\varphi_0$, $\Psi \to -\varphi_0$; at $u_l \to \varphi_0$, $\Psi \to \varphi_0$.

In the interval $< -\varphi_0 ; +\varphi_0 >$ function $\Psi(u_l)$ is continuous and assumes the value $\pm\varphi_0$ at the limits. Consequently, there exists only one point $u = u_l^*$, where $\Psi(u_l^*) = u^*$.

When the argument of the elliptic sine is small, it becomes possible to simplify the series and finish the solution:

$$\Psi(u_l) = u_l + \frac{\alpha l^2}{4}(\varphi_0^2 - u_l^2), \quad \Psi'' = 1 - \frac{\alpha l^2}{2} u_l, \quad \Psi''' = -\frac{\alpha l^2}{2}.$$

It is easy to see (Fig. 3) that in the last case the stationary state is unique, and $u_l^* < u^*$, i.e., the potential along the tube decreases. Assigning a limiting potential to the descending branch ($u^* > 0$), we, generally speaking, obtain u_l^* on the same branch. However, with a very small positive limiting potential u^*, the region of potentials, being realized along the tube, embraces a portion of the ascending branch, i.e. u_l^* becomes negative.

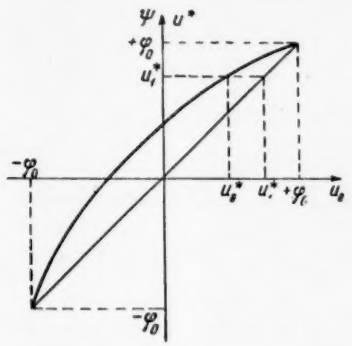

Fig. 3.

The region of strong anodic polarization (to the right of the inflection point in Fig. 1, a) permits a similar treatment. The stationary states are described by the equation

$$\frac{2[3(u_l^2 + \beta/\alpha)]^{1/2}\sqrt{(u-u_l)}}{u - u_l + \sqrt{3(u_l^2 + \beta/\alpha)}} = \operatorname{sn}\left[\left(\frac{2K}{3\varkappa r_0}\right)^{1/2}\left(3u_i^2 + \frac{3\beta}{\alpha}\right)^{1/4}(l-x)\right],$$

where $\beta = \beta^*/\varkappa r_0$, and β^* corresponds to the current in the region of the minimum on the polarization curve. For positive values of u_l^* independent of the absolute value of the latter, the region of the values of the potential is bounded by the ascending branch of the curve $j(\varphi)$.

Any stationary distribution requires an additional investigation for stability, which, however, is usually not taken into consideration when solving electrochemical problems. Strictly speaking, only the stable solutions are stationary ones. We will write the expression for the dissipated energy, which represents a particular case of the general vibration principle (the idea of the method and a number of applications are contained in [5]):

$$W = \varkappa r_0 \int \left(\frac{\partial\varphi}{\partial x}\right)^2 dx + 2\int\int j(\varphi)\, d\varphi\, dx.$$

The first integral corresponds to the ohmic losses, while the second corresponds to the energy that is dissipated in chemical resistance. It is known [6] that a stationary distribution of the current in a medium with a constant $\varkappa$ corresponds to the minimum dissipation of energy. The presence of a negative chemical resistance may prove to put the dissipated energy at a maximum. Calculation of the second variation $\delta^2 W$ reveals that the necessary condition for a minimum has the form $\varkappa > 0$ and is executed identically.

In our case the Jacobi equation has the form

$$\varkappa r_0 \frac{d^2\eta}{dx^2} - \frac{dj}{d\varphi}\eta = 0, \quad \eta_l(x)\Big|_{x=0} = 0, \quad \eta_l'(x)\Big|_{x=0} = 1.$$

If the solution $\eta(x)$ has roots inside the interval $[0, 2l]$, then the extremal cannot give the minumum of integral W [7]. In the Jacobi equation $dj/d\varphi$ is known from the previous discussion of the function of the x coordinate. Let $dj/d\varphi = K$. Then solution has the form $\eta \sim e^{-\alpha^* x}$, the roots are absent, and the dissipated energy is minimum. If $dj/d\varphi = -K$, then $\eta = \sqrt{\varkappa r_0/K} \times \sin\sqrt{K/\varkappa r_0}\,x$, and for the case $\sqrt{K/\varkappa r_0}\, l < \pi/2$ there are no roots, which corresponds to minimum W. If $\sqrt{K/\varkappa r_0}\, l > \pi/2$, then the dissipated energy in the given stationary state cannot be minimum. It seems natural to conclude that such stationary states are unstable, all the more so since exact calculation for the case of linear characteristic of both signs using the provisional equation

$C\frac{\partial\varphi}{\partial t} = \kappa r_0 \frac{\partial^2\varphi}{\partial x^2} - j(\varphi)$ leads to the following asymptotic expression: $\varphi \sim \exp\left\{\left[\frac{K}{C} - \left(\frac{\pi}{2l}\right)^2 a^2\right] t\right\}$, from which derives the same criterion of stability $\sqrt{K/\kappa r_0}\, l < \pi/2$.

A characteristic feature of systems with a falling characteristic consists in the fact that $R_{chem} < 0$ leads to a distribution of the current that is "unprofitable" for the ohmic resistance — a greater current travels a long way. However, since the total dissipated energy consists of two parts, the sum may be minimum. With increase in R_{ohm} or simply in the length of the tube the ohmic losses increase and, beginning with a certain critical value of the parameter $\left(\frac{K}{\kappa r_0}\right)^{\frac{1}{2}} l = \left(\frac{R_{ohm}}{R_{chem}}\right)^{1/2} \left(\frac{l}{r_0}\right)^{1/2}$, the system loses its stability; the chemical resistance can no longer impose an "unprofitable" distribution of the current on the system. The presence of an unstable stationary state is not sufficient proof of the creation of autovibrations. The possibility of unlimited increase in the potential should be excluded. Characteristics of the N-type satisfy this condition, since the ascending branches limit an increase in the potential, while the descending portion leads to the creation of instability. A unique difference from systems with one degree of freedom consists in the following. For atuovibrations to arise in the equipotential degenerate system $\partial\varphi/\partial t = F(\varphi)$ it is necessary that $F(\varphi)$ be unsynonymous. In distributed systems this limitation is removed due to the presence of the first term in the equation $C\frac{\partial\varphi}{\partial t} = \kappa r_0 \frac{\partial^2\varphi}{\partial x^2} - j(\varphi)$. Thus, there is basis to assume that the stationary state in the system is either a periodic or a quasiperiodic process.

The opinion has been frequently expressed that the presence of a descending branch of the characteristic in the system makes possible the establishment of a state that corresponds to a rectification of the polarization curve (Fig. 1, b). However, as has been indicated by A. N. Frumkin, such a state cannot be realized due to the fact that the potential suffers discontinuity here.

In conclusion I wish to express my deep gratitude to Academician A. N. Frumkin for arranging this problem and for valuable counsel, and to Acad. Sci. USSR Corresponding Member V. G. Levich for directing the work.

LITERATURE CITED

[1] U. F. Franck, Z. physik. Chem. [N.F.] 3, 183 (1955).

[2] A. A. Andronov and S. É. Khaikin, Theory of Vibrations [in Russian], 1937.

[3] A. N. Frumkin, J. Phys. Chem. (USSR) 23, 1477 (1949).

[4] A. A. Vitt, J. Tech. Phys. (USSR) 4, No. 1 (1934).

[5] V. G. Levich, Physicochemical Hydrodynamics [in Russian] (Izd. AN SSSR, 1954).

[6] L. D. Landau and E. M. Lifshits, Electrodynamics of Continuous Media [in Russian], 1957.

[7] V. I. Smirnov, Course in Higher Mathematics [in Russian], Vol. 4 (1956).

Received July 25, 1958

THE SALT EFFECT AT THE EXCHANGE OF DEUTERIUM IN LIQUID AMMONIA

A. I. Shatenshtein, Yu. P. Vyrskii and E. A. Rabinovich

L. Ya. Karpov Physicochemical Scientific Research Institute

(Presented by Academician V. N. Kondrat'ev on July 31, 1958)

There is little published information on salt effects in deuterium exchange. A convenient medium for use in the study of these effects is liquid ammonia, for it has a low dielectric constant and is a good solvent for many salts, as well as for organic substances.

Information on the influence of salts on the reaction kinetics of lactones, esters and halides were previously established [1]. Other authors confirmed the conclusions [2, 3]. Neutral salts accelerate these reactions the greater their charge and the smaller the radius of their ions, ($Ca^{++} > Sr^{++} > Ba^{++}$; $Li^{+} > Na^{+}$; $Cl^{-} > Br^{-} > NO_3^{-} > I^{-} > ClO_4^{-}$). The energy E and the entropy of activation $\Delta S^{\neq}$ also increase.

TABLE 1

Material	$k_0 \cdot 10^4$	$Ca(NO_3)_2$, N	$k \cdot 10^4$	k/k_0
Indene	4.9 ± 0.2 (8)	1.3	6.4 ± 0.6 (7)	1.3
Acetophenone	0.71 ± 0.01 (4)	3.1	2.9 ± 0.3 (9)	4.1

We assumed that the laws governing the salt effect at the deuterium exchange and the solvation reactions in liquid ammonia are similar. The preliminary experiments were performed with indene and acetophenone [4]. The velocity constants (sec^{-1}) were calculated from a first-order equation: k_0 without salt, k with $Ca(NO_3)_2$ addition (see Table 1; experiment number in parentheses; temperature kept at 25° ± 0.05°).

Systematic experiments (see Table 2; number of measurements in parentheses) were performed with methyl-β-naphthyl ketone (melting point before and after the experiments 52.5-53.3°). This substance (0.2 g) was dissolved in ammonia (~ 2.5 g) in the presence of the carefully dried salt (various preparations of the salt were often taken) at a concentration of about 2.5 N. Without salt the duration of the experiments was 0.5-2 hours, while with salt it was one-half hour. The reaction was quenched by pouring the mixture into 0° water. The ketone was extracted with ether and after separation was distilled in vacuum. The D concentration in the water, determined by combustion of the material after the experiment, was found to be C_W = 0.5 - 2 atomic % D, while the D concentration in the original ammonia was C_0 = 10-11 atomic % D.

For the determination of the activation energy and entropy (Table 3), the experiments were carried out with methyl-β-naphthyl ketone, the methyl group of which was partially deuterated (4.76 atomic % D) and with normal NH_3. For 0.2 gram ketone 12.9-13.0 grams NH_3 were obtained. For 1 gram-equivalent of the salt 8.0-8.3 moles of NH_3 were required.

We also studied (see Table 2) the displacement of the equilibrium of the formation of colored complexes of 3,5-dinitrobenzoic acid (I) and of phenolphthalein (II) with ammonia, when salts were added [5]. The spectrophotometric measurements [6] were performed by E. A. Rabinovich. In case (I), using $5 \cdot 10^{-4}$ M/liter, we determined $\lg \epsilon_{555}$ at 25 ± 0.2° in 0.1 N salt solutions. In case (II), at $4 \cdot 10^{-5}$ M/liter the measurements were performed at λ = 572 mμ with 0.01 N salt solutions; we lowered the pH of solution (II) in NH_3 by adding $6 \cdot 10^{-4}$ M/liter NH_4NO_3.

TABLE 2

Salt	Deuterium exchange at 25° ± 0.05, $k \cdot 10^4$, sec^{-1}	Equilibium of the complex formation	
		$\lg \varepsilon_{555}$	$\lg \varepsilon_{372}$
Without salt	0,91±0,02 (9)	—	—
$Ca(NO_3)_2$	3,8 ±0,1 (4)	—	—
$Sr(NO_3)_2$	3,2 ±0,2 (6)	—	4,49±0,03 (3)
$Ba(NO_3)_2$	3,1 ±0,1 (4)	—	4,54±0,02 (3)
$LiNO_3$	3,2 ±0,1 (6)	3,17±0,05 (7)	3,57±0,02 (4)
$NaNO_3$	2,1 ±0,1 (3)	2,91±0,03 (7)	3,52±0,05 (9)
KNO_3	—	2,70±0,03 (7)	3,26±0,06 (5)
$RbNO_3$*	—	2,65±0,02 (5)	3,35±0,03 (3)
NaCl	—	3,23±0,02 (5)	3,81±0,02 (3)
NaBr	3,6 ±0,1 (2)	3,09±0,05 (7)	3,60±0,02 (3)
$NaNO_3$	2,1 ±0,1 (3)	2,98±0,03 (7)	3,52±0,05 (9)
NaI	2,2 ±0,1 (3)	2,98±0,03 (7)	3,47±0,04 (3)
NaCNS	1,6 ±0,05 (2)	—	—
$NaClO_4$	1,1 ±0,05 (2)	2,86±0,02 (5)	3,39±0,03 (3)

*In 0.03 N solutions of $RbNO_3$ and $CsNO_3$ the following values were obtained for $\lg\epsilon_{555}$: 2.40 ± 0.12 (5) and 2.24 ± 0.08 (9). For $AgNO_3$ $\lg\epsilon_{555}$ = 2.76 ± 0.03 (5).

We also give here the results of kinetic experiments, carried out in the presence of 2.5 N ammonium salts (number of measurements in parentheses).

Salt	NH_4Cl	NH_4Br	NH_4CNS	NH_4I	NH_4NO_3	NH_4ClO_4
$k \cdot 10^4$	2,6±0,0 (2);	2,1±0,05 (2);	2,2±0,2 (5);	2,1±0,05 (3);	1,8±0,05 (2);	1,5±0,1 (3)

TABLE 3

Temperature °C	Duration of experiments, hr	C_W	$k \cdot 10^4$, sec^{-1}	Temperature °C	Duration of experiments, hr	C_W	$k \cdot 10^4$, sec^{-1}
Without salt				3,9 *N* $Ca(NO_3)_2$			
15	8	1,37	0,43	15	2	1,20	1,90
		1,43	0,42			1,19	1,90
		1,27	0,45	25	1	0,95	4,50
		1,52	0,40			0,91	4,60
		1,43	0,42	35	0,5	0,79	10,0
		1,44	0,42			0,77	10,0
25	4	1,53	0,79			0,81	10,0
		1,52	0,80	3,9 *N* $NaClO_4$			
		1,54	0,79				
		1,54	0,79				
		1,56	0,78	15	8	2,13	0,28
		1,50	0,80			2,11	0,28
		1,45	0,83			2,08	0,29
35	2	1,61	1,5	25	4	1,78	0,69
		1,55	1,6			1,81	0,68
		1,62	1,5			1,84	0,66
		1,67	1,5			1,75	0,70
						1,85	0,66
						1,82	0,67
				35	2	1,65	1,5
						1,63	1,5
						1,67	1,5

Kinetic measurements of the deuterium exchange confirmed the assumption expressed by stating the problem of this work. Deuterium exchange reactions are accelerated by salts and this behavior remains the same throughout the series of cations and anions which were previously determined by ammonolysis. This is illustrated by data presenting the value of $\frac{k \text{ in salt solution}}{k \text{ without salt}} \cdot 100$ for the deuterium exchange of methyl-β-naphthyl ketone (I), the ammonolysis of pilocarpine (II) [2c] and the ammonolysis of ethyl chloride (III) [1e] (Table 4).

The same regularity was observed in the case of santonin [1a], desmotroposantonin [1b], tartaric [1b] and benzoic [2a] esters, 2-chloro-benzothiazole [3b] and of 9-chloro-9-phenyl fluorene [3d].

Similar series of cations and anions were obtained by determining the shift of the complex formation equilibrium:

3,5-dinitro-benzoic acid: $Li^+ > Na^+ > K^+ \geq Rb^+ (\geq Cs^+)$; $Cl^- > Br^- > I^- \simeq NO_3^- \geq ClO_4^-$
Phenolphthalein: $Ba^{++} > Sr^{++} > Li^+ \geq Na^+ > K^+ \leq Rb^+$; $Cl^- > Br^- \geq NO_3^- \geq I^- > ClO_4^-$

The above-mentioned sequence of anions is contrary to the series determined by measurements of the electrical conductivity [7] and of the osmotic coefficients [8] of the very same salts in NH_3, showing that the salt effect is a function of the ionic field strength.

TABLE 4

Reaction	Salt conc. in N	Nitrate salts						Salt conc. in N	Sodium salts				
		Ca^{++}	Sr^{++}	Ba^{++}	Li^+	Na^+	NH_4^+		Br^-	I^-	NO_3^-	CNS^-	ClO_4^-
I*	2,5	420	350	350	350	230	190	2,5	400	240	230	170	115
II	1	1350	446	340	166	133	—	1	258	175	208	—	125
III	2	300	304	306	376	316	250	1	375	—	206	--	203

*Sodium bromide, iodide and nitrate accelerate the deuterium exchange more strongly than the ammonium salts, while ammonium thiocyanate, and perchlorate are more active than the sodium salts.

Let us investigate how the parameters of the Arrhenius equation change when salt is added. In the 3.9 N solutions of $Ca(NO_3)_2$ and $NaClO_4$ the activation energy E increases by 3.3 kcal/mole (14.5-11.2 kcal) and the first exponent increases by a factor of 1500 and 250 (without salt lg A = 4.1; with $Ca(NO_3)_2$ lg A = 7.3 and with $NaClO_4$ lg A = 6.5). The entropy of activation ($\Delta S^* = 4.576 \lg A/T - 49.203$) increases correspondingly by 15 and 11 entropy units. In the presence of salt the ammonolysis of pilocarpine [1c] is accompanied by an even more impressive change of the kinetic parameters. So, by raising the NH_4Cl concentration from 0.1 to 5.0 N, the value of E increases to 6 kcal and A - w increases $4 \cdot 10^6$ times. The salts increase the values of E and A also in the case of the ammonolysis of diethyl malonate, ethyl benzoate [3b] and of 9-phenyl-9-chlorofluorene [3d]. The activation energy and entropy of the ammonolysis of pilocarpine increase with increasing radius of the anion of the 2N salt. In Table 5 the kinetic parameters are compared or related to the same parameters obtained in the absence of the salts.

TABLE 5

Parameter	NaBr	$NaNO_3$	$NaClO_4$
ΔE, kcal	1.2	3.0	3.9
A/A_0	30	400	1000
$\Delta(\Delta S^*)$ entr.units	6.6	12.0	14.0

The theory of the kinetic and thermodynamic salt effect makes use of the theory of strong electrolytes, but like in the case of ammonia solutions of uni-univalent salts, this theory applies only at concentrations 10^6 times lower than those we had to deal with in the present work (see [9]). It is obvious that the current quantitative theory of the salt effect is not suitable for discussing the above described results.

Osmotic measurements [8] indicate that the ions are associated in concentrated ammonia solutions. The osmotic coefficients plotted as a function of concentration pass through a minimum which shifts toward the lower concentration region as the radius of the anion increases. The existence of the minimum may be understood by calculating the solvation of the salts. The constitution of the concentrated solutions does not differ much from that of higher crystal ammonates. (E.g., 8 moles of NH_3 are required for one gram-equivalent of the salt in an approximately 4 N solution.) The heat of formation and the stability of the crystal ammonates increase with increasing charge and decreasing size of the cation with the same anion and with increasing volume of the anion, if the cation is kept unchanged [10]. Coincidentally the number of ammonia molecules entering into the constitution of the highest ammonates increases also. By this means the location of the minimum of osmotic coefficients, plotted as a function of concentration, is adjusted.

In order to insure that reactions occuring in concentrated salt solutions will take place with the solvent participating, a molecule under the influence of the ionic field requires a larger activation energy than it would in the absence of the salt. The lower level of solvation of the activated complex in the salt solution is related to the increase of the reaction's entropy of activation which helps to accelerate it. The increase of the entropy of activation of the deuterium exchange in an approximately 4 N solution of $Ca(NO_3)_2$, compared to the hydrogen exchange in the absence of the salt, amounts to 14.7 entropy units, while the entropy of the melting process of NH_3 is equal to 7 entropy units. The entropy effect of the "thawing out" of the solvent's molecules prevails over the increase of the activation barrier. This is inferred from a nearly sixfold acceleration of the reaction.

It is known [11, 12] that for many reactions there is a linear correlation between the enthalpy change $\Delta H^{\neq}$ and the entropy of activation $\Delta S^{\neq}$. For the salt effect of the deuterium exchange of methyl- β-naphthyl ketone this is expressed by the equation $\Delta H^{\neq} = 20000 + 225\ \Delta S^{\neq}$ and for the salt effect at the ammonolysis of pilocarpine by the following equation $\Delta H^{\neq} = 19000 + 225\ \Delta S^{\neq}$.

The stated considerations agree well with previously described regularities of the salt effect of deuterium exchange and the ammonolysis in liquid ammonia and explain their correlation. The nature of the phenomenon under consideration is doubtless for more complicated and many sided. Further research is required to help in clarifying it.

We thank Ya. K. Syrkin, Corresponding Member, Academy of Sciences USSR, and Prof. M. B. Neiman for valuable observations.

LITERATURE CITED

[1] A. I. Shatenshtein, G. S. Markova, E. A. Izrailevich, a) J. Phys. Chem. 7, 26, (1936); b) 8, 696 (1936); c) 13, 1175 (1939); d) 17, 24 (1943); e) Proc. Acad. Sci., 35, 73 (1942).

[2] L. F. Audrieth, et al., a) J. Am. Chem. Soc. 60, 579 (1938); b) 61, 2387 (1939); c) 64, 2498 (1942).

[3] R. C. Anderson, G. W. Watt et al., a) J. Am. Chem. Soc. 63, 1953 (1941); b) 64, 467 (1942); c) 65, 49 (1943); d) 66, 376 (1944).

[4] A. I. Shatenshtein, and Yu. P. Vyrskii, Proc. Acad. Sci. 70, 1029 (1950); J. Phys. Chem. 25, 1206 (1951).

[5] A. I. Shatenshtein, E. A. Izrailevich and N. M. Dykhno, J. Phys. Chem. 13, 1791 (1939); 16, 73 (1942); Acta Physicochim. URSS, 17, 230 (1942).

[6] A. I. Shatenshtein, E. A. Izrailevich, J. Phys. Chem. 26, 377 (1952).

[7] V. A. Pleskov, A. M. Monoszon, E. N. Gur'yanova, J. Phys. Chem. 3, 221 (1932); 8, 345 (1936).

[8] A. I. Shatenshtein and L. Z. Uskova, J. Phys. Chem. 6, 985 (1935).

[9] V. A. Pleskov, J. Phys. Chem. 10, 601 (1937).

[10] Van Arkel, The Chemical Bond, 1934, p. 147.

[11] Ya. K. Syrkin and M. A. Gubareva, Proc. Acad. Sci. 23, 685 (1939).

[12] J. E. Leffler, J. Org. Chem. 20, 1202 (1955).

Received July 25, 1958

MEASUREMENT OF THE RATE OF COMBUSTION OF A POWDER UNDER DETONATION WAVE CONDITIONS

A. Ya. Apin and L. G. Bolkhovitinov

Institute of Chemical Physics of the Academy of Sciences of the USSR

(Presented by Academician V. N. Kondrat'ev August, 16 1958)

It is certain that the rate of combustion of individual grains in a detonation wave is less than the rate of detonation. But direct measurement of the rate of combustion of a powder, under pressures of the order of 20,000 kg/cm^2 is extremely difficult. The only data in the literature is that of Basset [1], who measured the rate of combustion at 10,000 kg/cm^2. Basset established that the combustion rate was directly proportional to pressure, and, for powders similar in composition to NB powder, he obtained an absolute value of the combustion rate of 0.95 m/second at 10,000 kg/cm^2. If the data of Basset is extrapolated to pressures of 50,000 and 100,000 kg/cm^2, then the time derived for the combustion of powder grains under detonation wave condition is greater than the time calculated from the data on critical diameter and on the change in detonation rate of the powder as a function of the diameter of the charge. The combustion of a grain of powder or explosive must occur more rapidly in a detonation wave than under static conditions, since, in the first case, it is heated by adiabatic compression during combustion.

We do not know how much a grain is heated, nor the temperature coefficient of the combustion rate at ultrahigh pressures, so that a direct measurement of the combustion rate was of interest. By means of the ionization zone method, we were able to measure very short time intervals, and hence to obtain a direct measurement of the rate of combustion of a powder grain in a detonation wave. (The oscillograph OK-17 m used had a maximum scanning speed of 30 cm/μ second, and its screen produced photographic impulses making it possible to measure short time intervals with a precision of 0.01-0.02μ seconds.)

In order to measure its rate of combustion, the tablet of NB powder was mounted on a strip of wood, 20 mm wide, as shown in Fig. 1. The tablet (4 x 4 x 0.3 mm) was placed over the detector, K_3. So as to prevent the eruption of gases, the tablet was covered with a thick layer of coating material, leaving only a small portion uncovered in the center of the upper surface. The top was all covered with copper foil except for a small opening over the free surface of the powder tablet.

A cardboard box, 20 x 20 mm, was glued to the wooden strip, and filled with a charge of powdered blend of TNT and trimethylene trinitramine TG 50/50, composed of small particles (about 0.02 mm). The detonation of this charge controlled the conditions for combustion. Since the particle size of this controlling charge was less by an order of magnitude than that of the powder tablet, it may be reckoned that the combustion of the tablet occurred mainly at the Zhuge point at nearly constant pressure. Under these conditions, a change in the density of the controlling charge could be used to alter the pressure at which combustion occurred.

When the controlling charge was detonated, the detonation wave was propagated in the direction shown by the arrow in Fig. 1. The oscillograph was triggered by the first detector. The oscillograph showed its first blip when the wave reached the edge of the detector K_2, located over the boundary of the free surface of the powder. It was reckoned that the powder ignited at this instant. The detector K_3 was energized when the powder was completely burnt, and produced a second blip on the oscillograph.

A small amount of air could always remain under the powder tablet. This air layer was compressed by the shock wave, and was thus heated and would set fire to the powder tablet. In this case, combustion of the tablet would proceed from both sides. Accordingly, the time interval should be doubled when calculating the rate of combustion from the equation $v = h_0/\Delta t$, where h_0 is the original thickness of the powder tablet, and Δt is the time interval between the first and second impulses. But in a number of cases there was no air layer, so that combsution would not take place from one side, and the combustion rate, calculated as above, would have to be doubled.

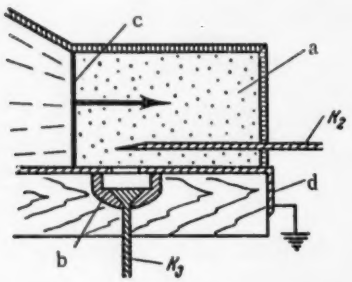

Fig. 1. Method of fixing powder tablet. a) Conditioning charge; b) powder tablet; c) detonation front of conditioning charge; d) foil.

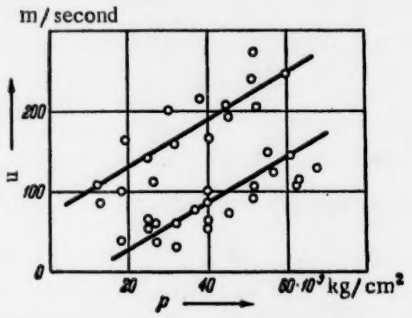

Fig. 2. Variation of the rate of combustion of the powder tablet with the pressure at the front of detonation of the controlling charge.

Since there was no means of telling in which way the tablet had combusted, the combustion rate was calculated in the same way for all the experiments, and the results are shown on a single graph. The density of the controlling charge varied from 0.60 to 0.90 g/cm³. The pressure at the Zhuge point, at which combustion occurred, was calculated approximately from the known formula $p = \rho_0 D^2/(k + 1)$, where k was taken as 3.

Figure 2 shows that the rate of combustion increased linearly with increasing pressure. All the experimental points fell into two groups, the mean values of which were approximately in the ratio of 1 : 2.

It may be finally concluded that, under the conditions of a detonation wave, the rate of combustion of NB powder is about 200-300 m/second (at a pressure of 60,000 kg/cm²).

LITERATURE CITED

[1] L. Basset and J. Basset, C. r. 14, 649 (1950).

Received August 23, 1958

THE ISOTOPE EFFECT IN THE CRACKING OF ETHANE

A. M. Brodskii, R. A. Kalinenko and Corresponding Member Acad. Sci. USSR K. P. Lavrovskii

This paper is concerned with the isotope effect in the cracking of ethane labelled with radioactive carbon C^{14}.

Experimental investigations have been published [1, 2] on the cracking of the propanes $C_2H_5-C^{13}H_3$ and $C_2H_5-C^{14}H_3$. In these, by measuring the activity of the methane formed by cracking,* it was established [2] that the $C^{12}-C^{12}$ bond was ruptured about 8% more frequently than $C^{14}-C^{12}$ or $C^{13}-C^{12}$ bonds. As was noted in [2], the large value of the effect, and the fact that it was the same for $C^{14}-C^{12}$ and $C^{13}-C^{12}$, were at variance with theoretical predictions [3], based on the use of the transition state method.

In our opinion, a possible explanation of this discrepancy is that, in the case of molecules with a plane of symmetry perpendicular to the direction of the chain, the introduction of a labelled carbon atom into the carbon skeleton disturbs the above mentioned symmetry and eliminates the quantum degeneracy [4]. The existence of degeneracy in unlabelled molecules and, associated with this, the preservation of symmetry during decomposition, restrict the number of possible end states of the decomposing molecule and, generally speaking, must produce a change in the rate of decomposition, as compared with labelled molecules. The above proposition is of a very general nature, and is not specially associated with the use of the concept of the transition state. It is clear that the existence and value of the isotope effect are of great importance for checking the position and for methods of calculating chemical kinetics.

In this connection, we investigated the isotopic effect in the high temperature cracking of the ethanes $C^{12}H_3-C^{12}H_3$ and $C^{12}H_3-C^{14}H_3$. The decomposition mechanism of ethane is essentially simpler than that of propane, since the molecule C_2H_6 differs from C_3H_8 in containing an even number of carbon atoms.

The experiments were carried out at ~850° and a pressure of 50-80 mm Hg, by the previously described [5,6] method, in a reactor with practically complete mixing. With such a reactor [5], the concentration of each product in the reaction mixture was directly proportional to the velocity constant of its formation, so that the specific activity of any final product was directly proportional to the ratio of the rates of formation of the corresponding active and unlabelled analogs. The separation and analysis of the reaction products was carried out chromatographically [7]. The original ethane, consisting of a mixture of $C_2^{12}H_6$ and $C^{12}H_3-C^{14}H_3$, had an activity A = 213 counts/minute, at 1 mm Hg, in an internally filled counter SBM-8, which corresponded to approximately 1520 counts/minute per normal cm^3. The original gas was purified chromatographically [7], in order to remove possible traces of inactive ethylene and methane. The results showed that over a wide range of conversions, the activity of the ethylene formed was the same as that of the original ethane, to a precision of 1%. But the activity of the methane was considerably less than A/2, the value to be expected if there were no isotopic effect.

Table 1 shows the activity of the methane, as a percentage of A/2, as a function of the ethylene content of the cracked gas. It is clear from the table that the methane activity was approximately 10% less than

*Cracking was carried out with a mixture of active and inactive propanes. The activities of the other products, besides methane, were not quoted in [2]. Data on the activity of the methane formed was only given in this for two very high degrees of conversion.

A/2 and altered relatively little with the extent of reaction. The values found for the isotopic effect were close to those obtained [1, 2] with propane.

TABLE 1

Pressure in mm Hg	Content of C_2H_4 in cracked gas, vol. %	Activity of CH_4 as % of A/2
50	7.7	90 ± 3
50	10.7	85 ± 3
30	11	86 ± 2
88	12.3	86 ± 2
90	16.2	87 ± 2
89	23.5	90 ± 2
84	23.7	88 ± 1

First and foremost, the results confirm, for the case of ethane, the large value of the isotopic effect in the methane formation reaction, previously observed with propane. The values of the effect are of the same order for methane from C_2H_6 and C_3H_8, and this provides an argument for the existence of the same stages in CH_4 formation in both cases.

Note added in proof. Preliminary experiments, on the cracking of a mixture of the ethanes $C^{12}H_3-C^{12}H_3$ and $C^{14}H_3-C^{14}H_3$, showed that the isotopic effect for methane was considerably less in this case than for the cracking of $C^{12}H_3-C^{14}H_3$. The activity of the methane was approximately 5% less than A/2. This serves to confirm the above proposition that the anomalously high value of the isotopic effect in the cracking $C^{12}H_3-C^{14}H_3$ is due to a quantum effect associated with disturbance of symmetry.

LITERATURE CITED

[1] D. P. Stevenson, C. D. Wagner, O. Beek, and J. W. Otvos, J. Chem. Phys. 16, 993 (1948).

[2] H. M. Frey, C. J. Danby and C. Hinshelwood, Proc. Roy. Soc., A, 234, No. 1198, 301 (1956).

[3] J. Bigeleisen, J. Chem. Phys., 17, 675 (1949); 56, 823 (1952).

[4] L. Landau and E. Lifschitz, Quantum Mechanics (1948).

[5] A. M. Brodskii, R. A. Kalinenko, K. P. Lavrovskii and V. B. Titov, Proc. Acad. Sci. USSR, 116, No. 5, 789 (1957).*

[6] A. M. Brodskii, R. A. Kalinenko, K. P. Lavrovskii and V. B. Titov, Proc. Acad. Sci. USSR, 117, No. 6, 1013 (1957).*

[7] A. M. Brodskii, R. A. Kalinenko and K. P. Lavrovskii, Problems of Kinetics and Catalysis, 9th edition, Acad. Sci. USSR (1957) p. 399;** Chem. and Technol. Fuels, No. 8, 18 (1956).

Received September 24, 1958

*Original Russian pagination. C.B. Translation.

**In Russian.

USE OF THE DROPPING MERCURY ELECTRODE FOR THE DETERMINATION OF DIFFUSION COEFFICIENTS

Evgenii Budevskii

Sofia State University, Sofia, Bulgaria

(Presented by Academician A. M. Frumkin, September 1, 1958)

I. Equation of Limiting Diffusion Current

From measurement of the limiting diffusion current with a dropping mercury electrode it is possible to calculate the diffusion coefficient of the material taking part in the electrode process. But for this purpose it is necessary to have a sufficiently precise diffusion current equation. The Ilkovic equation

$$\bar{i}_d = 0{,}627\, nFc_0 m^{2/3} t_0^{1/6} D^{1/2},$$

which has been used for this purpose [1], is only a very rough approximation [2], since a number of effects, characteristic of the dropping mercury electrode, are neglected in its derivation:

1. Spherical diffusion. It has been established, as the result of a large number of experimental and theoretical investigations [2], that curvature of the mercury drop is the cause of an increase in the diffusion current, as the result of spherical diffusion. An exact solution of this problem was given simultaneously in 1953 by Koutecky [3] and Matsuda [4], who showed that calculation of spherical diffusion leads to a correction factor $(1 + 3.9\ x)$ for instantaneous values of the current, or $(1 + 3.4\ x_0)$ for mean values of the limiting current, to be applied to the Ilkovic equation. Here $x = D^{1/2} m^{-1/3} t^{1/6}$ or $x_0 = D^{1/2} m^{-1/3} t_0^{1/6}$, t is the time from the beginning of the life of the drop, t_0 is the drop time in seconds.

2. Effect of screening. Diffusion to the upper part of the mercury drop is retarded by the proximity of the capillary. If it is assumed that the part of the drop surface, situated within a distance $\delta = \sqrt{3/7\ \pi Dt}$ from the capillary (δ is a measure of the depth of the change in concentration), does not take part in the electrode process, a correction factor is obtained equal to $(1 - 2.3\ x)$ and $(1 - 2.0\ x_0)$ for the instantaneous and mean currents respectively. Since x and x_0 are usually less than 0.1, it is permissible to neglect the square terms, and to combine the screening and spherical diffusion corrections to give the correction factors $(1 + 1.6\ x)$ and $(1 + 1.4\ x_0)$. It is obvious that this screening correction is exaggerated, since the effectively screened part of the surface does play some part in the electrode process. In his attempt to derive a more precise treatment, Matsuda [4] obtained an expression in which, as the result of a reduction in the screening effect, the combined correction factors were $(1 + 2.3\ x)$ and $(1 + 2.1\ x_0)$.

3. The effect of decrease of concentration of the electrochemically active component in the immediate vicinity of the drop surface was first investigated experimentally by Hans, Henne and Meurer [5]. These authors showed that the effect of impoverishment of electrolyte led to a decrease in the current, which was also proportional to the parameters x and x_0, and could be expressed by a further decrease in the correction factor for spherical diffusion.

These three effects can therefore be expressed by a single correction factor in the Ilkovic equation, which takes the form of $(1 + A'\ x)$ for instantaneous current and $(1 + A\ x_0)$ for mean current, where A' and A are empirical constants ($A' < 3.9$ and $A \leq 3.4$).

4. Effect of capillary pressure. All expressions for the limiting diffusion current are based on the assumption of a constant rate of flow of mercury. But it is known that the rate of flow is considerably reduced at the beginning of the life of a drop, owing to the high value of the capillary pressure $P_\sigma = 2\sigma/r$, which acts against the pressure producing the mercury flow. For this reason, the mean value of the rate of flow is used in the expression for the mean diffusion current. A somewhat better approximation is obtained if, in the expression for the instantaneous value of the diffusion current

$$i_d = nFc^0 q \sqrt{\frac{7}{3}\frac{D}{\pi t}}\,(1 + A'x)$$

the electrode surface, q, is calculated in the usual way from the drop weight, but using the drop weight given by the approximate Smith equation [6]

$$W = m_0 t\,(1 - {}^3/_2 s\,(m_0 t)^{-1/3} - {}^3/_2 s^2\,(m_0 t)^{-2/3}),$$

in which allowance is made for changes in the rate of flow of mercury for different stages in the development of the drop. Here $s = 5.79 \cdot 10^{-4}\,\sigma/h$, where σ is the surface tension of mercury, h is the pressure causing the mercury to flow, m_0 is the rate of flow of mercury into mercury (i.e., when $P_\sigma = 0$) in grams per second.

Integration of the equation obtained in this way gives, for the mean current

$$\bar{i}_d = 0{,}627\; nFc_0 m_0^{2/3} t_0^{1/6} D^{1/2}(1 + AD^{1/2} m^{-1/3} t_0^{1/6} -$$
$$- 1{,}4\; s\;(m_0 t_0)^{-1/3} - 2{,}9\, s^2\,(m_0 t_0)^{-2/3} - 1{,}4\; AD^{1/2} m_0^{-2/3} t_0^{-1/6}), \qquad (1)$$

in which all terms of the second order are omitted from the correction factor. The integration should not be carried out from t = 0, because the Smith equation gives negative values of W for very small values of t. The lower limit of integration is therefore taken as the value of t at which i_d is extinguished. The error involved may be calculated from a precise expression for the relation between W and t. This leads to a rather complicated expression. The corresponding correction, involving the capillary radius, is usually very small and may be neglected.

5. Deformation of drop under the influence of its weight. Photographs of large mercury drops [5, 6] show that the latter are pear shaped rather than spherical, i.e., they can be represented as spheres with greatly elongated necks. This deformation becomes significant at a drop weight greater than 4-5 mg. Although, in this case, the surface of a drop alters very little in comparison with the surface of a sphere of the same volume,* the deformation can lead to an increase in current for two reasons: a) removal of the drop from the screening surface of the capillary — the screening effect is reduced: b) because of the high linear rate of flow of mercury through the neck, convection currents may be set up in the electrolyte round the neck, in spite of the presence of surface active agents. At present, it is hardly possible to give a quantitative expression to this additional increase of current. It is therefore obviously more satisfactory to work with drops of weight less than 3-4 mg for which equation (1) remains valid.

II. Verification of Equation for Limiting Diffusion Current

The equation derived for the limiting diffusion current (I) contains two unknown quantities: the diffusion coefficient, D, and an empirical constant, A. These quantities can be determined by investigating the relation between the diffusion current and the rate of flow of mercury, m_0, the drop time, t_0, and the height of the mercury column, h, using the method of successive approximations. For this purpose, equation (I) was used in the form

$$y = \frac{\bar{i}_d}{KD'^{1/2}} - 1 + B = \frac{\bar{i}_d}{KD'^{1/2}}\,\delta + Ax_0, \qquad (1)$$

where D' is an approximate value of the diffusion coefficient, $D^{1/2} = D'^{1/2}(1 + \delta)$, and δ is the corresponding correction; $K = 0.627nFc_0 m_0^{2/3} t_0^{1/6}$, $B = 1.4\,s\,(m_0 t_0)^{-1/3} + 2.9 s^2 (m_0 t_0)^{-2/3} + 1.4\,Asm_0^{-2/3} t_0^{1/6} D^{1/2}$.

*For a drop of weight 16 mg the increase in surface only amounts to about 0.3% [5].

Since the value of $\bar{i}_d / KD^{1/2}$ is of the order of unity ($1 \cdot \pm 0.2$), provided that δ is small in comparison with unity, we may write, instead of (1*),

$$y = \delta + Ax_0.$$

In this equation, y is the experimentally determined value, if some provisional value is taken for A, for example $A \cong 2.0$ [7], in determining the third term, B. Investigation of the relation between y and x_0 then makes it possible to determine A and δ and, hence, D.

With this in view, an apparatus was constructed, with which, by adjusting the drop time, it was possible to measure accurately the relation between limiting current and m_0, t_0 and h. The device for varying and measuring the drop time consisted of a shortened pendulum with increased moment of inertia, controlled by a quartz prism. A mirror was fastened to the bottom of the pendulum, and this reflected a beam of light on to the photocell when the pendulum was in its lowest position. The periodic electrical pulses obtained in this way were fed to a thyratron relay, which energized an electromagnetic vibrator. This vibration was connected to the capillary in such a way as to ensure the absence of vibration after the mercury drop had broken away.

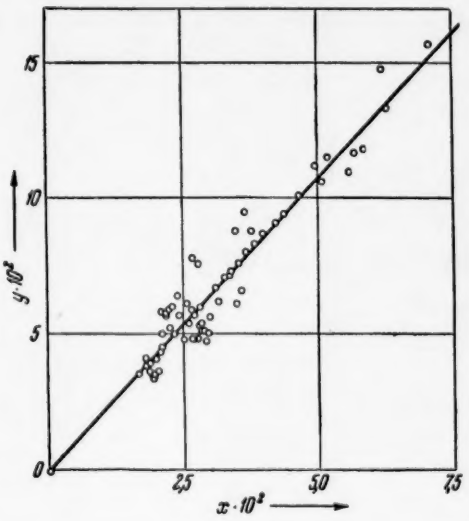

Fig. 1.

The current was measured by a galvanometer, shunted by a 3000 μf condenser, which reduced oscillations to about $\pm 1\%$ of the nominal value of the current. The condensers used were free from leakage and polarization. A correction for the residual current was applied in all cases. The investigation was carried out with approximately 1.5×10^{-3} M $PbCl_2$ in 0.1 N KCl containing 0.01% of gelatin at 25°, in a hydrogen atmosphere, with a potential of 0.7 v across the cell.

Figure 1 shows the experimental results for the relation between y and x_0. The following values were used for calculating y and x_0: $\sigma = 430$ dynes/cm, $D^* = 8.69$ cm²/second, A = 2.1. These values of D^* and A were obtained as the result of preliminary calculation. The final values $A = 2.17 \pm 0.08$, $D = (8.69 \pm 0.05) \cdot$

TABLE 1

Capillary No. 1, Diameter of Orifice 110 μ, h = 30.4 cm, $m_0 = 3.02 \times 10^{-3}$ g/second, $c_0 = 1.428 \times 10^{-6}$ mole $PbCl_2$ per ml

t_0,sec.	$\bar{i}_d$ meas. μa	$\bar{i}_d$ calc. μa	$\Delta\bar{i}/\bar{i}$, %	W,mg	t_0,sec.	$\bar{i}_d$ meas. μa	$\bar{i}_d$ calc. μa	$\Delta\bar{i}/\bar{i}$, %	W,mg
4,84	14,60	13,93	+4,8	14,6	1,23	10,58	10,59	+0,0	3,7
4,36	14,18	13,62	+4,1	13,2	1,00	10,07	10,14	—0,7	3,0
3,25	13,33	12,88	+3,5	9,8	0,80	9,59	9,66	—0,7	2,4
2,69	12,78	12,40	+3,1	8,1	0,69	9,32	9,38	—0,6	2,1
2,38	12,42	12,09	+2,7	7,2	0,61	9,07	9,11	—0,4	1,8
2,10	11,97	11,81	+1,4	6,3	0,51	8,73	8,74	—0,1	1,5
1,61	11,35	11,19	+1,4	4,9	0,32	7,88	7,89	—0,1	1,0

$\cdot 10^{-6}$ cm²/second were obtained by the method of least squares. The graph shown refers to a drop weight of 4 mg. Positive deviations of the measured current from that calculated from equation (1) were always obtained with large drops.

With 16 mg drops this deviation was about + 5%, which considerably exceeded the limits of the normal deviation (of the order ± 1%). Table 1 shows the results of such a set of measurements.

The value obtained for the diffusion coefficient is in excellent agreement with the diffusion coefficient of the lead ion measured by other methods for the same conditions: $D = 8.69 \times 10^{-6}$ cm^2/second (Stackelberg et al. by the Cottrell method [7]) and $D = 8.64 \times 10^{-6}$ cm^2/second (Yukhtanova [8]) by the rotating disc electrode method.

LITERATURE CITED

[1] K. Micka, Chem. Listy 50, 203 (1956).

[2] J. J. Lingane and B. A. Loveridge, J. Am. Chem. Soc. 66, 1425 (1944); L. Meites and T. Meites, J. Am. Chem. Soc. 72, 3686 (1950); 73, 395, 1581, 2035, 3724, 4257 (1951); H. Strehlow and M. v. Stackelberg, Zs. Elektrochem. 54, 51 (1950); H. Strehlow, O. Madrich, and M. v. Stackelberg, Zs. Elektrochem. 55, 244 (1951).

[3] J. Koutecky, Czechoslov. J. Phys. 2, 50 (1953).

[4] H. Matsuda, Bull. Chem. Soc. Japan 26, 342 (1953).

[5] W. Hans, W. Henne, and E. Meurer, Zs. Elektrochem. 58, 836 (1954).

[6] G. S. Smith, Trans. Farad. Soc. 47, 63 (1951).

[7] M. v. Stackelberg, M. Pilgram, and V. Toome, Zs. Elektrochem. 57, 342 (1953).

[8] V. D. Yukhtanova, Proc. Acad. Sci. USSR, 124, No. 2 (1959).*

Received September 1, 1958

*See C.B. Translation.

THE EFFECT OF CRYSTALLOGRAPHIC ORIENTATION ON THE REACTION OF ISOTOPIC EXCHANGE AT A METALLIC SURFACE

B. N. Bushmanov and G. S. Vozdvizhenskii

Kazan Aviation Institute.

(Presented by Academician A. N. Frumkin, September 13, 1958)

It was shown previously [1, 2] that the faces of a zinc monocrystal behave differently when in a solution of zinc sulfate containing the radioactive isotope Zn^{65}. The faces of the prism acquire a greater activity than does the base. From a large number of measurements, it was found that the mean value of the ratio of the acquired activities I_{prism}/I_{base} was 108 ± 1%. A difference was also observed [2] in the kinetics of the exchange process atom — ion on "fresh" (just polished) and "aged" (allowed to stand in air for 500 hours after electropolishing) samples of monocrystals of zinc. Exchange took place considerably more slowly with "aged" samples, and the effect of crystalline orientation was less marked (I_{prism}/I_{base} = 105%). This difference in the behavior of "fresh" and "aged" samples is obviously explained by the presence of an oxide film on the surface of the crystalline faces investigated, and quality of the film (thickness, continuity and crystallographic orientation) depending on the time of exposure to atmospheric oxygen before the exchange experiments and on the crystallographic orientation of the surface investigated. Further experimental work has been done on this subject, and the results are given in this paper.

EXPERIMENTAL

The results obtained previously with samples of area 1 cm^2 were confirmed for samples for which the area of the face investigated was 6 cm^2. Samples of dimensions 40 × 15 × 5 mm were sawed from large zinc monocrystals, grown by the method developed by one of us [3]. In order to eliminate the effects on the properties of a monocrystal of its conditions of growth (peculiar to each large monocrystal) [4], 7 to 8 samples for each of the three fundamental crystalline faces (0001), (10$\bar{1}$0) and (12$\bar{1}$0) were prepared from a single large monocrystal. X-ray investigation showed that the deviation of the working surface of each sample from the given crystalline orientation did not exceed 3-6°.

The preparation of the samples for test and the exchange process were carried out as described in [1, 2].

The results confirmed the previously obtained effect of anisotropy in exchange between the faces of the base (0001) and of the prism 1 position (10$\bar{1}$0). No difference was observed (within the limits of experimental error) in the intensities of exchange for the (10$\bar{1}$0) and (12$\bar{1}$0) faces.

Measurements were made of the activities of samples treated at different exchange temperatures (under strictly uniform conditions). The results of these measurements are shown in Fig. 1. It is evident that, with rising temperature from 0 to 69°, the activities of the treated samples increased by a factor of 3-4. The activation energy of the exchange process $Zn \rightleftharpoons Zn^{++}$ was calculated from these results. The mean activation energy, for the range of temperature 0 to 69°, was 3700 cal/mole for the base face and 3400 cal/mole for the prism faces.

We also investigated the reverse exchange process, when a radioactive metal sample was immersed in an inactive solution of zinc sulfate. The radioactivity was applied to the metal sample by direct exchange, i.e., by immersion of the sample in radioactive zinc sulfate solution. The reverse exchange process was very rapid

at the start. From a series of measurements, it was found that 30-40% of the radioactive zinc was transferred from the sample surface to a 1 M solution of zinc sulfate in 1 second. The process slowed up subsequently, and it was found that the curve for reverse exchange as a function of time approximated asymptotically to a horizontal straight line (Fig. 2). About 7 and 5-6% respectively of the original activity remained on the samples after 24 and 100 hours exposure to reverse exchange in 1 M solution. No differences were observed for reverse exchange (as also for direct exchange) between the (10$\bar{1}$0) and (1210) prism faces.

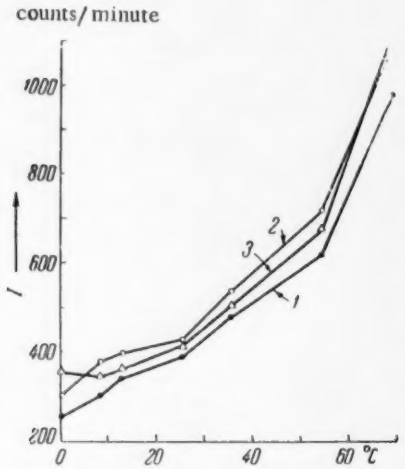

Fig. 1. Variation of activity of treated samples with exchange temperature (duration of exchange 1 minute, specific activity of solution 0.11 mC/ml; 8 individual samples were used in each series). 1) Base, 2) prism, 3) polycrystalline.

Reverse exchange took place more rapidly with more concentrated zinc sulfate solutions.

DISCUSSION OF RESULTS

The difference in exchange intensity between the faces of the base and of the prism are connected with their structural peculiarities. The base is a crystalline face, showing a denser packing and having a more positive electrode potential, and, for this reason, exchange occurs on it less intensively. The prism face has a less dense packing and a more negative potential, and exchange occurs on it more intensively.

A number of authors [5] have assumed that transfer of radioactivity to a metallic sample by immersion of the sample in a solution containing the appropriate radioactive ion, may be caused by the exchange atom $\rightleftharpoons$ ion and also by adsorption of radioactive ions by the metallic surface. But the nature of the variation of exchange with temperature enables us to conclude that the dominating process, involved in the transfer of radioactivity to the sample, is the exchange atom $\rightleftharpoons$ ion, and not an adsorption process.

The persistent residual activity, in reverse exchange, is clearly due to the diffusion of some radioactive zinc ion-atoms into the depth of the metal, where they cannot take part in exchange with the ions present in the solution. This process is aided by the screening action of the oxide film, whose thickness increases with increasing residence time of the metallic sample in the electrolyte solution.

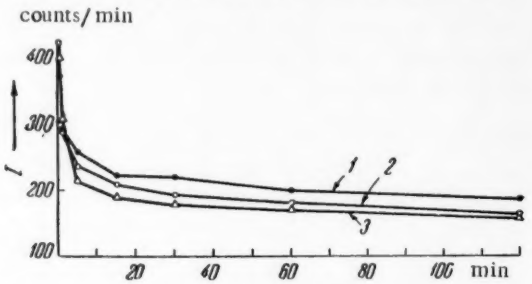

Fig. 2. Reverse exchange in a 0.03 M solution of zinc sulfate. 1) Base, 2) prism, 3) polycrystalline.

The effect of crystallographic orientation on the course of the reverse exchange process is also apparent (Fig. 2 and 3), but is less marked than for direct exchange. In our view, the cause of this is the formation of an oxide film on the surface of the metal, the structure and thickness of the film depending on the crystallographic orientation of the substrate.

An oxide film is already formed during the electropolishing of zinc samples [6]. During immersion of the sample in a radioactive solution of zinc sulfate (so that a radioactive deposit is formed on the surface of

the metal), and during subsequent washing, the thickness of the film increases. The rate of oxidation is different for faces of different crystallographic index [7-10]. For a zinc monocrystal, the base face is the most resistant to oxidation. It is therefore evident that the prism faces will acquire a thicker film, and that all the prism faces will thus be made passive to a greater extent than the base face. This increased passification weakens the effect of anisotropy observed in direct exchange.

The observed effect of the difference in the rates of the exchange atom $\rightleftharpoons$ ion on the faces of a zinc monocrystal may be explained as due either to a difference in the physicochemical properties of the different faces, determined by their structures, or to possible differences in the true surfaces of the faces with identical electrochemical behavior. We believe that the first suggestion is more plausible.

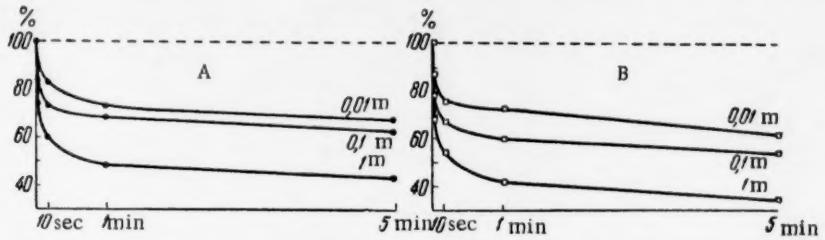

Fig. 3. Reverse exchange in solutions of zinc sulfate of different concentrations. A) On base face, B) on prism face.

We have not made any special investigation of the values of the true surfaces of our samples, but a number of investigators (9, 11-15) have shown that electrolytic polishing is a sufficiently reliable method of preparing monocrystalline samples for investigation, associated with a constant value of the true surface.

It might be supposed that the different behavior of the different faces of a zinc monocrystal in a solution labelled with the radioactive isotope could be explained by secondary causes, as, for instance, a difference in the distribution of impurities and lattice defects on the different faces, variations in the thickness and continuity of the oxide film, difference in the adsorptive powers of the faces, etc. But this would not diminish the role of crystallographic orientation in the processes investigated, since all these secondary causes are functions of the crystallographic orientation, and vary on the different faces in accordance with the different crystalline structures of the latter.

LITERATURE CITED

[1] B. N. Bushmanov, and G. S. Vozdvizhenskii, Proc. Acad. Sci. USSR 114, 1046 (1957).*

[2] B. N. Bushmanov, Trans. Kazan. Aviation Inst. 35, 37 (1957).

[3] B. N. Bushmanov, Phys. Met. and Metallogr. 4, 310 (1957).

[4] Li Choh Hsien, J. Washburn, and E. R. Parker, J. Metals 5, 1223 (1953).

[5] A. Baerg and C. A. Winkler, Canad. J. Chem. 31, 521 (1953).

[6] H. Ehlers, Zs. f. Phys. 136, 379 (1953).

[7] A. T. Gwathmey and A. F. Benton, J. Chem. Phys. 8, 9569 (1940).

[8] J. Bardolle and J. Benard, C. r. 239,706 (1954).

[9] T. Rodin, Collection: Catalysis, Investigation of Heterogeneous Processes, IL (1956), p. 45.**

[10] T. Kvan, Loc. cit., p. 314.

[11] T. N. Rhodin, J. Phys. Chem. 57, 143 (1953).

[12] S. Z. Roginskii, I. I. Tret'yakov and A. V. Shekhter, Proc. Acad. Sci. USSR 100, 487 (1955).

*Original Russian pagination. See C.B. Translation.

**Russian translation.

[13] V. A. Dmitriev, E. V. Rzhevskaya and V. A. Khristoforov, Bull. Kazan Branch Acad. Sci. USSR. Chem. Series, 4, 115 (1957).

[14] S. Yoshida, J. Phys. Soc. Japan 11, 129 (1956).

[15] F. Bouillon, Y. Bouillon-Nysen and A. Delplancke, Bull. Soc. Chim. Belg. 65, 245 (1956).

Received September 10, 1958

VOLTAGE-CURRENT CHARACTERISTICS OF AN ELECTROLYTE – N-TYPE SEMICONDUCTOR CONTACT

Yu. A. Vdovin, Corresponding Member Acad. Sci. USSR. L. V. Levich, and V. A. Myamlin

Moscow Physical Engineering Institute

Introduction. Up to the present time, the boundary separating an electrolyte from a semiconductor has not been studied well enough, neither experimentally nor theoretically. We decided to study this type of contact for the simple reason that in this case we had some essentially common properties as well as different ones from those exhibited by solid contacts between the metal and semiconductor, or semiconductor and semiconductor. Actually, the rectifying action of a semiconductor – metal contact is connected with the formation of a near-contact layer which is defective in charge carriers. As the direction of the current is alternated, this layer acquires an excess or deficiency of carriers and its resistance decreases or increases accordingly. All this takes place at the investigated contact, therefore, it is here that one would naturally expect to observe the rectifying effect. Besides, since in this case one can have a wide variety of electrode reactions and of electrolytes it opens new vistas in the choice of systems with various properties that one might need. Let us also note that the actual contact surface in this case far exceeds the corresponding surface at a contact between two solids.

In this paper we have analyzed the contact between an N-type semiconductor and an electrolyte. We have assumed (in contrast to paper [1]) that when the current flows an oxidation-reduction reaction of type

$$A^{+} + e^{-} \rightleftharpoons A, \tag{1}$$

takes place.

For the sake of simplicity, we have assumed that the ionic concentration at the reaction surface is large enough to exclude the transport of ions from the bulk of solution as a possible limiting step in Reaction (1). The potential drop in the electrolyte was neglected, which is justified if the solution contains some inert electrolyte at high enough concentration.

Fundamental equations. Let us write out the equations connecting current, charge density, and the electric field in a semiconductor. For the current, we have

$$j = eu\left(En + \frac{kT}{e}\frac{dn}{dx}\right) \quad (e > 0), \tag{2}$$

where u = mobility of electrons, n = concentration of electrons. The second equation we will chose in the form,

$$\operatorname{div}\mathbf{E} = -\frac{4\pi e}{\varepsilon}\left(n - \frac{n_{\infty}^2}{n}\right); \tag{3}$$

where n_{∞} = concentration of electrons in a region sufficiently far removed from the contact. Such a choice of current density corresponds to weakly ionized donor levels [2].

The system of Equations (2) and (3) may be conveniently transformed into a dimensionless form,

$$\frac{dz}{dt} - zy - \lambda = 0, \quad \frac{dy}{dt} = z - \frac{1}{z}. \tag{4}$$

The symbols introduced here are: $\lambda = j/j_\lambda = j/kTun_\infty \kappa$; $t = \kappa x$; $\kappa = \sqrt{4\pi e^2 n_\infty / kT\epsilon}$; $z = n/n_\infty$; $\psi = e\varphi/kT$; $y = d\psi/dt$.

We will assume that the contact is spread over a very thin plane x = 0. In the region x > 0, we have the semiconductor, while at x < 0 the electrolyte.

In the case of the metal-electrolyte contact, according to the theory of delayed discharge [3], the current density at the phase boundary satisfies equation

$$j = k_1 c_{ion} e^{-\alpha\Delta\psi} - k_2 e^{\beta\Delta\psi}, \tag{5}$$

which may be regarded as a boundary condition for the transfer equation. Here C_{ion} is the concentration of reacting ions right next to the electrode surface; $\Delta\psi$ is the drop of the dimensionless potential in the Helmholtz region of a double layer; α, β, k_1, k_2 are constants, and $\alpha < 1$, $\beta < 1$, $\alpha + \beta = 1$.

Unlike a metal, a semiconductor can undergo considerable changes in its electron concentration. Therefore, the following relation would be a natural simplification of the delayed discharge formula:

$$j = k_1 n_c c_{ion} e^{-\alpha\Delta\psi} - k_2 e^{\beta\Delta\psi}, \tag{6}$$

where n_c = concentration of electrons at the contact.

Let us represent the potential drop in a Helmholtz double layer in the form $\Delta\psi = \Delta\psi^0 + \Delta\psi'$, where $\Delta\psi^0$ = potential drop when the system is at equilibrium (j = 0). In addition to this, we can write the boundary conditions for Equation (6) in this convenient form

$$j = j_0 \frac{z_c}{z_c^0} e^{-\alpha\Delta\psi'} - j_0 e^{\beta\Delta\psi'}. \tag{7}$$

In accordance with what was said above, the ionic concentration C_{ion} we assume to be constant. In this case j_0 is the exchange current $j_0 = k_1 n_c^0 c_{ion} e^{-\alpha\Delta\psi^0} = k_2 e^{\beta\Delta\psi^0}$; z_c and z_c^0 are the dimensionless electron concentrations at the contact at a finite and zero current respectively.

The solvent Equation (4) it is convenient (see [4]) to introduce a subsidiary function $q = \frac{1}{z}\frac{dz}{dt}$, for which it is easy to get the equation

$$q\frac{dq}{dz} - \frac{z - 1/z}{z} + \frac{\lambda}{z^2} q = 0. \tag{8}$$

Let us at first analyze Equation (8) for small currents ($\lambda \ll 1$). The last condition is not a rigid limitation, since j_λ changes from approximately 0.1 to 10^3 a/cm^2, depending on the value of mobility u and of concentration n_∞. Expanding q into a series for small λ, we get

$$q = \frac{1 - z}{\sqrt{z}}\sqrt{2} - 2\lambda \frac{1}{1 - z}\left(1 - \frac{2}{3}\sqrt{z} - \frac{1}{3}\frac{1}{z}\right) + \ldots \tag{9}$$

By comparing the terms in Series (9) we can see that the expansion is really justified if $\lambda \ll \sqrt{z}$. With the help of Equation (9) is easy to find the connection between an electric field y and a concentration z,

$$y = -\lambda/z + q(z). \tag{10}$$

We can write the overall potential drop in a Helmholtz double layer and in a semiconductor (after subtracting the ohmic drop) in the form

$$\psi = \Delta\psi + \int_0^\infty (y - y_\infty)\, dt. \tag{11}$$

By using Equations (9) and (10) and by limiting ourselves only to terms linear in λ, we can readily calculate

$$\psi = \Delta\psi - \ln z_c - \lambda(\sqrt{2}/\sqrt{z_c} - \sqrt{2}). \tag{12}$$

If we take advantage of the fact that the inductions at a Helmholtz layer – semiconductor boundary are equal and assume that the potential function in the Helmholtz layer is linear, we can express $\Delta\psi$ in terms of a field y_c taken on the semiconductor surface. The we will get

$$\Delta\psi = y_c t_0, \tag{13}$$

where $t_0 = \kappa d\epsilon / \epsilon_1$, d and ϵ_1 are the width and the dielectric constant of the Helmholtz layer respectively.

Using Equations (7), (9), (10), (12), and (13) it is possible to get the voltage-current characteristic $\psi = \psi(j)$. However, since it is difficult to solve Equation (7) for $\Delta\psi'$, we will isolate a region of small currents $j \ll j_0 \ll j_\lambda$. In this case we can consider the deviations of all the numbers from their equilibrium values to be small, and therefore a series expansion is permissible for small j/j_0. The voltage-current characteric then looks as follows:

$$\psi = \psi_c - j/j_0 + {}^1/_2 (j/j_0)^2. \tag{14}$$

In deriving Equation (14) we assume that $j_0 \ll j_\lambda z_c^0 / t_0$ and $t_0 \ll \sqrt{z_c^0}$. In Equation (14) ψ_c = the equilibrium potential difference at the contact. Besides, it was assumed that at equilibrium the region near the contact is already defective in electrons, i.e., that $z_c^0 < 1$.

Let us now analyze the flow of barrier currents, i.e., let us study the case where $j < 0$, $-j < j_0$. This current flow can indeed be called a barrier since the electrons by moving away from the contact make the layer next to the electrode deficient in carriers. The deficient layer becomes wider. In this case we can assume that

$$\frac{z_c}{z_c^0} e^{-\alpha\Delta\psi'} \ll e^{\beta\Delta\psi'}. \tag{15}$$

And consequently, the voltage-current characteristic assumes the form

$$\psi = \Delta\psi^0 + \frac{1}{\beta} \ln \frac{-j}{j_0} - 2 \ln (\sqrt{2}\beta t_0) + 2 \ln \ln \frac{-j}{j_0} - \frac{2}{3} \frac{\lambda}{\beta t_0} \ln \frac{-j}{j_0}. \tag{16}$$

The condition that $-\lambda \ll \sqrt{z}$ leads to the requirement that $-\lambda \ll \beta t_0$. Since $\beta t_0 \sim 10^{-3}$, the last inequality may actually limit the range within which Formula (16) would be applicable.

We can see that in this case the change of potential vs. current is essentially determined by Tafel's law, since the first and the third members of the series are constants while the fourth constitutes a small correction to Tafel's law.

Since the magnitude of the current in Formula (16) is limited by the relationship $-\lambda \ll \beta t_0$, it is quite interesting to determine the law obeyed by a potential drop at large currents. In this case, to find q, we will have to look for a solution in the form of the following series,

$$q = \frac{1}{\lambda}\left(q_0 + \frac{q_2}{\lambda^2} + \frac{q_4}{\lambda^4} + \cdots\right) \tag{17}$$

(we have chosen this form of a solution due to the fact that with a barrier current the deficiency region expands and consequently the derivative dz/dt in the initial Equation (4) becomes small). Substituting Equation (17) into (8) and limiting ourselves to terms $\sim 1/\lambda^2$, we get

$$q = \frac{1}{\lambda}(z^3 - 1)\left(1 - \frac{2z^3}{\lambda^2}\right). \tag{18}$$

It can easily be shown that the expansion is justified when $-\lambda \ll \sqrt{z}$. With the help of Equation (18) it is easy to get the voltage-current characteristic

$$\psi = \Delta\psi^0 - \frac{\lambda}{\beta l_0} \ln \frac{-j}{j_0} - \lambda \frac{\sqrt{2}}{\sqrt{z_c^0}} + \frac{1}{\beta} \ln \frac{-j}{j_0}. \tag{19}$$

In deriving this formula we assumed that $\beta t_0 \ll -\lambda \leq 1$ and $(\beta t_0)^{2\beta-1}/(z_k^0)^{\beta} \ll j_\lambda / j_0$, and besides this, all the members of the order of one or less were left out of Formula (19). It is obvious from Formula (19) that in this case the potential drop substantially exceeds the potential drop as given by Tafel's law. Actually, the second term is considerably larger than the fourth. This is connected with the fact that a region deficient in current carriers is formed at the contact and the principal potential drop occurs in this region.

Let us now go over the conducting current flow, $j > 0$. By using Equation (7), (9), (10), (12), and (13), we can find the relationship

$$\psi = \Delta\psi^0 - \ln \frac{j}{j_0} - \ln z^0_c \tag{20}$$

which is valid if the inequalities $j_0/z_c^0 < j \ll j_0/z_c^0\ (\alpha t_0)^2$; $j < j_\lambda (z_c^0 < 1)$ are satisfied.

All the terms that were small as compared to one were left out of Formula (20). One can readily see that in this case the potential drop has the form of Tafel's law.

To get the asymmetry characteristic of the voltage-current curve it is interesting to compare the potential drop for a current $\pm j$. It should be noted that in accordance with the determination of ψ (see Formula (11)) this number does not contain any ohmic voltage drop which has the value $\lambda \kappa l$, where l is the length of the semiconductor in centimeters. It is easy to verify that at sufficiently small l ($l \sim 10^{-2}$ cm) the ohmic potential drop can be neglected in the case of a barrier current. In the case of a conducting current the ohmic voltage drop plays the principal role at $\lambda \sim 1$.

Let us estimate the ratio between the total potential drop at a barrier current $\Delta V(-j)$ and $\Delta V(+j)$. This can be readily accomplished with the help of Equation (19)

$$\frac{\Delta V(-j)}{\Delta V(+j)} = \frac{\ln(|j|/j_0)}{\beta l_0 \kappa l} = \frac{\ln(|j|/j_0) \cdot \varepsilon kT}{\beta \cdot 4\pi e^2 n_\infty l d}. \tag{21}$$

We can see now that the rectification depends not only on the electrochemical reaction occurring on the semiconductor (coefficients β and j_0), but also on the properties of the semiconductor itself (coefficient n_∞). At $l = 10^{-2}$ cm, $\kappa = 10^5$ cm^{-1}, $t_0 = 10^{-3}$, $\ln(|j|/j_0) = 10$ and $\beta = 1/2$ this ratio is equal to $\Delta V(-j)/\Delta V(+j) = 20$. Thus, under the indicated conditions the system possesses distinct rectifying properties.

The results of this work are also valid in the case where for different current directions different reactions predominate; for example, when $j > 0$ reaction of type $A^+ + e^- \rightarrow A$ takes place, while at $j < 0$ the $B^- \rightarrow B + e^-$ reaction. In this case it is necessary to substitute some constants characterizing the corresponding reactions into the final formulas. Let us note that for a porous semiconductor the obtained results can be generalized right away.

LITERATURE CITED

[1] Yu. A. Vdovin, V. G. Levich, and V. A. Myamlin, Coll. Some Problems in Theoretical Physics, Moscow, 1958.*

[2] A. L Gubanov, Theory of the Rectifying Action of N-type Semiconductors, Moscow, 1958.*

[3] A. N. Frumkin, V. S. Bagotskii, Z. A. Iofa, and B. N. Kabanov, Kinetics of Electrode Processes, Moscow, 1952.

[4] W. Schottky, Zs. f. Phys. 113, 367 (1939); W. Schottky and E. Spenke, Veroff. Siemens Werken 18, 1 (1939).

Received September 27, 1958

* In Russian.

APPLICATION OF THE EMANATION METHOD TO THE INVESTIGATION OF CATALYSTS

STUDY OF THE EMANATING POWER DURING THE PREPARATION OF OXIDATION CATALYSTS

G. M. Zhabrova, M. D. Sinitsyna, and Corresponding Member Acad. Sci. USSR S. Z. Roginskii

Institute of Physical Chemistry, Academy of Sciences, USSR

An uninterrupted measurement of the emanating power during the topochemical stages in the preparation of a catalyst provides a proper background for the control of structural changes in the formation of catalysts.

Earlier [1], we have carried out an investigation of the decomposition of magnesium and zinc carbonates and hydroxides by using radium as the indicator element. Magnesium compounds (carbonate and hydroxide) turned out to be interesting objects of inbestigation; when thermally decomposed they yield magnesium oxide which is a known catalyst for dehydrogenation [2] and certain other processes [3].

For the indicated compounds, we established a linear dependence between the emanation coefficient and the specific surface at constant distribution depth. However, in working with radium one had to interrupt the topochemical process to take out test samples and to gather the radon. This defect does not appear in the emanation method which is based on the determination of thoron resulting from the gradual radiochemical conversion of radiothorium. Therefore, it was interesting to study in detail one of the previously investigated systems, this time by the use of radiothorium. Magnesium hydroxide was precipitated from an alkaline solution of magnesium nitrate and was thoroughly washed with distilled water. A nitric acid solution of radiothorium containing 0.36 g ThO_2/ml was used as the emanation source. Radiothorium was introduced into the sample by the use of a method described by Jagitsch [4] – a magnesium hydroxide suspension was saturated with the indicated solution then evaporated over a water bath until the residue acquired a consistency convenient for the making of tablets. Hydroxide tablets were dried at 100° and left for 25-30 days to achieve a radiochemical equilibrium.

As is well known [5], tetravalent thorium ion precipitates from its nitrate chloride, and other solutions as the hydroxide at pH 3.51-3.60. Since the pH of dissolved magnesium hydroxide was 10, then it is obvious that in this case we had a complete precipitation of radiothorium. Radiothorium was bound very tightly to the magnesium hydroxide precipitate and could not be removed by washing with water.

A comparison between the emanating powers of magnesium hydroxide samples with different amounts of radiothorium introduced by impregnation indicates (see Table 1) that the amount of thoron isolated increases linearly with increase in the radiothorium contents, i.e., the emanation coefficient remains practically constant while the quantity of radiothorium trapped varies considerably. The data obtained agree with the assumption that the radiothorium atoms are homogeneously distributed, evidently in the form of microheterogeneous true solid solutions. Let us note that when magnesium hydroxide is dehydrated the formation of solid thorium dioxide and magnesium oxide solutions is so much more probable since the crystal structures of both oxides are similar.

By using radiothorium as the indicator element, we were able to study flow emanation [6, 7] in the process of preparation of a magnesium oxide catalyst. A sample of magnesium hydroxide with the incorporated radio-

thorium was placed into a quartz vessel which was then introduced into a thermally regulated electric furnace. At a fixed temperature, we passed through the sample a stream of dry air at a rate which ensured the maximum activity of the thoron for a given length of path to the electrometer (mark SG-1M). Water vapor formed during dehydration was frozen out in a trap submerged in a −78° cooling bath, and the stream of air containing thoron was passed through calcium chloride drying tubes. The electrometer was calibrated before the experiment with a thoron standard under similar conditions. The emanating power of thoron (measured at the experimental temperature) was expressed by the number of divisions through which the quartz thread in our instrument passed in a minute for each gram of magnesium hydroxide used. The degree of dehydration was determined by weighing. The specific surfaces of initial magnesium hydroxide, magnesium hydroxide samples at various stages of conversion, and of magnesium oxide samples prepared by dehydration at various chosen temperatures were computed from the n-heptane adsorption isotherms by the BET method.

TABLE 1

Dependence of the Emanating Power and the Emanation Coefficient of Magnesium Hydroxide on the Amount of Radiothorium Incorporated

Radiothorium incorp. per 1 g of $Mg(OH)_2$	Emanating power in g per 1 g of $Mg(OH)_2$	Emanation coefficient in %
$3.4 \cdot 10^{-4}$	$0.52 \cdot 10^{-4}$	15
$1.8 \cdot 10^{-3}$	$1.89 \cdot 10^{-4}$	10
$6.2 \cdot 10^{-3}$	$8.33 \cdot 10^{-4}$	13.4
$1.6 \cdot 10^{-2}$	$2.1 \cdot 10^{-3}$	13.2

Kinetic curves for the change in emanating power with time in the course of magnesium hydroxide dehydration were determined at 320, 350, 400, 450, 550, 600, 700, 800, and 1080° (see Fig. 1). Simultaneously, at fixed time intervals, we determined the percent of hydroxide converted to the oxide.

As may be seen from Fig. 1, at 320 and 350° the emanating power smoothly increases with time. At the end of dehydration the evolution of thoron slows down considerably, and is accompanied (after 90% conversion) by a slight decrease in the emanation coefficient. The smooth nature of the radioactivity vs. time function is disturbed at a dehydration temperature of 400° — a diffused maximum appears at about 75% conversion. At

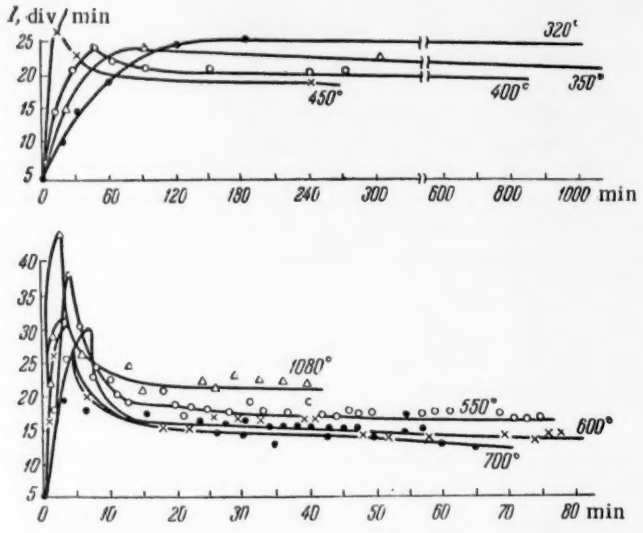

Fig. 1. Change in the emanating power of thoron (expressed in electrometer divisions per minute) during the dehydration of magnesium hydroxide at various temperatures.

450° a clearly outlined maximum is formed and corresponds to 70-80% conversion. As the dehydration temperature is further raised the radioactivity maximum becomes sharper and sharper, shifting toward shorter times (of the process). At temperatures above 500° the maximum can only be conjectured since it falls within the time interval during which the sample warms up to the reaction temperature. In all the cases the maximum

corresponded to a high percent conversion of hydroxide to oxide, and neither a maximum nor a minimum in radioactivity were observed at the beginning of the process.

The characteristic form of the kinetic curves for the change of emanating power vs. time at any experimental temperature evidently depended on the interaction between dehydration, which increased the specific surface, and the thermal fusion, which decreased it. The processes are characterized by different temperatures and time dependence, which determine the form and nature of the kinetic curves for the changes in emanating power shown in Fig. 1.

Simultaneously, with the measurements of the emanating power of magnesium hydroxide during dehydration, we carried out some measurements of its specific surface at various stages of conversion. We set up for this special experiments which involved interrupting the dehydration, measuring the emanation coefficient at room temperature, and determining the magnitude of the specific surface of the investigated samples. Just as in a preceeding investigation [1] (where the emanation coefficient was determined with radon), if the conversion depth was constant, we observed a linear dependence between the emanation coefficient based on thoron and the specific surface.

It was interesting to follow up the effect of dehydration temperature on the relationship between the emanation coefficient and the specific surface at practically complete conversion of magnesium hydroxide to oxide.

Figure 2 shows the curves for the change in the emanation coefficient and specific surface with respect to dehydration temperature of magnesium hydroxide at a constant conversion of 94-96%. As one may see from the figure, the emanating power of magnesium oxide samples (measured at room temperature) and the specific

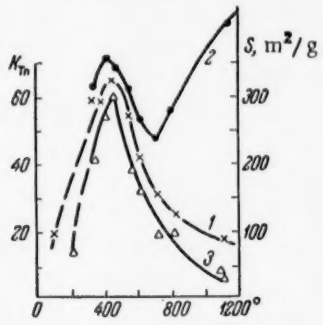

Fig. 2. Changes in the emanation coefficients of thoron measured at room temperature (1) and at the experimental temperature (2); and the specific surface (3) as a function of the magnesium hydroxide dehydration temperature.

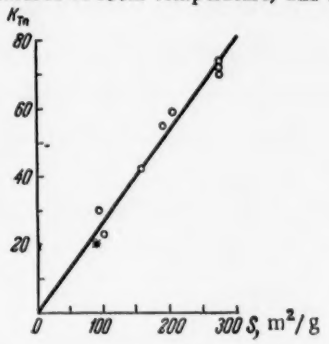

Fig. 3. Emanation coefficient of thoron measured at room temperature as a function of the specific surface of magnesium oxide samples obtained through dehydration at various temperatures. The asterisk refers to magnesium hydroxide.

surface both increase with increase in temperature, pass through a maximum at a dehydration temperature of 450°, then decrease. This mutual change in two structural characteristics of a solid results in a linear dependence between them, which is apparent in Fig. 3. Let us note, that the emanation coefficient and the specific surface values obtained with magnesium hydroxide samples at various dehydration depths as well as those obtained with magnesium oxide samples prepared at various magnesium hydroxide dehydration temperatures fall on the same straight line.

A more complex relationship is observed when the emanation coefficient is measured at the temperature of the topochemical process. In the 320-600° temperature range this coefficient changes side by side with the specific surface and the emanating power measured at room temperature, while the numerical values of both coefficients are almost the same. Deviations from this dependence show up at 700°, and if the temperature is further raised, sharp increase in the high-temperature emanation coefficient takes place accompanied by a decrease in the specific surface and low-temperature emanation coefficient.

It is interesting to analyze the possible causes of the difference observed in the dependence of emanation coefficients on the specific surface and on dehydration temperature.

The linear dependence between the emanation coefficient measured at room temperature and the specific surface can obviously be explained by the fact that the thoron produced is only eliminated from the surface layers of the investigated magnesium hydroxide and oxide samples, whereupon the nature of the distribution of the radiothorium indicator atoms is more or less the same in different samples. A similar type of thoron elimination takes place in the 320-600° temperature range. At higher temperatures (700° and up) the elimination mechanism changes. Evidently, as a result of increased atomic mobility in the crystal lattice, not only the surface but the whole volume begins to take part in the elimination of thoron. With a further rise in temperature the atomic mobility in the lattice and the structural break-up increase even more, which results in a sharply increased emanating power. Thus, at 1080° the emanation coefficient attains 81%, i.e., almost all the thoron formed in the sample is being eliminated. It is interesting that the temperature at which the nature of thoron evolution begins to change, which phenomenon is connected with the emergence of atomic mobility in the magnesium oxide crystal lattice, is far below the Tamm temperature at which sintering begins.

LITERATURE CITED

[1] G. M. Zhabrova, M. D. Sinitsyna and S. Z. Roginskii, Proc. Acad. Sci. USSR 117, No. 2, 255 (1957).•

[2] A. M. Rubinshtein, B. A. Zakharov, N. A. Pribytkova, and V. A. Afanas'ev, Proc. Acad. Sci. USSR 103, No. 6, 1134 (1955); 103, No. 1, 83 (1955).

[3] S. A. Ballard, M. D. Finch, and D. E. Winkler, Chemistry and Chemical Technology 12, 103 (1957).

[4] R. Jagitsch, Zs. Phys. Chem. B, 181, 215 (1937).

[5] Gmelins Handbuch d. anorg. Chem. 44, Thorium und Isotope, 1955.

[6] Coll. Pract. Works on Radiochemistry, Edited by I. E. Starik, A. N. Murin, A. P. Ratner, Leningrad, 1956.••

[7] H. Kaiser, Zs. Elektrochem. B, 58, No. 8, 601 (1954).

Received September 24, 1958

•Original Russian pagination. See C.B. Translation.

••In Russian.

THE EMULSIFYING ACTION OF HIGHLY DISPERSED SOLIDS

A. F. Koretskii and A. B. Taubman

Institute of Physical Chemistry, Academy of Sciences USSR

(Presented by Academician P. A. Rebinder, August 27, 1958)

Among the solid emulsifiers used in the preparation of commercial emulsions, bentonite occupies a special place; when peptized its hydrophilic particles produce a highly dispersed suspension with a tendency to structure formation.

However, even with the help of bentonite, in the absence of adsorbing layers of alkali metal soaps of a special composition, stable emulsions of pure hydrocarbon oils (as we have already shown in [1]) can only be obtained if the system contains a considerable amount of a solid phase (not less than 4%) which ensures the formation of a three dimensional hydrophilic coagulating structure. In the presence of the above mentioned adsorption layers, which possess pronounced structural and mechanical properties, the concentration of a solid emulsifier required for a lasting stabilization sharply decreases, until it corresponds to a monomolecular layer per drop [2].

With other hydrophilic powders which are unable to form hydrophilic coagulants in water, stable emulsification under similar conditions (i.e., in the absence of alkali soaps) can only be achieved if a large amount of solid phase is present; this corresponds to the formation of a protective multilayer coating of loosely packed solid particles — a structural network on the surface of each drop. Evidently, in this case the hydrophobic coagulating structure can already exhibit such a network; the structure is formed by hydrophilic emulsifier particles whose surface is rendered hydrophobic by the proper orientation of the adsorption layers.

Concentrated 50% emulsions of nonpolar vaseline oil (purified with silica gel) and of oils made hydrophobic by the addition of surface active agents (fatty acids, alcohols, and amines) were prepared just as in [1] by vigorous mechanical stirring in the presence of solid emulsifiers; as emulsifiers, we used pure reagent grade samples of calcium carbonate, titanium dioxide, and silicon dioxide. A 75-80% degree of powder dispersion corresponded to a less than 3μ particle size.

The choice of emulsifiers was determined by the fact that in the series $CaCO_3$–TiO_2–SiO_2, as the basicity of these minerals decreased and acidity increased, their tendency towards a chemisorption interaction with admixtures of surface active agents in the oil phase changes radically. This interaction was taking place in the process of emulsification, when the oil drops came into cotact with the emulsifier particles.

The stability of emulsions was estimated from the time required for a partial destruction and the separation of half the emulsified oil into a separate phase. Emulsions which were not destroyed within two days were considered stable (marked with an ∞ sign by Figs. 1 and 2).

As may be seen from the curves of stability (τ) vs. emulsifier concentration (C_s) in Fig. 1, highly dispersed particles which differ in their molecular nature form stable emulsions at very different solid phase concentrations. These differences are connected not only with the intrinsic inhomogeneity (mosaic structure) of particle surface (so that separate portions of the particle can be selectively wetted by both emulsion phases), but also with the possibility of forming a hydrophobic coagulating structure in the emulsion system.

Insignificant, frequently analytically undetectable acidic impurities seem to be always present, even in purified hydrocarbon oils, and in sufficient amounts to form on the surface of $CaCO_3$ particles a reactive

(toward the Ca portion of the compound) chemisorbed hydrophobic shell – an adsorbed layer of a Ca-soap, essential for the subsequent structure formation. Under these conditions at a relatively high C_s (not less than 2.5%) a stable emulsion of the oil water type is formed (Curve 1). Since titanium dioxide interacts much less with oleic acid,* at least 15% of it are needed to give the emulsion a lasting stabilization (Curve 2). At the same time the shape of the curves shows that, if C_s is even insignificantly decreased below the indicated values, a sharp decrease in stability results (for example, for $CaCO_3$ at C_s = 2.5% τ > 48 hours, but at C_s = 2.0% τ is only 2 hours). Finally, silicon dioxide, which is inert toward acidic compounds, regardless of its contents in the system does not form any emulsions at all (Curve 3).

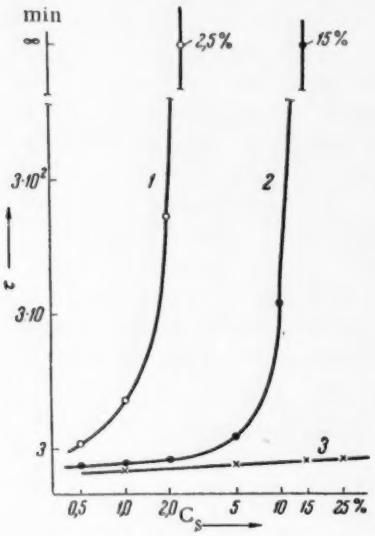

Fig. 1. Stability of a vaseline oil emulsion as a function of the solid emulsifier concentration. 1) $CaCO_3$; 2) TiO_2; 3) SiO_2.

The dependence of the emulsifying action on the contents of additives specially introduced into the oil phase to render it hydrophobic is shown in Fig. 2 and graphically confirms what was already said before. (These emulsions were prepared with only 2% emulsifier suspension, and, as was shown in Fig. 1, no emulsification would have occurred if the additives were absent. As one would expect, SiO_2 would not act as an emulsifier at any oleic acid concentration (Curve 1), but with TiO_2 emulsification sharply increased with the acid concentration, displaying maximum action at $C_{max} \approx 10^{-2} - 10^{-1}$%, after which, excessively hydrophobic surface reduced the stability of emulsions and converted it back into an oil phase as the particles migrated in solution (Curve 2).

Thus, as a result of a stabilized structure formed by the emulsifier particles under optimum hydrophobic conditions, the solid phase contents required for stable emulsification can be decreased appreciably; meanwhile there will be a transition from a loose multilayer coating on the surface of each drop to a thin protective layer which already possesses some structure.

Emulsifier particles, when rendered hydrophobic, show a similar effect on calcium carbonate (Curve 3) but due to its high reactivity of maximum action of oleic acid is observed at considerably lower acid concentrations ($C_{max} \approx 10^{-3}$%). When the oleic acid is replaced with pelargonic (Curve 4), due to a weaker hydrophobic action and a consequent lowering in the stability of the structure formed, the maximum emulsification is actually displaced toward higher concentrations of the added acid ($C_{max} \approx 10^{-2}$%). The fact that it is possible to activate inert silicon dioxide with basic additives is in full accord with the above described results. As may be seen in Fig. 2, 5, the oil which contains octadecylamine in place of oleic acid forms a stable emulsion in the presence of SiO_2 due to the fact that in this case a hydrophobic chemisorbed layer is formed on its surface [4].

On the other hand, it should be pointed out that cetyl alcohol, which formed only reversible loosely bound adsorbed layers on the solid surface, did not show any effect on the emulsifying action of the powders studied by us.

Everything so far indicates that any strong stabilization, necessary to obtain stable long lasting emulsions of the type oil/water with the help of small quantities of solid hydrophilic emulsifiers, can only be produced by sharply increasing the natural mildly pronounced mosaic nature of their crystal lattice surface. This type of a secondary "induced" mosaic nature is characterized by the widest possible variation in the molecular nature (with respect to selective wetting of the emulsion by both phases) of individual surface segments, and it may

*In the technology of oil paints and varnishes the "chalking" phenomenon in titanium white is well known, it consists of a gradual loss of free pigment from the dried paint cover due to the poor quality of the soap formed by TiO_2 and the fatty acids in the oil [3].

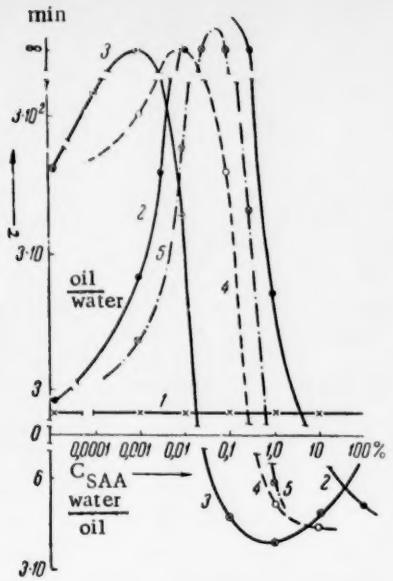

Fig. 2. Stability of emulsions as a function of the nature of the emulsifier and the contents of surface active substances–water repellents in the oil phase. 1) SiO_2, SAA* – oleic acid; 2) TiO_2, SAA – oleic acid; 3) $CaCO_3$, SAA – oleic acid; 4) $CaCO_3$, SAA–pelargonic acid; 5) SiO_2, SAA – octadecylamine.

be produced by partially covering the surface with chemisorbed hydrophobic layers of surface active agents bound irreversibly to it by covalent bonds [5].

At the optimum balance in the distribution of hydro- and oleophilic radicals (in the presence of an oil) on the particle surface, stable emulsions are formed protectively covered by hydrophobic coagulating structures [6]. These structures arise in the emulsion system when strong bonds are formed not only between particles and drops but also between emulsified particles on the water side of the emulsion.

The possibility of forming such structures on account of acidic impurities contained in many technical oils was disregarded by many authors, which also led them to interpret incorrectly the mechanism of emulsification by solid emulsifiers; they assumed a simple adhesion between a single layer of particles and the drop-medium surface on account of wetting forces [7-10]. Besides, oddly enough, they did not consider the fact that the emulsifier concentrations used exceeded by far the amounts required to form a monomolecular film on the oil phase drops. For the sake of comparison we may point out that according to our data in order to form such a film, if for example $CaCO_3$ powder with the usual degree of dispersion were used, we would need 2.5-3.0% of solid relative to the oil, whereas concentrations of the order of 25-30% of solid phase were usually used in these works [9, 10].

LITERATURE CITED

[1] A. B. Taubman and A. F. Koretskii, Proc. Acad. Sci. USSR, 120, No.1, 126 (1958).••

[2] A. B. Taubman and A. F. Koretskii, Colloid. J. 20, No. 5, 676 (1958).••

[3] W. Harkins, H. Ryan, and W. Hans, Ind. and Eng. Chem. 24, 1288 (1932); 36, 86 (1932).

[4] A. V. Kiselev, Coll. Chemical Surface Compounds and Their Role in the Adsorption Phenomena, Moscow 1957, p. 90;••• Proc. Acad. Sci. 106, No. 6, 1046 (1956).

[5] P. A. Rebinder, M. E. Lipets, M. L. Rimskaya, and A. B. Taubman, Physical Chemistry of Flotation Processes, 1933;••• P. A. Rebinder, Bull. Acad. Sci. USSR, Div. Math. and Nat. Sci. 5, 705 (1936).

[6] P. A. Rebinder, 3rd All-Union Conference on Colloid Chemistry, 1956, p. 7;••• P. Rebinder, Disc. Farad. Soc. 18, 151 (1954).

[7] W. Ramsden, Proc. Roy. Soc. 72, 156 (1903); W. Clayton, Emulsions, Theory and Technical Applications (IL, 1950, p. 366) [Russian translation]; U. Pickering, J. Chem. Soc. 91, 2010 (1907); W. Ramsden and K. Brook, Nature, 112, 671 (1923).

[8] P. Finkle, H. C. Draper, and J. H. Hildebrand, J. Am. Chem. Soc. 45, 2780 (1923); L. N. Mukerjee and S. N. Srivastava, Koll. Zs. 147, 146 (1956); 149, 35 (1956); 150, 144 (1957).

[9] D. L. Talmud and S. D. Sukhovol'skaya, J. Phys. Chem. 2, No. 1, 1 (1931).

[10] J. H. Schulman and J. Leja, Trans. Farad. Soc. 50, 598 (1954).

Received August 27, 1958

*SAA = Surface active agent.

••Original Russian pagination. See C.B. Translation.

•••In Russian.

THE THEORY OF THERMAL DETONATION OF CONDENSED EXPLOSIVES

A. G. Merzhanov and F. I. Dubovitskii

Institute of Chemical Physics, Academy of Sciences USSR

(Presented by Academician N. N. Semenov, September 9, 1958)

Elimination of gaseous products formed during the decomposition of explosives away from the reaction zone has a considerable effect not only on the formal kinetic laws governing the course of reaction under isothermal conditions, but also on the thermal equilibrium in nonisothermal decompositions. Due to this, the thermal detonation of condensed explosives can not in the majority of cases be described by the present theory so suitably developed by N. N. Semenov [1], D. A. Frank-Kamenetskii [2], and D. M. Todes [3] for the gaseous systems.

In the present work we will analyze a more general theory which takes into account the removal of a part of the reaction products from the reaction zone, and for explosives in the liquid state enables one to calculate all the fundamental characteristics of a thermal detonation: critical conditions, depth of predetonation decomposition, and the induction period.

Let us introduce the following symbols: V = reaction volume; V_0 = initial size of the reaction volume; m = mass of the material; m_0 = initial mass; d = diameter of the charge (in cm); l = initial charge length (in cm); T = average temperature of the material (in degrees); T_0 = temperature of surrounding medium (in degrees); t = time (in seconds); Q = heat of reaction (cal/cm^3); E = activation energy (cal/mole); k_0 = coefficient (1/sec); λ = thermal conductivity (cal/cm · sec · deg); c = specific heat (cal/g · deg); ρ = density (g/cm^3); η = depth of conversion; θ = dimensionless firing; τ = dimensionless time.

We will assume that the elimination of gaseous products from the reaction zone is in a state of quasi-equilibrium. This is justified at low rates of gas generation, where the outflow of gaseous products proceeds much faster than the reaction itself. For substances which remain practically undecomposed at the melting point there is always a temperature interval in which these conditions hold.

Under the conditions of quasi-equilibrium the reaction volume can be considered to be a homogeneous fluid, undisturbed by the bubbles of the evolving gases, while the relative volume change in the decomposition process may be taken to be proportional to the depth of conversion $\frac{V_0 - V}{V_0} = \mu\eta$. In the majority of cases the proportionality coefficient μ is constant for each substance. For gaseous systems $\mu = 0$. For most condensed explosives μ is almost one.

The removal of any gaseous products from the reaction zone has to be considered not only in the expressions for the rate of heat evolution (due to the increased fraction of the initial substance in a unit volume), but also in the expressions for the rate of heat conduction (on account of decreased geometrical dimensions).

The rate of heat evolution per unit volume is $\frac{Q}{1 - \mu\eta}\frac{d\eta}{dt}$. In the limiting case where $\mu = 1$ (all the products are gases) the reaction zone contains only the starting material and the specific decomposition rate appears in the expression for the inflow of heat.

According to Frank-Kamenetskii the rate at which heat is flowing out by the process of conduction from a vertical cylinder* is

$$4e\left[2{,}00+0{,}21\left(\frac{d}{l}\right)^2\frac{1}{(1-\mu\eta)^2}\right]\frac{\lambda}{d^2}(T-T_0).$$

We will neglect the heat exchange at the upper face of the cylinder.

Thus, in our case the system of equations describing a thermal detonation will look as follows:**

$$\gamma\frac{d\theta}{d\tau}=\frac{e^\theta\varphi(\eta)}{1-\mu\eta}-\frac{1}{\varkappa_\infty}\left[1+\frac{1}{\nu^2(1-\mu\eta)^2}\right]\theta, \tag{1}$$

$$\frac{d\eta}{d\tau}=e^\theta\varphi(\eta). \tag{2}$$

Initial conditions: $\tau=0$, $\theta=0$, $\eta=0$;

$$\eta=\frac{1}{\mu}\left(1-\frac{m}{m_0}\right);\quad \varkappa_\infty=\frac{1}{8e}\frac{Q}{\lambda}\frac{E}{RT_0^2}d^2k_0e^{-E/RT_0};$$

$$\theta=\frac{E}{RT_0^2}(T-T_0);\qquad \nu=3{,}08\frac{l}{d};\quad \tau=k_0e^{-E/RT_0}t;\quad \gamma=\frac{c\rho}{Q}\frac{RT_0^2}{E};$$

$\varphi(\eta)$ is a function defining the law according to which a reaction under isothermal conditions proceeds.

In calculating the gas evolution, we were obliged to introduce a new parameter μ into the system of equations. Besides this, parameters $\varkappa_\infty$ and ν, which appear in the gaseous reaction system in a combined form $\frac{1}{\varkappa}=\frac{1}{\varkappa_\infty}\left(1+\frac{1}{\nu^2}\right)$, now appear separately.

The removal of gaseous decomposition products from the reaction zone will have a substantial effect on the thermal detonation only in cases where the depth of the pre-explosion reaction is comparatively large. For reactions with normal kinetics the detonation occurs at low conversion depths, and the change in the reaction volume has to be considered mainly in calculating the corrections for the burning out during the induction period. From the point of view of the present theory the most interesting reactions are the ones which become self-accelerating under isothermal conditions.

Let us analyze a simpler and at the same time a more commonly encountered case – autocatalytic reactions of the 1st order. As was shown earlier [4], for the decomposition of liquid explosives autocatalyzed by the condensed end products

$$\varphi(\eta)=\left(\eta_0+\frac{\eta}{1-\mu\eta}\right)(1-\eta),$$

where η_0 is a criterion of the autocatalytic behavior. The solution of a quasi-stationary [5] system of equations yields the following expressions:

Critical conditions

$$\frac{1}{e\varkappa_\infty}=\frac{1-\mu\eta_0}{2\mu^2}\left\{\sqrt{\left[1+\frac{\nu^2}{(1-\mu\eta_0)^2}\right][1+(1-\mu)^2\nu^2]}-\left(1+\frac{1-\mu}{1-\mu\eta_0}\nu^2\right)\right\}; \tag{3}$$

*A vertical cylinder is most convenient for the analysis since in this case the charge model is not deformed in the decomposition process, while the change in geometrical dimensions (cylinder height) can be readily computed mathematically.

**The system is presented in a dimensionless form with the usual thermodynamic approximations and assumptions.

depth of pre-explosion decomposition,

$$\eta_{exp} = \frac{1 + \frac{2\mu}{e\varkappa_\infty} - \eta_0(1+\mu) - \sqrt{\left[\frac{1+(1-\mu)(1-\mu\eta_0)}{\mu}\right]^2 - 4\left(1 + \frac{\mu^2}{e\varkappa_\infty} - \mu\eta_0\right)\left(\frac{1-\mu}{\mu^2} + \frac{1}{e\varkappa_\infty \nu^2}\right)}}{2\left(1 + \frac{\mu^2}{e\varkappa_\infty} - \mu\eta_0\right)}; \tag{4}$$

induction period,

$$\tau_{ind} = \frac{1}{2\mu} \int_{\theta_0}^{1} \frac{[a + \sqrt{a^2 - 4\mu^4 F(\theta)\Phi(\theta)}]\,(1-\theta)\,e^{-\theta}}{\theta F(\theta)\sqrt{a^2 - 4\mu^4 F(\theta)\Phi(\theta)}}\, d\theta, \tag{5}$$

where

$$a = [1 + (1-\mu)(1-\mu\eta_0)]\,\nu, \quad F(\theta) = \frac{1-\mu\eta_0}{\mu^2} + \frac{1}{\varkappa_\infty}\theta e^{-\theta},$$

$$\Phi(\theta) = \frac{1-\mu}{\mu^2}\nu^2 + \frac{1}{\varkappa_\infty}\theta e^{-\theta};$$

θ_0 is calculated from the expression $\theta_0 e^{-\theta_0} = \kappa\,\eta_0$.

An analysis of Equation (1)–(2) and Formulas (3) – (5) shows that for condensed explosives the magnitudes of κ, η_{exp}, and τ_{ind} on the explosion boundary depend on the parameter ν which characterizes the conditions under which the experiment is carried out. Such a dependence arises as a consequence of increased effective heat transfer coefficient in the process of decomposition and is not needed in gaseous systems.

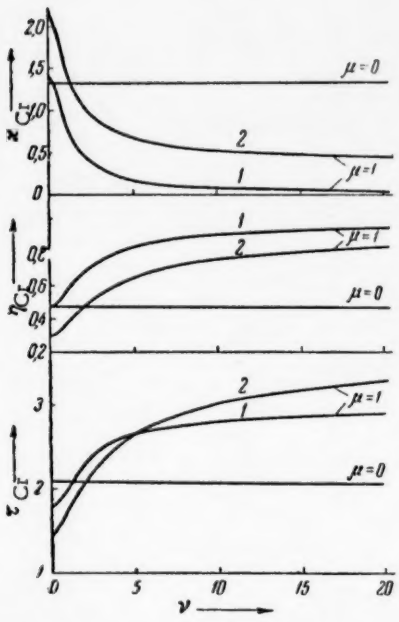

Fig. 1. Dependence of the critical condition κ_{Cr}, depth of pre-explosion decomposition under critical conditions η_{Cr}, and induction period under critical conditions τ_{Cr} on the parameter ν at $\eta_0 = 0.05$. 1) Autocatalysis by the condensed decomposition end products; 2) by the gaseous products.

In the case where the decomposition in a closed vessel is autocatalyzed by the gaseous end products $\varphi(\eta) = (\eta_0 + \eta)(1 - \eta)$. The critical condition looks as follows in the parametric form:

$$\frac{1}{e\varkappa_\infty} = \frac{2[1 + \mu(1-\eta_0)]\,\eta_{Cr} - 3\mu\eta_{Cr}^2 - [1 - \eta_0(1+\mu)]}{2\mu(1 - \mu\eta_{Cr})},$$

$$\nu^2 = \frac{2[1 + \mu(1-\eta_0)]\,\eta_{Cr} - 3\mu\eta_{Cr}^2 - [1 - \eta_0(1+\mu)]}{(1 - \mu\eta_{Cr})^2[\mu\eta_{Cr}^2 - 2\eta_{Cr} - \eta_0(1-\mu) + 1]}.$$

The depth of pre-explosion decomposition and the induction period can be easily computed numerically.

Some characteristics of a thermal detonation can be obtained within the framework of Frank-Kamenetskii's stationary theory. Analyzing δ and δ_{Cr} as functions of the conversion depth:

$$\delta = \frac{Q}{\lambda}\,\frac{E}{RT_0^2}\,\frac{d^2}{4}\,k_0 e^{-E/RT_0}\,\frac{\varphi(\eta)}{1 - \mu\eta},$$

$$\delta_{Cr} = 2{,}00 + 0{,}21\left(\frac{d}{l}\right)^2 \frac{1}{(1 - \mu\eta)^2},$$

by using the condition that $\delta = \delta_{Cr}$, it is possible to find expressions for the explosion limit and depth of pre-explosion decomposition. It is possible to apply Frank-Kamenetskii's theory to complex processes only under the conditions where the whole process occurs much slower than the explosion itself.

With heat transfer by convection (easily accomplished by vigorously stirring the substance) the thermal equilibrium equation looks as follows:

$$\gamma \frac{d\theta}{d\tau} = \frac{e^{\theta}\varphi(\eta)}{1-\mu\eta} - \frac{1}{\varkappa'_{\infty}}\left[1 + \frac{1}{\nu'(1-\mu\eta)}\right]\theta;$$

where

$$\varkappa'_{\infty} = \frac{1}{4}\frac{Q}{\alpha} d \frac{E}{RT_0^2} k_0 e^{-E/RT_0}, \qquad \nu' = 4\frac{l}{d},$$

α is a coefficient for the heat transfer from the inside surface of the vessel to the surrounding medium.

Expression for the thermal detonation characteristics can be obtained from the solution for a quasi-stationary system.

In Fig. 1 we have presented by results of some calculations.

LITERATURE CITED

[1] N. N. Semenov, Chain Reactions., Leningrad, 1934.*

[2] D. A. Frank-Kamenetskii, J. Phys. Chem. 13, 738 (1939).

[3] O. M. Todes, J. Phys. Chem. 13, 858 (1939); 13, 1594 (1939); 14, 1026 (1940).

[4] F. I. Dubovitskii, G. B. Manelis, and A. G. Merzhanov, Proc. Acad. Sci. USSR 121, 668 (1958).**

[5] A. G. Merzhanov and F. I. Dubovitskii, Proc. Acad. Sci. USSR 120, 1068 (1958).**

Received June 4, 1958

*In Russian.

**Original Russian pagination. See C.B. Translation.

THE RELATIONSHIP BETWEEN THE THERMAL DISSOCIATION RATE CONSTANTS OF DIATOMIC MOLECULES IN THE PRESENCE AND ABSENCE OF EQUILIBRIUM

E. E. Nikitin and N. D. Sokolov

Institute of Chemical Physics, Academy of Sciences USSR

(Presented by Academician V. N. Kondrat'ev, July 7, 1958)

Rice [1, 2] and Careri [3-5] have analyzed the thermal dissociation of diatomic molecules.

$$AB + M \rightarrow A + B + M$$

The latter, on the basis of simple collision theory [6], started with the assumption that molecular dissociation could take place through a direct transition from the lower vibrational levels of the bound state to the dissociated state. Theoretical calculations supported by direct experimental data (see for example [7]) indicate, however, that in molecular collisions the energy that is transferred with any appreciable probability is small compared to the dissociation energy.

In his calculations Rice [1, 2] began with the correct assumption that the transition of molecules into the continuous energy range takes place from the higher vibrational levels, but he did not take into account the disturbed Boltzman distribution in the molecular vibrational states, and it is this disturbance that is responsible for the nature of the thermal dissociation of diatomic molecules [15].

When the Boltzman distribution in the vibrational states of the dissociating molecule is disturbed, the number of occupied vibrational levels near the dissociation boundary decreases. This is connected with the fact that the transition rate of strongly vibrationally excited molecules into states with a continuous energy spectrum is much faster than the rate at which the molecules pass into the dissociation boundary; gradually the Boltzman distribution becomes more and more upset due to the decreased number of vibrational quanta near the dissociation boundary. Meanwhile, the dissociation constant will be determined by the rate at which vibrationally excited molecules are transferred to the upper vibrational levels. In connection with this, one would expect that the kinetics of the thermal dissociation and recombination would not obey the usual kinetic equation

$$\frac{d}{dt}[AB] = -k_d[AB][M] + k_r[A][B][M], \tag{1}$$

where k_d and k_r are constants determined by these two equations respectively,

$$k_d = -\frac{d}{dt}[AB]/[AB][M], \quad k_r = \frac{d}{dt}[AB]/[A][B][M], \tag{1a}$$

which describe the initial stages of the dissociation and recombination reaction.

In so far as the dissociation constitutes a multistage process, the kinetics of dissociation and recombination should be described by the following system of equations (for the sake of simplicity we will assume that [M] = 1)

$$\frac{d}{dt} x_n = -\sum_k P_{nk} x_n + \sum_k P_{kn} x_k, \tag{2}$$

Here x_n denotes a distribution function, i.e., the degree of occupancy of the n-th energy level of the AB system, while p_{kn} are the rotational and vibrational $k \to n$ transition probabilitites in the molecule AB. The summations in expression (2) include also the states in the continuous region of the spectrum, for which it should be understood that the summation over n involves integration over energy E where in this case $x_n \equiv x(E)\,dE$ and $P_{kn} \equiv P_{kE}$. Under the conditions where $[AB] \ll [M]$ the interaction between the AB molecules may be neglected, and consequently in that part of summation which corresponds to the rotational and vibrational transitions and to the dissociation of AB molecules, the number p_{kn} and P_{kE} do not depend on x_n and $x(E)$. At the same time, during the combination there is a real interaction just between the recombining atoms, leading to a linear relationship between the corresponding recombination probability P_{En} and $x(E)$, and also to a quadratic dependence between the recombination rates and atomic concentrations.

Let us analyze a simpler case where, if $[AB] \ll [M]$, then the $[A]_0$ and $[B]_0$ concentrations remain constant. In this case the system of Equations (2) becomes linear and can be rewritten in the form

$$\frac{d}{dt} \hat{X} = \hat{B}\hat{X} + \hat{C}[A]_0[B]_0, \tag{3}$$

where the single column of the $\hat{X}$ matrix consists of components of the distribution function x_n, while matrices $\hat{B}$ and $\hat{C}$ describe the subsequent dissociation and recombination respectively. A general solution of Equation (3) has the form

$$\hat{X} = \sum_\mu a(\mu)\hat{L}(\mu)\exp(-\mu t) + \hat{X}_0, \tag{4}$$

where μ is the real values of the matrix $\hat{B}$ ($\mu > 0$); $\hat{L}(\mu)$ = matrix constructed from the components of real vectors in matrix $\hat{B}$, which correspond to the real values of μ; $a(\mu)$ = arbitrary coefficients determined by the initial conditions, and $\hat{X}_0$ = a particular solution of the nonhomogeneous Equation (3).

The first real value of the $\hat{B}$ matrix (μ_0) corresponds to the dissociation rate constant and in the absence of recombinations can be determined from the expression [8]

$$\mu_0 = -\frac{d}{dt}[AB]/[AB]. \tag{5}$$

Under these same conditions (absence of recombinations) it is obvious that μ_0 coincides with k_d which was defined by Equation (1a). The second real value of the $\hat{B}$ matrix (μ_1) is approximately equal to the rate of vibrational energy relaxation in molecule AB, whereupon the inequality $\mu_0 \ll \mu_1$ is fulfilled [8, 9]. If the observation time t exceeds considerably the vibrational relaxation time, i.e., $t \gg 1/\mu_1$, then it follows from Equation (4) that the distribution function will be damped exponentially, which corresponds to dissociation. Since the relaxation time of translational motion is shorter than that of vibrational energy, then under the indicated conditions, we can assume that the energy distribution of atoms A and B is in a state of equilibrium. Then it is obvious that the solution of equation

$$\hat{B}\hat{X}_0 + \hat{C}[A]_0[B]_0 = 0 \tag{6}$$

will be an equilibrium distribution function

$$x_n^{(0)} = N\exp(-E_n/kT). \tag{7}$$

Let us now find the value of the constant N. One usually postulates that Equation (1) is valid for all values of [AB], [A], and [B], in particular at equilibrium $\left(\frac{d}{dt}[AB] = 0\right)$. However, we have no grounds to assume that numbers k_d and k_r will have the same values at equilibrium as at the initial stages of the dissociation and recombination reaction, where Equations (1a) hold. Therefore, in a general case one should introduce equilibrium values for the dissociation $k_d^{(0)}$ and the recombination $k_r^{(0)}$ rate constants, which are related

to the equilibrium constant K by the relation

$$\frac{[A]_0[B]_0}{[AB]_0} \equiv K = \frac{k_d^{(0)}}{k_r^{(0)}}. \tag{8}$$

Substituting Equation (7) in (8) and assuming that $[AB]_0 = \Sigma x_n^{(0)}$, we will find the constant coefficient in Equation (7):

$$N = \frac{k_r^{(0)}}{k_d^{(0)}} Q^{-1}, \tag{9}$$

where Q is the partition function for molecule AB.

Thus, when $t \gg 1/\mu_1$ the kinetics of thermal dissociation and recombination may be described by equation

$$[AB] = a \exp(-k_d t) + \frac{k_r^{(0)}}{k_d^{(0)}} [A]_0[B]_0. \tag{10}$$

At the same time integration of the inexact kinetic Equation (1) gives

$$[AB] = a \exp(-k_d t) + \frac{k_r}{k_d} [A]_0[B]_0. \tag{11}$$

Expression (10) and (11) are different, since, as one may readily see, the ratios $k_r^{(0)}/k_d^{(0)}$ and k_r/k_d are not equal to each other. Actually, under ordinary experimental conditions the recombination rate constant k_r will have the same value in the equilibrium as well as the nonequilibrium process. In fact, the experimental recomination rate constants of, for example, Br or I at T = 300° K are equal to 10^{-32} cm^6/mole^2·sec $\approx 10^{15}$ cm^6/mole^2·sec. In the recombination experiments the concentrations of Br and I atoms did not exceed several millimeters of Hg, i.e., about 10^{-7} moles/cm^3. The recombination reaction rate in this case was less than $10^{15} \cdot 10^{-7} \cdot 10^{-7}$ [M] sec^{-1} = 10 [M] sec^{-1}. At the same time it is known that the deactivation of vibrationally excited molecules occurs at practically every collision; under ordinary temperatures the number of collisions $Z \simeq 10^{14}$ cm^3/mole · sec. In addition, to this the deactivation rate of excited Br_2* or I_2* molecules is equal to $10^{14} \cdot 10^{-7}$ [M] sec^{-1} = 10^7 [M] sec^{-1}, i.e., much greater than the rate of the initial recombination process. It follows from this that the rate of the nonequilibrium recombination process is determined by the rate of transition (of atoms A and B) from states in the continuous energy spectrum to any of the upper levels in molecule AB. Moreover, the recombination equilibrium constant, when determined, turns out to be exactly equal to the rate constant of the latter process.

On the other hand, the equilibrium dissociation rate constant $k_d^{(0)}$ exceeds the rate constant of the nonequilibrium process k_d. This is due to two causes; greater occupancy of upper vibrational levels at equilibrium and the effects of long-range forces. The dependence of equilibrium dissociation rate constant on these forces follows from the work of Russel and Simons [14], who established a parallel relationship between k_1 (consequently $k_d^{(0)} = Kk_r$) and the degree of van der Waal's interaction among molecules M. The long range forces, however, do not effect the rate constant of the nonequilibrium dissociation (k_d), since they evidently are only effective in transitions from only the highest vibrational levels to the states of continuous energy spectrum, i.e., these forces determine that rate of the fastest stage.*

*Due to the difference between k_d^0 and k_d, there is no point in trying to combine into one interpolated formula the dissociation rate constants obtained from direct measurements of the nonequilibrium process (at high temperatures)with the ones calculated for the equilibrium conditions (at low temperatures) as was done, for example, by Palmer and Hornig [10]. One of us committed the same error in one of his communications [9].

The calculated values of k_d for the thermal dissociation of I_2, Br_2, and O_2 give a satisfactory agreement with the experimental values determined kinetically for molecular dissociation caused by a shock wave in an argon atmosphere at 1500-4000° K [10-12]. For example, for the thermal dissociation of bromine at T = 2000° K, we obtained in accordance with [9],

$$k_d \approx 4 \cdot 10^{14} \exp(-D/kT) \text{ cm}^3/\text{mole} \cdot \text{sec}.$$

According to Palmer and Hornig [10], the experimental value of k_d^0 at this temperature is

$$k_d^0 = 5 \cdot 10^{14} \exp(-D/kT) \text{ cm}^3/\text{mole} \cdot \text{sec}.$$

At other temperatures for which direct measurements are available the experimental dissociation constants exceed the theoretical ones by not more than a factor of 2 to 3.

According to Willard* the value of k_d for bromine dissociation at 300 °K is

$$k_d^{(0)} = 10^{16} \exp(-D/kT). \quad (12)$$

Formulas derived in [9] give for the same temperature

$$k_d = 10^{15} \exp(-D/kT).$$

Thus, the equilibrium dissociation rate constant is one order of magnitude larger than the nonequilibrium value.

A series of authors [1, 13] have noted the large value of the coefficient in Expression (12) for $k_d^{(0)}$ as compared with the gas kinetic number of collisions $Z \simeq 10^{14}$. This discrepancy can be explained, first by the causes which are responsible for making $k_d^{(0)}$ larger than k_d, and second, by factors such as rotation of the dissociating molecule [9], presence of several stable electronic states [1], and some increase in the molecular dimensions on account of vibrational excitation.

LITERATURE CITED

[1] O. K. Rice, J. Chem. Phys. 9, 259 (1941).

[2] O. K. Rice, J. Chem. Phys. 21, 750 (1953).

[3] G. Careri, Nuovo Cim. 6, 94 (1949).

[4] G. Careri, Nuovo Cim. 7, 155 (1950).

[5] G. Careri, J. Chem. Phys. 21, 749 (1953).

[6] R. Fowler, E. A. Guggenheim, Statistical Thermodynamics (IL, 1949) [Russian translation].

[7] J. C. McCoubrey and M. D. McGrath, Quart Rev. 11, 87 (1957).

[8] E. E. Nikitin, Proc. Acad. Sci. USSR 116, 584 (1957).**

[9] E. E. Nikitin, Proc. Acad. Sci. USSR 119, 526 (1958).**

[10] H. B. Palmer and D. F. Hornig, J. Chem. Phys. 27, 98 (1957).

[11] D. Britton, N. Davidson, and G. Schott, Disc. Farad. Soc. 17, 58 (1954).

[12] M. Camac, J. Camm et al. Chemical Relaxation in Air, Oxygen and Nitrogen, prepr. No. 802, Inst. Aeronaut. Sci., 1958.

[13] N. N. Semenov, Some Problems in Chemical Kinetics and Reactivity, Izd AN SSSR, 1954, p. 148.***

[14] K. E. Russel and J. Simons, Proc. Roy Soc., A. 271 (1953).

[15] B. J. Zwolinski and H. Eyring, J. Am. Chem. Soc. 69, 2702 (1948).

Received July 11, 1958

*Cited in [10].

**Original Russian pagination. See C.B. Translation.

***In Russian.

THE BEHAVIOR OF SULFATE ION IN THE ELECTROLYTIC PREPARATION OF MAGNESIUM

S. A. Pushkareva and E. A. Ukshe

Bereznikov Branch of the All-Union Aluminum-Magnesium Institute

(Presented by Academician A. N. Frumkin, July 31, 1958)

As was shown in papers [1-4], in the presence of sulfates there is an appreciable decrease in the yield of magnesium (for a given amount of current) electrolyzed from the fused chlorides. However, up until now the mechanism of this phenomena has not been discovered, despite the fact that it is of some interest not only for the solution of a series of practical problems but also for a fuller understanding of the kinetics involved in the electrolytic preparation of metals from their fused salts.

Since the electrolysis of fused magnesium salts is usually done in an electrolyte containing besides magnesium, potassium, and sodium chloride, also some dissolved metallic magnesium [5], it seems probable that at 700° the following equilibrium is established,

$$Mg^{+2} + 3\,Mg + SO_4^{-2} \rightleftarrows 4\,MgO + S, \qquad (I)$$

and is strongly displaced to the right, due to the fact that under the electrolysis conditions the standard free energy change for reaction (I) is about −267,170 kcal/mole.

However, the majority of workers claim that elementary sulfur could not remain for a long time dissolved in fused chlorides due to its low boiling point (441°). Therefore, a further reaction between sulfur and metallic magnesium to give sulfide is usually assumed, yet it is still not understood how the sulfide would affect the cathodic process.

We have established that when the sulfate ion (in the form of $MgSO_4$) is introduced into the fused chloride which contains metallic magnesium, then the electrolyte acquires a blue color and the color intensity increases if more sulfate is added. The blue color becomes detectable at 0.05-0.1 wt. % of $SO_4^{=}$ in solution, but if a large amount of magnesium oxide is suspended in the melt, the color disappears while a bluish sludge deposits on the bottom of the cell.

To find out why the melt becomes colored we carried out a series of experiments to test the effect of various sulfur compounds on the electrolyte color. The experiments were carried out in quartz cells in an argon atmosphere.

It was shown that:

1) When magnesium sulfate was introduced into fused $MgCl_2$ + KCl free of metallic magnesium, or in the presence of solid magnesium ($t < 650°$) no color appeared.

2) When $MgSO_4$ was introduced into fused $MgCl_2$ + KCl free of magnesium, sulfur, sulfites, or thiosulfites the blue color appeared, yet a qualitative analysis of the solidified salt failed to show any $SO_3^{=}$, $SO_4^{=}$, or $S^{=}$ ions.

3) In cases where the blue color was observed in the melt, we noticed that some elementary sulfur was being deposited on the walls of the quartz tube as time went on.

These qualitative experiments permit the assertion that when various sulfur compounds are introduced into the melt, then either due to the high temperature ($SO_3^=$, $S_2O_3^=$) or as a result of a reaction with dissolved magnesium ($SO_4^=$) they actually decompose to yield elementary sulfur, which evidently is soluble in the fused chloride and distills off very slowly.

The sulfur probably forms polymers or rings in the electrolyte of the composition S_8, S_6, etc.; these possess high surface activity in an ionic solution and can be adsorbed on the solid cathode to form a film which by impairing the wet contact between magnesium and the cathode leads to the formation of a more dispersed magnesium. This in its turn is connected with the decreased yield (for a given amount of current) due to a higher rate of solution and the anodic oxidation of the metal [6].

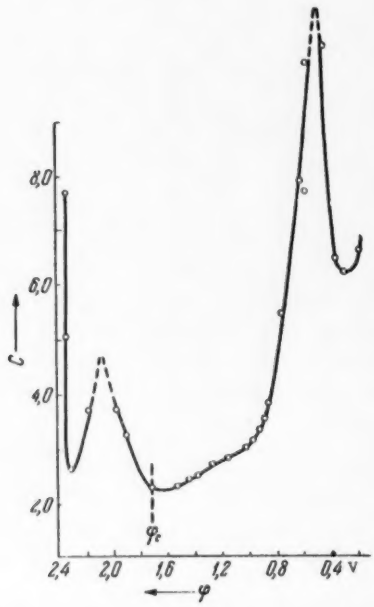

Fig. 1. Capacity of a double layer as a function of potential in fused chlorides. Electrolyte contents: KCl + NaCl + $MgCl_2$ (0.8 mole %), $SO_4^=$ 0.05 wt %. T = 720°, f = 500 hertz.

In order to varify this assertion, we measured the capacities of an electrolytic double layer on a molybdenum surface in fused chlorides. Measurements were done with an impedance bridge whose regulating arm consisted of variable resistors and condensers connected in series, while the two reference arms had a 1 mf capacitor each. A ZG-10 audio-frequency generator was used as the source of alternating current. An electronic oscillograph EO-7 was used as the balance indicator.

The experiments were carried out in a procelain crucible which was placed in a shaft electric furnace with automatically regulated temperatures. A layer of liquid magnesium (into which about 1.5 mole % of lead was added to increase the weight) severed simultaneously as the reference and the auxiliary electrode. A molybdenum wire was fused in a quartz tube and its end (approximate surface about 10^{-3} cm^2) served as the investigated electrode. A small amount of magnesium chloride (about 0.8 mole %) dissolved in a eutectic mixture of potassium and sodium chlorides served as the electrolyte. At 700° the potential of a magnesium electrode in this melt was about −2.9 v (on the chlorine potential scale). An LP- 5 vacuum-tube potentiometer was used to measure the molybdnum potential vs. the magnesium electrode. The amount of magnesium sulfate added corresponded to about 0.5 wt. % of $SO_4^=$ in solution.

Before beginning the experiment, we subjected the electrolyte for 1 hour to a direct current by using a special cathode. During this the Mg^{++} concentration in the melt changed, and therefore, we had to determine the magnesium contents after the experiment was over.

We used for our capacity measurements a 15 mv alternating current with a frequency of 500-1000 hertz. The results of these measurements are presented in Fig. 1.* The capacity vs. potential curve we obtained was quite reproducible and had the following characteristics:

1) The curve had two clear desorption peaks, and the peak on the cathode branch of the curve always seemed more pronounced than the one on the anode.

2) While in pure electrolytes a pronounced minimum was observed on the capacity vs. potential curve, in the presence of sulfur this minimum appeared spread out and slightly displaced toward more negative potentials.

*Due to unsufficiently smooth molybdenum surface the specific capacity values in our experiments are somewhat too high.

3) In the region of maximum desorption periodic fluctuations of capacity (attaining about 50% of the peak) were observed on the anodic branch of the curve.

4) When temperature was raised the minimum shifted slightly toward more positive potentials.

It is still difficult at the present time to give a full interpretation to the picture obtained due to a lack of reliable data on the structural properties of electric double layers in fused salts. However, it is entirely obvious that the presence of two desorption peaks on the C vs φ curve indicates that the adsorbed material is sulfur, a constituent of the uncharged particles. On the basis of the preceding discussion the most likely hypothesis is that the melt contains polyatomic polymers of type S_n with a high surface activity.

In concluding we consider it a pleasant duty to express out deep gratitude to B. N. Kabanov and D. I. Leikis for their comments on the results of this work.

LITERATURE CITED

[1] F. Oettel, Zs. Elektrochem. u. angew. phys. Chem. 2, 394 (1895).

[2] B. V. Strokan, Trans. Sci. Res. Inst. of Light Metals, No. 10, 22 (1934).

[3] A. A. Rudnitskii and I. P. Tverdovskii, J. Appl. Chem. 9, 26 (1936).

[4] Z. V. V..sil'ev and B. V. Popov, Trans. All-Union Alum.-Mag. Inst., No. 11-12, 169 (1935).

[5] A. I. Zhurin, Metallurgy 4, 87 (1935).

[6] E. L. Strelets, Trans. All Union Alum.-Mag. Inst. No. 39 (1957).

Received July 25, 1958

THE INFRARED SPECTRA OF WATER, ETHANOL, AND METHANOL ADSORBED ON CHROMIC OXIDE

L. M. Roev and Academician A. N. Terenin

A. A. Zhdanov Leningrad State University

Infrared spectroscopy provides one of the most fruitful methods for the study of adsorption and catalysis [1-5]. With its help it has been possible to establish the existence of a number of different adsorption centers on the surface of silicate adsorbents [2] and on that of an aluminosilicate catalyst [3]. Such centers consist of surface OH groups, and also groups of a second kind, which behave as electron acceptors. Infrared spectroscopy allows us to study the mechanism of catalytic reactions by establishing what is the primary step in the interaction of the reacting molecule with the catalyst. A. A. Babushkin and his co-workers[4] have confirmed spectroscopically that surface compounds are formed when alcohols are adsorbed on aluminum oxide.

In the present work the authors set out to explain the mechanism of the decomposition of alcohols on Cr_2O_3. The transition metal oxides, and in particular Cr_2O_3 and Fe_2O_3, are of great interest since on their surfaces it is possible to postulate several catalytically active centers. Cr_2O_3 is a catalyst for the dehydrogenation and for the dehydration of alcohols [6-7].

The Cr_2O_3 preparation at our disposal was obtained by the combustion of ammonium dichromate. Cr_2O_3 obtained in this way is catalytically active for the decomposition of alcohols [8] and has a high specific surface (176 m^2/g), which was also a determining factor in the choice of material for the present work. •

The Cr_2O_3 powder was pressed between NaCl plates to form a layer of thickness corresponding to 6-8 mg/cm^2. The conditioning of the surface was carried out by heating in air at 500° for 2 hours, followed by pumping continuously for $1\frac{1}{2}$ hours at 450°. After this the sample was cooled and its spectrum recorded, after which adsorption of vapor was allowed to go on for one hour. The preparation of the sample in vacuo, adsorption of the substance under consideration, and spectroscopic examination were carried out in a special vacuum cell described in [11]. The thickness of the free space through which the light beam passed was such that the vapor filling it did not contribute to the infrared absorption at the pressures used. Spectra were taken with a NaCl prism on an IKS-11 spectrograph. The spectra illustrated are expressed in terms of I/I_0, where I is the transmission of the sample after adsorption of the substance under investigation, and I_0 the transmission before adsorption. Such a presentation gives the clearest picture of the situation since spectra in the region 1500-1700 cm^{-1} are badly interfered with by the atmospheric water bands. The spectral range studied was between 800 and 1700 cm^{-1}. The transmission of samples in the 6-8 mg/cm^2 thickness range was about 10% at about 1800 cm^{-1}. The spectra were taken with slit widths ranging from 15-20 cm^{-1}.

H_2O. Adsorption of H_2O was carried out at 20° and at a vapor pressure of 4 mm. In Fig. 1 is shown the Cr_2O_3 spectrum after adsorption. In the region 800-1700 cm^{-1} the following absorption lines appear: 1645, 1492, 1336, 1180, 1042, 936 and 850 cm^{-1}. Besides these lines, which all have sharp maxima, it may be observed that there is an increase in general background over the whole region studied (800-1700 cm^{-1}).

•The Cr_2O_3 used was prepared at our request, and its surface area measured, by V. A. Komarov, to whom, we are very grateful. A second sample, which was also used in the investigation, was obtained from Academician A. A. Balandin, to whom we also refer our thanks.

Curve 2 in Fig. 1 shows the spectrum of the same sample after desorption of the H_2O for 1 hour at 20°.

The broad and intense absorption band at 1645 cm^{-1} belongs to water in the capillary condensed phase. The peaks at 1492, 1336 and 118 cm^{-1} obviously correspond to water molecules adsorbed on Cr_2O_3. The bonds to the surface are weak ones, since the absorption bands disappear on pumping out even at 20°.

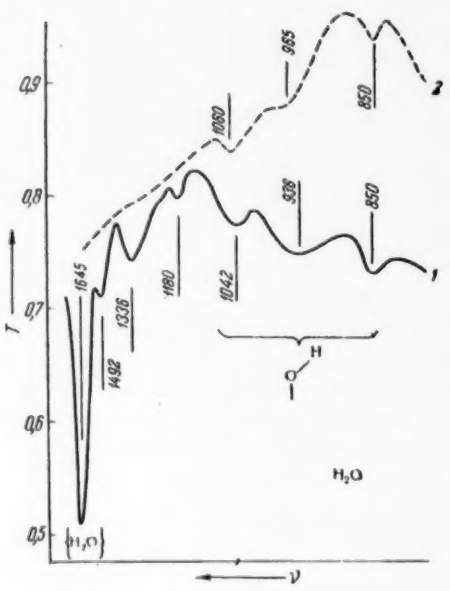

Fig. 1.

The peaks at 1042, 936 and 480 we may ascribe to OH groups, formed during the hydration process, which are bound to the surface. This assignment is based on the fact that most metallic hydroxides have their OH deformation frequencies in the region 600-1100 cm^{-1} [9]. Besides this, on pumping out, these bands, although they shift a little, do not disappear (Curve, Fig. 1). The shift obviously results from the removal of the interaction of the OH group with water molecules adsorbed or condensed on the surface.

The presence of such a large number of bands when water is adsorbed indicates the presence of several different types of adsorption centers on the Cr_2O_3 surface. As is well known, the OH deformation frequency of metallic hydroxides is very sensitive to the nature of the metal [9].

<u>C_2H_5OH.</u> The adsorption of ethanol vapor on Cr_2O_3 was carried out at a pressure of 40 mm and at two different temperatures, 20° and 150°. The sample was held under these conditions for one hour, after which it was cooled and the remaining vapor removed by pumping out at 20° for 15 min. Figure 2, Curve 1 shows the spectrum of Cr_2O_3 after absorption of C_2H_5OH at 20° and Curve 2 that after absorption at 150° and subsequent desorption at 20°.

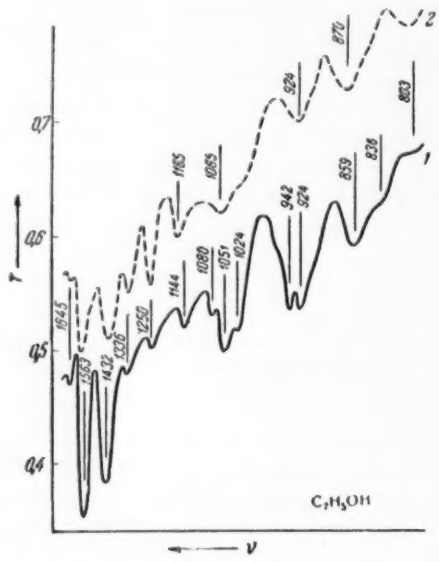

Fig. 2.

To simplify the interpretation, a comparison of the spectral lines observed is given in Fig. 3. It can be seen that the peaks at 1645, 1336, 942 and 859 correspond closely to the bands appearing when water is adsorbed on Cr_2O_3. From this it follows that the bands at 1645 and 1336 cm^{-1} are due to water molecules split off from the alcohol, and those at 942 and 859 cm^{-1} to surface OH groups. The desorption carried out at 20° for 15 min was obviously insufficient.

The presence of a peak at 1563 and the group of peaks at 803, 836 and 924 cm^{-1} indicates that when C_2H_5OH is adsorbed on Cr_2O_3, a compound is formed on the surface which possesses a carbon-carbon double bond. It is well known that the out-of-plane =CH deformation vibration lies very characteristicslly in the region 800-1000 cm^{-1}, and the presence of bands in this region is sufficient to justify our speaking of a C = C bond. The band at 1563 cm^{-1} borders on the region characteristic of the C = C stretching frequency. However it is not possible to decide on the basis of the present data what unsaturated compound is formed on the Cr_2O_3 surface when alcohol is adsorbed. From the fact that several = CH frequencies are observed, we must assume either that several different compounds are formed or that there are different adsorption centers.

The broad band with a maximum at 1432 cm^{-1} consists of superposed deformation vibrations of CH_3, CH_2, and CH groups and cannot be used for analytical purposes.

The bands at 1058 and 1051 cm^{-1} appearing when ethanol is adsorbed at 20°, belong to ethanol molecules weakly adsorbed on the Cr_2O_3 surface (in methanol the corresponding band is at 1033 cm^{-1}). The bands at 1065 and 1165 cm^{-1}, which appear on heating, may clearly be assigned to the surface compound $Cr - O - \overset{|}{C} - \overset{|}{C} -$, by analogy with the interpretation of the spectrum of ethanol on Al_2O_3 made by A. A. Babushkin and A. V. Uvarov [4]. The band at 1024 cm^{-1}, which does not disappear when the adsorption is carried out at 150°, possibly belongs to chemisorbed C_2H_5OH molecules. The adsorption of C_2H_5OH on Cr_2O_3 at 150° (Curve 2, Fig. 2), leads to some shifting of the 1563, 1144 and 859 cm^{-1} bands, and also to a change in the relative intensity of several of the bands.

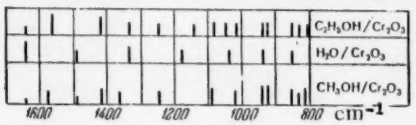

Fig. 3.

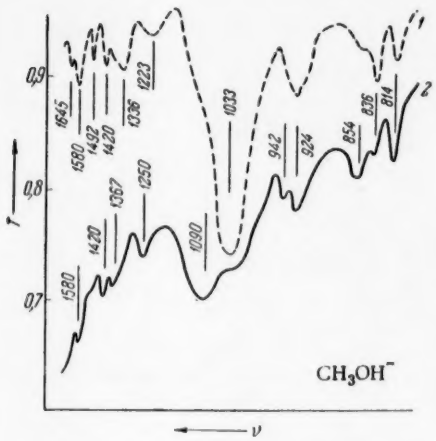

Fig. 4.

CH_3OH. The adsorption of methanol vapor was caried out at 20° and 150° at a pressure of 40 mm. Curve 1 of Fig. 4, corresponds to adsorption of methanol at 20° for 1 hour followed by desorption for 15 min at the same temperature. A comparison of the spectrum obtained with that of adsorbed C_2H_5OH (Fig. 3) shows that there is much common to both of them. The bands at 1645, 1492 and 1336 cm^{-1}, and the weak bands at 942 and 854 cm^{-1} may be assigned as before to H_2O molecules and OH groups split off from the alcohol molecule; the 1580 band, and those at 814, 836 and 924 cm^{-1} are attributed to the formation of a compound containing the C = C double bond. The intense 1033 cm^{-1} band (1051 and 1080 cm^{-1} for ethanol) belongs to the unbroken C-O bond of the CH_3OH molecule physically bound to the Cr_2O_3, but does not disappear on desorption at 20°. The band at 1223 cm^{-1} obviously corresponds to the 1250 cm^{-1} band which was observed when C_2H_5OH is adsorbed on Cr_2O_3.

Curve 2 of Fig. 4 shows the spectrum of Cr_2O_3 with adsorbed CH_3OH when both the adsorption and desorption were carried out at 150°. The relative intensity of the bands at 942 and 854 cm^{-1}, which belong to the OH group, has increased and that of the 1033 cm^{-1} band, which belongs to the C-O bond of physically adsorbed methanol, has decreased; meanwhile the band at 1223 cm^{-1} has shifted to 1250 cm^{-1}, obviously because of the decreased coverage of the surface, and a distinct band at 1090 cm^{-1} is exposed.

According to the data of Colthup and Bellamy [10], aromatic and unsaturated aliphatic ethers containing the group =C-O have a strong absorption band at 1250 cm^{-1}. The band at 1250 cm^{-1}, which appears when ethanol is adsorbed on Cr_2O_3, might therefore be attributed to the formation of adsorbed unsaturated ethers or of surface compounds such as $Cr - O - \overset{|}{C} = \overset{|}{C} -$. However, a similar band is also observed on the adsorption of methanol at 20°, in which case the formation of such compounds seems doubtful. The band at 1250 was also observed by A. A. Babushkin and A. V. Uvarov [4] when ethanol is adsorbed on Al_2O_3, and that at 1237 cm^{-1} when methanol is adsorbed on Al_2O_3. These authors ascribed the band to the Al-C linkage by analogy with compounds containing the Si-C bond, which show absorption at 1250 cm^{-1}. However, the observation of exactly the same frequency in the case of Cr_2O_3 throws some doubt on this interpretation, since it is hard to imagine that the Al-C and Cr-C bonds have identical frequencies.

On the basis of the interpretation of the spectra given here, we can say that even at 20° the adsorption of alcohols on Cr_2O_3 is accompanied by the following processes; a) splitting off of H_2O molecules and OH groups from the alcohols, with the formation of unsaturated compounds; b) elimination of hydrogen, with the

formation of surface compounds of the type Cr – O – C – in the case of methanol and Cr – O – C – C – in the case of ethanol. Increase of the temperature of adsorption to 150° does not substantially change the mode of decomposition of the alcohols.

Because of the complexity of the spectra obtained when alcohols are adsorbed on Cr_2O_3, it must be emphasized that our interpretation of the bands observed is not unambiguous, and that further experiments are required, using deuterated alcohols.

LITERATURE CITED

[1] A. N. Terenin, Zhur. Fiz. Khim. 14, 1362 (1940); N. G. Yaroslavskii and A. N. Terenin, Doklady Akad. Nauk SSSR 66, 885 (1949); V. N. Filimonov and A. N. Terenin, Doklady Akad. Nauk SSSR 109, 982 (1956); A. N. Sidorov, Zhur. Fiz. Khim. 30, 995 (1956).

[2] A. N. Sidorov, Doklady Akad. Nauk SSSR 95, 1235 (1954).

[3] L. M. Roev, V. N. Filimonov and A. N. Terenin, Optika i Spektroskopiya, 4, 328 (1958).

[4] A. A. Babushkin and A. V. Uvarov, Doklady Akad. Nauk SSSR 110, 581 (1956); A. A. Babushkin, A. V. Uvarov and A. A. Ignat'eva, Proc. 10th All-Union Symposium on Spectroscopy (in Russian) (1957) Vol. 1, p. 161.

[5] G. Pimental, J. Am. Chem. Soc. 75, 28 (1953); R. French and W. Wadsworth, J. Phys. Chem. 58, 805 (1954); R. P. Eischens, S. A. Francis, and W. A. Pliskin, J. Phys. Chem. 60, 194 (1956).

[6] P. Sabatier, Catalysis in Organic Chemistry (Leningrad, 1932).

[7] A. Eucken and K. Heuer, Z. physik. Chem. 40, 196 (1950).

[8] V. A. Komarov, E. A. Chernikova and V. M. Drozdova, Uchenye Zapiski Leningrad Univ. Ser. Khim. Nauk 9, 53 (1949); V. A. Komarov, Zhur. Fiz. Khim 27, 1754 (1954).

[9] O. Glemser and E. Hartert, Naturwiss 21, 552 (1953).

[10] N. B. Colthup, J. Opt. Soc. Amer. 40, 397 (1950); L. Bellamy, Infrared Spectra of Molecules [Russian Translation] (1957), p. 137.

[11] V. A. Nikitin, A. N. Sidorov and A. V. Karyakin, Zhur. Fiz. Khim. 30, 117 (1956).

[12] J. J. Kipling and D. B. Peakall, J. Chem. Soc. 1957, 834.

Received October 6, 1958

THE MIGRATION CURRENT ON A ROTATING DISC ELECTRODE

V. D. Yukhtanova

M. V. Lomonosov Moscow State University

(Presented by Academician A. N. Frumkin, September 18, 1958)

During electrolysis the oxidizable cations flow to the electrode surface by diffusion and migration. If the solution contains an excess of a supporting electrolyte, then the migration component of the limiting current can be made insignificantly small. In the region of highly dilute supporting electrolytes the migration component of the limiting current constitutes a large fraction of the total current, and therefore one should correct for it when calculating the true diffusion current.

Ilkovic and Hyrovsky [1], Kolthoff [2], and Levich [3] gave various expressions for the migration current on a mercury drop electrode. However, at a low relative concentration of the supporting electrolyte the measurements on a drop electrode present considerable experimental difficulties, and therefore no one has until now verified these equations experimentally with any degree of precision.

As early as 50 years ago Eucken gave the correct expression for the migration current during stationary electrolysis. If all the ions present in solution are univalent and the reducible cation has an anion in common with the supporting electrolyte, then Eucken's formula looks as follows:

$$I = 2I_d [M - \sqrt{M(M-1)}], \qquad (1)$$

where I_d is the limiting diffusion current in the absence of migration, while M is the ratio between the total anion concentration and the concentration of the reducible cation.

It seems that Eucken's formula has not been so far verified experimentally except by the author himself. Eucken's measurements were not accurate enough and covered only a small range of M values.

Eucken's results were given for an unstirred electrolyte, but they could be transposed to other cases if the electrolysis were carried out under strictly stationary conditions, for example, on a rotating disc electrode. The purpose of this investigation was to verify Eucken's formula at relatively low concentrations of the supporting electrolyte. If the supporting electrolyte is in a considerable excess (for example, by beginning with a 10 fold excess), Eucken's formula can be written in a more convenient form, namely

$$I = I_d \left[1 + \frac{1}{4}\frac{C_0}{C_1} - \frac{1}{8}\left(\frac{C_0}{C_1}\right)^2\right], \qquad (2)$$

where C_0 = concentration of the discharge cation, C = concentration of the supporting electrolyte.

Expression (2) was used in our preceding paper [5], and the experimental technique was also described there. The measurements were carried out by the compensation method with an amalgamated copper rotating disc electrode at 25° in a hydrogen atmosphere. The electrode potential was measured with reference to a 1 N calomel electrode. In all the cases the tip of the reference electrode jacket was placed as close as possible to the other electrode surface. To decrease the ohmic potential drop we tried to use as low as possible concentrations of the reducible cation (which is significant if the supporting electrolyte concentration is not too low) and proceeded in the order of decreasing electrode revolutions. The number of electrode revolutions was varied

in the 90-150 rpm range. In this range, the proportionality between current density and the square root of n.e.r.* was fulfilled just as required by Levich's formula. During each experiment we kept the rate of rotation constant. In the whole range of measurements, we observed good reproducibility in the experimental data.

In Fig. 1, we have drawn the polarization curves for Tl^+ ion.

Curve a was taken with a 50 fold excess of sodium perchlorate, i.e., under conditions where the action of the electric field on the reducible cation was practically nil, and the resulting current was a diffusion current. In this case the limiting current I = 5.4 μa.

The polarization Curve b was taken for Tl^+ ion at the same concentration but in the absence of inert electrolyte. Despite an appreciable ohmic potential drop, the curve had a suffuciently distinct plateau from which the limiting current could be computed readily, I = 10.6 μa. In this case the limiting current has increased to double (deviation was not more than 2%) the value it has at the same Tl^+ ion concentration in the presence of excess supporting electrolyte. The obtained dependence is in accord with Eucken's formula. Eucken was not able to obtain very clear plateaus for the limiting current in the absence of supporting electrolyte.

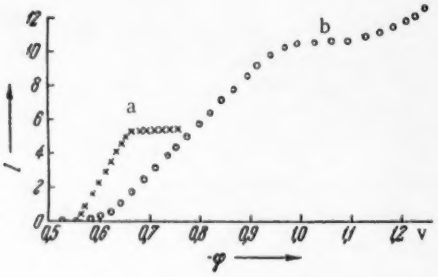

Fig. 1. Polarization curves for the reduction of Tl^+ ion: a) with excess of supporting electrolyte ($NaClO_4$); b) in the absence of supporting electrolyte.

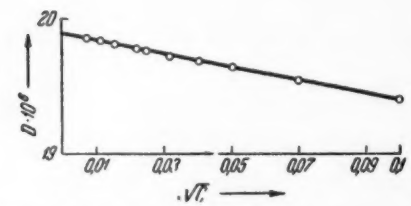

Fig. 2. Tl^+ diffusion coefficient as a function of the square root of the supporting electrolyte concentration.

Eucken's formula makes it possible to calculate true diffusion currents in the presence of highly dilute supporting electrolytes. Thus, in a series of measurements on the Tl^+ ion, by using the obtained diffusion currents, we calculated the diffusion coefficients according to Levich's formula; these coefficients, when plotted against the square root of the supporting electrolyte concentration, fell on a straight line (Fig. 2); extrapolation to infinite dilution gave the diffusion coefficient $D_e = 19.90 \times 10^{-6}$ which is in good agreement with the value calculated by the use of Nernst equation from the ionic mobility at infinitely dilute solutions, $D_\lambda = 19.94 \times 10^{-6}$ cm^2/sec. According to a recent paper by Gregory and Riddiford [6], a slight correction should be introduced into Levich's formula. Introduction of this correction is of no importance in the calculations on which Table 1 is based. These results may be considered to be the most reliable proof for the usefulness of Eucken's formula in calculating the migration current on a solid rotating electrode.

Since, as may be seen in Fig. 2, the diffusion coefficient is a function of the solution concentration while within the limits of a diffusion layer this concentration changes from $C_0 + C$, at a sufficiently large distance from the electrode, to $(C_0 + C_1)^{1/2} C_1^{1/2}$ at the electrode surface [7], then the choice of the concentration values to be used on the abscissa becomes difficult if the magnitudes of C_0 and C_1 are comparable. Therefore, in plotting Fig. 2, we used the mean concentration values, namely

$$\sqrt{1/2\,[(C_0 + C_1) + (C_0 + C_1)^{1/2} C_1^{1/2}]}.$$

If we disregard the dependence of the diffusion coefficient on the solution concentration in the range of sufficiently dilute solutions, then we can verify Eucken's formula in a more graphic, though somewhat less accurate form, and namely: by calculating I_d according to Levich's formula from the diffusion coefficient at infinite dilution, which was determined by extrapolation (as shown in Fig. 2) or calculated from the electrical conductance at infinite dilution (which is practically the same thing), and then comparing the calculated values

*n.e.r. = number of electrode revolutions.

of I_d with the experimental values of I. In Table 1, we have compared this determined I/I_d values with the ones calculated from Eucken's formula.

TABLE 1

M	I/I_d exper.	I/I_d calc. from Eucken's eq.
50	1.002	1.004
30	1.005	1.008
20	1.003	1.012
10	1.016	1.023
5	1.046	1.050
2	1.121	1.124
1	1.247	1.249

In concluding, we take a great pleasure in expressing out deep gratitude to Acad. A. N. Frumkin for some valuable comments in connection with this work.

LITERATURE CITED

[1] I. Kolthoff and D. Lingane, Polarography 1, 1952.

[2] D. Lingane and I. Kolthoff, J. Am. Chem. Soc. 61, 1045 (1939).

[3] V. G. Levich, Physicochemical Hydrodynamics, 1952.*

[4] A. Eucken, Zs. phys. Chem. 59, 72 (1907).

[5] V. D. Yukhtanova, Proc. Acad. Sci. USSR 120, No. 1 (1958).**

[6] D. Gregory and A. Riddiford, J. Chem. Soc. 1956, 3756.

[7] A. N. Frumkin, Proc. Acad. Sci. 117 USSR 117, No. 1 (1957).**

Received September 12, 1958

*In Russian

**See C.B. Translation.

THE SURFACE CHARGES OF SEMICONDUCTING OXIDES IN THE ADSORPTION OF GASES AND VAPORS

É. Kh. Enikeev, L. Ya. Margolis and S. Z. Roginskii, Corresponding Member, Acad. Sci. USSR

The Institute of Physical Chemistry of the Academy of Sciences of the USSR

A knowledge of the electrical state of the adsorbed molecules is essential for an understanding of the mechanisms of many surface processes. Although a number of papers have dealt with the surface charges which arise on semiconductors during the adsorption of various substances [1, 2] there is almost no data to indicate how these charges are affected by the type of bonding between the adsorbed molecules and the semiconducting surface. Measurement of the work function is a sensitive method for the detection of the surface charge [3].

The vibrating condenser technique [4] was selected for studying the relation between the adsorption and the surface charge. The experimental semiconductor, in powdered form, served as the fixed plate of the condenser, the vibrating plate being a gold sheet. The accuracy of the readings was approximately 0.01 v. Investigation was made of the adsorption of O_2, H_2, CO, CO_2, C_3H_6, and isopropyl alcohol vapors, on ZnO, V_2O_5, CuO and NiO, the first two being electronic, and the last two hole, semiconductors. The surface coverage by the adsorbent, θ, was determined manometrically and independently of the measurements of V_C. In the various experiments, θ ranged from 0.001 to 0.5-0.7. The specimens were heated (250-400°) under continuous evacuation to a vacuum of about 10^{-6} mm.

In Fig. 1, there is shown the relation between the contact potential, V_C, of NiO and the time of aging of a specimen which had earlier been held in an atmosphere of oxygen. The marked decrease in the work function is clearly due to the desorption of oxygen from the catalyst surface.

The high sensitivity of V_C to the amount of oxygen on a semiconducting oxide surface indicates that comparison of the work functions of specimens which have been held in an atmosphere of O_2 can be made only if the specimens have been treated under strictly comparable conditions.

Adsorption of the various gases and vapors, at room temperature and above, was studied after aging had led to an approximately constant value for the contact potential of the given semiconductor.

Table 1 presents data on the surface charges of semiconducting oxides in the adsorption of gases (at 20°). With the exception of oxygen, the adsorption of each gas either decreases the work function, i.e., the gas acts as an electron donor [5], regardless of the type of semiconduction (an inversion of charge sign for adsorption on n- and p-conductors, was not observed), or else leaves the work function unaltered (CO_2 and C_3H_6 on ZnO). It should be noted that the adsorption takes place very rapidly in this case, the desorption of each gas being almost complete at 80°; it is very likely that this adsorption is physical.

Confirmation of this conclusion is to be found in the adsorption of C_3H_6 on CuO (Fig. 2). In this case, there is also observed a rapid reversible adsorption, but at higher temperatures (50-120°), a fact which clearly points to the chemical nature of the process. There is an accompanying sharp decrease in the work function.

Oxygen, adsorbing firmly and irreversibly on NiO (20°), changes (diminishes) the work function still more markedly (Fig. 3).

TABLE 1

The Signs of the Surface Charges of Semiconductors In the Adsorption of Gases

Semi-conductor	Absorbate				
	O_2	H_2	CO	CO_2	C_3H_6
CuO	—	no adsorp.	+	unchanged	+
NiO	—	no adsorp.	+	unchanged	+
V_2O_5	—	+	+	unchanged	+
ZnO	—	no adsorp.	no adsorp.	unchanged	unchanged

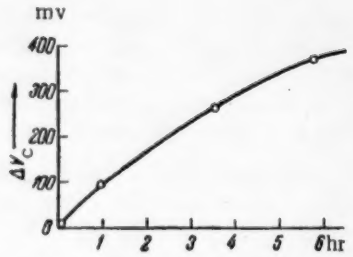

Fig. 1. The relation between the contact potential, V_C, and the time of aging of the specimen.

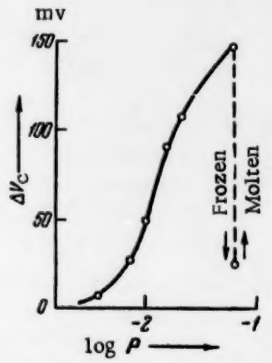

Fig. 2. The surface charge in the adsorption of C_3H_6 on CuO (80°).

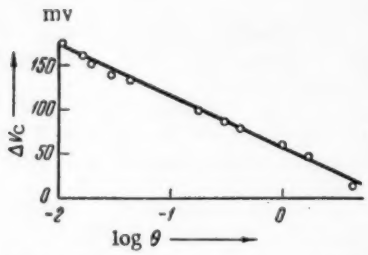

Fig. 3. The relation between the contact potential, V_C, and the degree of surface coverage.

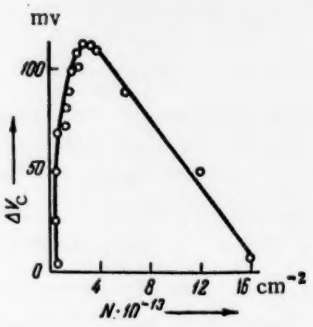

Fig. 4. The variation of the contact potential of ZnO in the adsorption of isopropyl alcohol (20°).

Peculiar results are observed in the adsorption of isopropyl alcohol vapors on ZnO at 20° (Fig. 4). The contact potential passes through a maximum (and the work function, through a minimum) when 10% of the adsorbent surface is covered with the alcohol. The work function falls on the left branch of the curve which is associated with the firm, irreversible adsorption of the alcohol, and rises on the right branch where the adsorption is weak and reversible. Desorption of the weakly bound portion of the alcohol takes place on elevating the temperature, and at 80° there remains of the $V_C(\theta)$ curve (θ is the surface coverage) only that left section which is associated with the firmly bound alcohol. Thus, the weak, reversible, adsorption of carbon dioxide

and propylene on ZnO at 20° does not bring about any alteration in the work function, whereas this same type of adsorption in isopropyl alcohol (the right branch of the curve of Fig. 4) increases this function. The weakly and reversibly adsorbed portion of the alcohol does not bring about any alteration in the surface charge, as has been shown by the measurements of electrical conductivity which have been carried out by G. M. Zhabrova on these same specimens.

In this case, it is possible that the change in the work function could be explained in terms of the dipolar nature of the adsorbed alcohol molecules as contrasted with the symmetry of the molecules of CO_2 and C_3H_6. Evaluation of the dipole from Fig. 4 actually gives $3 \cdot 10^{-8}$ cm, a result which is not too far from the accepted value of $1.38 \cdot 10^{-8}$ cm.

Thus, the measurment of differences in the contact potentials is a promising method for studying the character of the bonds which exist between the adsorbed molecules and a semiconducting surface.

LITERATURE CITED

[1] P. Aigrain and C. Dugas, Zs. Elektrochem. 56, 363 (1952); L. E. Germain, C. r. 236, 238, 345 (1954).

[2] H. I. Engel and K. Hauffe, Zs. Elektrochem. 57, 762 (1953); H I. Engel, Halbleiter Probleme, No. 1, 249 (1954); F. F. Vol'kenshtein, Bull. Moscow, Univ. 12, 79 (1957).

[3] V. I. Lyashenko and I. L. Stepko, Problems of Kinetics and Catalysis 8, 180 (1955).

[4] S. Rosenfeld and W. M. Hoskins, Rev. Sci. Instr. 16, 343 (1945).

[5] V. I. Lyashenko, Dissertation, Kiev, 1955.*

Received August 14, 1958

*In Russian.

AN INVESTIGATION OF THE ELECTRODE REACTIONS ON THE SILICON CATHODE

E. A. Efimov and I. G. Erusalimchik

(Presented by Academician A. N. Frumkin, September 11, 1958).

A number of papers [1-5] have shown the kinetics of the electrochemical reactions on the germanium electrode to be distinguished by certain peculiarities which arise from semiconduction in the metal. In this connection, it is of interest to determine the extent to which these same peculiarities can appear in other semiconducting materials such as silicon, especially so since the literature contains no work devoted to this problem.

By using polarization measurements, over the interval of current densities from 10^{-6} to 10^{-1} amp/cm^2, the present work has studied the electrolytic evolution of hydrogen, and the reduction of potassium ferricyanide, at t = 20°, on monocrystalline silicon of the p- and the n- types, oriented according to the 111 planes. The construction of the electrodes and the electrolyzer, and the technique of the polarization measurements, were the same as those described in [6]. Electrical contact with the silicon was made through an electrolytic deposit of rhodium. Prior to each experiment, the electrode was treated with a HF : HNO_3 mixture (1 : 2) and with 42% HF. The same results were obtained through a preliminary treatment of the electrode with boiling KOH (5-10%). A hydrogen half-cell served as the comparison electrode in the acidic solutions, and a calomel half-cell, in the alkaline solutions.

In Fig. 1, there is shown the relation between the logarithm of the current density in 2 N H_2SO_4 solutions and the hydrogen overvoltage on n- and p- type silicon of various specific areas, the minority carrier lifetime being 30-40 μ sec. These curves are practically coincident over the interval of current densities 10^{-6}-10^{-4} amp/cm^2, and have a slope of b = 0.18. Divergences are observed at higher current densities. Similar curves were obtained in 1 N KOH (Fig. 2). Each of the curves of Figs. 1 and 2 was developed with the electrolyzer completely darkened. Over the entire range of investigated current densities, illuminating the p-type silicon electrode (ρ = 10 ohm·cm) with a 200 candlepower arc lamp caused a 100-200 mv shift of potential in the positive direction. This effect was not observed with n-type silicon. Thus the hydrogen overvoltage curves for silicon are quite different from those for germanium [6] where the value of the overvoltage is independent of the type of conduction in the electrode.

It might be supposed, as Brattain and Garrett have done [1], that the curves of Fig. 1 diverge because of the suppression of the diffusion of electrons, the minority current carriers, from the interior of the p-type semiconductor to its surface. This would, however, scarcely correspond with the facts. If the deflection of Curve 1 at I $\approx 10^{-4}$ amp/cm^2 is due to the appearance of a limiting diffusional current of electrons, it is then difficult to admit that this same effect would arise at I $\approx 10^{-3}$ amp/cm^2 in n-type silicon where the electrons are the principal carriers. Moreover, if suppression of the electronic diffusion actually plays a decisive role in silicon, it could be anticipated that the deviation between Curves 3 and 4 would be much more pronounced than it is, and that these curves would not lie so close to Curve 1.

In our opinion, the differences existing between the curves of Fig. 1 arise, not from the effect of the type of conduction in the silicon on the hydrogen overvoltage, but rather from the ohmic potential drop in the impoverished layer of the semiconductor which is included in the measured value of the overvoltage. In order to confirm this supposition, the differential capacity of the silicon electrode was measured at a frequency of 200 kc. In sufficiently concentrated electrolytic solutions, the calculations of Bohnenkamp and Engell [5] have

shown the capacity of a semiconducting electrode to be fixed by the width of the impoverished layer, and not by the electrochemical processes. It would thus follow from our results (Fig. 3) that the maximum width of the impoverished layer and the largest ohmic potential drop would be shown by the p-type silicon with ρ = 10 ohm · cm. The p- and n-types with ρ = 25 ohm · cm would follow closely thereafter. Taking the four cases

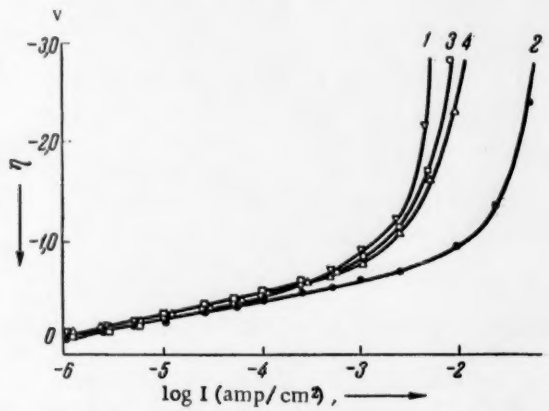

Fig. 1. The hydrogen overvoltage on silicon in 2 N H_2SO_4: 1) p-type, ρ = 10 ohm · cm; 2) n-type, ρ = 10 ohm · cm; 3) p- type, ρ = 25 ohm · cm; 4) p-type, ρ = 25 ohm · cm.

together, the maximum capacity and the minimum values of the width of the impoverished layer and the ohmic potential drop should be observed in the n-type silicon with ρ = 10 ohm · cm. The position of the curves in Fig. 1 is in full agreement with this interpretation.

In the light of these facts, it becomes understandable that there would be no sharp deflection of the η vs log I curve for germanium [6] at $I < 10^{-1}$ amp/cm². Measured under our conditions, the capacity of the germanium electrode at ρ = 1 ohm · cm is 10-90 mf/cm². This is much higher than the capacity of the silicon electrode (Fig. 3). It could thus be expected that the ohmic potential drop in the impoverished layer would distort the η vs log I curve at higher current densities. With germanium, supplementary experiments showed that such a distortion is actually observed at about $3 \cdot 10^{-1}$ amp/cm².

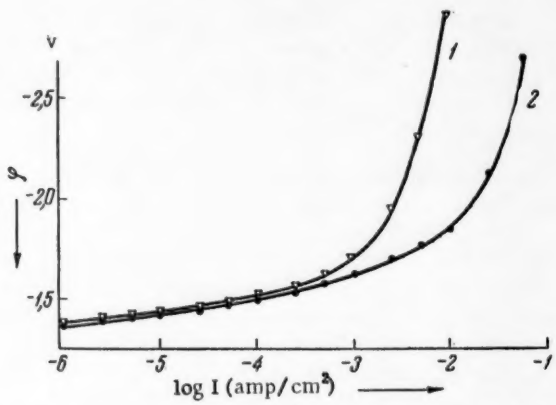

Fig. 2. The potential of the silicon cathode (vs the calomel electrode) in 1 N KOH: 1) p-type, ρ = 10 ohm · cm; 2) n-type, ρ = 10 ohm · cm.

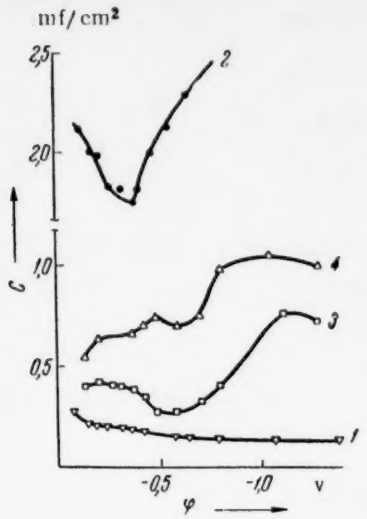

Fig. 3. The capacity of a silicon electrode in 2 N H_2SO_4: 1) p-type, ρ = 10 ohm · cm; 2) n-type, ρ = = 10 ohm · cm; 3) p-type ρ = 25 ohm · cm; 4) n-type, ρ = 25 ohm · cm.

Nevertheless, the action of illumination in diminishing the hydrogen overvoltage on p-type silicon by 100 - 200 mv indicates that there is a certain suppression of the passage of electrons from the interior of the semiconductor to its surface. However, this is not the principal cause of the hydrogen overvoltage. With silicon, just as with germanium, the kinetics of the hydrogen evolution is clearly limited by processes occurring in the electric double layer, rather than in the interior of the semiconductor. The high value of the coefficient b = 0.18 v is obviously related to a certain oxidation of the electrode surface at the higher negative potentials.

In order to interpret the effect of the type of conduction in the silicon cathode on the course of other electrochemical reactions, polarization curves were developed for the reduction of $K_3Fe(CN)_6$ (Fig. 4). It is to be seen from Fig. 4 that the kinetics of the ferricyanide reduction depends not only on the ionic concentration of the solution, but also on the type of semiconduction in the cathode, this latter factor being much more significant here than it is in the evolution of hydrogen. On illuminating an electrode of the p-type, Curve 3 is markedly displaced toward Curve 4. This indicates that the divergences between Curve 3 and 4, and 5 and 6, are the result of a deficiency of electrons on the surface of the p-type silicon.

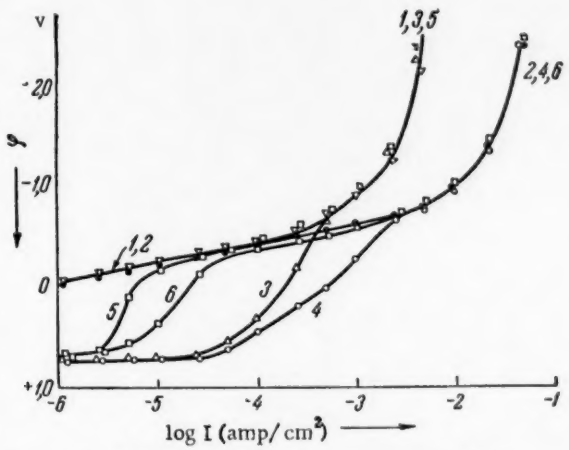

Fig. 4. Polarization of a silicon electrode during the reduction of potassium ferricyanide: 1) p-type in 2 N H_2SO_4; 2) n-type in 2 N H_2SO_4; 3) p-type in 2 N H_2SO_4 + 5 g/liter $K_3Fe(CN)_6$; 4) n-type in 2 N H_2SO_4 + 5 g/liter $K_3Fe(CN)_6$; 5) p-type in 2 N H_2SO_4 + 0.5 g/liter $K_3Fe(CN)_6$; 6) n-type in 2 N H_2SO_4 + 0.5 g/liter $K_3Fe(CN)_6$.

Thus these experiments show that semiconduction in the cathode variously affects the kinetics of various electrochemical reactions. The type of conduction is without influence on the evolution of hydrogen on germanium [6], but it affects this process on silicon to a certain degree, and quite markedly influences the ferricyanide reduction.

It is clear that the lower the electrochemical polarization of the cathodic reaction, the more marked is the effect of the semiconduction of the material constituting the electrode.

LITERATURE CITED

[1] W. Brattain and C. Garrett, Bell. Syst. Techn. J. 34, 129 (1955).

[2] D. Turner, J. Electrochem. Soc. 103,252 (1956).

[3] H. Gerischer and F. Beck, Zs. Phys. Chem. 13, 389 (1957).

[4] E. A. Efimov and I. G. Erusalimchik, J. Phys. Chem. 32, 413 (1958); 32, 1103 (1958).

[5] R. Bohnenkamp and H. Engell, Zs. Elektrochem. 61, 1184 (1957).

[6] E. A. Efimov and I. G. Erusalimchik, J. Phys. Chem. 32, vol. 9, (1958).

Received September 10, 1958

RESISTANCE OF SOME DEFORMED MATERIALS TO CORROSION CRACKING

Yu. S. Zuev and A. Z. Borshchevskaya

The Scientific Research Institute of the Rubber Industry

(Presented by Academician P. A. Rebinder, September 26, 1958)

One of the most dangerous types of structural breakdown is the so-called corrosion cracking which arises from the simultaneous action of a stress and an adsorptionally active and chemically agressive agent. The role of the surface active agent in such cases was first pointed out, and then extensively investigated, in the papers of P. A. Rebinder and his school [1-3]. Corrosion cracking is observed in many materials (metals [4], glasses [3], and plastics [5]) and is especially marked in rubbers which have been attacked by ozone [6, 7]. The present work aimed at disclosing other instances of corrosion cracking in rubbers, where determination could be made of the role of the chemical activity of the aggressive agent, its diffusibility and adsorbability. The working specimens were so chosen as to have the same thickness after extension. The relative error in the determination of the life (τ) of 20 specimens amounted to 4%.

Analysis of the results indicates that cracking will occur in a rubber when interaction with the aggressor results in a pronounced breakdown of the elements of the space lattice. Processes of this kind are known to occur in reactions between: ozone and unsaturated rubbers; HCl and HF, and polydimethylsiloxyl rubber (SKT [8]); Na_2S and HCl, solutions and thiokol which has been prepared from dichloroethylformal [9]; HNO_3 and polyisobutylene [10]; and acids and vulcanizates of carboxyl-containing rubbers [11]. Corrosion cracking* of the deformed specimen is observed in each of these cases, and in the action of nitrogen dioxide on polychloroprene, as well, the external picture being approximately the same in every instance (Fig. 1). On the other hand, it is known that the attack of NK, SKB and SKS by such agents as Br_2 and HCl is principally through reactions of combination and displacement. In these systems, cracking is not observed [6].

The effect of deformation on the rupture time. In the system SKT - HCl (gas), polychloroprene - nitrogen dioxide, and carboxyl rubber - HCl (gas)(see Fig. 2), the rupture time passes through a minimum (in the region of critical deformation, ϵ_{cr}) as the deformation increases, and then increases toward a definite limit as the deformation continued to rise. This is the same relation as has been observed earlier in the ozone cracking of practically all rubbers [12, 13]. More detailed investigations on a vulcanizate of the carboxyl-containing rubber SK-1-30 (5 parts per weight of MgO, and 2 parts per weight of stearin, per 100 parts of rubber) have made it possible to test the effects of various aggressive agents which react with different structural elements (ozone attacks the double bonds of the polymer, and acids, the cross-linkages) and to determine the effect of differences in the dissociation constants, and the adsorptional and diffusional properties of the acids relative to the polymer.

A comparison of ϵ_{cr} values for the action of various aggressors on SK-1-30 rubber (Fig. 2) show this quantity to be displaced toward higher deformations (about 90%) under the action of HCl, or CH_3COOH, than is the case for action under O_3 (about 40%). On the basis of our interpretation of the phenomenon of critical deformation,** these facts would indicate that the disorientation of the polymer in the fissure opening under

*The divinylnitrylacrylcarboxyl vulcanizate is an exception.

**The existence of ϵ_{cr} is to be explained as resulting from the fact that the strengthening of the rubber by orientation in the fissure openings predominates (at ϵ_{cr}, and above) over the destructive action of the stress [12].

rupture of the cross-linkages (action of HCl) is more extensive than is the destruction of the molecules along bonds under the action of O_3.

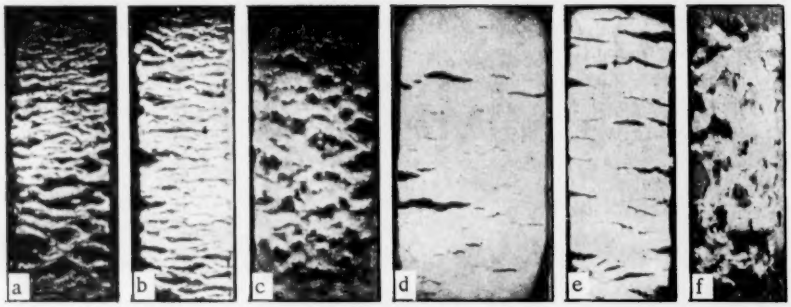

Fig. 1. The external appearance of rubbers after corrosion cracking in various media: a) "Nairite" in nitrogen dioxide, b) SKT in HCl; c) butyl in HNO_3; d) thiokol in NaOH; e) SKS-30 in O_3; f) SKS-50K in CH_3COOH.

The effect of the concentration of the aggressive agent on the rupture time. For a vulcanizate of SK-1-30 in HCl, or in CH_3COOH, this relation is the same as in the ozone cracking of rubber [7, 14], i.e., $\tau = kc^{-\alpha}$, the position of ϵ_{cr} being independent of the concentration of the aggressive agent in both cases [14].

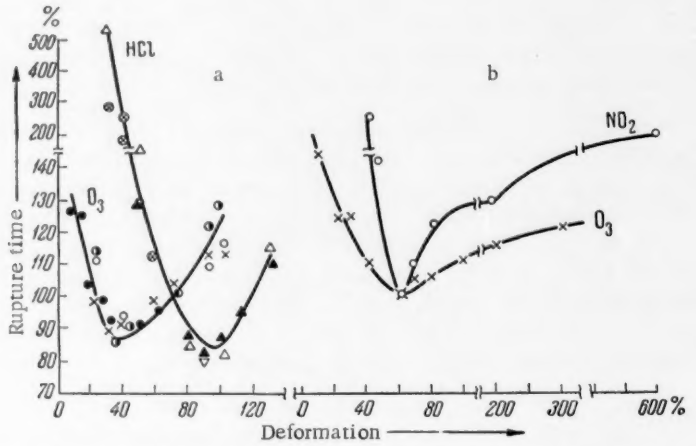

Fig. 2. a) Relation between the rupture time and the deformation of SK-1-30 rubber under the action of O_3, and HCl, the time being expressed as the percentage of the time for rupture of a rubber which had been elongated by 70%; b) relation between the rupture time and the deformation of polychloroprene rubber under the action of NO_2, and O_3, the time being expressed as the percentage of the time for rupture of a rubber which had been elongated by 60%.

The established rules concerning the effects of deformation and O_3 concentration, and the displacement of ϵ_{cr} into the region of higher deformation when orientation is hindered [12, 13], all point to a similarity in the corrosion cracking of rubber under the action of various aggressive agents. Analysis of the experimental data also shows that there are a number of relations which apply to both corrosion cracking and static fatigue of rubbers, metals, and other bodies [7, 20]. Thus, there is a similarity in the time dependence of the strength (at $\epsilon < \epsilon_{cr}$) [3, 12, 15-17], in the kinetics of rupture [18, 19], and in the concentration dependence of the life of metals [17], and rubbers [7, 14].

The effect of the dissociation constant of the acid. Test was made of two pairs of acids having the same molecular weights (this excluding diffusional effects) and different dissociation constants: α-chloracetic ($K = 14 \cdot 10^{-4}$) and isovaleric ($K = 0.15 \cdot 10^{-4}$); pyruvic ($K = 32 \cdot 10^{-4}$) and butyric ($K = 0.15 \cdot 10^{-4}$). The following values were obtained for the rupture times of SK-1-30 rubber: in a C_2H_5OH solution, 7 mM/liter, 12 minutes for α-chloracetic acid, and 64 minutes for isovaleric acid; in a n-C_4H_9OH solution, 28 mM/liter, 65 minutes for pyruvic acid, and 115 minutes for butyric acid. The fact that the rupture time decreases with an increase in the dissociation constant of the acid indicates that the rate of corrosion cracking undoubtedly rises as the strength of the acid increases.

TABLE 1

Rupture Times for Rubbers in Acid Solutions, and in Acid Vapors

Aggressive agent	Conc. of agent (mmoles/liter)	Rupture time (min)	
		in solution	in gaseous phase
SK-1-30 rubber (or SKT)			
HCl	1,9	> 2days	10
HNO_3	1,9	1day	—
CH_3COOH	1,9	120	28
C_3H_7COOH	1,9	34	26
O_3	1,9	—	1—2
HCl	19	228	—
HCl + aerosol OT	19	97	—
HNO_3	19	11	—
SK-1-30 rubber (or SKT)			
HCl	2,4	> 2days	20

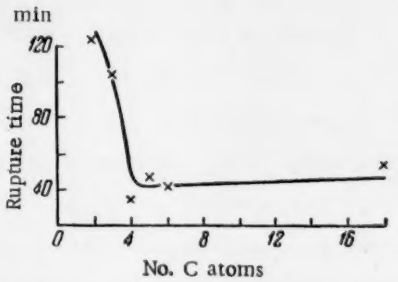

Fig. 3. The relation between the rupture time of a SK-1-30 rubber in acid solutions and the number of carbon atoms per acid molecule.

The role of adsorption. In order to understand the role of adsorption, corrosion cracking was studied in aqueous solutions of inorganic acids (HCl, HNO_3), in aqueous, and in alcoholic solutions of fatty acids of a homologous series, and in vaporized acids. In Fig. 3 there are shown the results of experiments which were carried out on SK-1-30 rubber in ethyl alcohol solutions of acids (2.4 mM/liter) at 50°. From this figure, it is clear that there is a marked increase in the reaction velocity (i.e., a decrease in τ) on passing from acetic to propionic and butyric acids; τ remains practically constant on going to the higher members of this series. When it is considered that the value of the dissociation constant is essentially the same for all of these acids ($K = 0.15 \cdot 10^{-4}$), and that the diffusion rate diminishes on going to the higher members of the series, it then becomes clear that an increase in the rate of cracking could only be due to a rise in the adsorption of the acid on the rubber, with an accompanying diminution in the strength of the latter [1, 20].

The relative roles of the strength, and adsorbability (wetting), of the acid. In treating this problem, experiments were carried out with acids of markedly different chemical activity (acetic and butyric acids being compared with hydrochloric and nitric acids), other comparative experiments being set up with acids in the vaporous form and in aqueous solution (Table 1). From Table 1, it is to be seen that the rate of cracking of SK-1-30 is greater in HCl vapors than it is in the vapors of acetic or butyric acid; in an aqueous solution of butyric acid the process proceeds at the same rate as in vapors of same concentration; in a CH_3COOH solution the rate is appreciably less than in the vapors; and, in a HCl solution, the rate is markedly lowered in comparison with its value in the vapors. These results can be explained by the fact that water hydrates an acid, and impedes its adsorption on the rubber surface. The hydration of HCl is especially strong, and it is for this reason that this acid acts more slowly than acetic acid, even though it has a much higher activity. The introduction of a wetting agent in the form of 1% OT aerosol (sodium dioctyl-sulfosuccinate) enhances the action of HCl. HCl proves to be more aggressive in the gaseous phase, where there is no hydration, than in aqueous solution, whereas acids of the same strength (acetic and butyric) have the same activity under these conditions.

The rate of interaction of SK-1-30 is greater with HNO_3 than it is with HCl, this being due to the oxidizing action which makes the rubber hydrophilic and much easier to wet. Thus, in terms of decreasing rate of

corrosion cracking, the aqueous solutions of the acids can be arranged in the sequence: butyric ≯ acetic ≫ nitric > hydrochloric; in acid vapors, the sequence is different: hydrochloric > acetic > butyric.

From this it follows that the rate of corrosion cracking of rubber is not determined by the stress and the concentration of the aggressive agent alone, the activity of the aggressor and its adsorbability being other significant factors.

LITERATURE CITED

[1] P. A. Rebinder, Jubilee Meeting in Honor of the 30th Anniversary of the Great Socialistic Revolution of October, Acad. Sci. USSR Press, 1947, page 531; J. Tech. Phys. 2, Nos. 7-8 (1932).

[2] V. I. Likhtman, P. A. Rebinder and G. V. Karpenko, The Effect of Surface Active Agents on the Deformation of Metals (in Russian), Acad. Sci. USSR Press, 1951.*

[3] M. S. Aslanova, Proc. Acad. Sci. USSR 95, No. 6 (1954).

[4] G. A. Shvarts and M. M. Kristal', The Corrosion of Chemical Equipment (in Russian), Moscow, 1958.

[5] E. E. Ziegler, Mater. and Methods 39, No. 6. 93 (1954).

[6] Yu. S. Zuev and A. S. Kuz'minskii, Proc. Acad. Sci. USSR 89, No. 2, 325 (1953).

[7] Yu. S. Zuev, Proc. Acad. Sci. USSR 93, No. 3, 483 (1953).

[8] K. A. Andrianov, The Silicoorganic Compounds (in Russian), Moscow, 1955.

[9] N. P. Apukhtina, R. A. Shlyakhter and F. B. Novoselov, Kauchuk i Rezina, No. 6, 7 (1957).

[10] I. D. Zakharov and S. A. Pavlov, Scientific Reports, Moscow Institute of Technology for Light Industry 1, 1 (1955).

[11] B. A. Dolgoplosk, E. N. Tinyakova, et al., Kauchuk i Rezina, No. 3, 11 (1957).

[12] Yu. S. Zuev and S. I. Pravednikova, Proc. Acad. Sci. USSR 116, No. 5 (1957).**

[13] Yu. S. Zuev and S. I. Pravednikova, J. Phys. Chem. 31, 2586 (1957).

[14] Yu. S. Zuev and S. I. Pravednikova, Reports of the Scientific Research Institute for the Rubber Industry, Vol. 6 (1959).

[15] S. N. Zhurkov and B. N. Narzulaev, J. Tech. Phys. 23, No. 10 (1953).

[16] G. M. Bartenev, Prog. Chem 24, vol. 7, 815 (1855).

[17] K. Matthaes, Zs. Metallkunde, 47, 37, (1956).

[18] F. F. Azhogin, Monograph, The Corrosion and Protection of Metals (in Russian), Moscow, 1957, p. 98.

[19] Yu. S. Zuev and S. I. Pravednikova, J. Phys. Chem. 32, No. 7, 1457 (1958).

[20] P. A. Rebinder, with M. E. Lipets, M. M. Rimskoi and A. B. Taubmana, The Physical Chemistry of Flotation Processes (in Russian), 1933.

Received September 4, 1958

*In Russian.

**See C.B. Translation.

THE CHEMICAL MODIFICATION OF ADSORBENT SURFACES AND ITS EFFECT ON THE ADSORPTIONAL CHARACTERISTICS

A. V. Kiselev, N. V. Kovaleva, A. Ya. Korolev and K. D. Shcherbakova*

(Presented by Academician M. M. Dubinin, September 6, 1958)

Until recently, the alteration and improvement of the characteristics of an adsorbent has been achieved by increasing the porosity, i.e., by modification of the geometrical structure of the adsorbent. This line of development culminated in the production of charcoal, xeronic gels, and porous crystals (molecular sieves) of high activity. Recently, it has become clear that profound alterations in the characteristics of adsorbents can be brought about by the chemical modification of their surfaces [1, 2]. The nature of the surface exercises a profound influence on the behavior of an adsorbent or catalyst and frequently determines the fundamental physico-mechanical properties of such substances as filled rubbers and plastics, lacquer coloring materials, lubricating greases, and others, as well. Work in the field of the chemistry of surfaces has been almost entirely limited to the study of the existing natural and synthetic adsorbents, and very simple reactions such as dehydration [1], have been carried out on these surfaces. It is possible to regulate the characteristics of adsorbents by carrying out the most varied of chemical reactions on their surfaces, thus forming dispersed materials and other substances having the requisite properties.

The present communication will consider the modification of the adsorptional characteristics of siliceous substances and graphitic bodies. In recent years, siliceous materials have been used in carrying out reactions of alkylation, and, in particular, methoxylation [3-11], chlorination [8], fluorination [12, 13], and reactions with alkyl chlorosilanes [14-17]. There is also indication that the surface properties of carbon black can be altered through chemical treatment [18], especially with oxidizing agents in aqueous solution [19-22]. The present work has dealt with aerosil, a highly dispersed silica, and a channel Ukhtinian carbon black. Modification was undertaken with the aim of rendering the silica hydrophobic and the carbon black hydrophilic.

Modification of silica. Hydrated silica surfaces are good adsorbents of polar substances. Through reactions with silicoorganic compounds, it is possible to bring about fundamental surface alterations which tend to give stable hydrophobic properties to these surfaces, a fact which is of interest in connection with the use of silica as a filler of polymeric materials and a thickener for lubricants. Modification was carried out by combining the hydroxyls of the silica with trimethylchlorosilane according to the reaction:

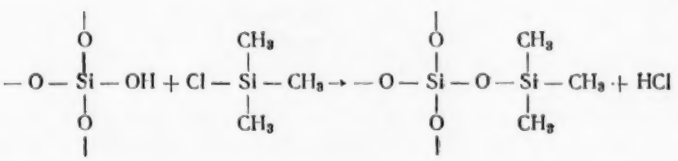

(1)

*With the participation of I. Yu. Babkin and G. M. Lyulina.

The aerosil, with a surface area of approximately 150 m^2/g, was treated with saturated vapors of trimethylchlorosilane, or with a solution of the latter in benzene, for 8 days at 20°. Prior to the adsorption experiments, both the initial and the modified specimens were evacuated in the adsorption system at 200°.

The greatest difference was observed in the isotherms for water vapors. As is to be seen from Fig. 1, the isotherm for the adsorption of water vapors on the original specimen with hydrated surface had the form which is characteristic of the polymolecular adsorption of a strongly adsorbing substance with capillary condensation in the fissures between the aerosil particles. On the modified specimen, the adsorption of these same vapors was only one tenth as large. On the modified specimen, the adsorption isotherm for water vapors was reversible and remained unaltered even after extended contact (several months) with water, a fact which pointed to the stability of the surface compound which had been formed. The isotherm was concave, as is characteristic of those cases in which there is a weak interaction between the absorbent and the adsorbate [23]. On the surface of the modified specimen, the formation of a dense monolayer of adsorbed water molecules capable of completely eliminating the capillary condensation in the fissures between the particles was not observed even when $p/p_s \rightarrow 1$. There was absolutely no wetting of the modified specimen by the water.

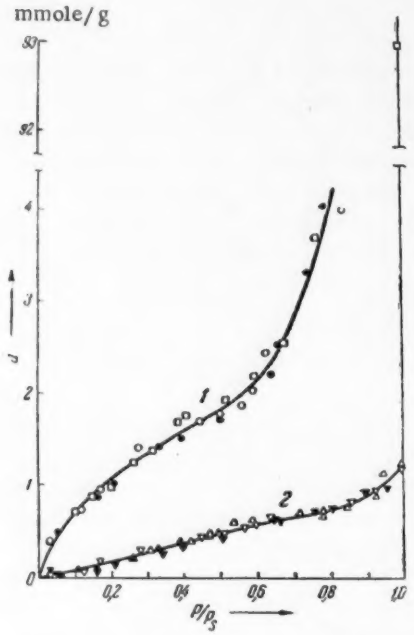

Fig. 1. Adsorption isotherms for water vapor on aerosils: 1) specimen with hydrated surface; 2) specimen with surface modified through reaction with trimethylchlorosilane. The various point designations refer to different series of experiments, the solid points being for desorption.

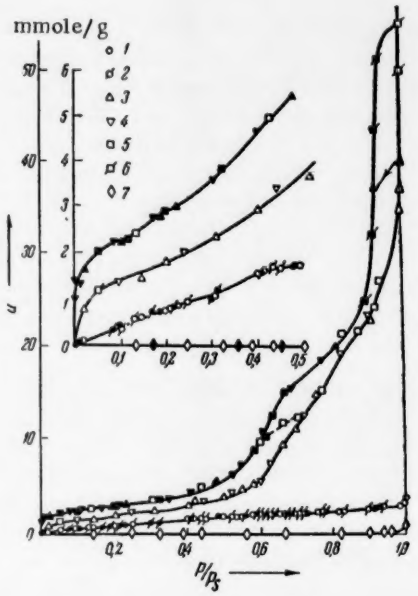

Fig. 2. Adsorption isotherms for water vapor on carbon black: 1) original specimen, evacuated at 25°; 2) the same, evacuated at 200°; 3) oxidized specimen, evacuated at 25°; 4) the same, evacuated at 200°; 5) oxidized specimen, evacuated at 25° after a second series of measurements; 6) the same, after a second evacuation at 200°; 7) specimen treated at 1700° in a current of hydrogen.

Modification of carbon black. The amount of oxygen which is contained in a carbon black fixes its adsorptional characteristics with regard to many adsorbates, especially polar ones. Modification of the channel black was carried out with the view of furthering the graphitization and increasing the oxidation. Calcination at temperatures above 1500° markedly diminishes the adsorption of vapors of water, methanol, ammonia, methylamine, sulfur dioxide, and other polar substances by breaking down the acid surface compounds and inducing the growth of graphite crystals (chemical and crystallochemical modification) [23]. Thermal treatment, particularly above 2500°. makes the surface of the carbon black more uniform, and diminishes the adsorption of nonpolar

substances in the region of low values of p/p_s [23, 24]. Such treatment also makes the hydrophobic nature of the carbon black more pronounced.

Increasing the affinity of the carbon black for polar substances in general, and for water, in particular, is of practical interest in connection with colored printing inks [22], in the strengthening of rubber in latex [25], in the production of emulsified black coloring agents and india ink, as well as in other fields. In the present work, the oxidation of the carbon black was brought about by sodium hypochlorite. There was an accompanying evolution of gas and a heating of the suspension to 75°. Neutralization was carried out with hydrochloric acid after the reaction was completed and the carbon black suspension had been cooled. As a result, the pH of the carbon black suspension, measured against a glass electrode, fell to 3.75. The suspension was then filtered and the precipitate washed with distilled water until the carbon black began to pass through the filter as a result of the removal of electrolytes. The carbon black was dried, first at room temperature, and then at 100°.

The oxidizing treatment was continued until there was a marked alteration in the surface, and in the chemical and colloidal properties of the carbon black. An increase was observed in the amount of chemically bound oxygen (from 4.1 to 17.3%), and in the amount of volatile materials. The content of carboxyl and hydroxyl (phenol) groups was much higher in the modified carbon black than in the original material. Such modification profoundly altered the adsorptive properties of the carbon black. There was an improvement in the bonding between the particles of the carbon black and the molecules of the polar medium in technically important colloidal systems, the carbon black showing an unusually pronounced ability to disperse in water to form very fine suspensions which gave a clear-cut Tyndall effect.

The modification of the carbon black sharply altered the adsorption of water vapors. In Fig. 2 there are shown isotherms for the adsorption of water vapors on the original, the oxidized, and the graphitized, specimens of the carbon black. Prior to each experiment, the specimens were evacuated at 25° and at 200°. For the original specimen, the isothermhad the usual form, being concave over the initial segment and showing two points of inflection. The adsorption and the desorption curves coincided. On the other hand, the isotherm for the oxidized specimen was convex, even at low values of the relative pressure, and rose quite steeply. Further on, this isotherm passed through a first inflection point at $p/p_s \approx 0.35$ and then rose sharply, once more. The isotherms for desorption fell above those for adsorption,* at all values of p/p_s. After the desorption measurements and evacuation for 10 hours at 25°, the water was still not completely removed from the specimen, a part of it (1.6 mmoles/g) remaining bound to the surface of the carbon black. A second series of measurements was carried out after evacuation at 200°. Both the adsorption and the desorption curves coincided with the corresponding curves of the first series of measurements. After evacuation for 2 days at 25°, a part of this water (1.05 mmoles/g) also remained bound to the surface. This water could not be removed by further evacuation in the cold. A subsequently developed third adsorption curve (without heating to 200°) coincided with the desorption curve up to $p/p_s \approx 0.45$ (reversibly and physically adsorbed water), following which it fell below the desorption curve and, from $p/p_s \approx 0.7$ on coincided with the desorption curve for the second series of measurements. The desorption curve for the third series of measurements coincided with the desorption curves for the first and second series. Once more, a part of the water remained bound with the surface of the carbon black after evacuation for 12 hours in the cold. The water was completely removed only after evacuation for 18 hours at 100°.

Complex hysteresis of this type is typical of cases involving the superposition of chemisorption (hysteresis at low values of p/p_s, firm binding of water without heating) and capillary condensation (hysteresis at high values of p/p_s, third series of measurements after hydration without subsequent removal of the chemisorbed water). It is clear that the action of the oxidizing agent led, first, to a strong oxidation of the external surfaces of the crystallites which formed the particles of the carbon black, this change occurring principally at the junction postions of the hydrocarbon radicals which had not been decomposed in the formation of the carbon black, and, second, to a penetration of a portion of the oxygen into a space between the crystallites, or even into the space between the layers. This last statement is supported by a certain similarity between the experi-

*Up to $p/p_s \approx 0.6$, equilibrium was established in 3-4 hours, both in adsorption and in desorption; beginning with $p/p_s \approx 0.6$, at least 10-12 hours were required to reach equilibrium.

mentally developed isotherms and the isotherm for the adsorption of water vapor on oxidized graphite. It is likely that the irreversibly adsorbed water was taken up through chemical adsorption and that it hydrated the surface oxides, penetrating the spaces between the crystallites and, possibly, between the graphite layers as well through the oxidized positions. The reproducible hysteresis in the region of high p/p_s values could have been due to the capillary condensation of water vapors in the fissures between the particles of the carbon black, or, possibly, in the fissures which were formed between the crystallites during oxidation. This last must, however, have been of minor importance, since the adsorption of nitrogen was not increased as the result of modification. Further work is needed to fix the details of this description.

A comparison of the isotherms of Fig. 2 for the various specimens of carbon black shows that thermal treatment and the liquid phase oxidation can so markedly modify a carbon black that the adsorption of water vapors on it is altered by many fold.

These measurements point to the importance, and the practical value of the modification of adsorbents by surface chemical reactions. By covalent linking of various radicals to adsorbent surfaces, it becomes possible to prepare materials which differ in their surface properties and on these radicals various organic and heteroorganic reactions can then be carried out. As a result, the surfaces of stable adsorbents of favorable geometrical structure can be rendered good fillers or selective adsorbents, or even rendered capable of carrying on exactly determined processes of separation and catalysis.

LITERATURE CITED

[1] A. V. Kiselev, Bull. Acad. Sci. USSR, No. 10, 43 (1957); Proc. Symposium on the Structure and Properties of Porous Materials, Bristol, 1958.

[2] A. Ya. Korolev, Review of Reports, Fourth All-Union Conference on Colloid Chemistry, Acad. Sci. USSR Press, 1958.*

[3] Monograph, The Surface Chemical Compounds and Their Role in Adsorption (in Russian), A. V. Kiselev, editor, Moscow, 1957.

[4] O. M. Dzhigit, A. V. Kiselev, N. N. Mikos-Avgul' and K. D. Shcherbakova, Proc. Acad. Sci. USSR 70, 441 (1950).

[5] R. K. Iler, The Colloid Chemistry of Silica and Silicates, 1957.

[6] US Pat. 2657149, 1953.

[7] K. V. Topchieva and A. P. Ballod, Proc. Acad. Sci. USSR 75, 247 (1950).

[8] K. D. Shcherbakova and K. L. Slovetskaya, Proc. Acad. Sci. USSR, 111, 855 (1956).

[9] H. Devel and R. Gentili, Helv. Chim. Acta 39, 1586 (1956).

[10] K. H. Ebert, Monatsh. f. Chem. 88, 275 (1957).

[11] W. Stober, Koll. Zs. 149, 39 (1956).

[12] A. P. Ballod and A. V. Topchiev, Monograph, The Surface Chemical Compounds and Their Role in Adsorption (in Russian), Moscow, 1957, p. 146.

[13] I. E. Neimark, R. Yu. Sheinfein and L. G. Svintsova, Proc. Acad. Sci. USSR 108, 871 (1956).

[14] R. K. Iler, The Colloid Chemistry of Silica and Silicates 1957, p. 257.

[15] Anon., J. Am. Ceram. Soc. 32, 157 (1949).

[16] F. Runge and W. Zimmerman, J. prakt. Chem. 1, 283 (1955).

[17] H. W. Kohlschutter, P. Best, and G. Wirzing, Zs. anorg. u. allgem. Chem. 285, 236 (1956).

[18] U. Hoffman and G. Ohlerich, Angew. Chem. 62, 16 (1950).

[19] G. Genin, Peintures, Pigments, Vernis, 30, 639 (1954).

*In Russian.

[20] Z. Vanuto, Paint Manufact. 24, 227 (1954).

[21] English Patent, 668724, 1952.

[22] A. Ya. Korolev, T. N. Malova and V. I. Ramanova, Poligraf. Proizvodstvoi 7, 25 (1957).

[23] A. V. Kiselev, Colloid J. 20, 338 (1958);* A. V. Kiselev, N. V. Kovaleva, V. A. Sinitsyn and E. V. Khrapova, Colloid J. 20, 444 (1958).*

[24] N. N. Avgul', A. V. Kiselev and A. Ya. Korolev, Colloid J. 20, 298 (1958).*

[25] B. A. Dogadkin, L. G. Senatorskaya, et al., Colloid J. 5, 528 (1956).*

Received September 5, 1958

*Original Russian pagination. See C.B. Translation.

A POLARIZATION MECHANISM OF THE SUPPRESSION OF STRUCTURAL ETCHING DURING ELECTROCHEMICAL POLISHING

S. I. Krichmar

The Dneprodzerzhinskii Nitrogen Fertilizer

(Presented by Academician A. N. Frumkin, September 2, 1958)

At the present time, electrochemical polishing is considered to involve a leveling out the microrelief of the metal under the action of various factors. Quantitative investigations have shown, for example, that the smoothing out which takes place in electrochemical polishing can result either from concentration polarization [1, 2] or from the effect of the curvature of the microrelief [3]. Despite the fact that satisfactory experimental confirmation of derived relations has been obtained in certain instances [1, 2, 3] (and this is undoubtedly the most convincing argument in favor of the correctness of the basic theoretical concepts), careful study shows the assumptions lying behind this quantitative work to contain no special features which would distinguish electropolishing from ordinary anodic dissolution. Thus, it is known that the most characteristic instances of polishing (the dissolution of copper, and its alloys, zinc, etc.) are those which occur in the region of the limiting current. But, although the quantitative calculations have been confirmed in this region, they clearly retain their validity for lower values of the current density as well. Accordingly, the smoothing process should also be possible at these lower values. Metal etching comes to the fore at low current densities, however, and this, in many cases, considerably complicates the picture.

By way of example, a photomicrograph is shown in Fig. 1, to illustrate the removal of traces of mechanical treatment in copper by chemical dissolution in 15% HNO_3. Another example (see Fig. 2) is seen in the dissolution of a stainless steel, EYa-IT, in aqua regia at 70°. Measured in a Linnik stereoscopic microscope, the height of the original protrusions was 2-5 μ and the final height, 0.5-1 μ. These examples make it clear that the removal of traces of mechanical treatment occurs not only in electrochemical dissolution, but in ordinary chemical dissolution, as well. These cases differ from electropolishing in that structural etching does not arise, and the quality of the surface is not, as a rule, improved.

On the basis of what has been said, it can be concluded that the suppression of structural etching is the most outstanding characteristic of electrochemical polishing. Together with the smoothing, this gives the most complete characterization of the process. But although the conditions for smoothing are realized in almost every case of anodic dissolution, the suppression of etching occurs only in electropolishing.

The formation of complex compounds in many instances of electrochemical polishing [6], and the high viscosity of the electrolytes which are employed, both indicate that through the formation of these complexes, and stable supersaturated solutions, there arise those conditions which favor a considerable increase in the solubility of the metal, up to complete exhaustion of the activity of the electrolyte. This claim is supported by the fact that the characteristic volt – ampere curves are, in many instances of electropolishing, those showing a limiting current region at the beginning of the polishing range [7, 8].

It has been noted in [5] that the suppression of etching during electrochemical polishing under concentration polarization is associated with a conformity in the region of the limiting current of the separate volt – ampere characteristics for the structural elements of the surface. In this connection, study will be made of the potentials of the anode, and its separate components, and their relation to the polarization current. Since the

theory of concentrated electrolytes has been only imperfectly developed, consideration will be limited here to the crude approximation of the dissolution of a metal in a dilute solution of a strong acid (for example, iron in hydrochloric acid, etc.). Since the salt of the type Me_xA_y which is formed in the course of the reaction is but poorly dissociated, its dissociation constant can be represented as:

$$K = \frac{a^x_{M^+} a^y_{A^-}}{a_{MA}} = \frac{\gamma^x_{M^+} \gamma^y_{A^-}}{\gamma_{MA}} \frac{C^x_{M^+} C^y_{A^-}}{C_{MA}}, \tag{1}$$

a_{A^-}, a_{M^+}, and a_{MA} being respectively, the activities of the anion, the cation, and the salt: γ_{A^-}, γ_{M^+}, and γ_{MA}, their respective activity coefficients; C_{A^-}, C_{M^+}, and C_{MA}, the respective concentrations; and x and y, the stoichiometric coefficients.

It is, at the outset, possible to replace C_{A^-} in(1) by C_a, the concentration of the acid, since the acid is strong and the salt poorly dissociated.

It is then clear that C_a is equal to the difference between the initial acid concentration, C_0, and the concentration of the acid which has been expended in the formation of the salt (C_{as}); i.e.,

$$C_a = C_0 - C_{as} = C_0 - \frac{y}{x} C_M \tag{2}$$

(C_M is here the concentration of the metal in the solution).

Finally, the concentration of the salt in the solution, C_{MA}, can be replaced by the total concentration of the metal in solution, C_M. Imposing these changes on (1), taking (2) in account, and solving the resulting equation for a_{M^+}, there is obtained:

$$a_{M^+} = \left[\frac{\gamma_{MA}}{\gamma^y_{A^-}} \frac{K C_M}{\left(C_0 - \frac{y}{x} C_M \right)^y} \right]^{1/x}. \tag{3}$$

Since the reaction product is but weakly dissociated, the current density at the anode will be essentially determined by the diffusion of the reaction products into the body of the solution:

$$i = nFD \frac{C_M}{\delta}, \tag{4}$$

here n is the valence of the metallic ion: D is the effective coefficient of diffusion of the reaction products; δ is the effective depth of the diffusion layer, and i is the current density. The concentration of the metal in solution at the anode cannot be greater than $(x/y)\, C_0$, which is the concentration which the metal would have if all of the acid were to be expended in forming the compound. Thus, a limiting current

$$i_0 = nFD \frac{x}{y} \frac{C_0}{\delta} \tag{5}$$

will arise when $C_M = (x/y)\, C_0$.

The anode potential is equal to

$$e = e'_0 + \frac{RT}{nF} \ln a_{M^+}. \tag{6}$$

Introducing the value of a_{M^+} from (3), and taking (4) and (5) into account, there is obtained

$$e = e_0 + \frac{RT}{xnF} \left[\ln \frac{i}{(i_0 - i)^y} + \ln \frac{\gamma_{MA}}{\gamma^y_{A^-}} \right], \tag{7}$$

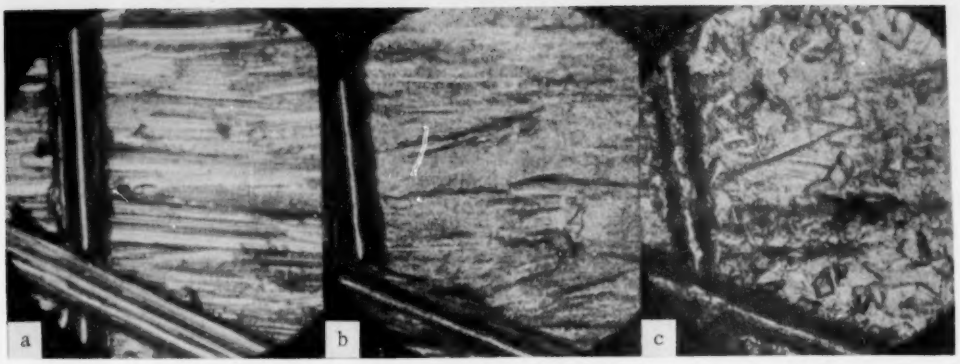

Fig. 1. The smoothing out of irregularities left in the microrelief by mechanical working; the case of the dissolving of copper by 15% nitric acid: a) before dissolution, b) after 3 minutes, c) after 6 minutes. 140 ×.

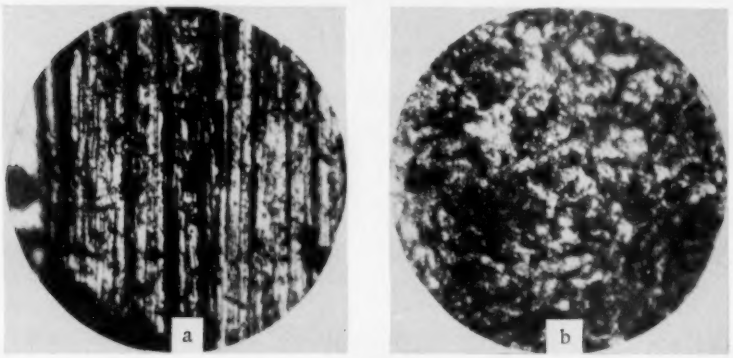

Fig. 2. The smoothing out of irregularities left in the microrelief by mechanical working; the case of the dissolving of ÉYa-1T steel by aqua regia: a) before dissolution, b) after 5 minutes of dissolution. 280 ×.

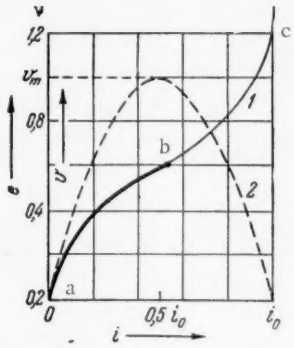

Fig. 3. The relation between $\underline{e}$ and $\underline{i}$, (1); and between $\underline{v}$ and $\underline{i}$, (2). Section ob is the region of etching, and bc, is the region of the suppression of etching.

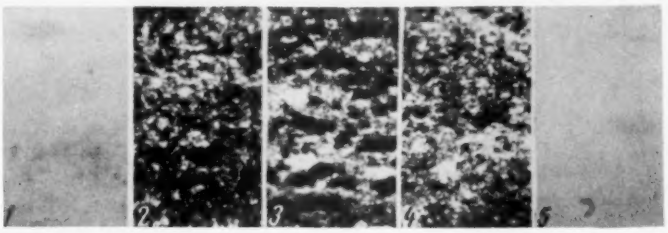

Fig. 4. Photomicrographs of a specimen of copper which was electropolished and then subjected to 6 minutes of dissolution in 7.5 M H_3PO_4 at various current densities, i_0 = 0.04 amp/cm^2: 1) i = 0; 2) i = 0.2i_0; 3) i = 0.5i_0; 4) i = 0.8i_0.

where e_0 is a constant combining the standard electrode potential and other constants. Unfortunately, an experimental test of (7) is rendered difficult by the absence of trustworthy data on the γ, C relation. Analysis of (7) shows the variation of potential with current density to be of the type which is shown in Fig. 3, i.e., of the type which is actually observed in many cases.

We will now consider the behavior of two sections of the anode having different normal potentials, e_{01} and e_{02}. Opposite each of these sections, the potential drop in the bath is the same and we will therefore have, according to (7)

$$e_c - \left[e_{01} + \frac{RT}{xnF}\left(\ln\frac{i_1}{(i_0 - i_1)^y} + \ln\frac{\gamma_{MA_1}}{\gamma^y_{A_1^-}}\right)\right] = e_c - \left[e_{02} + \frac{RT}{xnF}\left(\ln\frac{i_2}{(i_0 - i_1)^y} + \ln\frac{\gamma_{MA_2}}{\gamma^y_{A_2^-}}\right)\right], \tag{8a}$$

where e_c is the cathode potential, or

$$\Delta e_0 = \frac{RT}{xnF}\left[\ln\left(\frac{i_0 - i_2}{i_0 - i_1}\right)^y \frac{i_1}{i_2} + \ln\left(\frac{\gamma_{A_2^-}}{\gamma_{A_1^-}}\right)^y \frac{\gamma_{MA_1}}{\gamma_{MA_2}}\right]. \tag{8b}$$

γ varies more slowly with the potential than does the concentration, so that when account is taken of the smallness of the value of Δe_0 it becomes possible, in a first approximation, to neglect the second member of (8a) in comparison with the first. Introducing the notation $\Delta i = i_1 - i_2$, and substituting into (8b), there is obtained

$$\Delta e_0 \approx \frac{RT}{xnF}\left[\ln\left(1 + \frac{\Delta i}{i_1}\right) - y\ln\left(1 - \frac{\Delta i}{i_0 - i_1}\right)\right]. \tag{9}$$

Decomposing this result into a series and neglecting members of higher order, we have

$$\Delta i \approx \Delta e_0 \frac{xnF}{RT}\frac{i_1(i_0 - i_1)}{i_0 + i_1(y - 1)}. \tag{10}$$

It is clear that the difference between the rates of dissolution (the rate of etching) will be equal to

$$v = \frac{M}{\rho nF}(i_1 - i_2) = \frac{M\Delta i}{\rho nF}. \tag{11}$$

Substituting the expression for Δi from (10), there results

$$v = \Delta e_0 \frac{Mx}{\rho RT}\frac{i_1(i_0 - i_1)}{i_0 + i_1(y - 1)}. \tag{12}$$

This function has a maximum at the value

$$i_m = i_0/(1 + \sqrt{y}). \tag{13}$$

Here the rate of etching will be

$$v_m = \Delta e_0 \frac{Mx}{\rho RT}\frac{i_0}{(1 + \sqrt{y})^2}. \tag{14}$$

On the other hand, an analysis of expressions (9) and (10) shows the rate of etching to tend to zero as $i \to 0$, and as $i \to i_0$. For a 1 – 1 electrolyte, the rate of etching varies with the value of the current density in the manner shown by Fig. 3, 2 (see also Fig. 4). From the preceding equations, it is to be seen that when the current density is considerably less than the limiting value (from what has gone before, this situation is seen to arise from an exhaustion of the acid anions at the electrode surface), the rate of etching will at first increase with increasing current. This is the effect which is met in the usual anodic etching, where even an insignificant accumulation of salt in solution at the anode surface leads to a precipitation of a solid phase, and a further rise in the current results in the initiation of a number of new processes which make for complexities in the polarization curve. It follows from (13) that the rate of etching can increase to the value $i_m = i_0/(1 + \sqrt{y})$. Further increase in the current density once more results in a diminution of the rate of etching and the suppression of etching is complete when the limiting current is reached (see Fig. 4).

It is thus possible that the suppression of etching results, in many cases, from a considerable depletion of the electrolyte anions in the layer adjacent ot the anode through formation of supersaturated solutions and complexes. Electropolishing can be realized only when the conditions are such that etching is suppressed.

The polarization theory which has been outlined represents only one of the possible mechanisms for the suppression of etching. The possibility is not to be excluded that suppression can arise from other factors such as the existence of a thin amorphous layer of solid salt, or an oxide film. Some aspects of this question have been considered in [15].

LITERATURE CITED

[1] S. I. Krichmar, Proc. Acad. Sci. USSR 100, No. 3, 481 (1955); S. I. Krichmar, J. Phys. Chem. 31, No. 7, 1593 (1957).

[2] R. Wagner, J. Electrochem. Soc. No. 5, 225 (1954).

[3] S. I. Krichmar, Proc. Acad. Sci. USSR 101, No. 2, 297 (1955).

[4] S. I. Krichmar and V. P. Galushko, J. Phys. Chem. 31, No. 8, 1762 (1957); J. Nicolas and N. Tegart, J. Electrochem. Soc. 102, No. 4, 93 (1955).

[5] S. I. Krichmar and V. P. Galushko, J. Phys. Chem. 30, No. 3, 578 (1956).

[6] S. I. Krichmar and V. P. Galushko, J. Inorg. Chem. 1, No. 10, 2423 (1957); L. Ya. Popilov and L. P. Zaitseva, The Electropolishing and Electroetching of Metallographic Sections (in Russian), 1955, pages 141, 155; V. I. Lainer, The Electropolishing and Electroetching of Metallographic Sections (in Russian), 1947, p. 141.

[7] K. P. Batashev, Proc. Conference on Electrochemistry, Acad. Sci. USSR Press, 1953, p. 414 (in Russian).

[8] I. P. Fedot'ev and S. Ya. Grilikhes, J. Appl. Chem. 30, No. 3, 233 (1957).*

Received May 17, 1958

*Original Russian pagination. See C. B. Translation.

THE EFFECT OF VARIOUS FACTORS ON THE MAGNITUDE OF THE SPECIFIC SURFACE AND THE POROSITY OF CHROMATE CATALYSTS

T. V. Rode and A. E. Agronomov

The N. S. Kurnakov Institute of General and Inorganic Chemistry of the Academy of Sciences of the USSR

(Presented by Academician A. A. Balandin, September 24, 1958)

The effect of the method of synthesis of chromic oxide catalysts on their catalytic activity with respect to two reactions has been investigated in a paper by one of us [1]. In the present work, study has been made of the effect of the method of synthesis on the magnitude of the specific surface, and the formation and dimensions of pores. For this purpose, isotherms were developed for the adsorption of benzene at 0°, this work being carried out in a high vacuum system by a method of direct weighing. The benzene which was used had been carefully freed from thiophene, moisture, and dissolved air, and had a boiling-point of 79.7-80° (at 755 mm of Hg) and a n_D^{20} value of 1.5035. The catalyst specimens were held in vacuum (at 250°) to constant weight. The weight variation resulting from sorption was measured with an accuracy of $1 \cdot 10^{-5}$ g. The specific surfaces were determined from the adsorption isotherms by applying the BET method over the interval of relative pressures, p/p_s, from 0.1 to 0.3. The area occupied by the benzene molecule was assumed to be equal to 46.5 A^2 [3]. The distribution of the pore radii was developed from the desorption branch of the isotherm using the equation $RT \ln \frac{p_s}{p} = \frac{2\sigma v_m}{r}$ [4], where p/p_s is the relative pressure, σ is the surface tension of the benzene at 0°, v_m is the molar volume of the benzene, and r is the pore radius, in angstroms.

The methods of synthesis of the tested catalysts are shown in Table 1, and the experimental results, in Table 2.

It is a characteristic of the hydrated chromic oxide from which these chromate catalysts were prepared that it appears in two forms; a greyish blue and a dark yellow which on pressing and drying gives black cylinders fracturing along glossy conchoidal surfaces. These are not different crystalline modifications, since each proves to amorphous when subject to x-ray examination [1].

The form of hydroxide which is obtained depends only on the rate at which precipitation takes place; with rapid mixing of concentrated solutions, a greyish blue precipitate is formed immediately, whereas a very gradual, drop-wise addition of the precipitant to a dilute solution of chromium salt yields a soluble, basic chromic salt at the point of entry of the drop, this salt dissolving to later precipitate on further addition of the precipitant as a dark yellow chromium hydroxide of special properties. Kohlschütter [5] refers to the blue hydroxide as being "discretely dispersed" and the black, as being "compactly dispersed", and considers that particles of the latter are bound only along the edges and at the corners.

The present investigation has indicated that the factors responsible for the differences in the colors and properties of the two forms of the hydroxide lead to high porosity in the catalysts formed from dehydration of the black hydroxide and to a lack of pores in those catalysts which come from the blue form. By way of example, Fig. 1, I gives the adsorption isotherm for specimen 26 which had been obtained by dehydration of the blue hydroxide and Fig. 1, II, the isotherm for a specimen obtained from dehydration of the black hydroxide.

The desorption branches, b, point to the lack of pores in specimen 26 (the sorption curve a, and the desorption curve b practically coincide) and the presence of pores in specimen 27 (the a and b curves form a wide hysteresis loop). The adsorption isotherms for specimens 7 and 23, which had also been obtained from the blue hydroxide, were similar to that for specimen 26, while the isotherms for specimens 4,5 and 37, which came from the black hydroxide were similar to the isotherm for specimen 27. In order to retard the true aggregation of particles

TABLE 1

No. specimen	Precipitant*	Normal conc. of solution	Precipitation		Activation in H_2	
			temp., in °C	rate	temp., in °C	duration, hr
4	NaOH	0,1	20	Slowly, dropwise	450	2
4a	NaOH	0,1	20	The same	450	8
4b	NaOH	0,1	20	The same	525	2
5	NaOH	0,1	20	The same	450	6
7	NaOH	2	20	Rapidly	450	6
23	NH_4OH	2	80	The same	450	6
26	NH_4OH	2	20	The same	450	6
27	NH_4OH	0,1	20	Slowly, dropwise	450	6
37**	NH_4OH	0,1	20	The same	450	6
42	By thermal decomposition of ammonium dichromate					

*Initial solution, chromic nitrate.

**Precipitated in the presence of the reaction products (NH_4NO_3).

during precipitation of the hydroxide, specimen 37 was synthesized in the presence of the reaction product (chromic nitrate). After activation, the pore dimensions, the maximum in the distribution of pore volumes, the value of the specific surface, and the catalytic activity [1] were all greater for specimen 37 than for specimen 27 (see Table 2).

TABLE 2

No. of specimen	Specific surface, in m^2/g	Pore radii, in A	Max. in the distrib. of pore vol. over radii, A	Total benzene adsorbed at saturation, mmoles/g	Volume wt. of specimen, in g
4	70	20 — 40	31	1,4	10,36
4a	25	Small number of coarse pores	—	1,0	—
4b	30	The same	—	1,2	—
5	75	18 — 36	32	1,6	9,81
7	125	Nonporous	—	2,4	3,48
23	140	Nonporous	—	3,4	5,23
26	200	Nonporous	—	3,1	5,60
27	70	27 — 38	34	1,7	10,77
37	95	35 — 100	70	3,6	10,67
42	135	Nonporous	—	1,9	1,08

Judging from the desorption branch of its isotherm, specimen 42, which had been obtained by heating ammonium dichromate, was also nonporous. The high value of the volume weight of the powder is noteworthy.

The possibility of varying the specimen color from greyish blue to dark yellow by altering the rate of precipitation is readily explained in terms of differences in the porosity.

A comparison of the effects of various factors on the properties of chromate catalysts must be limited to specimens which have been obtained from the same form of the hydroxide.

Extensive investigations are needed to bring out the effect of the initial materials on the properties of the resulting catalyst, but the studies which have already been made indicate that the precipitant (NaOH in the case of specimens 4 and 5, and NH_4OH in the case of specimen 27) was without measurable significance in fixing the properties of specimens obtained from the black hydroxide. Here the surface area was practically the same for each specimen (70-75 m^2/g), the pore radii varied within the limits 20-40 A, and there was approximate constancy in the maximum in the distribution of the pore volume, the total amount of benzene adsorbed at saturation, and the powder volume weight (see Table 2). The properties of specimen 37 were somewhat different, but this is to be explained by the details of its synthesis (see above).

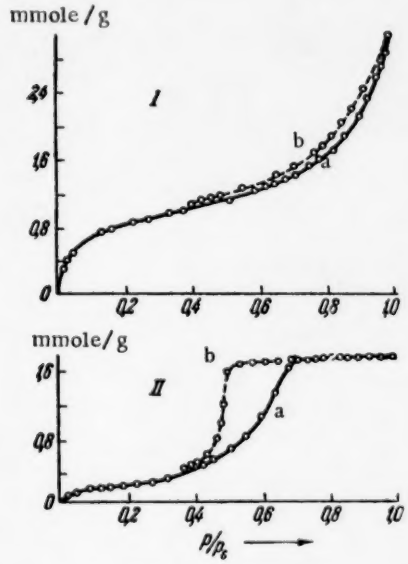

Fig. 1. Adsorption isotherms for benzene vapors at 0°; I) for specimen 26, II) for specimen 27. a) adsorption branch of isotherm, b) desorption branch.

The situation is different with specimens which have been prepared from the blue hydroxide. The values of the specific surface, the total amount of benzene adsorbed at saturation, and the powder volume weight were all greater in specimen 26 which had been prepared from a hydroxide precipitated with ammonia than they were with specimen 7 which had been obtained from a hydroxide precipitated with NaOH (see Table 2).

In order to bring out the effect of the temperature and duration of activation, various specimens of the black hydroxide were subjected to activation at 450° for 2 hours (specimen 4), and for 8 hours (specimen 4a), and at 525° for 2 hours (specimen 4b). Increasing the time of heating at 450° from 2 to 8 hours led to a diminution of the specific area from 70 to 25 m^2/g and resulted in an almost complete disappearance of the pores; the total amount of benzene adsorbed at saturation fell from 1.4 to 1.0 m moles/g. Similar effects accompanied a rise in the activation temperature from 450 to 525° (specimen 4b). In this case, the specific surface fell from 70 to 30 m^2/g, and the amount of benzene adsorbed at saturation decreased from 1.4 to 1.2 m moles/g (see Table 2). In addition, this specimen had only a small number of coarse pores.

In order to elucidate the effect of the aging of a hydroxide on the properties of a catalyst obtained from it, specimen 23 was synthesized from solutions which were heated to 80°, and activation was carried out 2 years afterward. The remaining details of the preparation of 23 were similar to those for the preparation of specimen 26 (see Table 1). The adsorption isotherms for the two specimens showed that the aging of the hydroxide, and the supplementary elevation of the temperature of precipitation had diminished the specific surface and the powder volume weight (see Table 2).

LITERATURE CITED

[1] T. V. Rode, Dissertation, N. S. Kurnakov Institute of General and Inorganic Chemistry of the Acad. Sci. USSR, 1956. (In Russian).

[2] S. Brunauer, P. Emmet, and A. Teller, J. Am. Chem. Soc. 48, 690 (1926).

[3] A. P. Karnaukhov, A. V. Kiselev and E. V. Khrapova, Proc. Acad. Sci. USSR 92, No. 2, 361 (1953).

[4] A. V. Kiselev, Prog. Chem. 14, 367 (1945).

[5] H. Kohlschütter, Koll. Zs. 77, 299 (1936); 96, 237 (1941).

Received September 17, 1958

THE ISOTOPIC EXCHANGE BETWEEN CO AND $C\overset{*}{O}_2$ ON VARIOUS SURFACES

S. S. Stroeva, N. V. Kul'kova and M. I. Temkin

The L. Ya. Karpov Scientific Research Institute for Physical Chemistry

(Presented by Academician S. S. Medvedev, September 29, 1958)

The theory of the catalytic activity of surfaces must assume simpler form in the reactions of isotopic exchange than in other heterogeneous catalytic processes [1]. For this reason investigation has been made of the rate of exchange of atomic oxygen between CO and CO_2 on various surfaces. The kinetics of this exchange on Fe_3O_4 has been studied earlier with the aid of tagged oxygen [2]. From this earlier work the conclusion was drawn that this reaction proceeds through a simpler two-step mechanism involving the participation of oxygen atoms from the catalyst surface. Radiocarbon, C^{14}, was employed for following the oxygen exchange in the present work. In this way the reaction

$$C^{14}O_2 + CO = C^{14}O + CO_2 \tag{1}$$

was observed. To this reaction there corresponds the two-step scheme:

$$C^{14}O_2 + (\ ) = C^{14}O + (O), \tag{2}$$

$$CO + (O) = CO_2 + (\ ). \tag{3}$$

Here, (O) represents a surface oxygen atom, and ( ), a surface position which is free of oxygen.

If Reaction (1) proceeds in the region of moderate coverage on a surface having a constant degree of inhomogeneity with respect to the heat of adsorption of oxygen, i.e., if those conditions are fulfilled under which application can be made of a logarithmic isotherm, and if there is a linear relation between the heats of reaction and the energies of activation of processes (2) and (3) at different surface postions, it is then possible to describe the rate of reaction by the equation [1, 2]

$$\omega = k^{\bullet}\left[P_{C^{14}O_2}\left(\frac{P_{CO}}{P_{CO_2}}\right)^{\alpha} - P_{C^{14}O}\left(\frac{P_{CO_2}}{P_{CO}}\right)^{1-\alpha}\right], \tag{4}$$

in which $k^{\bullet}$ is the rate constant, $P_{C^{14}O_2}$ is the partial pressure of the $C^{14}O_2$, etc, and α is the constant of the linear relation. In the case of a Fe_3O_4 catalyst, this equation gives agreement with the experimental data when $\alpha = 0.5$ [2]. For this surface, the logarithmic isotherm for oxygen has been indirectly developed [3].

It can be readily shown from general equations [1] that when Reaction (1) proceeds by this same mechanism on a surface which is poorly covered with oxygen, the rate is to be expressed by:

$$\omega = k^{\bullet}\left(P_{C^{14}O_2} - P_{C^{14}O}\frac{P_{CO_2}}{P_{CO}}\right). \tag{5}$$

Formally, Equations (4) and (5) can be looked upon as special instances of the relation

$$\omega = k^{\bullet}\left[P_{C^{14}O_2}\left(\frac{P_{CO}}{P_{CO_2}}\right)^{m} - P_{C^{14}O}\left(\frac{P_{CO_2}}{P_{CO}}\right)^{1-m}\right] \tag{6}$$

which correspond to m = α, and to m = 0, respectively. In a similar manner, the kinetics corresponding to a coverage close to surface saturation can be obtained from Equation (6) with m = 1.

It should be noted that

$$\omega = k^{\bullet} (P_{C^{14}O_2} - P_{C^{14}O}) \qquad (7)$$

when $P_{CO} = P_{CO_2}$, regardless of the value of m; in order to evaluate m, it is necessary to make use of data on the relation between the reaction rate and the composition of the gaseous mixture.

The study of the kinetics of Reaction (1) was carried out in a static system in which circulation was achieved by means of a glass electromagnetic pump. In measuring the radioactivity of CO and CO_2, precipitated $BaCO_3$ was investigated with an end-window counter. Evaluation of the exchange rate constant was through the equation:

$$k = \frac{1}{\tau (P_{CO}/P_{CO_2} + 1)\,(P_{CO_2}/P_{CO})^{1-m}} \ln \frac{S}{S - R_{CO}(P_{CO}/P_{CO_2} + 1)}, \qquad (8)$$

which follows from (6). Here, S is the total radioactivity of the gas $S = R_{CO_2} + \frac{P_{CO}}{P_{CO_2}} R_{CO}$; R_{CO_2} and R_{CO} are, respectively, the radioactivities of CO_2, and of CO, at the end of the experiment; and τ is the time of contact of the gaseous mixture with the catalyst as determined from the equation $\tau = t(W/V)$. W being the volume of the catalyst, V, the volume of the gaseous mixture in the system, reduced to the working temperature and t, the duration of the experiment. The constant k is related to the $k^{\bullet}$ of Equation (6) by the relation $k = \rho\sigma RTk^{\bullet}$, where ρ is the powder volume weight of the catalyst and σ is the specific surface.

The catalysts employed in these experiments had the form of tablets 2-5 mm in diameter (Ag, Cu, Pt, Co, Fe_3O_4, Ni and W),or foils (Ag, Pt, and Ni). The results of the measurements are shown in Table 1.

Under the experimental conditions which are used with each catalyst except Fe_3O_4, the point of equilibrium in the reaction

$$CO + MeO = Me + CO_2 \qquad (9)$$

was almost fully displaced toward the formation of the metal. The phase composition of the magnetite, Fe_3O_4, remained unaltered when $P_{CO_2} : P_{CO} \geq 2$.

Silver. Reaction (1) could not be observed on the tablet-form Ag powder (24 g) over the temperature interval 175-350°, or on the Ag foil (10.5 g) at 700°.

Copper. Kinetic measurements were carried out in the temperature interval 250-400° on a copper (3 g) which had been obtained by the reduction of CuO by carbon monoxide. If it was assumed that m = 0, the value of k was constant under alteration of the total pressure of the gaseous mixture, $P = P_{CO} + P_{CO_2}$, and independent of the composition (Table 1).

Platinum. Experiments were carried out on Pt black (1 g) at 250-300° and on Pt foil (1.89 and 3.7 g) at 600-740°. On Pt black, (1) is accompanied by the reaction $2\,CO = C + CO_2$, in which the point of equilibrium at t < 700° is on the side of the formation of carbon [4]. This reaction does not take place in the absence of a catalyst, but it proceeds with appreciable velocity on Ni, Co, Fe [5], and even Pt, as our experiments have shown. The carbon which separates out on the Pt black surface diminishes the activity of the catalyst and for this reason it was impossible to carry out kinetic measurements. In order to avoid carburization, experiments were performed with Pt foil at 700°.

Cobalt. On cobalt (6 g), Reaction (1) can be observed at 265°, and above. Because of carburization, the activity of the catalyst relative to this reaction diminishes, and kinetic studies were not made. Table 2 gives the largest of the values obtained for $k^{\bullet}$ on cobalt at 300°.

Ferrous and ferric oxides. Experiments with Fe_3O_4 (2.6 g) were carried out at 250-300° with gases in which $P_{CO_2} : P_{CO} > 1$. The results of the kinetic measurements confirmed the conclusions which had been drawn in [2]. The high value of k in Experiment 29 can be explained by the reduction of the Fe_3O_4 and the high catalytic activity of Fe as compared with magnetite.

Nickel. On tablet-form Ni powders (2.5 g), Reaction (1) proceeds with measurable velocity at 200°, and above. The activity of the catalyst diminishes because of carburization. For this reason the kinetic measurements were carried out on Ni foil (5.12 g) at 700°.

TABLE 1

Expt. No.	P, mm	P_{CO_2} : P_{CO}	τ, sec	k, sec^{-1}			Expt. No.	P, mm	P_{CO_2} : P_{CO}	τ, sec	k, sec^{-1}		
				$m=0$	$m=0,5$	$m=1$					$m=0$	$m=0,5$	$m=1$
	Cu, 340°							Fe_3O_4, 270°					
11	43	1 : 1	4,98	0,037	0,037	0,037	25	176	5 : 1	7,4	0,0246	0,055	0,123
5	80	1 : 1	5,84	0,050	0,050	0,050	27	176	3 : 1	7,1	0,0260	0,045	0,078
7	83	1 : 1	5,96	0,048	0,048	0,048	45	176	2 : 1	3,7	0,0326	0,046	0,065
13	117	1 : 1	11,44	0,037	0,037	0,037	29	176	1 : 1	7,4	0,0640	0,064	0,064
12	249	1 : 1	4,98	0,041	0,041	0,041							
							46	45	2 : 1	2,4	0,0587	0,083	0,117
18	196	1 : 5	6,26	0,056	0,026	0,011	44	60	2 : 1	3,7	0,0600	0,085	0,120
14	130	1 : 3	10,86	0,046	0,033	0,015	41	77	2 : 1	3,7	0,0495	0,070	0,098
16	200	1,5 : 1	5,26	0,035	0,045	0,052	40	120	2 : 1	3,7	0,0400	0,056	0,079
15	127	3 : 1	8,48	0,040	0,073	0,120	33	238	1 : 1	5,5	0,059	0,059	0,059
17	190	5 : 1	8,00	0,045	0,100	0,225	31	318	1 : 1	5,5	0,061	0,061	0,061
	Pt foil (1.9 g), 700°							Ni foil, 700°					
34	88	1 : 1	0,633	0,332	0,332	0,332	16	235	1 : 8	1,9	0,595	0,210	0,073
33	172	1 : 1	0,633	0,332	0,332	0,332	15	120	1 : 1	1,6	0,364	0,364	0,364
35	265	1 : 1	0,633	0,305	0,305	0,305	12	194	4 : 1	0,74	0,253	0,505	1,030
	Pt foil (3.7 g) 700°						13	312	7,85 : 1	0,51	0,195	0,545	1,530
9	573	3,7 : 1	0,153	0,56	1,66	4,90	14	341	12,2 : 1	0,43	0,078	0,280	0,960
3	301	5,6 : 1	0,220	0,78	1,83	4,40				W, 550°			
6	172	2 : 1	0,362	1,26	1,79	2,52	7	259	4 : 1	3,12	0,0118	0,0236	0,0472
7	176	1 : 1	0,416	1,73	1,73	1,73	8	134	1 : 2,25	11,33	0,1240	0,0825	0,0550
8	166	1 : 2	0,416	2,34	1,66	1,17	9	105	1 : 3,66	10,30	0,2060	0,1340	0,0870

Tungsten. Experiments on tungsten were carried out at 550-700°. Under the experimental conditions, the W phase showed low stability. Beginning at 550°, isotopic exchange became appreciable, and the formation of tungsten carbide commenced at this same temperature. The oxidation of tungsten by carbon dioxide takes place at higher temperatures. It was not possible to attain constant catalytic activity, and for this reason the kinetics of reaction could only be surmised.

TABLE 2

Catalyst	ρ, g/cm^3	σ, m^2/g	k* · 10^8, moles/(atm · m^2 · sec)	q, kcal/mole	Reference	m
Ag	1,2	0,4	—	16	[6]	—
Cu	0,75	12,9	2,64	80	[7]	0
Pt foil	21,4 *	0,014	10,4	100	[8]	0,5
Co	1,2	4,5	14,2	111	[9]	—
Fe_3O_4	1,18	14,6	29,6	125	[3]	0,5
Ni foil	8,9 *	0,0045	1000	130	[10]	0,5
W	3,9	3,5	0,0029	155	[11]	1

*Density

X-ray studies of the catalysts, carried out by N. G. Sevast'yanov at the conclusion of the kinetic measurements, showed that the iron oxide catalyst had the magnetite structure, that the Ni and Co metals were contaminated with carbon, that small amounts of alloying CuO were to be detected in the copper, and that the tungsten catalyst contained a considerable amount of tungsten carbide, WC.

Evaluation of the specific surfaces of the catalysts was made from the low-temperature nitrogen adsorption, with the results which are shown in Table 2.

The experimental data will now be compared with the theoretical conclusions concerning the maximum catalytic activity [1]. On a surface for which the heat of adsorption is independent of the degree of coverage, the maximum rate is reached in Reaction (1) when the surface coverage by oxygen is equal to 0.5. The corresponding value of the heat of adsorption of oxygen, which will be designated as optimal, can be estimated in the following manner. It will be assumed that the standard entropy change, ΔS°, for (3) is approximately the same as the value of ΔS° for reaction (9). A typical value for Reaction (9) would be $\Delta S^\circ = 2$ cal/deg (Me = Ni, Cu). At half coverage, the standard free energy change of Reaction (3) is $\Delta G^\circ = 0$; since $\Delta G^\circ = \Delta H - T\Delta S^\circ$, the value $\Delta H = 1100$ cal is obtained at 300°. Combining this result with the value of the change in free energy for the reaction $CO + 1/2\ O_2 = CO_2$, we obtain $\Delta H = -138{,}000$ cal for the reaction $O_2 + 2(\ ) = 2(O)$.

In the case of a surface whose heat of adsorption varies linearly with the coverage, the highest catalytic activity occurs when the heat of adsorption at half coverage is close to the optimal value. Reaction will then take place in the region of moderate coverage, i.e., with m = 0.5. If the heat of adsorption is much less than the optimal, the kinetics must correspond to low coverage and m = 0; if the heat of adsorption is much greater than the optimal, the kinetics must correspond to high coverage and m = 1. The catalytic activity will be low in both cases. In Table 2 the activities of the catalysts are compiled as a characterized by the values of the constant k^* at 300°, the heats of adsorption of oxygen according to the data of the literature, and the values of the constant m. The k^* values for Pt and Ni foils, and for tungsten, have been extrapolated to 300° with the aid of the Arrhenius Equation. It should be noted that the available data on the heat of adsorption are not uniformly significant. Preference has been given here to results which have been obtained by direct calorimetric measurements. Maximal activity for Reaction (1) is shown by Ni, and by Pt, Co, and Fe_3O_4. For these catalysts, the heat of adsorption of oxygen is clearly close to the optimal value, m = 0.5. With copper, this heat of adsorption is considerably less than the optimal value and its catalytic activity is less than the maximal, m = 0; with tungsten, the heat of adsorption is much greater than the optimal and its catalytic acitivity is also less than maximal, m = 1. With Ag where the heat of adsorption of oxygen is 16 kcal/mole, i.e., very small, exchange could not be detected. Thus the experimental data are in quantitative agreement with the predictions of the theory.

LITERATURE CITED

[1] M. L. Temkin, J. Phys. Chem. 31, 3 (1957).

[2] N. V. Kul'kova, É. D. Kuznetz and M. L. Temkin, Proc. Acad. Sci. USSR 90, 1067 (1953).

[3] N. V. Kul'kova and M. L. Temkin, J. Phys. Chem. 31, 2017 (1957).

[4] A. A. Vvedenskii, Thermodynamic Calculations for the Reactions of the Fuel Industry (in Russian), 1949.

[5] W. Baukloh, B. Chatterjee and P. P. Das, Trans. Indian Inst. Metals 4, 271 (1950).

[6] A. F. Benton and L. C. Drake, J. Am. Chem. Soc. 56, 506 (1934).

[7] A. W. Russel and O. C. Bacon, J. Am. Chem. Soc. 54, 54 (1932).

[8] G. B. Taylor, G. B. Kistiakowsky, and J. H. Perry, Zs. phys. Chem. 34, 799 (1930).

[9] R. Rudham and F. S. Stone, Trans. Farad. Sci., 54, 420 (1958).

[10] O. Beeck, Advances in Catalysis 2, 151 (1952).

[11] J. K. Roberts, Proc. Roy. Soc. A, 152, 445 (1935).

Received September 20, 1958

THE MECHANISM OF THE LOW TEMPERATURE POLYMERIZATION OF MONOMERS UNDER THE ACTION OF GAMMA RADIATION

A. P. Sheinker, M. K. Yakovleva, E. V. Kristal'nyi and A. D. Abkin

The L. Ya. Karpov Scientific Research Institute for Physical Chemistry

(Presented by Academician S. S. Medvedev, October 30, 1958).

It is one of the characteristics of the radiational polymerization of the vinyl compounds that these processes can be carried out at comparatively low temperatures. This results from the fact that the energy of activation for polymerization under the action of radiation is relatively low [1] in comparison with the activation energy for polymerization with material initiators. In spite of this, it would be anticipated that any considerable diminution in the temperature would bring about a significant decrease in the rate of polymerization. But, as we have shown, the polymerization of certain monomers (isobutylene, the nitrile of acrylic acid, and others) under the action of γ-radiation proceeds with measurable velocity even at very low temperatures (-195°).

By work in the field of radiational polymerization, it is established that the process at ordinary temperatures is carried on through a radical mechanism [2]. The experimental observations (the relatively high rate of polymerization of various monomers at low temperatures; the polymerization of isobutylene, which is known to follow a nonradical mechanism, etc.) force one to conclude that low temperature polymerization does not proceed through a radical mechanism. The literature contains only one communication dealing with this question [3].

The present work outlines results which have been obtained in an investigation of the mechanism of the low temperature polymerization of various vinyl compounds under the action of γ-radiation. In this study of mechanisms, use was made of the method of copolymerization, through which the necessary information concerning the nature of the active particles (radicals, ions) promoting the polymerization process can be obtained from data on the kinetics and the copolymer compositions [4].

Study was made of the copolymerization of isobutylene with vinylidene chloride (in "bulk") over the temperature interval −78 to 0°, and of methylmethacrylate with styrene in ethyl chloride solution at −78° to + 25°.

Polymerization was carried out in ampules in a Co^{60} source with a source strength of 20,000 gram equivalents at an intensity of 230-250 r/sec. Exposure of the carefully purified monomers in ampules was performed in vacuum under such conditions as to assure the absence of atmospheric oxygen. The precision of the dosing of the isobutylene and the vinylidene chloride amounted to 2-3%. Depending on the composition, the time of polymerization of these monomers varied from 2 to 8 hours. The degree of polymerization did not exceed 10%. The yield of polymer was determined by weighing. Determination of the compositions of the copolymers of isobutylene with vinylidene chloride was through analysis for the content of chlorine.

In Fig. 1, data on the isobutylene – vinylidene chloride system is presented to show the relation between the composition of the starting mixture and the compositions of copolymers formed by polymerization at various temperatures. From these data there were obtained the copolymerization constants, α (for isobutylene) and β (for vinylidene chloride), use being made of a simplified integral composition equation [5]. Numerical values of these constants are presented in Table 1.

It follows from these data that the compositions of the copolymers alter markedly with the temperatures of copolymerization, and in such a manner that the copolymers are enriched with vinylidene chloride in the

temperature region (0°), and with the isobutylene component in the region of low temperatures. It is especially significant that this enrichment increases sharply on decreasing the temperature from −40 to −78°. It is well known that with fixed mechanism of initiation, variation of the polymerization temperature alters the composition of the copolymer only insignificantly.

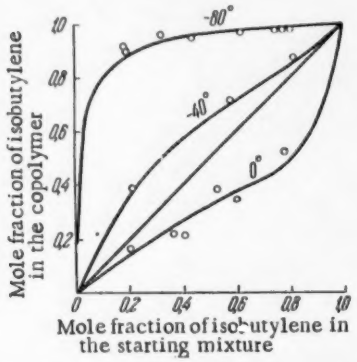

Fig. 1. The relation between the composition of the copolymer and the composition of the starting mixture in the polymerization of isobutylene with vinylidene chloride. The points represent experimental data; the curves have been calculated from the experimentally determined values of α and β.

TABLE 1

Temperature of polymerization, °C	α	β
−78	25	0
−40	1.27	0.21
0	0.03	1.3

Thus, the observed inversion of the relative reactivities of the monomers indicates that polymerization under the action of radiation proceeds according to different mechanisms at low, and at high, temperatures.

For a radical initiation mechanism, the copolymerization constants for the system isobutylene – vinylidene are $\alpha = 0$ and $\beta = 1.5$ [6]. These are close to the values which have been found here for radiational polymerization at 0°. This fact can serve as a proof that the radiational polymerization of isobutylene and vinylidene chloride proceeds according to a radical mechanism at high temperatures (in this case, at 0°).

It is clear that a diminution of the temperature brings into play ionic type reactions, the contribution of such reactions increasing as the temperature falls.

Isobutylene with its two electropositive substituents is known to be characterized by the ability to undergo cationic polymerization. In terms of the carbonium mechanism, vinylidene chloride fails to polymerize because of the presence of electronegative substituents (chlorine atoms) at the molecule's double bond. This is in full agreement with the data on the separate radiational polymerization of isobutylene, and vinylidene chloride.

Thus, at −78°, the initial rate of polymerization of isobutylene is 0.31 M/liter · hr, whereas the rate of polymerization of vinylidene chloride is only 1/15th this large and amounts to 0.023 M/liter · hr. On the other hand, at 0°, the rate of polymerization of vinylidene chloride is almost 50 times higher than that of isobutylene.

These facts justify the supposition that copolymerization of isobutylene with vinylidene chloride at low temperatures under the action of γ-radiation proceeds through a carbonium mechanism, or, in any case, through something which is very close to a carbonium mechanism.

Considerable interest attaches to the study of the polymerization of other monomers at low temperatures. Here, the principal interest is directed to the copolymerization of styrene and methylmethacrylate, since the relation between the polymerization mechanism and the compositions of the resulting polymers has been studied in detail for this monomer pair [7].

At 25°, the polymerization of styrene and methylmethacrylate follows a radical mechanism, as has been shown earlier [8]. In this case, the copolymer formed from an equimolar mixture of the monomers contains approximately equal amounts of the two components. The study of this pair of monomers has added significance in view of the fact that styrene is known to be capable of polymerizing according to either a radical or an ionic mechanism.

Polymerization was carried out on styrene, and on an equimolar mixture of styrene and methylmethacrylate in ethyl chloride (styrene concentration, 2.51 M/liter; total monomer concentration, 4.03 M/liter). The compositions of the resulting copolymers were determined by infrared spectroscopy of the band at 1725 cm^{-1} which is characteristic of the CO groups of polymethylmethacrylate. The results are presented in Table 2, and in Fig. 2.

TABLE 2

Polymerization temperature, °C	Degree of polymerization, %	Mole ratio of components in copolymers, styrene: methylmethacrylate
25	7.9	0.55 : 0.45
0	2.38	0.66 : 0.34
−30	1.38	0.71 : 0.29
−78	4.3	0.79 : 0.21

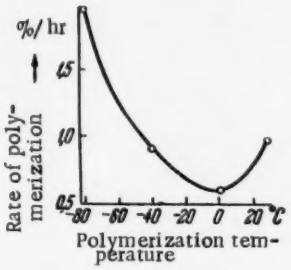

Fig. 2. The relation between the rate of polymerization of styrene and the polymerization temperature.

It follows from the data of Table 2 that the relative amount of the methylmethacrylate in the copolymer diminishes markedly with a decrease in the polymerization temperature, a fact which points to an increase in the contribution made by the ionic reactions. In this connection, it is interesting to note that lowering the temperature of polymerization of styrene from + 25° to −78° at first decreases, and then increases, the rate of polymerization (Fig. 2). Here, the rate of polymerization at −78° is greater than the rate at +25°.

The rise in the rate of polymerization of styrene with diminishing temperature could only be due to the formation of chains of ionic type in the system, the contributions of the ionic and the radical reactions being dependent on the reaction temperature. The possibility of low temperature radiational polymerization according to an ionic (carbonium) mechanism clearly arises from the formation in the system of those conditions which favor a lengthening of the life of the ions which are produced under the action of the radiation. This is also a determining factor in the production of chains of ionic type in the system. The data available at the present time is not sufficiently detailed to permit a consideration of the mechanism of the formation of ionic chains. This problem will be dealt with in future investigations.

The authors wish to express their indebtedness to Academician S. S. Medvedev for his interest in this work and for a discussion of the results.

LITERATURE CITED

[1] D. S. Ballantine, P. Colombo, A. Glines and B. Manowitz, Chem. Eng. Progr. Sympos. Series 50, No. 11, 267 (1954).

[2] T. S. Nikitina and Kh. S. Bagdasar'yan, Collected Papers on Radiation Chemistry (in Russian), Acad. Sci. USSR Press, 1955, p. 183.

[3] W. H. T. Davison, S. H. Pinner and R. Worral, Chem. and Ind. No. 38, 1274 (1957).

[4] A. D. Abkin, Problems of Chemical Kinetics, Catalysis and Reactivity (in Russian), Acad. Sci. USSR Press, 1955, p. 338.

[5] L. M. Gindin, A. D. Abkin and S. S. Medvedev, J. Phys. Chem. 21, 1269 (1947).

[6] T. A. Alfrey, J. Bohrer and G. Mark, Copolymerization (Russ. trans.) Foreign Lit. Press, 1953, p. 37.

[7] C. Walling, E. R. Briggs, W. Cummings and F. R. Mayo, J. Am. Chem. Soc. 72, 48 (1950).

[8] W. H. Seitzer, R. H. Goeckermann and A. V. Tobolsky, J. Am. Chem. Soc. 75, 755 (1953).

Received October 27, 1958

THE FORMATION AND PROPERTIES OF METAL SOAPS IN DILUTE AQUEOUS SOLUTIONS

N. A. Aleinikov and A. M. Makarova

S. M. Kirov Kola Section of the Academy of Sciences USSR

(Presented by Academician P. A. Rebinder, September 6, 1958)

The study of the composition and properties of metallic soaps prepared in dilute aqueous solutions can be of considerable help in explaining the changes in the surface properties of particles during flotation [1], the phase transitions in emulsions, stabilities of emulsions and foams, flocculation, ion exchange, and other phenomena occurring in dispersed systems.

While analyzing the crystals of saturated aliphatic acids with ion exchange in mind, A. A. Trapeznikov [2] showed that the amount of exchange between H^+ and Cu^{++} when plotted against the pH of the solvent passed through a maximum (pH ~ 4.75). A similar type of change was observed in the viscosity and related properties of Al soaps of naphthanoic acids [3]. When the properties of metallic soap films formed on the surface of aqueous solutions were compared with those formed on the surface of minerals, it was found [4, 5] that the interaction between the polyvalent cation in solution and a film of palmitic or myristic acids occurred at a relatively low pH. The surface area of the film (calculated by assuming a unimolecular layer) also showed characteristic changes with respect to pH, a maximum in the acid region (cations were Al, Co, Cu)* where "solid" films were formed [5].

This kind of a change is undoubtedly connected with a variable composition of the soaps being formed.

The formation of metallic soaps with polyvalent cations, depending on the pH of the aqueous solution, can be represented as a process in which there is a simultaneous formation of "acidic" and "basic" soaps. The first soaps are formed under conditions where the hydrolytic dissociation of the polyvalent cation salt is small, and as the pH decreases their composition changes from fully substituted (stoichiometric) soaps to dissociated soap molecules, by going through stages with various amounts of H^+ incorporated into their colloidal ions or polymeric complexes. In this case alongside an ionic exchange we can also assume a molecular mechanism involving the adsorption of palmitic acid on the micelles of "basic" soaps, followed by a chemical reaction.

Basic salts formed by hydrolysis (among them complex cations) readily form the "basic" soaps whose composition will vary with increase in pH from soaps with incompletely substituted palmitic acid to alkaline soaps with different amounts of chemisorbed hydroxyl ions. The first soaps will have cation-like properties, the latter ones anion-like. It is obvious that, with increased pH of the solution, the amount of "acidic" soaps being formed will go through a maximum, while the amount of "basic" soap will keep increasing without interruption. The investigation of the hydrolysis kinetics of dilute salts and of its effects on the mechanism of formation and the composition of metallic soaps is quite important; however, in this work we did not investigate it particularly.

To prove the general scheme of metallic soap formation we prepared Fe^{++} and Fe^{+++} palmitates. The method by which these soaps are formed from the reaction solutions can represent the processes normally

*No determination was made with Fe.

occurring in the presence of these soaps. In our case it was important to carry out the addition of sodium palmitate solution, containing various amounts of free NaOH, by pouring it into an iron sulfate solution which contained various amounts of free H_2SO_4. The concentration of sodium palmitate in the original solution was fixed at $3.9 \cdot 10^{-3}$ moles/liter, and at 44-45° this solution was only slightly colloidal. After the iron salt solution ($FeSO_4$ or $Fe_2(SO_4)_3$) was heated to the above mentioned temperature we added to it the stoichiometric amount of sodium palmitate contained in an approximately equal volume of solution. After the solutions were mixed, the mixture was stirred for 5 minutes at the same temperature, then the pH was measured at 20° and the reaction mixture extracted with diethyl ether. The ether layer contained the most hydrophobic compounds: "acidic" soaps, that part of "basic" soaps which contained the largest amount of palmitic acid, and the free palmitic acid if there was any left in solution. Typical "basic" soaps were insoluble in ether. A determination of the total amount of iron in the isolated products gave its distribution among the two types of soaps and indicated their relative amounts. Since the quantitative results were reproducible, it indicated that some sort of an equilibrium was achieved in these reactions.

The general form of the experimental function representing the change of soap composition vs pH agrees well with the assumed one (Fig. 1). With the $Fe_2(SO_4)_3$ salt, which is hydrolyzed more completely than $FeSO_4$, the maximum in the formation of "acidic" soaps is displaced in the direction of lower pH.

To determine the composition of the "acidic" soaps prepared in acidic media, we extracted the free palmitic acid from the reaction mixture by using dioxane, and determined the bound palmitic acid and iron in the residue. The ratio between the palmitic acid and iron equivalents varied from 0.44 to 1.0. With typical "basic" soaps the same ratio had a value of about 0.06.

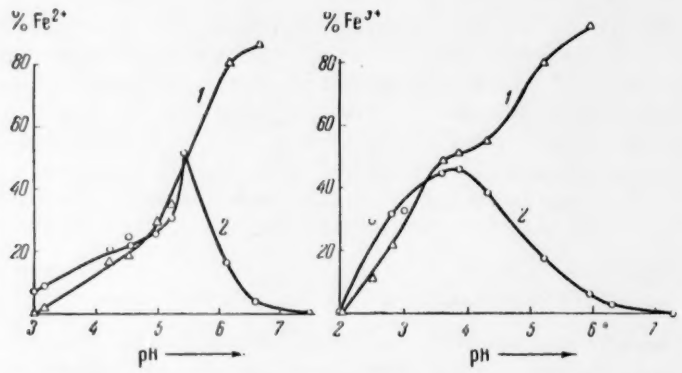

Fig. 1. The distribution of Fe^{++} and Fe^{+++} among the palmitic acid soaps as a function of pH. 1) Basic soaps; 2) acidic soaps.

With increased pH the stability of "basic" soaps in solution increased, and at a pH 10-11, beside the salting out of sodium palmitate, we detected the formation of a highly stable sol. When we agitated the aqueous solutions by bubbling air, the "acidic" soaps readily flocculated and formed flakes exhibiting froth flotation, in a manner which resembled the surface coagulation observed in colloidal solutions [6]; the "basic" soaps showed less tendency toward flocculation.

On the basis of the observed properties of iron soaps one can assume that the flotation of natural iron oxides (hematite and magnetite) by carboxylic acids results from the formation of similar compounds on the surface of the particles. Actually at pH < 6 the flotation of iron oxides proceeds primarily on account of the surface compounds of the "acidic" soap type which also contain some carboxylic acid molecules. In this case the formation of flotation aggregates from particles and air bubbles exhibits fast kinetics, which is also confirmed by the great number of recommendations prescribing flotation of iron oxides at low pH. When pH > 7 the flotation of iron oxides proceeds through the formation surface compounds which are primarily composed of "basic" soaps and chemisorbed compounds while the formation of aggregates is retarded.

We are extremely grateful to Acad. P. A. Rebinder and A. B. Taubman for their valuable advice and interest in this work.

LITERATURE CITED

[1] M. E. Lipets, J. Phys. Chem. 16, 59 (1942).

[2] A. A. Trapeznikov, Proc. Acad. Sci. USSR 114, No. 6, 1280 (1957).*

[3] G. V. Belugina and A. A. Trapeznikov, Colloid. J. 20, No. 1, 3 (1958).*

[4] A. A. Trapeznikov, J. Phys. Chem. 12, 583 (1938); 13, 406 (1939); Proc. Acad. Sci. USSR 47, 349 (1945).

[5] G. A. Wolstenholme and I. H. Schulman, Trans. Farad. Soc. 46, 475 (1950); 47, 788 (1951); I. H. Schulman and T. D. Smith, Recent Developments in Mineral Dressing, London, 1953, p. 393; H. Kimizuka, Bull. Chem. Soc. Japan, 29, 123 (1956).

[6] S. G. Mokrushin, Trans. 3rd All-Union Conference on Colloidal Chemistry, 1956, p. 357; H. Freundlich and S. Loebman, Kolloidchem. Beihefte 28, 391 (1929).

Received September 30, 1958

*Original Russian pagination. See C.B. Translation.

THE ANODIC PASSIVATION OF SILVER IN ALKALINE SOLUTIONS

G. L. Vidovich, D. I. Leikis, and B. N. Kabanov

Institute of Electrochemistry of the Academy of Sciences USSR

(Presented by Academician A. N. Frumkin, October 1, 1958)

As is well known [1], the anodic oxidation of silver in alkaline solutions proceeds in two steps – first Ag_2O is formed, then at higher potentials the Ag_2O is converted to AgO. The described oxidation process does not proceed until all the silver is used up, but stops after a while due to the passivation of the metal.

In this work we have investigated the passivation of silver in KOH solutions, in the 0.01 to 10 N concentration range. The work was carried out by a method in which the capacity and ohmic components of the impedance of the electrode were measured at a constant current density or potential. The impedance was measured by compensation. In the compensating arm of the bridge of the electrode represented a capacitance C_2 and resistance R_2 connected in parallel, both in series with a resistance corresponding to that of the solution. With this measuring technique R_2 corresponded to the resistance of the reaction or of one of its stages, while C_2 corresponded to the capacity of the double layer.

As may be seen in Fig. 1, when a small positive potential was applied to the electrode (0.3 v, with reference to a mercuric oxide electrode in the same solution) the rate at which silver dissolved rapidly declined with time, and was accompanied by a parallel decrease in the capacity of the electrode's double layer. These large changes in the solution current and the electrode capacity occurred after only a small amount of electricity was passed (approximately 20 mcoul / cm^2), an amount corresponding to about 10 molecular layers of Ag_2O. It seems that the drop in capacity may be connected with the semiconducting properties of Ag_2O [2]. Moreover, we are assuming that the forming layer of Ag_2O covers the electrode relatively evenly.

On the basis of the data presented we may assume that at first (before a solid layer of Ag_2O has formed on the surface) the process proceeds through solution and a primary formation of a supersaturated solution followed by a deposition on the crystallization centers.*

After a compact layer of Ag_2O has formed on the silver surface, it seems that the $Ag \rightarrow Ag_2O$ process continues at the solid interface; this is similar to the process occurring during the passivation of iron in acidic solutions [4], with the difference that the growing Ag_2O film will not dissolve any more in alkali. Therefore, it is natural that the rate of the $Ag \rightarrow Ag_2O$ process should decrease with the formation of a compact Ag_2O layer. We call this the first stage of passivation.

However, even at this decreased rate the process proceeds for only a limited length of time. This may be seen in Fig. 2, where we have shown the dependence of the potential φ, the capacity C_2 and ohmic R_2 components of the impedance of a silver electrode in a 0.1 N KOH solution on the amount of current passed at a constant current density and $3 \cdot 10^4$ hertz.** One can see in Fig. 2 that at a constant current strength during a fixed time interval (point a) the potential sharply increases (by approximately 0.3 v) and the second stage of passivation sets in.***

*That this electrochemical process can proceed through solution in 3 to 12 N alkali was proven in work [3].

**Similar dependence was observed within the whole investigated KOH concentration range and also at lower frequencies.

***It is possible that this is caused by an enrichment of the Ag_2O layer, adjacent to the silver, in oxygen, or by the adsorption of oxygen at the Ag/Ag_2O boundary.

Simultaneously there is a sharp increase in R_2, i.e., a retardation of some electrochemical process. We are not dealing with the $Ag \rightarrow Ag_2O$ process as whole, since the resistance of this reaction (calculated from the slope of the overvoltage curve) is larger than the measured R_2 by two orders of magnitude. Probably the measured R_2 characterizes one of the stages in the $Ag \rightarrow Ag_2O$ process. It is possible that an electrochemical adsorption of oxygen on the silver surface constitutes this stage, just as it happens during the solution and passivation of iron in alkali [5].

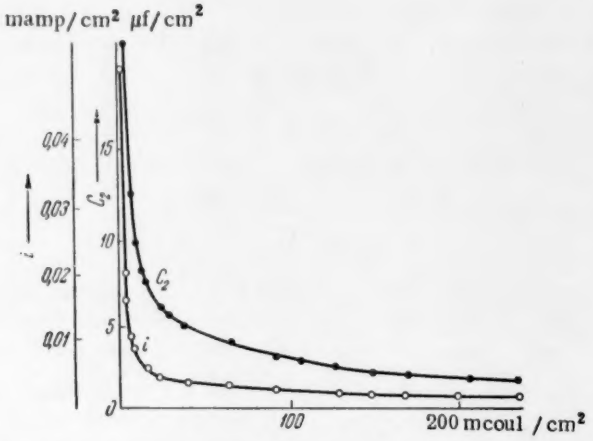

Fig. 1. The anodic current density and the capacity of a double layer on a silver electrode at 0.3 v in 0.1 N KOH as a function of the current passed through.

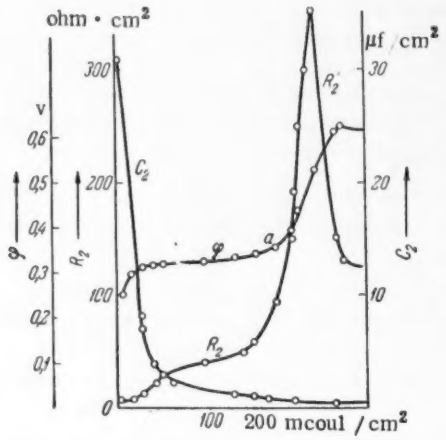

Fig. 2. Changes in the potential, the capacity of the double layer, and the electrode resistance at a 0.08 ma/cm² current density.

As soon as the electrode potential exceeds the $Ag_2O \rightarrow AgO$ standard electrode potential, the $Ag_2O \rightarrow$ $\rightarrow AgO$ reaction begins to proceed alongside the $Ag \rightarrow$ $\rightarrow Ag_2O$ reaction, which is equivalent to introducing one more parallel conductance, the reciprocal of which corresponds to the resistance calculated from the curve we obtained for the overvoltage in the $Ag_2O \rightarrow AgO$ reaction. Since the resistance of the $Ag_2O \rightarrow AgO$ reaction is small as compared to R_2 (which was increased as a result of passivation), the measured total resistance R'_2 sharply drops after the $Ag_2O \rightarrow AgO$ reaction sets in (Fig. 2).

Interestingly, after the second passivation stage the silver still continues to undergo anodic oxidation. The second anodic plateau on the charge curve which corresponds to the formation of AgO is evidence of this, as it is usually shorter than the first. That this extended delay is caused by the oxidation of silver and not by some extraneous process is evident from the fact that the total amount of electricity used in the two plateaus of the cathodic reduction is always equals to the total amount of electricity expended in the anodic oxidation. The oxidation of silver on the second plateau proceeds at a rate which is lower (by nearly 5 orders of magnitude) than the rate extrapolated (to 0.6 v) from the first plateau of the overvoltage curve for the $Ag \rightleftharpoons Ag_2O$ process (in estimating the rate we have assumed that the rate of this process changed insignificantly over the length of the second plateau). Thus, we can assume that the second stage of passivation results in a retarded silver solution rate (by several orders of magnitude).

It should be noted that at high current densities, the oxidation of metallic silver is not observed; for example, at 0.73 v (vs a standard hydrogen electrode) in 0.1 N KOH. In this case the amount of electricity used in the $Ag \rightarrow Ag_2O$ process is equal to the amount used in the $Ag_2O \rightarrow AgO$ reaction, i.e., at a potential above 0.73 v (vs a standard hydrogen electrode) silver is almost completely passive in 0.1 N KOH. A similar passivation of silver in 10 N KOH occurs at potentials above 0.64 v. We call this practically complete discontinuity in the oxidation of silver the third stage of passivation.

It should be note that all the observed passivation stages do not occur independently of each other, but follow each other. Thus, for example, if the first anodic plateau is established at such high current densities (0.5 ma/cm^2) that its length is considerably decreased then the third passivation stage is not observed at the potentials at which it usually occurs.

Therefore, the anodic passivation of silver in alkali proceeds in three successive stages, and each stage is accompanied by a sharp decline in the oxidation rate. We are currently continuing our investigation of the mechanism of these stages.

LITERATURE CITED

[1] R. Luther and F. Pokorny, Zs. anorg. Chem. 57, 291 (1908); A. Rakov, Dissertation at the L. Ya. Karpov Moscow Phys. Chem. Inst. 1947.

[2] A. Rakov, T. Borisova, and B. Érshler, J. Phys. Chem. 22, 1390 (1948).

[3] Yu. V. Pleskov, Proc. Acad. Sci. USSR 117, No. 4, 645 (1957).*

[4] K. F. Bonhoeffer, Zs. Electrochem 59, No. 7, 594 (1955).

[5] D. I. Leikis, Dissertation at the Inst. Phys. Chem. Acad. Sci. USSR, 1958.**

Received September 11, 1958

*Original Russian pagination. See C.B. Translation.

**In Russian.

PHASE COMPOSITION STUDY OF THE COPPER CATALYST USED IN THE OXIDATION OF PROPYLENE TO ACROLEIN

O. V. Isaev and M. Ya. Kushnerev

Institute of Physical Chemistry of the Academy of Sciences, USSR

(Presented by Academician V. L Spitsyn, October 6, 1958)

In a previous work [1] we have shown that depending on the composition of the reaction mixture and the temperature during the catalytic oxidation of propylene to acrolein the phase composition of the catalyst changes; there is either an enrichment of the cuprous oxide by metallic copper or an increase in the oxygen content in the cuprous oxide. The x-ray analysis of the catalyst was done not during the oxidation of propylene, but periodically after each experiment, which made this work inadequate.

The purpose of the present work was to investigate the phase changes in the copper catalyst during the oxidation of propylene to acrolein.

To have an uninterrupted control over the phase changes we used a technique which made it possible to take x-ray pictures during the reaction itself. The x-ray pictures were taken in an especially designed chamber, whose structural characteristics are shown in Fig. 1.

A powdered sample of cuprous oxide (2-3 mg) was placed in reactor 1, which was made of a thin (diameter 0.7-1.0 mm) molybdenum glass capillary and was heated by a coiled electric heater 2. The reactor was linked to a system which permitted a continuous addition of the gaseous mixture and collection of the reaction products. The temperature of the catalyst was registered with the help of a thermocouple and maintained constant within $\pm$ 1°. The x-ray beam scattered by the sample was recorded on a flat film placed in the box 3.

With the catalyst under investigation we obtained good resolution and satisfactory reflection intensities by using a BSV-5-Cu x-ray tube (without a β-ray filter), with a distance of 25-26 mm between the sample and the film and a 15-30 min exposure.

As in our previous work, we used cupric oxide, cuprous oxide, and copper metal as our starting materials. Cupric oxide was prepared by the oxidation of Cu and Cu_2O with air oxygen. Cuprous oxide was prepared by a method proposed by D. N. Finkel'shtein [2]. Copper metal was made by reducing copper oxides with propylene at 350-400° [1]. All the experiments were carried out at atmospheric pressure on a gaseous mixture of the following composition: 15% propylene, 15% oxygen, and 70% nitrogen. Contact time was maintained for about 2 seconds.

In Fig. 2 and 3, we have presented the results from our identifaction of the x-ray pictures taken on the catalysts. We plotted sin θ on the abscissa and line intensity (determined visually) on the ordinate.

During the oxidation of propylene on cupric oxide (see Fig. 2) at 310°, we observed a reduction of the catalyst; after 210 min the catalyst showed the presence of cuprous oxide. A rise in temperature (343 and 370°) resulted in a sharply increased reduction rate. Besides the formation of cuprous oxide, in both cases we have detected the presence of a metallic phase, and the higher the temperature the sooner it appeared. When the oxidation of propylene was carried out at 370° on CuO, after 135 minutes only one phase was observed – copper metal.

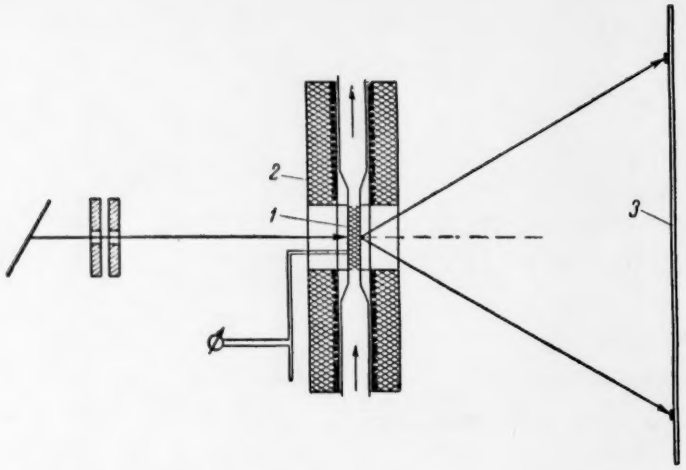

Fig. 1. The basic scheme of an x-ray. chamber for the investigation of copper catalysts during the oxidation of propylene to acrolein.

Similar results were obtained when propylene was first oxidized on cuprous oxide. As may be seen in Fig. 3, after the gaseous mixture was passed for 150 min over Cu_2O at 300° a metallic phase appeared. At 400° the cuprous oxide was fully reduced after only 65 min. When fresh copper metal was treated with the gaseous mixture in the 370-450° temperature range it did not undergo any phase changes. However, additional electron diffraction study of a thin copper film showed that some cuprous oxide was formed after the gaseous

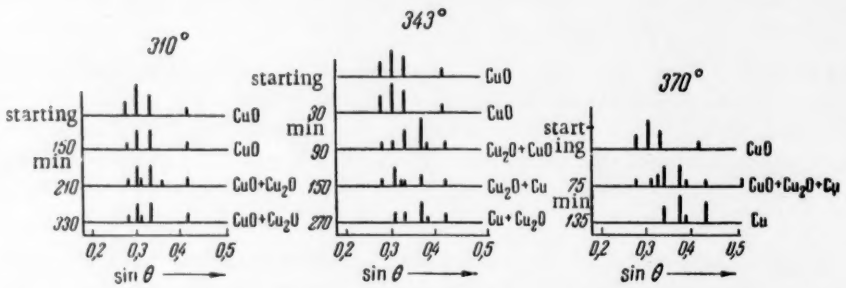

Fig. 2. Phase composition changes in the catalyst during the oxidation of propylene to acrolein on cupric oxide at 310, 340, and 370°.

mixture was passed over it at 400°. It is probable that during the oxidation of propylene to acrolein the catalyst surface is always covered with a layer of cuprous oxide which is not detected by the x-rays. The composition of the outgoing gases formed in the oxidation of propylene was constant with all the studied catalysts. Only on cupric oxide did we initially observe a slightly increased CO_2 yield, but it rapidly achieved a constant value. This may possibly be connected with the establishment of a constant phase composition on the catalyst surface.

The oxidation of propylene on a copper oxide catalyst results in the formation of a very reactive compound – acrolein, which can be oxidized and polymerized at 400-450° not only in the gas phase but also on the surface of the catalyst. Therefore, it was interesting to investigate the effect of acrolein on the phase changes in cupric oxide. The experiment showed that by passing a mixture of acrolein vapor (0.5%) and nitrogen over cupric oxide we reduced it to Cu_2O + Cu.

Addition of oxygen to the gaseous mixture strongly inhibited the reduction of the catalyst, and a polymeric film formed on its surface.

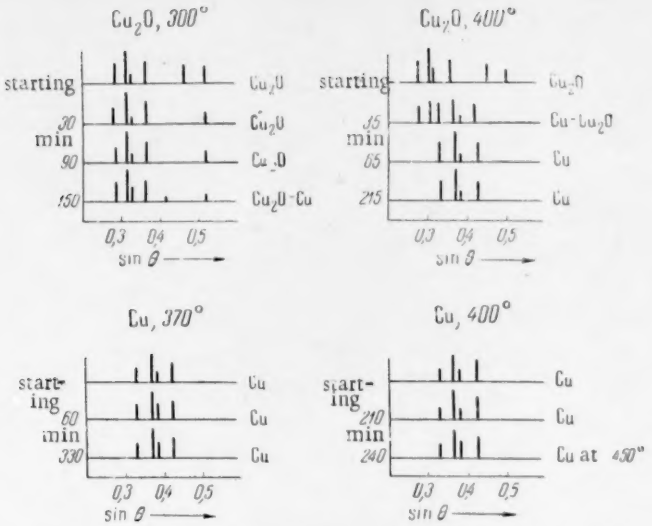

Fig. 3. Phase composition changes in the catalyst during oxidation of propylene to acrolein on cuprous oxide, at 300 and 400°.

By means of a special electron diffraction study we showed that a treatment of a copper film with a mixture containing acrolein (0.5-5.0%), oxygen (15%), and nitrogen for 2-3 hours at 400° resulted in the oxidation of copper to cupric oxide and a simultaneous deposition of a polymeric film on the catalyst surface (Fig. 4). It seems that a large excess of oxygen in the gaseous mixture may be responsible for the poisoning of the copper catalyst, not only as a result of the contact surface oxidation, but also due to an appreciable surface covering by a polymeric film.

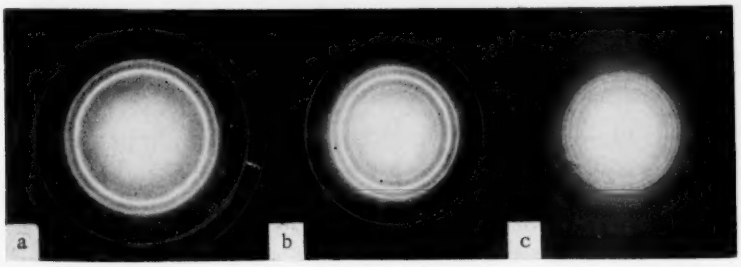

Fig. 4. Electron diffraction patterns of a thin copper film. a) The original copper film (Cu); b) copper film treated with the operational gaseous mixture (Cu_2O); c) copper film treated with a mixture composed of acrolein vapors (0.5-5.0%), oxygen (15%), and nitrogen (CuO plus polymer).

LITERATURE CITED

[1] O. V. Isaev, M. Ya. Kushnerev, and L. Ya. Margolis, Proc. Acad. Sci. USSR 119, No. 1, 104 (1958).*

[2] Yu. V. Karyakin and I. I. Angelov, Pure Chemical Reagents, Moscow, 1955. **

Received October 3, 1958

*Original Russian pagination. See C.B. Translation.

**In Russian.

THE GAS-CRYSTALLINE STATE OF MATTER IN POLYMERS

A. I. Kitaigorodskii

Institute of Heteroorganic Compounds of the Academy of Sciences, USSR

(Presented by Academician V. A. Kargin, October 3, 1958)

1. Gas-crystalline state in low-molecular weight compounds. The literature does not give enough emphasis to the fact that one of the most widespread phase states among molecular substances is the state where the molecular "centers" form a true three-dimensional lattice, while the molecular azimuths are randomly distributed and satisfy either a spherical or an axial symmetry. Timmerman's book [1] is the only exception; it contains a large list of compounds with their transition temperatures which enabled us to fix the stability ranges of this state. The existence of a gas-crystalline state may be detected by measuring the dielectric constant, and also from the heats of transition. Direct proof is obtained by x-ray structural analysis, which proves the random statistical distribution of the molecules.

The nature of molecular motion in the gas-crystalline state can not as yet be regarded as explained; there is no general, common movement. Probably the most frequent form is a vibration about the numerous equilibrium positions accompanied by intermittent transitions from one position to another.

The term we proposed, the "gas-crystalline state," emphasizes quite well the structural pecularities of this state: presence of a large scale order in the distribution of molecular centers, and the absence of any close range order in the molecular orientations. The gas-crystalline state arises in all the cases where the molecular rotations (of spherically or cylindrically shaped molecules) do not produce any appreciable changes in the density of packing.

The available structural data indicate that in almost every case the volume available to each molecule in the gas-crystalline state is somewhat smaller than the volume of the solid described by the rotating molecule. This means that not all the mutual orientations can exist in the crystal, but only those where the "protruberance" of one molecule fits into the "recess" of another [2]. Nevertheless, the large number of variations even among similar distributions makes the existence of the gas-crystalline state possible.

Ya. I. Frenkel' gave a very descriptive name to the transition from a normal crystalline state to the gas-crystalline – "orientational melting" [3]. He, however, as did many authors, erroneously assumed that the orientational melting always occurs at the λ-point, i.e., that it is a phase transition of the second type. The inaccuracy of this assumption was demonstrated by direct measurements of the heats of transition [1]. In certain cases, for example among paraffins, the abrupt volume changes were also measured [4]. A transition of the 2nd type – from a gas-crystalline to a crystalline state – constitutes an exception and not the rule.

2. The packed structure of polymers. In a recently published paper [5] we presented a new way of looking at the polymeric structure. We proposed that the structural "unit" of a polymer be a packet of chains.

The degree of regularity in polymers depends on the fraction of completely amorphous material located outside the packets and on the amount of order inside the packets. Let us discuss the nature of the order inside the packets (which was not done before). We are assuming that each packet, consisting of numerous parallel molecular chains, can exist in either the crystalline, the liquid, or the gas-crystalline state.

In the crystalline state the chains have a large scale orderly distribution not only with respect to their axes, but also with respect to orientation. In the amorphous (liquid) state there is a close range order diagonally

across the packets both with respect to the axes, as well as the orientation. In the gas-crystalline state there is a large scale order in the distribution of molecular axes across the packets but no regular orientation.

The specificity of polymeric chains — a periodic repetition along the chain — leads to two variations in the amorphous and gas-crystalline states. Each of them can exist with or without an arbitrary displacement of each chain along the general axis of chains. By using the terminology now accepted in liquid crystals, we can say that the amorphous and gas-crystalline states in polymers can exist in nematic (arbitrary displacement down the chain) or smectic (no displacement) modifications.

3. Indications of the gas-crystalline state in polymers. The cross section of either of the two modifications exhibited by the gas-crystalline portion of each packet should exhibit a hexagonal lattice to fit the close packing of cylinders. The circular cross section of any cylinder should be equal to the average cross sectional area S of the chain molecule. Therefore, the axis a of the two-dimensional hexagonal lattice should be approximately equal to $a = 1.1\sqrt{S}$. The maximum interplanar distances in a two-dimensional lattice of cylinders are: $a\frac{\sqrt{3}}{2}$, $a\frac{1}{2}$, ...

Theoretically it is easy to calculate the x-ray diffraction patterns for samples in the gas-crystalline state. This state exhibits characteristic sharp 1-3 equatorial reflection ("crystalline") and rapidly declining scattering intensities. Such an x-ray pattern could not be produced by either a liquid or crystalline state. The above mentioned pecularities in the intensity distribution arise as a result of the fact that the average "cylindrical" molecule has a wide and approximately homogenous (good for a rough calculation) electron density distribution in the cross section perpendicular to the chain axis. Beside this, some gaseous scattering should be observed near the original undiffracted beam. The presence of the latter type of scattering was demonstrated a long time ago [6].

The intensity of the x-rays scattered by such a system of closely packed cylinders can be calculated either for an infinite lattice or for a system consisting of n chains.

In the first case [7] the diffraction pattern is reduced to a series of equatorial reflections which can be described by the two indexes h and k of a two-dimensional lattice. The square of the structural factor can be written in the form

$$F_{hk0}^2 \approx f^2 \frac{(1+\cos^2 2\theta)}{\sin 2\theta}\left[\frac{J_1(sR)}{s}\right]^2,$$

where f = the atomic scattering factor, 2θ = scattering angle, $S = 4\pi \sin\theta/\lambda$, λ = wave length, J_1 = Bessel function; R = radius of the cylinder.

In the second case [8] we calculate the uninterrupted intensity curve from the formula

$$I \approx f^2(1+\cos^2 2\theta)\left[\frac{J_1(sR)}{s}\right]^2 (n + 2\sum_{m,m'}^{m'>m} J_0(s\rho_{m,m'})).$$

Summation is carried out over all the chain pairs m, m'; $\rho_{mm'}$ = distance between the chains.

For n of the order of 100 both analyses give similar results. Scattering by gas-crystalline polymers should satisfy the above written formulas.

So far we have discussed only the indications of the gas-crystalline state established by diffraction methods. Yet the existence of the gas-crystalline state should show up in many other properties. Here, we do not have enough space for a detailed analysis of this problem. We will only show, as an example, that the gas-crystalline state should become apparent in the morphology of substances, i.e., promote the formation of packets covered with regular faces.* The gas-crystalline state should also make the nuclear magnetic resonance lines narrower. The discovery of this effect in polystyrene [9] above 110° indicates, in our opinion, the formation of the gas-

*Packets with regular faces were first discovered by V. A. Kargin, H. F. Bakeev, and Kh. Vergin in the polymers of acrylamide, salvarsan, and the copolymers of methylmethacrylate and methacrylic acid [10].

crystalline state. Any movement of the molecular components can only occur in one manner – rotation about single C-C bonds, provided these bonds are located parallel to the packet of chains. Any other form of rotation is forbidden for steric reasons.

4. The gas-crystalline state in polyacrylonitrile. As an example of a high polymeric substance whose packets (to a substantial degree at least) are gas-crystalline we take polyacrylonitrile; its x-ray picture (in an extended state) consists of two sharp equatorial reflections with the interplanar distance $d_1 = 5.45$ and $d_2 = 3.15$ ($d_1/d_2 = \sqrt{3}$). Besides these reflections the photograph also shows a diffuse halo, which corresponds either to a completely amorphous material, or to portions of the packets where the molecules are distributed in the liquid state. The experimental intensity curve agrees extremely well with the calculated one.

TABLE 1

hkl	R = 2.5 A	R = 2.85 A	R = 3.15 A
100	100.0	100.0	100.0
110	7.4	20.0	57.0
200	3.4	1.62	4.0
210	0.24	1.70	2.5
220	0.00	0.30	0.8

We calculated the intensities for an infinite lattice made of cylinders and from these obtained the values of F^2 for three different cylinder sizes with the radii covering all the stereochemically possible variations in the conformation of the chains; these are tabulated in Table 1. We observed two experimental lines with the ratio between their F^2 values approximately equal to 5.

θ, degrees	3	4	5	6	7	8	9	10	11	12	13	14	15	16	17	18
I	55,2	34,7	18,1	58,5	94,5	224	5,46	0,4	4,2	4,2	10,0	**39,0**	9,5	5,2	0,5	0,03

It is interesting that the calculation for a finite number of chains also gives good results; in Table 2 we have done it for a small number, n = 25. The maxima corresponding to the (100) and (110) indices of a hexagonal lattice are shown in bold print.

It seems to us that here, we have a direct proof for the existence of the gas-crystalline state in polyacrylonitrile. A further search for the gas-crystalline state in polymers may be of considerable interest.

I would like to thank D. Ya. Tsvankin for his help in the calculations.

LITERATURE CITED

[1] J. Timmermans, Les constantes physiques des composés organiques cristallises, Paris, 1953.

[2] A. I. Kitaigorodskii, Organic Crystal Chemistry, Izd AN SSSR, 1955.*

[3] Ya. I. Frenkel', The Kinetic Theory of Liquids, Izd AN. SSSR, 1945.*

[4] A. E. Smith and A. Shearer, J. Am. Chem. Soc. 77, 2015 (1955).

[5] V. A. Kargin, A. I. Kitaigorodskii and G. I. Slonimskii, Colloid. J. 19, 131 (1957). **

[6] V. I. Kasatochkin and B. V. Lukin, J. Tech. Phys. 20, 1160 (1950).

[7] R. Bear and O. Bolduan, Acta Cryst. 3, 936 (1950).

[8] D. Ya. Tsvanskin, Proc. Acad. Sci. 120, No. 5 (1958). **

[9] L. V. Holroyd et al., J. Appl. Phys. 22, 696 (1951).

[10] V. A. Kargin, N. F. Bakeev, and Kh. Vergin, Proc. Acad. Sci. 122, No. 1 (1958).***

Received July 18, 1958

*In Russian.

**Original Russian pagination. See C.B. Translation.

***See C.B. Translation.

THE ULTRAVIOLET AND VISIBLE ABSORPTION SPECTRA OF AROMATIC AMINES ADSORBED ON SPECIFIC CENTERS OF ALUMINOSILICATE CATALYSTS

E. I. Kotov and Academician A. N. Terenin

Physical Scientific Research Institute of the A. A. Zhdanov Leningrad State University

The infrared spectroscopic investigation of the aluminosilicate catalysts showed that their surfaces contain hydroxyl groups (OH) whose spectra did not differ (in frequency or perturbation by extraneous molecules) from those exhibited by hydroxyls on the surface of silica gel and microporous glass [1]. This evidently resulted from the fact that our samples of the aluminosilicate adsorbent had a predominance of the silicate component. Nevertheless, the ultraviolet absorption spectra of the adsorbed aromatic amines showed that the aluminosilicate catalyst surface contained some acid centers, which, unlike silica gel, alumina gel, and microporous glass, reacted in the same way with the amines as do the protons in HCl and H_2SO_4 solutions [2].

On the other hand, the visible absorption spectra exhibited by some adsorbed aromatic amines [4, 5], and also the infrared spectra of adsorbed NH_3 and CH_3CN [6] indicated that the surface of the aluminosilicate catalysts contained some electron-acceptor centers which were capable of ionizing the aromatic amines and coordinating with the ammonia and acetonitrile.

It was interesting to carry out a spectroscopic study in order to explain the function of the proton-donor or electron-acceptor centers with respect to the activity of the aluminosilicate cracking catalysts.

M. A. Kaliko (VNII NP)* and K. V. Topchieva (MGU) kindly supplied us with some industrial and laboratory samples of various synthetic aluminosilicate catalysts. Later L. F. Moskovskaia (MGU) prepared for us some samples of the aluminosilicate catalyst and poisoned them with Na^+ and Li^+ ions in $NaOOCCH_3$ and $LiOOCCH_3$ solutions. According to K. V. Topchieva's and L. F. Moskovskaia's data, the activities (α) of the initial sample, the one poisoned with Na^+ and with Li^+ ions were : 0.41, 0.01 and 0.04 respectively.

We hoped that by comparing the absorption spectra of the molecules adsorbed on the original sample with the spectra on the poisoned one, we would be able to isolate those specific adsorption centers which were not associated with protons.

For the spectroscopic investigation we used the aromatic amines previously used in our laboratory: aniline, dimethylparaphenylenediamine and benzidine. As adsorbents we used: 1) silica gel (prepared in the GDR** and characterized by the lowest level of impurities); 2) γ-Al_2O_3; 3) industrial alumina gel I in the form of pills; 4) laboratory-made alumina gel II; 5) industrial silica-alumina gel I in the form of pills, and of the composition Al_2O_3 : SiO_2 = 12 : 88; 6) industrial silica-alumina gel II of the composition Al_2O_3 : SiO_2 = 25 : 75; 7) laboratory-made silica-alumina gel III in the form of pellets, of the composition Al_2O_3 : SiO_2 = 30 : 70; 8) laboratory-made silica-alumina gel IV in the form of pellets, of the composition Al_2O_3 : SiO_2 = 50 : 50; 9) laboratory-made silica-alumina gel V in the form of pellets, of the composition Al_2O_3 : SiO_2 = 80 : 20; 10) Na-silica-alumina gel III; 11) Na-silica-alumina gel IV; 12) Li-silica-alumina gel IV; 13) Na-silica-alumina gel V.

*All-Union Sci. Res. Inst. of Petroleum Industry.

**German Democratic Republic.

All the adsorbents were ground in a mortar and passed through a calibrating sieve. The resulting powder was composed of irregularly shaped particles whose size was about 50 μ. The specific surface of these powders was not determined but may be estimated as 300-500 m^2/g.

To prepare the adsorbents for the experiment we kept them in vacuo for 30 min at 20° and for 2 hrs at 350-400°. The adsorption of the aniline and dimethyparaphenylenediamine was carried out in vacuo at 20° by allowing the amine vapor to pass from a trap (in a vacuum apparatus) to a bulb containing the adsorbent. The adsorption of benzidine was carried out at 100° by distilling it in vacuo, onto the adsorbent maintained at 100°. The absorption spectra of the adsorbed molecules were measured with the diffused reflected light on a SF-4 spectrophotometer with a specially designed set up [2]. The measurements were done at low concentrations of the adsorbate, before the appearance of distortions observed in the spectra of diffused reflected light at higher concentrations [7].

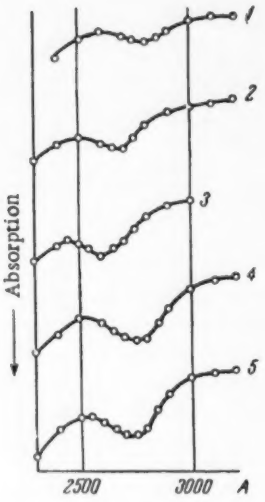

Fig. 1. Aniline absorption spectra. 1) Adsorbed on silica gel; 2) on alumina gel I; 3) on silica-alumina gel IV, $Al_2O_3 : SiO_2 = 50 : 50$; 4) on Na-silica-alumina gel IV; 5) on Li-silica-alumina gel IV.

In Fig. 1, we have drawn the aniline absorption spectra.* The spectra were obtained after the first portion of aniline vapor (at a pressure of 0.4 mm in a previously calibrated volume) was introduced into the bulb containing the adsorbent. The number of molecules in this portion was such that if they were spread out flat they would cover 5-10% of the adsorbent's surface. In Fig. 2, we have drawn a schematic representation of the observed absorption bands when aniline was adsorbed on other adsorbents.**

A comparison between the spectra indicates that the 2800 A absorption band seen in fairly unperturbed aniline adsorbed on silica gel (compare with the methanol solution) changes to a 2600 A band, when the amine is adsorbed on the catalytically active silica-alumina gels; the same band is observed when aniline is dissolved in strong protonic acids (HCl, H_2SO_4) and corresponds to the $C_6H_5NH_3^+$ cation [3]. A complete absence of the 2600 A band in the spectra of aniline adsorbed on the catalysts which were poisoned by Na^+ and Li^+ confirms the fact that the silica-alumina gel contains proton-donor acids centers. In our opinion the ultraviolet absorption bands located between 2750 and 2650 A, which were observed with aniline adsorbed on γ-Al_2O_3, alumina gel, and silica-alumina gels poisoned with alkali metal cations, indicate that the surface contained nonprotonic acid centers; these were capable of accepting electron pairs and had an effect similar to that of a proton but to a lesser degree. A very similar effect was observed by V. A. Khadeev when aniline was allowed to react with sublimed anhydrous $AlCl_3$ in vacuo to form an addition compound [8].

In Fig. 3, we have drawn the visible absorption spectra of dimethylparaphenylenediammonium $(CH_3)_2N-C_6H_4-NH_2^+$ [9] and benzidinium $H_2N-C_6H_4-C_6H_4-NH_2^+$ [5] ions, which (according to our spectroscopic data) were formed when the vapors of the corresponding amines were adsorbed (in a manner already described) on the surfaces of silica-alumina gel IV, Na-silica-alumina gel IV, and Li-silica-alumina gel IV.

*The absorption spectra of the adsorbed molecules in Fig. 1 and 3 are represented as curves of the relative transmittance,

$$T\,(\%) = \frac{\text{Light beam diffused and reflected by the adsorbent + adsorbed material}}{\text{Light beam diffused and reflected by adsorbent itself}}\,.$$

Minima on the curves correspond to maxima on the absorption bands.

**Here the rest of each band is omitted, only the maxima on the absorption bands were fixed (within the limits of ± 25 A).

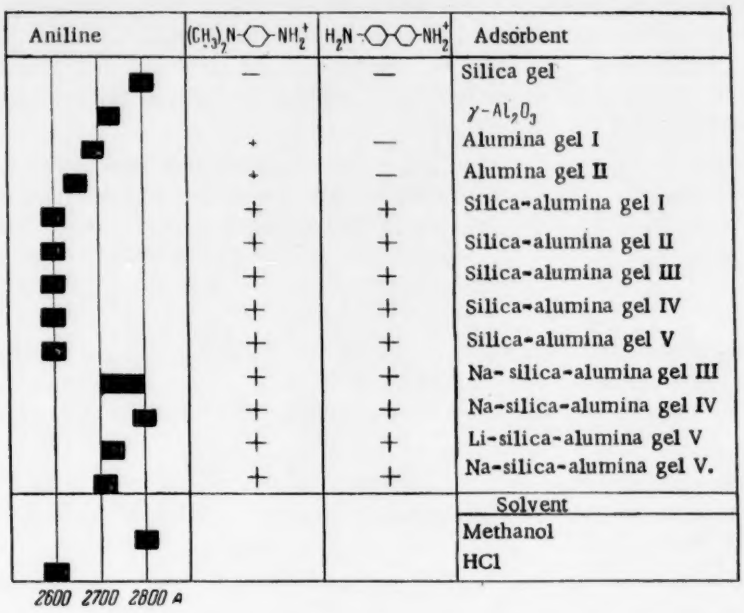

Fig. 2.

The results obtained with dimethylparaphenylenediamine and benzidine adsorbed on all the investigated adsorbents are tabulated in Fig. 2, where the plus sign denotes the presence and minus the absence of the spectrum shown in Fig. 3. It should be noted that the ionic spectrum was also observed when dimethylparaphenylenediamine was adsorbed on alumina gel; however, its intensity was 1/5 to 1/10 of that observed for the same cation on silica-alumina gel catalysts, and this we denoted by a smaller plus sign. No benzidinium spectrum was detected on alumina gel.

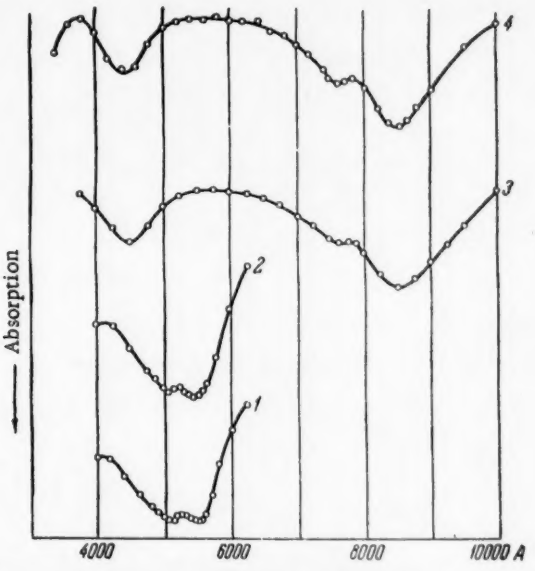

Fig. 3. Dimethylparaphenylenediamine absorption spectra: 1) adsorbed on silica-alumina gel IV, Al_2O_3: SiO_2 = 50:50; 2) on Li-silica-alumina gel IV. Benzidine absorption spectra: 3) adsorbed on silica-alumina gel IV; 4) on Na-silica-alumina gel IV.

A combination of the last few facts indicates that the surfaces of aluminosilicate catalysts (including those poisoned with alkali metal ions) contain oxidation — electron-acceptor — centers. These centers have an electron affinity strong enough to detach the electrons from the adsorbed dimethylphenylenediamine (at 20°) and benzidine (at 100°), but too weak to detach them from the adsorbed aniline (at 20-100°). The latter forms only a coordinate bond with the catalysts.

The absence of a benzidinium spectrum and the weak intensity of the dimethylparaphenylenediammonium spectrum on alumina gel indicate that the alumina gel surface also has some oxidation electron-acceptor centers; these are similar to the ones on aluminosilicate catalysts, but are at a lower concentration or have a lesser electron affinity.

SUMMARY

1) When the aluminoslicate catalysts are poisoned with Na^+ and Li^+ ions,the oxidation electron-acceptor centers survive and remain accessible to the extraneous adsorbed molecules. The loss of catalytic activity indicates that the activity of aluminosilicate cracking catalysts can not be directly connected with the presence of such centers.

2) When the aluminosilicate cracking catalysts are poisoned with the alkali metal ions, the loss of activity is accompanied by the disappearance of the proton-donor centers which are detected through their effect on the adsorbed molecules.

We wish to express our deep gratitude to K. V. Topchieva, I. F. Moskovskaia, and M. A. Kaliko for their cooperation and advice.

LITERATURE CITED

[1] V. N. Filimonov and A. N. Terenin, Proc. Acad. Sci. 109, 982 (1956); V. N. Filimonov, Optics and Spectroscopy 1, 490 (1956); A. N. Terenin and N. G. Yaroslavskii, Proc. Acad. Sci. 66, 885 (1949); L. N. Kurbatov, and N. G. Neuimin, Proc. Acad. Sci. 68, 341 (1949); N. G. Yaroslavskii, J. Phys. Chem. 24, 68 (1950); A. V. Karyakin and N. G. Yaroslavskii, Proc. Acad. Sci. 85, 1103 (1952); A. N. Sidorov, Proc. Acad Sci. 95, 1235 (1954); J. Phys. Chem. 30, 995 (1956); A. N. Terenin, Coll. Chemical Surface Compounds and Their Role in the Adsorption Phenomena, Moscow 1957, p. 206.*

[2] E. L Kotov and A. N. Terenin, Proc. of the 1st Inter-University Confer. on Catalysis MGU, 1958 (in press); * E. L Kotov, Optics and Spectroscopy 3, 115 (1957).

[3] G. Kortun, Zs. Phys. Chem., B, 42, 39 (1939); W. D. Kumler and L. A. Strait, J. Am. Chem. Soc. 65, 2349 (1943).

[4] A. L Sidorova and A. N. Terenin, Bull. Acad. Sci. USSR, Div. Chem. Sci. 1950, 152; A. I. Sidorova, Proc. Acad. Sci. 77, 327 (1950); J. Phys. Chem. 28, 525 (1954).

[5] E. L Kotov, Optics and Spectroscopy 1, 500 (1956).

[6] L. M. Roev, V. N. Filimonov, A. N. Terenin, Optics and Spectroscopy 4, 328 (1954).

[7] E. L Kotov, Optics and Spectroscopy 3, 368 (1957).

[8] A. N. Terenin, Bull. Acad. Sci. USSR, Div. Chem. Sci. 1940, 59.

[9] L. Michaelis, M. Schubert, and S. Granick, J. Am. Chem. Soc. 61, 1981 (1939)

Received November 3, 1958

*In Russian.

THEORY OF THE NONEQUILIBRIUM ELECTRICAL DOUBLE LAYER

Corresponding Member Acad. Sci. USSR V. G. Levich

Institute of Electrochemistry of the Academy of Sciences USSR

In paper [1] we developed a theory for the nonequilibrium double layer at the boundary between a metal and solution. In particular, we showed that during the discharge of ions the voltage—current characteristic on the similarly charged electrode (for example on the negatively charged electrode during the reduction of anions) should have a decreasing curve (i.e., the current should decrease as the negative potential and the corresponding negative surface charge increase). This phenomenon was discovered independently by T. A. Kryukova in A. N. Frumkin's laboratory [2], and it was very thoroughly investigated by A. N. Frumkin and co-workers [3-6]. At the same time they established the fact that the voltage–current characteristic for the reduction of $S_2O_8^{2-}$ anion has a complicated V-shaped form with a distinct minimum. A. N. Frumkin and G. M. Florianovich proposed [3] an explanation for this form of a curve by starting with the theory of delayed discharge and by assuming that the distribution of the reacting ion between the double layer and the solution adjacent to the electrode is in a state of equilibrium.

In the present work we have endeavored to combine both points of view. In it, we have taken into account not only the deviations of the discharging ion concentrations from the equilibrium value in the double layer during the flow of current, but also the final rate of the discharge reaction. Meanwhile, we have assumed that the current density is low in comparison to the limiting diffusion current, so that we could neglect any changes in the concentrations of the reacting species in the volume outside the double layer. We also assumed that the solution contains some inert electrolyte, and that far away from the electrode the concentration of the reacting ions c_1 is very small compared to the concentration of the nonreacting ions c_2 and c_3.

The equations for the migration of ions look as follows:

$$-j = -FD_1z_1\frac{\partial c_1}{\partial x} + D_1F^2z_1^2c_1\frac{\partial \varphi}{\partial x}; \tag{1}$$

$$0 = -FD_2z_2\frac{\partial c_2}{\partial x} - D_2F^2z_2^2c_2\frac{\partial \varphi}{\partial x}; \tag{2}$$

$$0 = -FD_3z_3\frac{\partial c_3}{\partial x} + D_3F^2z_3^2c_3\frac{\partial \varphi}{\partial x}. \tag{3}$$

Here D_i, z_i (i = 1, 2, 3) are the diffusion coefficients and the charge of the ions respectively; φ is the electrical potential, measured in units of $RT/F = 25 \cdot 10^{-3}$ v.

We are taking the electrode potential to be negative, the x-axis directed away from the electrode toward the solution, and the current flow in the negative direction on the x-axis.

The electrical potential satisfies Poisson's equation,

$$\Delta\varphi = -\frac{4\pi}{\varepsilon}\frac{F^2}{RT}\sum c_iz_i. \tag{4}$$

Let us note that outside the double layer $x > \lambda$ (where λ is the Debye length) while the concentrations approximately fulfill the requirement of electrical neutrality

$$\sum c_i z_i = 0, \tag{5}$$

and Poisson's equation for φ changes to Laplace's equation.

The boundary conditions require that inside the solution, at a distance from the electrode, we fix a specific potential (whose value may be taken as zero) and take the concentrations

$$c_1 = c_1^{(0)}, \quad c_2 = c_2^{(0)}, \quad c_3 = c_3^{(0)}. \tag{6}$$

Near the electrode we will analyze the distribution of the potential and concentrations only in the diffuse portion of the double layer, i.e., at $x \geq x_0$, where x_0 = thickness of the Helmholtz layer (we are disregarding any differences between the x_0 values of the cations and anions).

At the point x_0 the potential assumes the value ψ_1, while the current density satisfies the expression from the delayed discharge theory

$$j = kc_1(x_0)e^{-\alpha(\varphi_0 - \psi_1)}, \tag{7}$$

where $c_1(x_0)$ = concentration of reacting ions; ψ_1 = potential at the boundary of the Helmholtz layer, i.e., at the distance of one ionic radius from the electrode surface; φ_0 = electrode potential; α = a constant smaller than one; and k = the rate constant for the electrode reaction.

In order to find the distribution of the potential and the concentration within the entire solution (at $x_0 \leq x < \infty$) we will take advantage of the fact that the concentration of the inert electrolyte is large as compared to that of the reacting ions; moreover, the potential satisfies Poisson's equation, while the concentrations satisfy the usual transference equations and all the boundary conditions. Thus, we can discard the concentration of the reacting ions in equation (4). At the same time it follows from Equations (2), (3), and (4) that the distribution of concentrations and of the potential φ in the double layer coincides with the distribution in an equilibrium double layer. In particular, when $z_2 = z_3 = 1$, we can write

$$c_2 = c_2^{(0)}e^{-\varphi}; \quad c_3 = c_3^{(0)}e^{\varphi}; \tag{8}$$

$$\varphi = -2\ln\frac{(e^{\psi_1/2}+1) + (e^{\psi_1/2}-1)\,e^{-x/\lambda}}{(e^{\psi_1/2}+1) - (e^{\psi_1/2}-1)\,e^{-x/\lambda}}. \tag{9}$$

Knowing the potential distribution we can integrate Equation (1) directly and get the distribution of the concentrations of the reaction ions. This gives us

$$c_1(x) = e^{z_1\varphi}\left(\text{const} + \frac{j}{Fz_1D_1}\int e^{-z_1\varphi}\,dx\right). \tag{10}$$

Equation (10) contains two unknown constants – the current density j and the integration constant. The latter may be determined from the condition that the solution of Eq. (10) must have a closed form and from the distribution of the concentration c_1 in the $x > \lambda$ region. The solution yields const $= c_1^{(0)}$.

Substituting the potential distribution into Eq. (10) we can get the final expression for $c_1(x)$. An analysis of the integral in Eq. (10) reveals that the major contribution to this integral comes from the region $x \ll \lambda$, where the expression φ can be simplified if $\psi_1 \gg 1$. The solution gives the following for $c_1(x_0)$,

$$c_1(x_0) \cong e^{z_1\varphi}\left[c_1^{(0)} - \frac{2\lambda j}{(2z_1-1)D_1z_1F}\exp\left\{-z_1\varphi - \frac{\psi_1}{2}\right\}\right]. \tag{11}$$

The boundary condition (7) gives

$$j = \frac{kc_1^{(0)} \exp\{(z_1 + \alpha)\psi_1 - \alpha\varphi_0\}}{1 + \frac{2\lambda k}{(2z_1 - 1) D_1 z_1 F} \exp\left\{\left(\alpha - \frac{1}{2}\right)\psi_1 - \alpha\varphi_0\right\}} . \quad (12)$$

At the same time the potential at the boundary of the Helmholtz layer, ψ_1 (when $\psi_1 \gg 1$), can be expressed as a function of the electrode potential by the equilibrium relationship

$$\psi_1 \cong -2 \ln(-\varphi_0) + \text{const.} \quad (13)$$

When the inequality

$$1 \gg \frac{2\lambda k}{(2z_1 - 1) D_1 z_1 F} \exp\left\{\left(\alpha - \frac{1}{2}\right)\psi_1 - \alpha\varphi_0\right\} \quad (14)$$

is fulfilled, Equation (12) reduces to the equilibrium equation derived by A. N. Frumkin and G. M. Florianovich and corresponds to the curve with a minimum. At high negative electrode potentials, Inequality (14) is reversed and Eq. (12) changes into the limiting expression

$$j_{\text{lim}} \simeq \frac{(2z_1 - 1) D_1 z_1 F}{2\lambda} \exp\left\{\left(z_1 + \frac{1}{2}\right)\psi_1\right\}, \quad (15)$$

which was obtained by us in [1], and which corresponds to a relatively slowly decreasing j_{lim} with change in the electrode potential φ_0.

Thus the full change in $j(\varphi_0)$ is expressed by a curve with one minimum and one maximum. For certain values of the constants the maximum and the minimum come close to each other, with the result that over a segment of the curve the current will change relatively little with change in φ_0.

In the present work, we are not taking into consideration the detailed structure of the double layer or any possible local variations in the functions affected by the cations located nearest to the reaction anion. If, we were to consider such a case, we would have to alter radically our computational method; at the present state of the theory of the double layer such a thing is not feasible.

In passing to the comparison between Eq. (12) and the experimental data, we have to point out that the experiments with divalent or other polyvalent anions either yield V-shaped curves (without a subsequent drop), or, as in the case of $Fe(CN)_6$ [3, 6], curves which at first drop with increase in φ_0 then terminate in a broad plateau.

The discrepancy between the theoretical Eq. (12) and the experimental data could be connected with the fact that we did not consider the changes in the potential ψ_1 along the electrode surface, nor any other changes in the nature of the elementary processes during the transition towards more negative potentials, for example, the changed adsorption conditions or the increased probability of nonadiabatic electronic processes on highly charged negative surfaces.

As we have already pointed out in [1], the problem connected with the formation of ion-pairs or ionic complexes of the type $KS_2O_8^-$ during the reduction of $S_2O_8^{2-}$ deserves a particular attention. At the same time we have to distinguish two limiting cases.

1) A case where the ion-pairs participate in the reaction while in the bulk of the solution the equilibrium between the ion-pairs and their components is preserved. In this case, Equation (12) is valid for the treatment of the problem, provided the equation is appropriately changed, for example, by decreasing the value of z_1 to one.

2) In the second limiting case we can assume that the concentration of the ion-pairs in the bulk of solution is very low and that the reaction rate is determined by the rate at which they are formed within the double layer. For this it is necessary that the anions with charge z_1 be able to approach the cations forming the Helmholtz shell of the double layer. Under these conditions it should be possible to express the reaction rate by an equation of type (15), provided it were possible to correct it so as to account for the changes in the potential along the electrode surface.

It may so happen that when the ion-pairs participate in the electrode reaction the nature of the reacting species changes with a changing potential. In other words, that with an increasing negative potential the fraction of the ion-pairs participating in the reaction may increase.

I take a great pleasure in expressing my gratitude to Acad. A. N. Frumkin for a highly valuable discussion of the problems covered in this communication.

LITERATURE CITED

[1] V. G. Levich, Proc. Acad. Sci. 67, No. 2, 309 (1949).

[2] T. A. Kryukova, Proc. Acad. Sci. 65, 517 (1949).

[3] A. N. Frumkin and G. M. Florianovich, Proc. Acad. Sci. 80, 907 (1951); J. Phys. Chem. 29, 1827 (1955).

[4] A. N. Frumkin, Zs. f. Elektrochem 59, 807 (1955).

[5] A. N. Frumkin, Proc. 2nd Congr. Surface Activity, London 1957, p. 58.

[6] A. N. Frumkin and N. V. Nikolaeva, Chem. Phys. 26, 1552 (1957).

[7] A. N. Frumkin, Bull. Acad. Sci. USSR, Div. Chem. Sci. 1957, 1429.*

[8] A. N. Frumkin and N. V. Nikolaeva-Fedorovich, Bull. Moscow Univ., Chem. Ser. No. 4, 169 (1957).

[9] A. N. Frumkin, B. B. Damaskin, and N. V. Nikolaeva-Fedorovich, Proc. Acad. Sci. 115, 751 (1957).*

[10] D. Graham, Zs. f. Elektrochem. 62, 264 (1958).

Received October 1, 1958

*Original Russian pagination. See C.B. Translation.

INFRARED ABSORPTION SPECTRA OF ETHYLLITHIUM DISSOLVED IN BENZENE, HEXANE AND DIETHYL ETHER

V. N. Nikitin, G. V. Rabova, and N. V. Mikhailova

Institute of High-Molecular Compounds of the Academy of Sciences USSR

(Presented by Academician A. N. Terenin, September 23, 1958)

Certain organolithium compounds exist in the associated state in solutions. This fact was variously established, particularly through cryoscopic measurements [1, 2] and infrared absorption spectra [2, 3]. However, in the case of ethyllithium the cryoscopic measurements did not allow any unequivocal conclusions as to the structure of the complexes formed. Thus, in work [1], the authors maintained that in benzene the ethyllithium is dimerized. Similar measurements conducted by other authors [2] led them to the conclusion that the ethyllithium exists in the form of hexamers.

The infrared absorption data also needs some refinement. Thus, in a short communication [3] the 875 cm^{-1} band (observed in a benzene solution of ethyllithium) was assigned to the C – Li bond vibration in associated molecules, while in paper [2] this same band was assigned to the unassociated molecules. Besides this, the two works report a different number of absorption bands in one and the same region.

In the present work, we studied the absorption spectrum of ethyllithium in benzene, hexane, and diethyl ether. One would expect that the ether oxygen, by acting as an electron-acceptor, would be able to complex with ethyllithium.

EXPERIMENTAL

The crystalline ethyllithium was prepared from lithium metal and ethyl chloride in a benzene solution, followed by the evaporation of the solvent. The crystalline C_2H_5Li was washed three times with cold hexane and dried in vacuo. All the operations were carried out under dry purified nitrogen. We took all the necessary precautions to protect C_2H_5Li from decomposition. The absorption spectrum of the dissolved ethyllithium was determined in a single-beam infrared spectrophotometer with a NaCl prism. To exclude the solvent absorption, the spectra were recorded in two identical cells, whose thickness was d = 0.2 mm. One of the cells was especially built by us and had a variable thickness [4]. The spectra were registered by means of successive solvent – solution absorption measurements. The cell with the fixed thickness was sufficiently tight [5], and no visible decomposition of ethyllithium occurred during the measurements. The cell lining, which determined the thickness d, was made of polyethylene.

In Fig. 1, I, we have drawn the absorption spectrum of ethyllithium dissolved in benzene.

To resolve the question regarding the state of association of ethyllithium in benzene, and to find out which absorption bands correspond to the associated and which to the unassociated molecules, we studied the optical density ratios at two concentrations. Let the optical density be D_{C_1} when the concentration of ethyllithium is C_1, and D_{C_2} after a two-fold dilution ($C_2 = 1/2\ C_1$). If there were no association, then according to Beer-Lambert's law we would have

$$\frac{D_{C_1}}{D_{C_2}} = \frac{kC_1 d}{kC_2 d} = 2. \qquad (1)$$

The ratio (1) is larger than 2 for bands belonging in the associated molecules and smaller than 2 for bands belonging to the bonds in unassociated molecules.

Let us look at the optical density ratios for the absorption bands of ethyllithium dissolved in benzene; the two concentrations are: $C_1 = 0.64$ mole/liter and $C_2 = 0.32$ mole/liter (cell thickness d = 0.2 mm).

ν in cm^{-1}	1104	1054	968	926	885
D_{C_1}/D_{C_2}	0.6	0.7	2.6	2.5	1.6

This is a pretty rough estimate of the D_{C_1}/D_{C_2} ratio since we did not consider the overlap of the absorption bands. However, one can be fairly certain that the 1104 and 1054 cm^{-1} frequencies are characteristic of the unassociated molecules, since the intensity of these vibrational bands are considerably increased when the C_2H_5Li concentration is lowered.

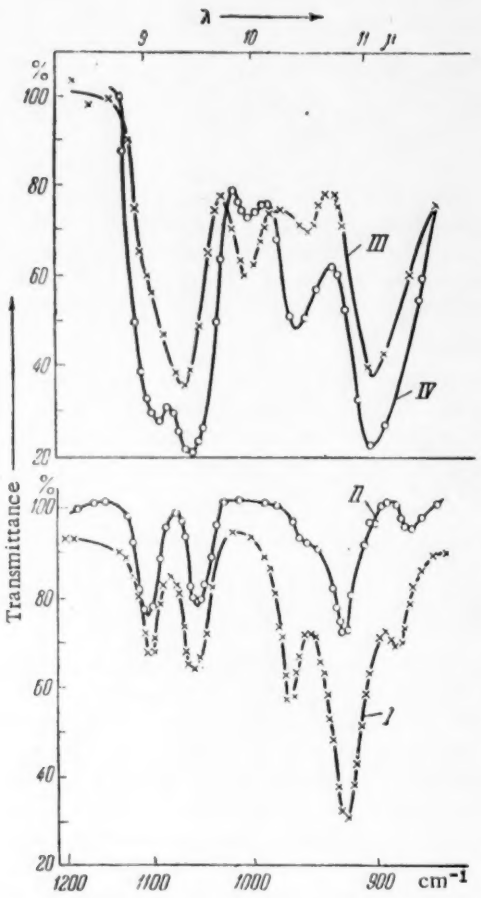

Fig. 1. Ethyllithium absorption spectra. I) In benzene, C = 0.64 mole/liter, cell thickness d = 0.2 mm; II) in hexane, C ≃ 1.4 mole/liter, d = 0.2 mm; III) in diethyl ether, C = 1.7 mole/liter, d = 0.06 mm; IV) in benzene with some diethyl ether added (7%), C = 1.1 mole/liter, d = 0.2 mm.

Most probably the 1104 and 1054 cm^{-1} frequencies are connected with the vibrations of the C-C-Li bonds in unassociated molecules.* The 968 and 926 cm^{-1} frequencies may be assigned to the C-C-Li vibrations in the associated molecules, since the ratio (1) is larger than 2. The assignment of the 962 cm^{-1} to the vibrations in the associated molecules agrees with the assignments made in papers [2, 3]. In paper [3] the 875 cm^{-1} frequency (according to our data 885 cm^{-1}) was assigned to the associated molecules. Our data on 885 cm^{-1} frequency indicate that the ratio (1) is equal to 1.6. This result is in accord with that of paper [2], where the indicated frequency was assigned to the unassociated molecules.

In Fig. 1, II we have shown the C_2H_5Li absorption spectrum in hexane. As may be seen, the same absorption bands are observed in hexane as in benzene solutions of C_2H_5Li.

We also studied the absorption spectra of ethyllithium dissolved in diethyl ether. These investigations are of a considerable interest, for there are some indications that the addition of a small amount of ether has an effect on the catalytic polymerization of dienes [7]. There is a hypothesis that the ethyllithium complexes with diethyl ether. It is also known that the ether oxygen can participate in intermolecular hydrogen bonding. In Fig. 1, III we have drawn the spectrum of ethyllithium dissolved in diethyl ether. As in the preceeding experiments the solvent absorption was subtracted.

Ether itself absorbs strongly in the investigated region, and therefore in the range of the ether bands we had to use the maximum slit opening. In such a case there is a danger that the recorded spectrum of

*One cannot assign these frequencies in C_2H_5Li to the characteristic C-Li bond vibrations, as was done in papers [2, 3], since these frequencies fall in the same region as the C-C bond vibrations (see [6]).

C_2H_5Li in ether may be strongly distorted. In the present work we were mainly interested in observing the changes in the spectrum of C_2H_5Li when it was dissolved in diethyl ether instead of benzene. In connection with this we obtained an additional spectrum of C_2H_5Li in benzene; the spectrum was recorded under conditions similar to those used with the ether solution (same slit openings and similar pointer deflections on the EPP-09 recorder, while the amplification coefficient in the amplifier was decreased). When recorded under these conditions the spectrum of C_2H_5Li in benzene was practically identical with the one obtained at smaller slit openings and which is shown in Fig. 1, I. By comparing the C_2H_5Li spectrum in benzene with that in ether (see Fig.1), we can see that when the compound is dissolved in ether the location and number of the absorption bands are considerably changed. We may assume that the observed changes in the absorption of C_2H_5Li in diethyl ether are connected with the formation of an ethyllithium – ether adduct. We have also studied the absorption spectrum of C_2H_5Li dissolved in benzene to which some diethyl ether was added (7%).

One can see that the absorption bands observed on Curve III are also observed on Curve IV. This can be explained by the fact that in the benzene solution there are also quite a few molecules of C_2H_5Li associated with the added ether.

We also attempted an investigation of the absorption spectrum of C_2H_5Li dissolved in dioxane. The experimental results seem to indicate that at room temperature the dioxane undergoes a chemical reaction with C_2H_5Li.

We would like to thank A. A. Korotkov for suggesting this subject and M. V. Vol'kenshtein for some valuable advice.

LITERATURE CITED

[1] K. B. Piotrovskii and M. P. Ronina, Proc. Acad. Sci. 115, No. 4, 737 (1957).*

[2] T. L. Brown and M. T. Rogers, J. Am. Chem. Soc. 79, 1859 (1957).

[3] A. Rodionov, D. Shigorin, T. Talalaeva, and K. Kocheshkov, Bull. Acad. Sci. USSR, Div. Chem. Sci. 1958, 120.*

[4] V. V. Nikitin, Instruments and Experimental Techniques (1959, in print).

[5] V. N. Nikitin, Bull. Acad. Sci. USSR, Phys. Ser. 17, No. 5, 674 (1933).

[6] M. V. Vol'kenshtein, Structure and Physical Properties of Molecules, IZD AN SSSR, 1955, p 426.**

[7] K. B. Piotrovskii, Thesis Reports Delivered at the 9th Conference on the General Problems in the Chemistry and Physics of High-molecular Compounds, Moscow 1956, p. 51.**

Received September 17, 1958

*Original Russian pagination. See C.B. Translation.

**In Russian.

CAUSES FOR THE DECREASED STABILITY OF THE CRYSTALLINE STRUCTURE OF MONOCALCIUM ALUMINATE FORMED AT ELEVATED TEMPERATURES

E. E. Segalova, Z.D.Tulovskaya, E. A. Amelina and Academician P. A. Rebinder

The Chair of Colloidal Chemistry at the M. V. Lomonosov Moscow State University

One of the most serious defects encountered with aluminate cements consists of the fact that when they are allowed to set at higher temperatures their mechanical strength is reduced. While studying the structure formation (by crystallization) in water suspensions of monocalcium aluminate, $CaO \cdot Al_2O_3$ (CA)* (the principal mineral in aluminate cements) we confirmed the fact that the solidified structure formed at elevated temperatures was always weaker (Fig. 1). This has usually been blamed on the accelerated transition from the unstable dicalcium aluminate hydrate (formed through the hydration of CA) to the stable tricalcium aluminate hydrate [4, 5]. However, a thermographic investigation of the hydration products showed that the compounds formed at 20 and at 60° C were identical. This fact is in full agreement with the results obtained by several other authors [6].

Consequently, the weaker structure resulting from crystallization at elevated temperatures has to be explained not by the formation of a different compound, but by the changed crystallization conditions of the hydrate composing the structure. Actually, the maximum strength among the investigated suspensions of monocalcium aluminate was attained in 3-4 days at 20° and in 3-4 hours at 60° (Fig. 1). And as one would expect, the hydration was over at the same time. Such an increase in reaction rate with the rise in temperature could only result from a change in the value and kinetics of the supersaturation in the solidifying suspension; these changes will essentially determine the nature of the structure formation taking place in the suspension [1-3].

The supersaturation observed in CA suspensions has been measured by several authors who determined the CaO and Al_2O_3 contents in the liquid phase of the suspensions [7-10]. Yet, none of them had noted that the stable supersaturation had a maximum value, which could be regarded as the nominal solubility of the anhydrous compound. All the authors referred to concluded that the supersaturated CA suspensions were unstable. If should be noted that in their experiments they usually used suspensions of some fixed concentration; this prevented them from discovering the maximum supersaturation which is independent of the CA concentrain the suspension.

We studied the supersaturation kinetics conductometrically at the optimum mixing rate (400 rpm). To protect the suspension from carbonation all our measurements were carried out under nitrogen.

One may see in Fig. 2 that the electrical conductance attained a constant level in all sufficiently concentrated suspensions; it corresponded to the maximum supersaturation value or to the nominal solubility of anhydrous CA. With CA suspensions the constant supersaturation level was achieved much sooner than with tricalcium aluminate suspensions [11], but much later than with gypsum hemihydrate [2]. The rate at which

*We used in these experiments (as is usually done in our laboratory [1-3]) suspensions which contained a large amount (80-95%) of an inert filler (ground quartz sand) besides the cement.

the maximum supersaturation value was attained increased considerably with increase in the concentration of the suspension.

That stable supersaturated suspensions which are independent of the concentration can exist is also indicated by the results obtained through a quantitive determination of the CaO and Al_2O_3 concentrations in the liquid phase of the suspension, after the electrical conductance had attained its maximum value. The samples

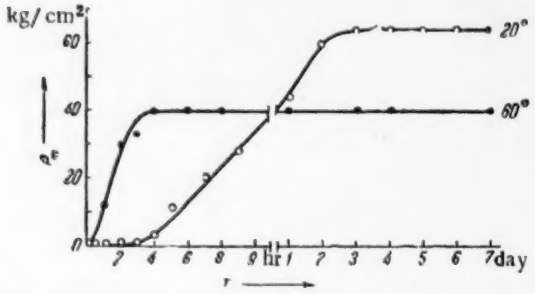

Fig. 1. Kinetics of structure formation in Ca suspensions at 20 and 60° C. P_m = plastic strength [1-3]. The composition of the suspension was: 5% CA, 95% ground quartz sand, and water 30% with respect to dry mixture.

TABLE 1

Starting material	Expt. temp. °C	Sample removed after	CaO, g/liter	Al_2O_3, g/liter	CaO / Al_2O_3
CA	20±0,3	30 min	1,10	2,01	0,99
		1 hr	1,03	2,02	0,91
		2 hr	1,09	2,00	0,95
		4 hr	1,06	2,07	0,93
C_2A·aq	20±3	4 days	0,26	0,23	2,15
CA	60±0,3	6 min	0,53	0,85	1,14
		20 min	1,40	2,02	1,25
		30 min	1,35	2,27	1,06
		50 min	1,49	2,50	1,09
C_2A·aq	60±3	2 hr	0,27	0,23	2,11

removed for the analysis were taken out of the same suspension in which the electrical conductance was measured. Analytical results (Table 1) enabled us not only to confirm the existence of stable supersaturated CA suspensions, but also to characterize them quantitatively.

The maximum supersaturation value at 20° corresponds to a solution containing 3.12 g/ liter of CA; one should therefore consider it the nominal solubility of CA at this temperature. The data obtained indicate that CA dissolves congruently, since the CaO/ Al_2O_3 concentration ratio in the liquid phase of the suspension is 1, which corresponds to the ratio in the anhydrous compound.

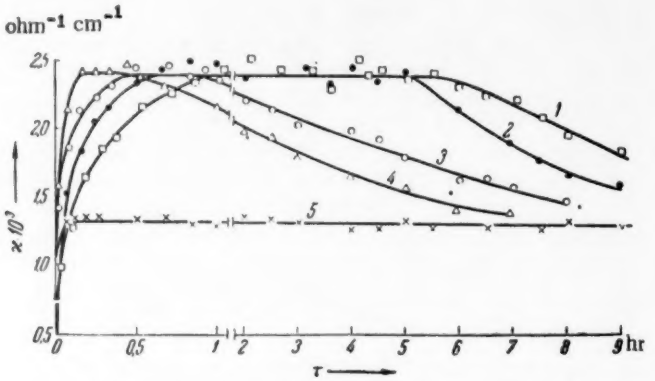

Fig. 2. Specific electrical conductance kinetics at 20° of suspensions contained in 125 ml of water. 1) 3.5 g of CA; 2) 9.4 g of CA; 3) 12.5 g of CA; 4) 18.25 g of CA; 5) 5 g of C_2A · aq.

At the same time we determined the solubility of the 2 CaO · Al_2O_3 · aq hydrate (C_2A · aq), which was prepared by the hydration of CA at 20°. The solubility turned out to be 0.49 g of C_2A per liter of solution; it was in good agreement with the literature data [8]. The ratio between the CaO and Al_2O_3 concentrations corresponded to the dicalcium aluminate hydrate (CaO/ Al_2O_3 = 2).

We carried out similar experiments at 60°. At first, we did not detect any constant supersaturation level when measuring the electrical conductance (Fig. 3A). A distinct maximum was observed on the experimental conductance curve; as the concentration of the suspension was increased this maximum sharply increased and was attained in a shorter time.

Such supersaturation curves were usually observed in highly concentrated CA suspensions, where the hydration was so extensive that the constant supersaturation level could not be experimentally detected [8, 10]. When we tried to detect the supersaturation conductometrically we ran into complications, since as a result of sharply accelerated hydration rate a large quantity of heat was given off in a short time interval, resulting in a temporary temperature rise and consequently also in an increased conductance. Thus, it is possible that in this case the sharp rise in the electrical conductance was not connected with any increase in the concentration of ions.

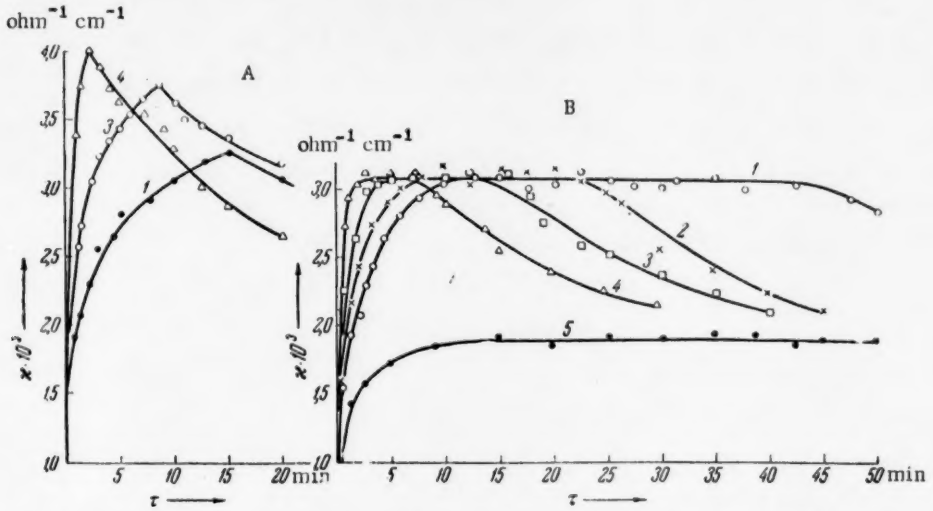

Fig. 3. Specific electrical conductance kinetics in CA suspensions at 60°. A) In pure water; B) in a 0.003% SCB solution. The liquid phase of the suspension (125 ml) contained: 1) 1.5 g of CA; 2) 2.5 g of CA; 3) 3.5 g of CA; 4) 5.0 g of CA; 5) 1.5 g of $C_2A \cdot aq$.

These experiments have shown beyond any doubt that the rate of solution sharply increases with rise in temperature, but they did not make it possible to determine the value of the stable supersaturation. To achieve our goal we had to retard the solution of CA, without changing, however, the experimental temperature. For this purpose we introduced some surface-active agents—sulfite cellulose brine products (SCB); small amounts of these were completely adsorbed on the particles of the starting material while leaving the electrical conductance of the suspension practically unchanged [11]. We found it to be most convenient to add an amount corresponding to a 0.003% solution of SCB. We have previously measured the electrical conductance of a plain SCB solution and found it to be insignificant in comparison with that of the suspension.

By measuring the electrical conductance at 60° we found out that under these conditions, just as at 20°, during the hydration of CA, stable supersaturated solutions of the hydrate were formed (Fig. 3B). The maximum supersaturation level does not depend on the concentration of the suspension but is attained sooner at higher concentrations. At 60° the hydration proceeds much more rapidly, since CA dissolves extremely fast.

Through a concurrent chemical analysis we determined the concentrations of CaO and Al_2O_3 in the liquid phase of the suspension; on the basis of this we were able to make a quantitative estimate of the maximum supersaturation value, i.e., the nominal solubility of CA at 60° (Table 1). As it turned out, the nominal solubility of CA at 60° (Table 1) was only insignificantly larger than that at 20°; its value was 3.67 g/liter.

At 60° the solubility of the aluminate hydrate, which was prepared by hydration of CA at the same temperature, was practically the same as that of the aluminate hydrate at 20° and had a value of 0.50 g/liter of C_2A. This is in good agreement with the literature data [8].

The results of these experiments indicate that the sharply increased rate of hydration and structure formation in the suspensions of CA at elevated temperatures is essentially connected with the higher rate of solution, since the change in the supersaturation value resulting from the increased solubility is very insignificant.

While investigating the processes of structure formation in suspensions of gypsum hemihydrate [1], it was discovered that the strength of the solidifying structure was greatly reduced when the initial binder was more finely ground. The same phenomenon was observed in our present case. Not only a finely ground original binder, but particularly the raised temperature, sharply increased the solubility rate. At the same time the high supersaturation value lasted much longer in the solidifying suspension, which produced very finely divided crystals in the solidifying structure and thus highly reduced its strength.

LITERATURE CITED

[1] E.E. Segalova, V. N. Izmailova and P.A. Rebinder, Proc. Acad. Sci. 110, No. 5 (1956).

[2] E. E. Segalova, V. N. Izmailova and P. A. Rebiner, Proc. Acad. Sci. 114, No. 3 (1957).*

[3] E. E. Segalova, E. S. Solov'eva, and P.A. Rebinder, Proc. Acad. Sci. 113, No. 1 (1957).*

[4] O. M. Astreeva and L. Ya. Lopatnikova, Investigation of the Hydration Processes by Means of Petrographic Analysis, 1954.**

[5] P. P. Budnikov, and L.V. Kravchenko, Colloid. J. 13, No. 6 (1951).

[6] V. A. Tikhonov, L. S. Ingul'skaya and E. V. Zdanevich, Proc. Lvov Polytech. Inst. 1, No. 1 (1955).

[7] L. S. Wells, J. Res. Bur. Stand. 1, 6 (1928).

[8] J. Brocard, Chim. et Ind. 59, 431 (1948).

[9] R. H. Boque, The Chemistry of Portland Cement, N. Y., 1952.

[10] A. M. Kuznetsov and A. I. Sosnina, Bull. Nat. Sci. Inst. Perm State Univ. 13, No. 6 (1952); A. M. Kuznetsov, Bull. Nat. Sci. Inst. Perm State Univ. 14, No. 1 (1957).

[11] E. E. Segalova, E. S. Solov'eva, and P. A. Rebinder, Proc. Acad. Sci. 117, No. 5 (1957).*

Received October 15, 1958

*See C.B. Translation.

**In Russian.

THE EFFECT OF ALKALI METAL HALIDES ON THE MECHANISM OF THE CATALYTIC HYDROGENATION OF CYCLOHEXENE

Academician (Acad. Sci. Kazak SSR) D. V. Sokol'skii and

G. D. Zakumbaeva

Institute of Chemical Sciences of the Academy of Sciences Kazakh SSR

The effects of salts on the rates of catalytic hydrogenation in solution have not been very extensively investigated [1, 2]. We have investigated the hydrogenation of cyclohexene on Raney nickel (0.3 g) in 0.01, 0.1, 0.5 and 1 N solutions of KCl, KBr and Ki in 50% ethyl alcohol at 20, 30 and 40°. For the sake of comparison we also carried out similar experiments without the salts. Alongside the hydrogen absorption kinetics we measured the potential of the powdered catalyst [3].

In Fig. 1, we have drawn the kinetic and potential curves obtained during the hydrogenation of cyclohexene at 20° in the presence of KCl. As may be seen from the figure, the rate of hydrogenation decreased with increased KCl concentration. The potential of the catalyst shifted toward the anodic region by 90 mv during the hydrogenation of cyclohexene in 50% alcohol in the absence of salts. In the presence of KCl the potential curves were displaced toward more negative potentials. One should note, though, that with increased KCl concentration the potential drop ΔE decreased.

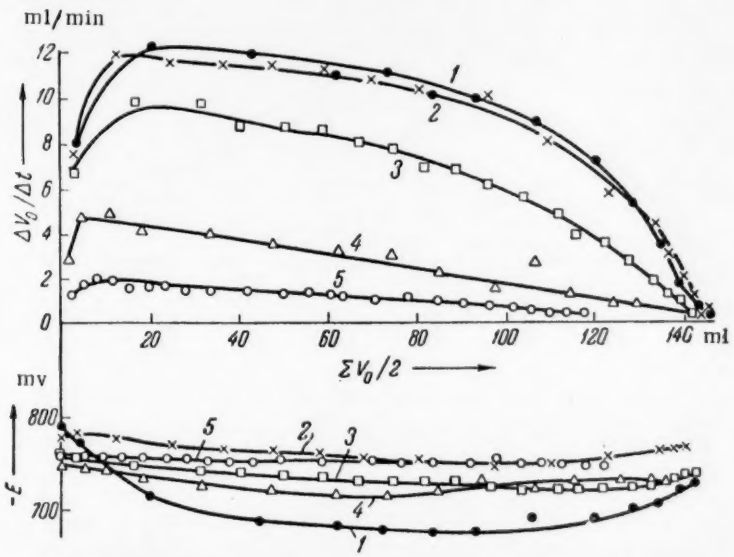

Fig. 1. The effect of KCl on the hydrogenation of cyclohexene over a Ni catalyst (0.3 g). Solvent – 50% ethyl alcohol. T_{exp} = 20°. 1) 50% alcohol; 2) 0.01 N KCl; 3) 0.1 N KCl; 4) 0.5 N KCl; 5) 1 N KCl.

In Fig. 2, we have drawn the kinetic and potential curves obtained during the hydrogenation of cyclohexene in the presence of KBr. As one may see from Figs.1 and 2, KCl and KBr had almost identical effects; only in the potential curves was there any difference observed. The reversible hydrogen potential attained 760-770 mv with all the investigated KCl concentrations, but with KBr it was only 800 mv. The potential drop ΔE in the course of the reaction was greater in the KBr solution.

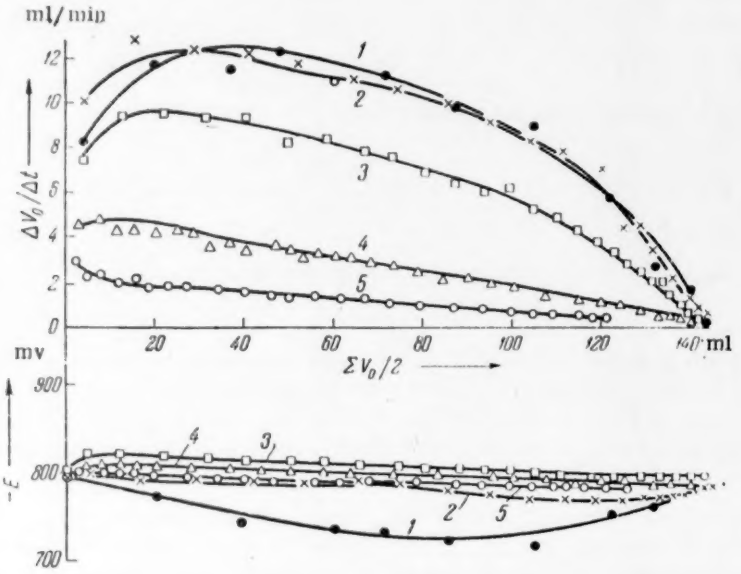

Fig. 2. The effect of KBr on the hydrogenation of cyclohexene over a Ni catalyst (0.03 g). Solvent – 50% ethyl alcohol. T_{exp} = 20°. 1) 50% alcohol; 2) 0.01 N KBr; 3) 0.1 N KBr; 4) 0.5 N KBr; 5) 1 N KBr.

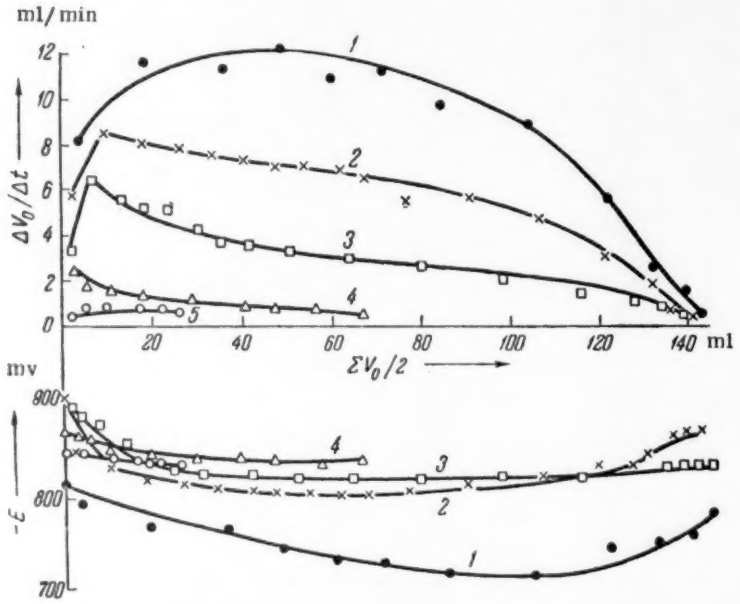

Fig. 3. The effect of KI on the hydrogenation of cyclohexene over a Ni catalyst (0.3 g). Solvent–50% ethyl alcohol. T_{exp} = 20°. 1) 50% alcohol 2) 0.01 N KI; 3) 0.1 N KI; 4) 0.5 N KI; 5) 1 N KI.

Thus the hydrogenation of cyclohexene proceeded at more negative potentials and the rate correspondingly decreased when the KCl and KBr were added. It seems that in the presence of the salts this must be connected with a decreased adsorption of cyclohexene on the catalytic surface.

The activation energy for the hydrogenation of cyclohexene increased from 2 to 6 kcal/mole as the salt concentration was raised.

As may be seen from Fig. 3, addition of KI decreased the rate of hydrogenation of cyclohexene even more. It seems that the dependence of hydrogenation rate on the concentration and nature of the anion is connected with the screening of the catalytic surface, which hinders the adsorption of the hydrogenated compound and correspondingly increases the hydrogen concentration. The higher the salt concentration and the larger the ionic radius, the more effectively will the anion screen the catalytic surface.

The potential of the catalyst increased in the order: $Cl^- < Br^- < I^-$.

When we measured the pH of the experimental media, we found out that the pH was slightly altered after each experiment (see Table 1); with KCl the medium became more acidic, while with KBr and KI more alkaline. It seems, that the change in the pH of the medium after each experiment can be explained by the changed structure of the electrical double layer.

TABLE 1

Anion	Radius, in A	Electron affinity, in kcal	Halide concentration, in N	pH before the experiment	pH after the experiment	The reversible hydrogen potential of the catalyst, in mv.
Cl^-	1.81	86	0.1	6.8	6.5	760
Br^-	1.96	84	0.1	6.9	7.8	800
I^-	2.2	76	0.1	7.3	8.3	870

A. N. Frumkin and co-workers have shown [4] that when the cations in a neutral solution are absorbed on the electrode surface the solution becomes acidic, while in case of anions basic.

On the basis of pH measurements we may assume that in a KCl solution it is the potassium cation that is adsorbed on the catalytic nickel surface; charge curves [4, 5] indicate that the adsorption of a cation increases the bond energy between the adsorbed hydrogen and the catalyst.

By contrast, it is the anions that are adsorbed in the KBr and KI solutions [6]; adsorption of anions on a negatively charged surface increases the cathode potential even further. It seems that the Ni and the anion form a dipole, with the anionic electron cloud displaced toward the Ni, and consequently the adsorbed hydrogen becomes much more loosely bound to the catalytic surface [4]. The smaller value of the reversible hydrogen potential in the case of KBr is connected, first, with the greater electron affinity of the Br^-, and second, with a smaller adsorbability.

The bond energies of the adsorbed hydrogen decrease in the order: $Cl^- < Br^- < I^-$.

LITERATURE CITED

[1] T. Erdey-Gruz and K. Zimmer. Magyar kem folyoirat 62, 9, 302 (1956).

[2] K. Hoshino and J. Miyata, J. Chem. Soc. Japan, Ind. Chem. Sec. 59, No. 2, 236 (1956).

[3] D. V. Sokolskii and V. A. Druz', J. Phys. Chem. 28, 364 (1952).

[4] A. N. Frumkin, The Kinetics of Electrode Reactions, Moscow, 1952, p. 24;* A. N. Frumkin and A. L. Shlygin, Bull. Acad. Sci. USSR, Chem. Ser. No. 5, 773 (1936); A. N. Frumkin, J. Phys. Chem. 14, 1200 (1940); A. N. Frumkin and A. L. Shlygin, Acta Physicochem. URSS 3, 701 (1935).

*In Russian.

[5] B. V. Érshler, J. Phys. Chem. 14, 708 (1940).

[6] K. Schwabe, K. Wagner and C. Weissmantel, Zs. phys. Chem. 206, 5-6, 309 (1957).

Received August 25, 1958

DETERMINATION OF THE ELEMENTARY CONSTANTS IN THE OXIDATION OF ETHYLBENZENE BY THE METHOD OF INTERRUPTED ILLUMINATION

V. F. Tsepalov and V. Ya. Shlyapintokh

Institute of Chemical Physics of the Academy of Sciences USSR

(Presented by Academician V. N. Kondrat'ev, October 11, 1958)

According to current ideas the liquid-phase oxidation of hydrocarbon proceeds through a chain mechanism involving the formation of substituted hydrogen peroxide as the primary stable oxidation product [1]. At low temperatures the substituted hydrogen peroxide is also the final reaction product. In this case the reaction scheme looks as follows:

Chain initiation

Formation of radicals $\dot{R}$ and $\dot{R}O_2$, rate w_i. (I)

Chain propagation

$$\dot{R} + O_2 \xrightarrow{k_2} \dot{R}O_2; \quad \text{(II)}$$

$$\dot{R}O_2 + RH \xrightarrow{k_3} RO_2H + \dot{R}. \quad \text{(III)}$$

Chain break

$$\left.\begin{aligned} 2\,\dot{R} &\xrightarrow{k_4} \\ \dot{R} + \dot{R}O_2 &\xrightarrow{k_5} \\ 2\,\dot{R}O_2 &\xrightarrow{k_6} \end{aligned}\right\} \text{inactive products.} \quad \begin{matrix}\text{(IV)}\\ \text{(V)}\\ \text{(VI)}\end{matrix}$$

Here RH = hydrocarbon, $\dot{R}$ and $\dot{R}O_2$ = alkyl and peroxyl radicals.

In cases where the chains are long this scheme results in the following rate equation [2]:

$$\left(\frac{d[O_2]}{dt}\right)^{-2} = w_i^{-1}\left(k_2^{-2}k_4[O_2]^{-2} + 2k_2^{-1}k_3^{-1}k_5[RH]^{-1}[O_2]^{-1} + k_3^{-2}k_6[RH]^{-2}\right). \quad (1)$$

If the oxygen concentration O_2 is sufficiently large, then Equation (1) assumes the form

$$\frac{d[O_2]}{dt} = w_i^{1/2}k_3k_6^{-1/2}[RH]. \quad (2)$$

In the case of a short chain we have to add the initial rate w_i to the right side of Eq. (2).

Equation (2) contains three unknowns: w_i, k_3, and k_6. And accordingly, we need three independent equations to get a solution for each parameter.

By carrying out the oxidation under conditions of continuous illumination we can determine the values

of w_i and $d[O_2]/dt$ by the usual kinetic methods, and thus obtain a relationship between the constants k_3 and k_6. To get an individual solution for each constant it is necessary to have one more independent equation. Such an equation could be obtained by measuring the concentration of $\dot{R}O_2$ radicals ($[\dot{R}O_2] = \sqrt{w_i / k_6}$). However, the concentration of $\dot{R}O_2$ in the investigated reaction is too low and cannot be determined directly. For this reason, in order to get the missing equation, we used in our work a special method – the method of interrupted illumination.

The theory of interrupted illumination was reviewed in full detail in [3]. By means of this method it was possible to measure the average life time of a chain or in other words, the average life time of the radicals, τ. The determination yields

$$\tau = \frac{[\dot{R}O_2]}{k_6 [\dot{R}O_2]^2} = \frac{1}{k_6 [\dot{R}O_2]}.$$

Assuming that $k_6[\dot{R}O_2]^2 = w_i$, we will get the equation

$$\tau = \frac{1}{\sqrt{k_6 w_i}}, \qquad (3)$$

from which k_6 is calculated by substituting into it the known values of τ and w_i.

The experimental method. The reaction rate was determined in a vacuum apparatus from the absorption of oxygen whose pressure was automatically regulated and recorded (see Fig. 1, where: 1 = light source; 2, 6 = lenses; 3, 7 = light filters; 5= diaphragm). The pressure was regulated by means of manometer 12 whose contacts k and l were linked with the electrolytic cell 11 through a current amplifier. In order to record automatically the reaction rate we passed a steady current through a platinum wire which was stretched in the gas burette 10. The outlet 13 of this wire was hooked up to the EPP-09.

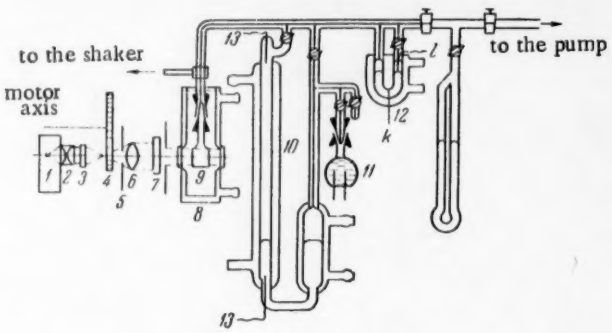

Fig. 1. Schematic diagram of the apparatus.

For a light source we used a mercury lamp SVDSh-250, which operated on direct current. As may be seen in Fig. 1, the light, ($\lambda > 380$ mμ) after passing through an appropriate optical system, falls in a parallel beam on the reaction vessel 9 (volume 5.5 cm^3) placed in the thermostat 8. The light was interrupted by means of a rotating disc 4 with slits (the ratio of light interval to the dark one was 1 : 3). The length of the light impulse could be varied from 0.002 to 10 sec. During the experiment the reaction vessel with agitated in the direction of the light beam at the rate of 8 cycles per second. At this rate the diffusion of oxygen into the liquid phase did not limit the reaction. We purified the ethylbenzene by shaking it with 5% fuming sulfuric acid, then with sodiummetabisulfite, after which we washed it several times with water, dried over sodium metal, and distilled at 15 mm. To determine the initiation rate, we used as inhibitors α- and β-naphthols (analytically pure grade). Chemically pure anthraquinone was used as a sensitizer. The concentration of anthraquinone in ethylbenzene was 1.4×10^{-4} mole/liter. At this concentration less than 9% of the incident light was absorbed. The experiments were carried out at $P_{O_2} = 1$ atm in the 0-90° temperature range. The degree of conversion did not exceed 0.5% of ethylbenzene. Without the sensitizer the rate of this photochemical reaction was almost nil.

Determination of the initiation rate. In the presence of an inhibitor, which reacted with the radical $\dot{R}O_2$, an additional reaction was introduced into the oxidation scheme

$$\dot{R}O_2 + B \xrightarrow{k_3} \text{destruction of the radical.} \qquad \text{(VII)}$$

At a sufficiently high inhibitor concentration the rate of the inhibited reaction would be

$$\frac{d[O_2]}{dt} = w_i\left(1 + \frac{k_3[RH]}{k_7[B]}\right), \qquad (4)$$

where [B] = concentration of the inhibitor.

One can see from Eq. (4) that $d[O_2]/dt$ is a linear function of $1/[B]$. In the limiting case where $1/[B] = 0$ $d[O_2]/dt = w_i$. The experimentally determined $d[O_2]/dt$ as a function of $1/[B]$ is shown in Fig. 2. As is clear from the Figure, the experimental data satisfies Equation (4) fairly well. The fact that the lines for the two inhibitors, though at various temperatures, meet at one point indicates that the addition of inhibitors does not change the initiation rate proper,* and that the rate of initiation is independent of temperature.

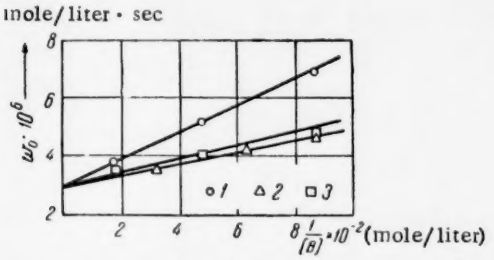

Fig. 2. Dependence of the initial reaction rate on the inhibitor concentration. 1) β-Naphthol, 70°; 2) α-naphthol, 70°; 3) β-naphthol, 29° C.

The latter fact that utilized in the direct determination of w_i. We measured the reaction rate as a function of temperature (Fig. 3). From the shape of the obtained curve it is evident that at sufficiently low temperatures (5-15°) the reaction rate is independent of temperature. In this temperature. Experiments have demonstrated that the values of w_i obtained by the inhibitor method and from the temperature dependence of the reaction rate are in practically full agreement. Later on the initiation rate was always determined by the second method, since it gave more exact results with a smaller loss of time.

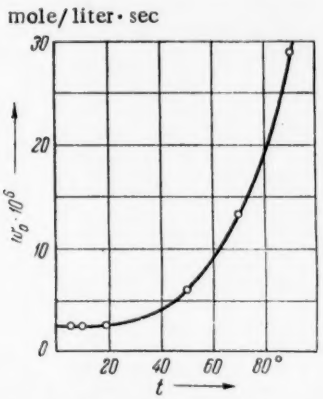

Fig. 3. Reaction rate as a function of temperature.

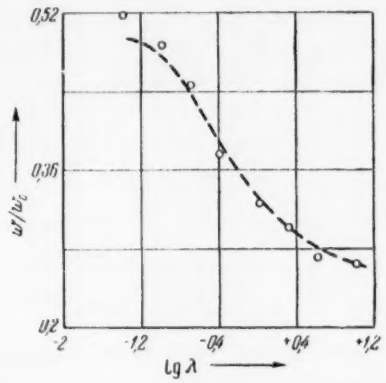

Fig. 4. Determination of the life-time of the RO_2 radicals. The circles denote experimental data at 70°; the dotted line gives the theoretical curve for $\tau = 0.13$ sec.

Determination of the life time of peroxide radicals. In Fig. 4, we have drawn one of the curves obtained by the method of interrupted illumination. This curve represents w/w_0 as a function of log λ, where w = reaction rate with interrupted illumination, w_0 = reaction rate with continuous illumination, and λ = length of a light impulse, in seconds. The theoretical curve for $\tau = 0.13$ sec was constructed according to the tabulated data in [3]. As is clear from the graph, the experimental points fit fairly well on the theoretical curve.

*This method of determining w_i was described in paper [4].

From Equation (3) it follows that at a fixed temperature

$$\tau \sqrt{w_i} = \frac{1}{\sqrt{k_6}} = \text{const.}$$

TABLE 1

Temp. °C	$w_i \cdot 10^8$, mole/liter·sec	$(w_0 - w_i) \times 10^8$ mole/liter·sec	τ, sec	$\tau\sqrt{w_i} \cdot 10^4$
70	2,63	11,4	0,148	2,2
	1,98	9,8	0,142	2,0
	2,48	11,0	0,139	2,2
90	2,14	24,5	0,133	1,9
	2,24	25,0	0,143	2,1
	0,15	6,1	0,574	2,2

The values of $\tau \sqrt{w_i}$, obtained for various w_i at two temperatures (70 and 90°), are listed in Table 1.

It is evident from the table that, within limits of experimental errors, k_6 has the same value at 70 and 90°. Therefore, from now on we will assume that the activation energy for the recombination reaction $E_6 = 0$.

From the average value of k_7, and from the measured values of $d[O_2]/dt$ at various temperatures, we determined the rate constant k_3 by using Equation (2), and then the value of k_7 for α- and β-naphthol from Equation (4):

$$k_3 = 1.2 \cdot 10^{-13} e^{-11400/RT} \text{ cm}^3/\text{sec},$$

$$k_6 = 3.6 \cdot 10^{-14} \text{ cm}^3/\text{sec},$$

$$k_7 = 3.5 \cdot 10^{-12} e^{-7900/RT} \text{ cm}^3/\text{sec} \text{ (for β-naphthol)},$$

$$k_7 = 8.3 \cdot 10^{-18} \text{ cm}^3/\text{sec} \text{ (for α-naphthol at 70°)}$$

On the basis of general concepts one would expect that the reactivity of various R–O–O·radicals should not depend on the nature of the hydrocarbon radical $\dot{R}$, since it is far removed from the location of the free valence. Indeed, when compared, the values of k_6 obtained by various authors are quite similar for the majority of hydrocarbons. The values of k_6 for ethylbenzene and tetralin [4] are practically identical. For a series of unsaturated hydrocarbons the constant k_6 is smaller by 1-1.5 orders of magnitude [5]. Cumene (isopropylbenzene) is an exception [6] ($k_6 = 6.6 \times 10^{-17}$ cm^3/sec).

The literature does not list any values of k_7 for α and β-naphthol. From the data listed in work [7], we calculated k_7 for the reaction between β-naphthol and tetralin peroxyl radicals, $k_7 = 3.3 \times 10^{-17}$ cm^3/sec (at 25°). According to our data for ethylbenzene, $k_7 = 0.6 \times 10^{-17}$ (at 25°); so that the difference in the values of the k_7 constant is also small.

LITERATURE CITED

[1] D. G. Knorre, Z. K. Maizus, L. K. Obukhova, and N. M. Émanuél', Progr. Chem. 26, 416 (1957).

[2] L. Bateman, Quart. Rev. London. Chem. Soc. 8, 147 (1954).

[3] G. M. Burnett and H. W. Melville, Technique of Organic Chemistry 8, 1953, p. 133.

[4] C. H. Bamford and M. J. S. Dewar, Proc. Roy. Soc. A, 198, 252 (1949).

[5] H. R. Cooper and H. W. Melville, J. Chem. Soc. 1951, 1984, 1994.

[6] H. W. Melville and S. Richards. J. Chem. Soc. 1954, 944.

Received September 20, 1958

THE VIBRATIONAL RELAXATION OF DIATOMIC MOLECULES

E. E. Nikitin

Institute of Chemical Physics USSR Academy of Sciences

(Presented by Academician V. N. Kondrat'ev, October 25, 1958)

The question of the relaxation of the nonequilibrium vibrational distribution function and its relationship to the theory of nonequilibrium chemical reactions has been the subject of a number of works (see, for example, [1, 2]). For the case of a harmonic oscillator [1], the transition probabilities are usually calculated using the formula of Landau and Teller [3]

$$P_{n,\,n+1} = k(n+1); \qquad P_{n,\,n+p} = 0, \quad p > 1, \tag{1}$$

in which n denotes the number of the vibrational level.

For the case of an anharmonic oscillator, it has been assumed in [2] that $P_{n,n+p}$ satisfy the relationships

$$P_{n,\,n+1} = k(n+1)[1+\varepsilon(n+1)]; \qquad P_{n,\,n+2} = \frac{k}{4}(n+1)(n+2);$$
$$P_{n,\,n+p} = 0, \quad p > 2, \tag{2}$$

where the anharmonicity coefficient ϵ is equal to $\hbar\omega_0/4D$ (ω_0 is the fundamental frequency of a diatomic molecule and D is the dissociation energy).

The difference between (1) and (2) is due solely to the fact that the calculation of the transition probabilities was carried out in the first case using the wave functions for a harmonic oscillator and in the second case using the wave functions for an anharmonic oscillator. It can be easily shown, however, that the formula of Landau and Teller applied to an anharmonic oscillator leads to a different relationship between the transition probabilities and the vibrational quantum numbers.

According to [3] we may write, for a one-quantum transition

$$P_{n,\,n+1} = c(n+1)\exp[-3\ \chi(n)] \tag{3}$$

where the magnitude of $\chi(n)$ is proportional to $(E_{n+1} - E_n)^{2/3}$ and is equal to 5-10 for different molecules at ordinary temperatures [4], while c is independent of n. For a Morse oscillator, which describes a diatomic molecule with sufficient accuracy when $n \ll \frac{1}{2}\epsilon$, we may write

$$(E_{n+1} - E_n)^{1/3} = [\hbar\omega_0(1 - 2\ \varepsilon n)]^{1/3} = (\hbar\omega_0)^{1/3}\left(1 - \frac{4}{3}\varepsilon n\right). \tag{4}$$

Substituting (4) in (3), we have

$$P_{n,\,n+1} = c(n+1)\exp[-3\chi(0) + 4\chi(0)\varepsilon n] = k(n+1)\exp[4\chi(0)\varepsilon n] \equiv$$
$$\equiv k(n+1)\,\gamma^n, \tag{5}$$

from which (1) follows when $\epsilon = 0$. It is important, however, that even at a low anharmonicity the exponential term in (5) may be large, since $\chi(0)$ is a comparatively large quantity.

For many quantum transitions $n \to n + p$, the probability $P_{n,\,n+p}$ is proportional to the factor $\epsilon^{p-1}\exp[-3p^{2/3}\chi]$ and is smaller by many orders of magnitude than the probability $P_{n,n+1}$. We may therefore assume with sufficient accuracy that

$$P_{n,\,n+p} = 0, \quad p > 1. \tag{6}$$

Since the expressions (5) and (6) are essentially different from (1) and (2), it is to be expected that the relaxation of a system of anharmonic oscillators differs considerably from the relaxation of a system of harmonic oscillators. We would point out that the opposite conclusion is reached in [2].

The relaxation of the vibrational distribution function $x_n(t)$ for an anharmonic oscillator is described by the system of equations

$$\frac{d}{dt}\,x_n(t) = \sum_m B_{nm}\,x_m(t), \tag{7}$$

in which the elements of the matrix $\hat{B}$ are expressed by the transition probabilities (5) and (6). The approximation of $x_n(t)$ to equilibrium may be characterized by the relaxation times, defined by the expression

$$\tau_n = \int_0^\infty t\,\frac{d}{dt}\,[x_n(t) - x_n(\infty)]\,dt = \int_0^\infty [x_n(t) - x_n(\infty)]\,dt. \tag{8}$$

τ_n in this expression is dependent on the initial distribution $x_n(0)$. Let us examine the δ-type initial distribution $x_n(0) = \delta_{nm}$ and introduce the corresponding notation τ_{nm}. The magnitude of τ_n for any initial distribution may be expressed in the form $\tau_n = \sum_m a_m \tau_{nm}$ in view of the linearity of (8).

An integral of the type in (8) may be formally expressed by the matrix $\hat{B}^{-1}$ (see, for example, [5]). When this is actually calculated it must be borne in mind that the first (μ_0) true value of the matrix $\hat{B}$ corresponds to the equilibrium distribution and is equal to zero, so that the reciprocal matrix B^{-1} does not exist. It is, however, easy to overcome this difficulty if we consider first of all a decaying oscillator with a finite number of discrete levels and then reduce the decay rate constant to zero. In this way the expression (8) can be used to give the expression

$$\tau_{nm} = \lim_{\mu_0 \to 0} [B^{-1}_{nm}(\mu_0) - x_n(\infty)/\mu_0]. \tag{9}$$

Following [5] in the calculation of B^{-1}, and using for μ the expression derived previously [6], we can show that when $n, m \gg 1$

$$\begin{aligned} \tau_{nm} &= \exp(-E_n/kT) \sum_{j=0}^{n} \frac{1}{P_{j,\,j+1}\exp(-E_j/kT)}, \qquad n \ll m; \\ \tau_{nm} &= \exp(-E_n/kT) \sum_{j=0}^{m} \frac{1}{P_{j,\,j+1}\exp(-E_j/kT)}, \qquad n \gg m. \end{aligned} \tag{10}$$

Substituting the value of $P_{j,\,j+1}$ from (5) in (10), and assuming that when $j \ll 1/2\,\epsilon$, $\hbar\omega(j)/kT = \hbar\omega_0 j/kT = \theta j$, we have

$$\begin{aligned} \tau_{nm} &= \{[1 - \gamma\exp(-\theta)]\,\gamma^n (n+1)\,k\}^{-1} + O\left(\frac{1}{n^2}\right), \quad n \ll m; \\ \tau_{nm} &= \{[1 - \gamma\exp(-\theta)]\,\gamma^m (m+1)\,k\}^{-1} \exp[\theta(m-n)] + O\left(\frac{1}{m^2}\right), \qquad n \gg m. \end{aligned} \tag{11}$$

For a harmonic oscillator (i.e., when $\epsilon = 0$) the magnitude of τ_{nm} (11) agrees with that calculated earlier by a different method [7].

When n, m ~ 1, the value of τ_{nm} is not defined by the expressions (10) and (11). Moreover, when $\underline{n}$ is of the order of several units, τ_{nm} becomes negative. This means that as equilibrium is approached the distribution function in the lower vibrational levels remains smaller than the equilibrium function. The change in the sign of τ_{nm} at low values of $\underline{n}$ also follows from the normalization condition $\Sigma\tau_{nm} = 0$.

As an example of the application of expression (11) let us consider the vibrational deactivation of an oxygen molecule

$$O_2^*(n) + N_2 \rightarrow O_2^*(n-1) + N_2, \tag{12}$$

which has been studied by Norrish and co-workers [8] in an examination of the flash photolysis of chlorine dioxide. The vibrational relaxation of the oxygen molecules in reaction (12), with an initial δ-distribution, at m = 8, corresponding approximately to the experimental conditions for the formation of O_2, * has been examined by Shuler [9] on the basis of a harmonic oscillator model. It was found that the calculated half-decay time for the population of the sixth level was greater by approximately one order of magnitude than the experimental value, even at the very high nitrogen pressures at which the experiment was carried out (≃ 600 mm). From this it follows [9] that reaction (12) cannot complete with the parallel reaction involving deactivation of oxygen

$$O_2^*(n) + ClO \rightarrow O_2^*(n-1) + ClO. \tag{13}$$

According to [8] this conclusion is accurate within the range of N_2 pressures studied.

In the calculation of τ_{nm}, however, the anharmonicity of the vibrations of the O_2 molecule must be taken into account. From (11) it follows that

$$\tau_{nm}(\text{harm})/\tau_{nm} \simeq \gamma^n, \quad n \ll m, \tag{14}$$

where $\tau_{nm}(\text{harm})$ is the relaxation time for a harmonic oscillator. Using the calculation method of Schwartz and Herzfeld [4], together with the spectroscopic data for the oxygen molecule [10], we obtain $\chi(0) = 10$ (T = 288° K) $\omega_0 = 1580$ cm^{-1} and D = 118 kcal/mole, from which we find that $4\chi(0)\epsilon \simeq 2/5$ and that

$$\tau_{68}(\text{harm})/\tau_{68} \simeq 10. \tag{15}$$

It is thus shown that at N_2 pressures greater than 600 mm, reaction (12) may compete with reaction (13).

By making use of the relaxation time τ_{nm}, we may calculate comparatively easily the relaxation time of any physical quantity characterizing a molecule. Let us calculate, for example, the relaxation time of the vibrational energy defined by the expression:

$$\tau_E = \int_0^\infty \frac{E(t) - E(\infty)}{E(0) - E(\infty)}\, dt = \frac{1}{E(0) - E(\infty)} \sum_n E_n \tau_{nm}. \tag{16}$$

Assuming $1 \ll m \ll 1/2\epsilon$, we may approximate and write $E_n = \hbar\omega_0 n$, and also neglect the inaccuracy introduced into the sum in (16) by two or three of the first terms, which is related to the fact that the expression (11) is not applicable when n ~ 1. For simplicity, we also assume that $\exp(-\theta) \ll 1$, so that the terms decreasing exponentially in the sum in (16) when n > m may be neglected. We then have $E(0) - E(\infty) \simeq \hbar\omega_0 m$ and

$$\sum_n \hbar\omega_0 n\tau_{nm} \simeq \sum_{n=0}^{m} \hbar\omega_0 [1 - \gamma\exp(-\theta)]^{-1} \frac{n}{n+1}\gamma^{-n}. \tag{17}$$

From (16) and (17) we obtain accurately, up to terms of the order of $1/m^2$,

$$\tau_E = \{k[1 - \gamma\exp(-\theta)]\}^{-1} \frac{1 - \gamma^{-m}}{(1 - \gamma^{-1})\, m}. \tag{18}$$

For a harmonic oscillator $\gamma = 1$ and (18) acquires the form:

$$\tau_E = \{k[1 - \exp(-\theta)]\}^{-1}. \quad (19)$$

We thus obtain the well-known result for the relaxation of the vibrational energy of a harmonic oscillator: the relaxation time is independent of the initial distribution [3]. We would also point out that in this case the approximate formula (19) coincides with the exact expression for the relaxation time [3]. For an anharmonic oscillator the relaxation time for the vibrational energy decreases with increase in the energy at the initial moment of time. The fact that this relationship exists indicates that the relaxation of the vibrational energy of an anharmonic oscillator cannot be described by the differential equation

$$\frac{dE}{dt} = \frac{1}{\tau_E}[E - E(\infty)]. \quad (20)$$

I have to express my gratitude to Professor N. D. Sokolov for discussion of the present work.

LITERATURE CITED

[1] E. W. Montroll and K. E. Shuler, J. Chem. Phys. 26, 454 (1957).

[2] N. W. Bazley, E. W. Montroll, R. J. Rubin, and K. E. Shuler, J. Chem. Phys. 28, 700 (1958).

[3] L. Landau and E. Teller, Physik. Z. Sowjetunion 10, 34 (1936).

[4] R. N. Schwartz and K. F. Herzfeld, J. Chem. Phys. 22, 767 (1954).

[5] Kim, Shoon-Kyung, J. Chem. Phys. 28, 1057 (1958).

[6] E. E. Nikitin, Dokl. Akad. Nauk. 119, No. 3 (1958).*

[7] E. E. Nikitin, Dokl. Akad. Nauk. 116, No. 4 (1957).*

[8] F. J. Lipscomb, R. G. W. Norrish and B. A. Thrush, Proc. Roy. Soc. A, 233, 455 (1955).

[9] K. E. Shuler, J. Phys. Chem. 61, 849 (1957).

[10] G. Herzberg, The Structure and Spectra of Diatomic Molecules, IL, 1949.**

Received October 22, 1958

*See C.B. Translation.

**Russian translation.

THE ISOTOPIC EXCHANGE OF NITROGEN BETWEEN AMINO COMPOUNDS AND LIQUID AMMONIA

L. L. Strizhak, S. G. Demidenko and Corresponding Member AN SSSR A. I. Brodskii

L. V. Pisarzhevskii Institute of Physical Chemistry, Ukr. SSR Academy of Sciences

The isotopic exchange of nitrogen has been little studied up to the present [1]. In particular, little attention has been paid to the exchange of nitrogen in organic compounds, ammonia and its derivatives. No appreciable exchange has been detected in solution between the ammonium ion and the nitrate ion [2], between ammonia and a number of amino acids [3], or between ammonium chloride and a number of primary and secondary aromatic amines [4].

In the chemistry of organic nitrogen-containing compounds, the study of the relationship between structure and the mobility of amino and imino groups is of particular interest. We have therefore made a study of the exchange of nitrogen between liquid ammonia and substances containing these groups. Qualitative data for a number of these compounds, together with preliminary data on the kinetics of exchange in a nunber of cases, have been published by us earlier [5]. The present article presents new results of a more accurate study of the kinetics of the exchange and of its acid catalysis. These new data are in complete accordance with the exchange mechanism suggested earlier.

The experiments on the study of the exchange process were carried out as follows. The ammonia was prepared in an evacuated apparatus by the reaction between KOH and ammonium nitrate containing 8-9% N^{15}; it was then dried thoroughly by being frozen and evaporated three times in three traps in series cooled with liquid air, after which it was collected in a vessel for storage.

The experiments were carried out using thick-walled ampoules of molybdenum glass, with an internal diameter of 2-3 mm. The ampoule containing the weighed sample of the organic substance was connected to the apparatus, evacuated, and cooled with liquid air, after which the calculated quantity of ammonia was frozen into it from a measured volume. The ampoule was disconnected and heated for the necessary time in a thermostat, after which it was frozen, opened and transferred to a tube connected to the apparatus. The calculated quantity of hydrochloric acid was added to another tube of the same apparatus. Both tubes were cooled with liquid air and evacuated; the coolant was then removed and the ammonia liberated was absorbed by the acid.

When the ammonia had been distilled off, the organic compound was treated with concentrated sulfuric acid according to Kjeldahl's method, the reaction mass neutralized with alkali and the ammonia produced distilled into a solution of hydrochloric acid.

The NH_4Cl samples obtained from the ammonia or from the organic substance were oxidized with sodium hypobromite. The isotopic composition of the elementary nitrogen liberated in the process was determined using a mass spectrometer, with a total relative error of 3-5%.

All the solutions studied were homogeneous at the temperature of the exchange. After the exchange and removal of the ammonia by distillation, the melting points of the substances remained the same as before the experiment. The exchange in acid medium was carried out in N NH_4Cl. The latter was prepared from the

original ammonia containing 8% of the heavy nitrogen isotope, and was added to the ampoule before the latter was filled with the ammonia.

In previous experiments the percentage exchange was found from the change in the N^{15} content of the ammonia, which is insufficiently accurate when the exchange is slight or when a large excess of ammonia is

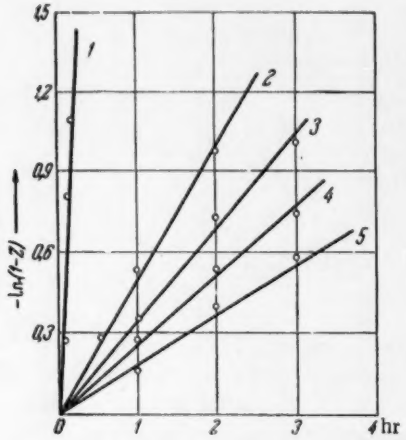

Fig. 1. Change in -ln(1-z), where z is the exchange fraction, with time. 1) trichloroacetamide, 25°; 2) 2,4-dinitroaniline, 150°; 3) urethan, 140°; 4) 2,4,6-trinitroaniline, 100°; 5) p-nitrobenzamide, 180°

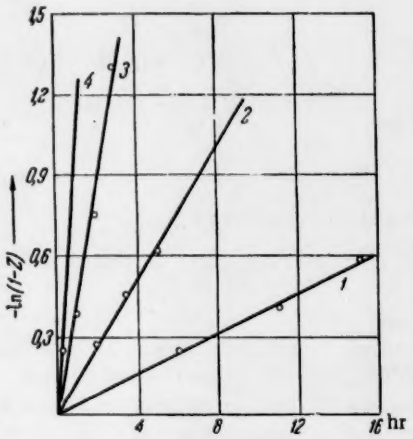

Fig. 2. Change in -ln(1-z) with time for urea: 1) at 80°; 2) at 90°; 3) at 100°; 4) in 1.0 N NH_4Cl at 100°.

used. In the experiments which we carried out, the percentage exchange was found chiefly from the N^{15} content of the dissolved substance. In a number of experiments the N^{15} content of the ammonia was also measured.

The rate constant and half-exchange period were calculated as usual from the monomolecular equation, without corrections for concentration, since in this case these are smaller than the experimental errors. It can be seen from Figures 1 and 2 that the exchange kinetics are given exactly by this equation. The wide differences

TABLE 1

Exchange in Acetamide and Benzamide

Moles amide per mole of NH_3	Time, hours	Exchange, % from NH_3	Exchange, % from the amide	k, hours^{-1}	Moles amide per mole of NH_3	Time, hours	Exchange, % from NH_3	Exchange, % from the amide	k, hours^{-1}
Acetamide, 180°					Benzamide, 180°				
0,8	2,5	26,2	25,0	0,118	1,0	3,0	17,4	—	0,064
1,0	4,0	39,0	42,7	0,131	1,1	5,0	25,9	23,6	0,057
1,0	6,0	54,5	56,8	0,135	1,0	8,0	39,4	36,0	0,059
1,0	8,5	67,0	70,8	0,137					
Acetamide + 1.0 N NH_4Cl, 120°					Benzamide + 1.0 N NH_4Cl, 160°				
1,0	0,7	—	33,3	0,578					
1,0	1,3	54,4	55,0	0,609	1,0	0,7	43,2	—	0,809
0,8	1,3	56,8	52,8	0,611	0,9	1,3	61,4	54,8	0,667
1,0	2,0	70,1	73,9	0,635	1,0	2,0	70,2	—	0,605

in the rates of exchange and solubilities made it impossible to compare the exchange kinetics at identical temperatures and concentrations. In each case the experimental conditions were chosen on the basis of the results of a number of preliminary experiments, in such a way as to make possible a comparison of the effects

of substituents in substances of the same general type. The concentrations were chosen in such a way as to ensure that the solutions were homogeneous at the temperature of the experiment and to give as closely as possible a molar ratio of ammonia to dissolved substance of 1 : 1. The fact that the densities of the solutions were not known made it impossible to calculate all rate constants for unit concentration. Recalculation in this way would change the values of certain of the rate constants by less than 50%, which is not significant for the purposes of the comparisons made below.

TABLE 2

Rate Constants and Half-Exchange Period

Substance	Temp., °C	Moles substance per mole of NH_3	k, hours^{-1}	$\tau_{1/2}$, hours
Trichloroacetamide	25	0,4—0,5	3,6	0,19
The same + NH_4Cl*	25	0,4	exchange complete in 2 min	
Acetamide	180	1,0	0,13	5,3
The same + NH_4Cl	120	0,8—1,0	0,61	1,1
Benzamide	180	1,0—1,1	0,060	12
The same + NH_4Cl	160	0,9—1,0	0,69	1,0
p-Nitrobenzamide	180	0,2	0,19	3,7
The same + NH_4Cl	180	0,2	1,51	0,46
Urethan	140	1,0	0,35	2,0
2,4-Dinitroaniline	150	0,2	0,53	1,3
The same + NH_4Cl	150	0,2	3,6	0,20
2,4,6-Trinitroaniline	100	0,2—0,3	0,25	2,8
Urea	80	1,0	0,037	19
The same	90	1,0	0,13	5,3
The same	100	1,0	0,39	1,8
The same + NH_4Cl	100	1,0	2,9	0,24

*1.0 N NH_4Cl in all cases.

The exchange in urea was studied at three temperatures. The rate constant is given by the Arrhenius equation with an apparent activation energy of 30 kcal/mole.

The results of the measurements for acetamide and benzamide are given in Table 1. To save space, the data for the other substances are given in less detail in Figures 1 and 2 and Table 2.

DISCUSSION OF RESULTS

As a result of measurements published earlier [5], which have been supplemented by certain new data, we have found no appreciable exchange at 200° over periods of 50-100 hours in experiments with o-, p- and m-nitroanilines, nitrobenzene, p-toluidine, p-anisidine and benzylamine; at 120° over periods of 100-200 hours with o- and p-aminophenols, o- and p-phenylenediamine hydrochlorides, p-chloroaniline, p-bromoaniline, p-iodoaniline, benzidine, benzidine hydrochloride, α- and β-naphthylamines, α-aminoanthraquinone, phenazine carboxylamide, pyridine, α- and β-aminopyridine, methylamine hydrochloride, ethylamine, 2,4-dinitrophenol and picric acid. In studies of the mechanism of the condensation of aromatic amines, B. A. Geller, R. Yu. Sheinfain and one of us [4] detected no exchange at 170-240° over periods of 6-30 hours with aniline, diphenylamine, benzanilide, benzo-α-naphthalide and phenyl-α-naphthalide with NH_4Cl.

It follows from these data that even under very severe conditions, liquid ammonia does not exchange nitrogen with the nitro group, with the nitrogen of the pyridine ring, or, which is more important in the present instance, with the amino group, when this is directly attached to the carbon of an aromatic nucleus or alkyl group.

Exchange with the amino group takes place when strongly negative substituents, such as the nitro group or the sulfonic acid group, are introduced into the nucleus. No exchange takes place with o-nitroaniline, but exchange takes place with 2,4-dinitroaniline and much more rapidly with 2,4,6-trinitroaniline. As was found

earlier [5], no exchange takes place with 2-aminopyridine but exchange takes place slowly with 5-nitro-2-aminopyridine. Exchange is also observed with sulfanilic and naphthionic acids. The considerable increase in the rate of exchange for trichloroacetamide compared with acetamide, and the smaller increase in the rates of exchange for p-nitrobenzamide and 4-nitrophthalimide compared with unsubstituted benzamide and phthalimide, must also be ascribed to this same influence of the negative substituents.

Comparatively rapid exchange is observed in the case of those compounds in which the amino group is attached directly to the strongly polarized carbon of the carbonyl or analogous groups C = X, where X is O, S or NH, as in the amides or derivatives of urea. The rates of exchange for the amides decrease along the series:

$$CCl_3 \cdot CO \cdot NH_2 > CH_3 \cdot CO \cdot NH_2 > C_2H_6O \cdot CO \cdot NH_2 > NO_2C_6H_4 \cdot CO \cdot NH_2 > C_6H_5 \cdot CO \cdot NH_2,$$

in which the half-exchange period varies between 0.2 hours at 25° and 11. hours at 180°. This series shows clearly the increase in the rate of exchange with increase in the electrophilic nature of the carbon atom, resulting both from conjugation and from the inductive effect of the negative substituents in the group

$$\leftarrow C^+ - NH_2 \cdot$$
$$\quad \| \quad$$
$$\quad O^-$$

Similar relationships are observed in the case of derivatives of urea, where the exchange again depends on the electrophilic nature of the carbon atom to which the amino group is attached. Thus, comparison of the data in Table 2 with those obtained earlier show that

$$NH_2 \cdot CO \cdot NH_2 > NH_2 \cdot CS \cdot NH_2 \text{ and } NH_2 \cdot CO \cdot NH \cdot NH_2 \cdot HCl > NH_2 \cdot CNH \cdot NH_2 \cdot HCl.$$

It can be seen from Tables 1 and 2 that the rate of exchange is greatly increased by the presence of the ammonium ion, which behaves as a strong acid in liquid ammonia. This is again related to the increase in the electrophilic nature of the carbon atom when a proton is attached to the C = X group.

All the features of the exchange of nitrogen in amino compounds which have been considered indicate bimolecular mechanism of (SN2) nucleophilic substitution of the amino group in the organic substance by an amino group from the ammonia molecule, with transfer of the proton from the latter to the amino group which is displaced:

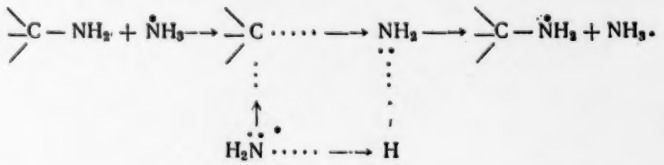

As has already been pointed out, this mechanism is analogous to that put forward earlier [4] for the condensation reaction between primary and secondary aromatic amines. The relationship between the mobility of amino groups and structure, and the mechanism of a number of other reactions connected with the removal of amino groups, may evidently be explained from these standpoints.

LITERATURE CITED

[1] A. L Brodskii, Isotope Chemistry, Izd. AN SSSR, 1957, p. 327.*

[2] H. G. Thode and H. C. Urey, J. Chem. Phys. 7, 34 (1939).

[3] R. Schoenheimer, D. Rittenberg, et al., J. Am. Chem. Soc. 59, 1768 (1937); K. Bloch and R. Schoenheimer, J. Biol. Chem. 131, 111 (1939); V. Vigneaud, S. Simmonds, and M. Cohn, J. Bio. Chem. 166, 47 (1948).

[4] A. L Brodskii, B. A. Geller, and R. Yu. Sheinfain, Dokl. Acad. Nauk. 95, 273 (1954).

*In Russian.

[5] A. I. Brodskii, N. A. Vysotskaya, L. I. Kukhtenko, G. P. Miklukhin, L. L. Strizhak, and L. V. Sulima, Coll. Isotopes and Radiation in Chemistry, Izd. AN SSSR, 1958, page 20;* A. E. Brodsky, J. Chim. Phys. 56, 40 (1958).

Received November 3, 1958

*In Russian.

THE SURFACE TENSION OF METALLIC INDIUM

O. A. Timofeevicheva and P. P. Pugachevich

N. S. Kurnakov Institute of General and Inorganic Chemistry USSR Academy of Sciences

(Presented by Academician I. I. Chernaev, October 25, 1958)

The aim of the present work was to study the variation in the surface tension of indium with change in temperature; a knowledge of this relationship is required for the solution of certain problems arising in connection with preparation of semiconducting materials.

The earliest reports on the surface tension of indium are apparently those given in the Liquid Metals Handbook [1]. In this work it is reported that the surface tension of indium in the temperature range 170-250° is equal to 340 dynes / cm.

Melford and Hoar [2] report that they have adopted an improved method involving the use of two capillaries and have found a linear relationship between the surface tension σ of indium and the temperature, within the temperature range from 156 to ~400°

$$\sigma = 574.7 - 0.10\,t, \qquad (1)$$

where t is the temperature in °C.

The difference between the values of σ for indium given in these two works [1, 2] is considerable and amounts to almost 220 dynes /cm at 170°.

The improved method involving the use of two capillaries required the use of an inert gas, while it was assumed that the wetting angle between the molten indium and the material of the capillary was equal to 180° and independent of temperature. This assumption, which is valid only as a first approximation when certain pure metals are being considered, cannot be made in the case where measurements are being made of the surface tension of metallic solutions containing added surface-active materials. For this reason, we have based our measurements of the surface tension of indium and its alloys on the maximum drop pressure method, by which it is not necessary to take into account the wetting angle, and have carried out the studies on the surface tension of indium using gravity apparatus of molybdenum glass under conditions of high vacuum.

The gravity apparatus (see Figure 1) was given a thorough high-temperature treatment under vacuum for many hours, after which approximately 10 cc of molten indium was introduced through the tube E; the apparatus was sealed off while still hot and disconnected from the vacuum assembly, after which it was placed, together with the rotating frame to which it had been previously attached, in an air thermostat fitted with observation windows. When the apparatus was rotated clockwise in the plane of Figure 1 through an angle slightly greater than 90°, the liquid indium from B and C was transferred to the reservoir P. When the apparatus was returned to its original position, the indium began to flow slowly through the capillary f into the manometer tube C, at the same time filling the calibrated capillary F. When the maximum pressure was reached in the drop which formed at the end of the capillary F, drops of indium began to detach themselves. From a knowledge of the radius of the capillary F, the height of the column of liquid indium above the end of the capillary and the density of indium at the temperature in question, it was possible to calculate the surface tension of indium using Cantor's formula [3].

When the surface tension had been measured at different temperatures, the liquid indium was transferred to the vessel D by rotating the apparatus clockwise through an angle of 360° about an axis perpendicular to the plane of Figure 1, after which the apparatus was cooled.

The indium which was studied was 99.995% pure and contained 0.003% Pb, 0.0001% Cd and 0.0001% Zn, together with traces of Cu, Fe, Ge, Ag and Sn. These impurities are either weakly surface-active relative to indium (Pb, Sn, Zn) or surface-inactive (Cd, Fe, Cu, Ge, Ag), so that their presence in small quantities in the indium could have no significant influence on its surface tension.

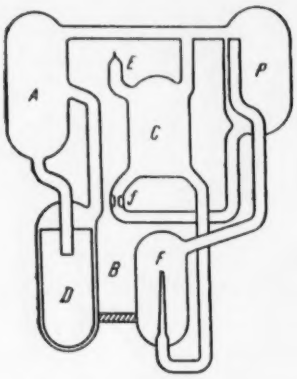

Fig. 1. Gravity apparatus for the measurement of the surface tension of indium.

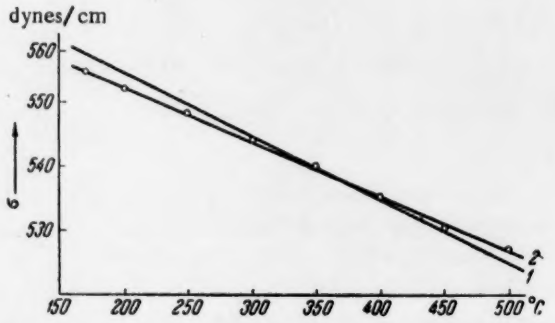

Fig. 2. The surface tension of indium according to the data of Melford and Hoar (1) and according to our data (2).

We have made approximately 500 separate measurements of the surface tension of indium in the temperature range 170-500° and have found that the surface tension is a linear function of the temperature (Figure 2) and may be expressed by the equation

$$\sigma = 569.3 - 0.085\,t, \qquad (2)$$

calculated by the method of least squares.

In order to calculate the surface tension from Cantor's formula it is necessary to know the density of indium at the temperature of the experiment. We did not measure the density of liquid indium, but used the data of Williams and Miller [4].

It can be seen from Figure 2 that our data for the surface tension of indium differs little from the results obtained by Melford and Hoar [2]. If, however, we assume, following the authors of paper [2], that the wetting angle between the wall of the capillary tube and the indium surface inside it is equal to 171° and independent of temperature, then the difference is more significant and amounts to 8-10 dynes/cm at a temperature of 170°.

LITERATURE CITED

[1] R. N. Lyon, Liquid Metals Handbook, Washington, 1952.

[2] D. A. Melford and T. P. Hoar, J. Inst. Metals 85, No. 5, 197 (1956-1957).

[3] M. Cantor, Ann. d. Phys. 47, 399 (1892).

[4] D. D. Williams and R. R. Miller, J. Am. Chem. Soc. 72, 3821 (1950).

Received October 21, 1958

THE CALCULATION OF THE ACIDITY FUNCTION AND MOLECULAR COMPOSITION OF HYDROFLUORIC ACID FROM THE NUCLEAR MAGNETIC RESONANCE DATA FOR F^{19}

E. Z. Utyanskaya, A. U. Stepanyants, M. I. Vinnik and N. M. Chirkov

Institute of Chemical Physics USSR Academy of Sciences

(Presented by Academician V. N. Kondrat'ev, October 29, 1958)

The Hammett acidity function is measured by an indicator method and is equal to

$$\mathcal{H}_0 = -\lg a_{H^+} \frac{f_B}{f_{BH^+}}, \tag{1}$$

where f_B and f_{BH^+} are the activity coefficients of the ionized and un-ionized forms of the indicator, and a_{H^+} is the activity of the protons in the medium in question [1].

The following equilibria are present in aqueous solutions of HF:

$$HF \rightleftarrows H^+ + F^-; \tag{2}$$

$$HF + F^- \rightleftarrows HF_2^-; \tag{3}$$

$$K_1 = a_{H^+} a_{F^-} / a_{HF} \tag{4}$$

$$K_2 = a_{HF_2^-} / a_{HF} a_{F^-}, \tag{5}$$

where $K_1 = 6.89 \cdot 10^{-4}$, $K_2 = 2.695$ are the equilibrium constants expressed in activity units [2].

It follows from equation (4) for the dissociation of hydrofluoric acid that

$$-\lg a_{H^+} = -\lg K_1 + \lg \frac{a_{F^-}}{a_{HF}}. \tag{6}$$

Replacing a_{F^-} by $m_{F^-} f_{F^-}$ (m_{F^-} is the molal concentration of F^- ions) in equation (6), we have:

$$-\lg K_1 - \lg \frac{a_{HF}}{m_{F^-}} = -\lg a_{H^+} f_{F^-} = \mathcal{H}_0 + \lg \frac{f_B}{f_{BH^+} f_{F^-}}. \tag{7}$$

For aqueous solutions of HCl and HBr up to concentrations of 16 molal, the quantity $f_B / f_{BH^+} f_{A^-} = 1$, where f_{A^-} is the activity coefficient of the Cl^- or Br^- anions [3]. If we assume that a similar relationship holds for aqueous solutions of HF, then the acidity function $\mathcal{H}_0$ may be calculated from a knowledge of the values of K_1, a_{HF} and m_{F^-}.

The composition of dilute solutions of HF is known [2]. In order to obtain quantitative data on the composition and acidity of more concentrated aqueous solutions of HF, we have measured the chemical shifts of the resonance of F^{19} in aqueous solutions of hydrofluoric acid at various concentrations.

The observed chemical shift

$$\delta_{obs} = \frac{H_0 \text{ spec} - H_0 \text{ stand}}{H_0 \text{ stand}} \cdot 10^4,$$

where H_0 spec and H_0 stand are the resonance values of the external magnetic field for the F^{19} nucleus in the specimen under study and in the standard [CF_3COOH] at a fixed frequency of a radio-frequency field. The values obtained were used to calculate the chemical shift of each specimen relative to F_2, δ CF_3COOH = $= 5.03 \cdot 10^{-4}$ [5].

For a system of several exchanging components [4], the observed chemical shift

$$\delta_{obs} = \sum \delta_i p_i \qquad (8)$$

where δ_i is the chemical shift of the individual fluorine-containing components and p_i is the fraction of the total number of F^{19} nuclei under study in a given component. The observed chemical shift of the solution depends on the HF concentration [7].

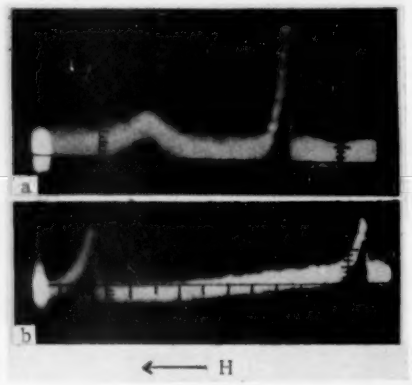

Fig. 1. Oscillograms of the F^{19} signals. The signals on the right are those of the standard CF_3COOH; the signals on the left belong to: a) aqueous KF solution (calibration material), b) 25% HF solution. Amplitude of modulation 0.4 oersteds, frequency of modulation 0.5 cycles/second.

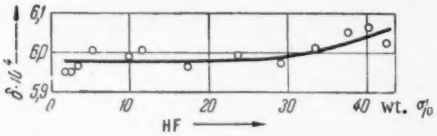

Fig. 2. Chemical shifts of the resonance of F^{19} in the system $HF-H_2O$.

Expressing p_i by the corresponding molal concentrations of the fluorine-containing species, we have

$$\delta_{obs} = \delta_{F^-} \frac{m_{F^-}}{m} + \delta_{HF_2^-} \frac{2m_{HF_2^-}}{m} + \delta_{HF} \frac{m_{HF}}{m}, \qquad (9)$$

$$m = m_{F^-} + 2m_{HF_2^-} + m_{HF}, \qquad (10)$$

where m is the total molal concentration of dissolved HF; m_{HF} is the molal concentration of the un-ionized HF present as monomeric and polymeric forms [6]; δ_{obs} is the chemical shift of the HF solution; δ_{HF} is the chemical shift of the monomeric and polymeric forms, averaged by exchange, and δ_{F^-} = $= 5.48 \cdot 10^{-4}$ [5].

The chemical shift of anhydrous HF relative to F_2 is $\delta_{HF} = 6.25 \cdot 10^{-4}$ [5]. For the want of better data, we assume that this value may also be used for aqueous solutions of HF, although the ratio of monomeric to polymeric forms for aqueous solutions is not the same as that for anhydrous HF. For an HF concentration of 2% by weight, the quantities m_{F^-}, m_{HF_2} and m_{HF} are known [2]; using these data and equation (9) we may calculate the chemical shift of the HF_2^- ion relative to F_2; it is found to be equal to $3.4 \cdot 10^{-4}$. From equations (4) and (5), we have

$$a_{HF} = \frac{1}{K_2} \frac{a_{HF_2^-}}{a_{F^-}} = \frac{1}{K_2} \frac{m_{HF_2^-}}{m_{F^-}} \frac{f_{HF_2^-}}{f_{F^-}}. \qquad (11)$$

It may be assumed that up to a molar ratio HF : H_2O = 1 :1 the activity coefficients of the anions f_{F^-} and $f_{HF_2^-}$ are equal. Then

$$a_{HF} = \frac{1}{K_2} \frac{m_{HF_2^-}}{m_{F^-}}. \qquad (12)$$

Simultaneous solution of the three equations (9), (10) and (12), with the three unknowns m_{F^-}, $m_{HF_2^-}$ and m_{HF}, enables us to calculate the molality of the ions and the undissociated fraction of the acid.

The quantity $\log(a_{HF}/m_{F^-})$ may be written in the form

$$\lg \frac{a_{HF}}{m_{F^-}} = \lg a_{HF} - \lg m + \lg \left\{(\delta_{FH} - \delta_{F^-}) + \right.$$

$$\left. + \frac{a_{HF}}{a_{1HF}} \left[\frac{m_1}{m_{1F^-}} (\delta_{HF} - \delta_{1\,obs}) - (\delta_{HF} - \delta_{F^-}) \right] \right\} - \lg (\delta_{HF} - \delta_{obs}). \qquad (13)$$

The index 1 refers to an HF concentration equal to 2% by weight. The acidity function

$$\mathcal{H}_0 = N + \lg (\delta_{HF} - \delta_{obs}), \qquad (14)$$

where N is a parameter which may be calculated from available data for every hydrofluoric acid specimen studied.

TABLE 1

The Chemical Shifts of the Resonance of F^{19} in Solutions of Hydrofluoric Acid. A) HF concentration, % by weight; m) molal concentration, moles HF/1000 g H_2O; H_0) strength of the main magnetic field, oersteds; δ') chemical shift measured relative to CF_3COOH; ϵ) mean square error in the measurements; δ) chemical shift recalculated relative to F_2

A	m	H_0	$\delta' \cdot 10^4$	$\epsilon \cdot 10^4$	$\delta \cdot 10^4$	A	m	H_0	$\delta' \cdot 10^4$	$\epsilon \cdot 10^4$	$\delta \cdot 10^4$
2,00	1,02	3347	0,92	0,011	5,95	23,7	15,5	3330	0,96	0,005	5,99
2,46	1,26	3342	0,92	0,005	5,95	28,8	20,3	3347	0,94	0,006	5,97
3,57	1,85	3342	0,93	0,010	5,96	33,4	25,1	3322	0,98	0,007	6,01
5,57	2,95	3329	0,98	0,011	6,01	37,7	30,2	3330	1,02	0,010	6,05
10,0	5,56	3342	0,96	0,007	5,99	40,3	33,8	3322	1,03	0,004	6,06
11,5	6,51	3322	0,98	0,005	6,01	42,5	37,0	3330	0,99	0,005	6,02
17,3	10,5	3347	0,94	0,008	5,97						

TABLE 2

The Molecular Composition and Acidity Function of Hydrofluoric Acid Solutions (m in moles per 100 g H_2O)

m	a_{HF} (*)	m_{F^-}	$m_{HF_2^-}$	m_{HF}	$\mathcal{H}_0 + \lg \frac{f_B}{f_{BH^+} f_{F^-}}$	$\mathcal{H}_0$ **
1,016*	1,05	0,0168*	0,0506*	0,898*	+1,37	+1,30
1,26	1,36	0,0175	0,064	1,11	+1,27	+1,22
1,85	2,05	0,0166	0,092	1,65	+1,07	+1,04
2,95	3,43	0,0132	0,122	2,69	+0,75	+0,72
5,56	7,26	0,0129	0,252	5,04	+0,41	+0,36
6,51	8,88	0,0114	0,273	5,95	+0,27	+0,25
10,5	17,4	0,0110	0,515	9,46	−0,04	−0,16
15,5	33,6	0,0078	0,706	14,1	−0,47	−0,63
20,3	57,3	0,0065	1,00	18,3	−0,78	−1,00
25,1	82,5	0,0048	1,07	23,0	−1,07	−1,34
30,2	16,0	0,0025	1,08	28,0	−1,64	−1,69
33,8	268	0,0016	1,16	31,5	−2,06	−1,91
37,0	380	0,0015	1,54	33,9	−2,24	−2,08

*See [2]

**See [9]

It can be seen from Table 1 that δ_{obs} is of the order of $(5.95\text{-}6.05) \cdot 10^{-4}$ for various concentrations of hydrofluoric acid. From this it follows that in order to obtain a value for the acidity function with an accuracy of $\pm$ 0.05, δ_{obs} must be known with an accuracy of $\pm\ 0.03 \cdot 10^{-4}$.

The measurements were carried out in a field of ~3300 oersteds. The uniformity of the magnetic field in the working part of the gap was not poorer than $\Delta H/H = 2 \cdot 10^{-6}$ in a volume of 1 cc.

The nuclear magnetic resonance signal was observed using an autodyne detector [8]. A serrated modulation of the main magnetic field was used for the measurements.

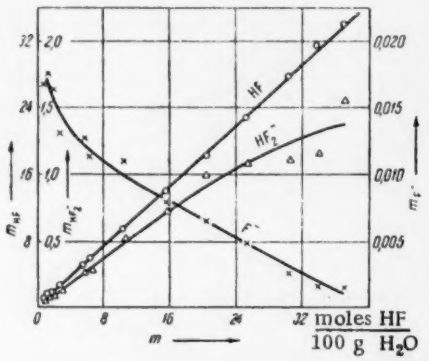

Fig. 3. The variation in the molal concentration of the ions $m_{HF_2^-}$ and m_{F^-} and of the undissociated fraction of the acid m_{HF} with change in the total molal concentration m of dissolved HF.

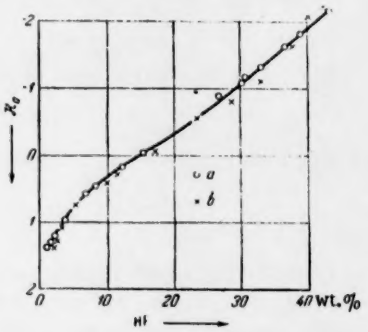

Fig. 4. The relationship between the acidity function $\mathcal{H}_0$ for hydrofluoric acid and the concentration: a) values obtained from measurements using the indicator method (Bell's data); b) values calculated from nuclear magnetic resonance data.

The measurements were carried out using spectroscopically pure hydrofluoric acid containing no silicon. The measurments were made at room temperature. The total systematic error in the measurements of the chemical shifts amount to 2% ($\Delta(\Delta H/H) = 2 \cdot 10^{-6}$). The results of the measurements are given in Table 1 and Figure 2. It can be seen from Figure 2 that the change in the chemical shifts with concentration (up to 30%) lies within the limits of the experimental error.

Table 2 and Figures 3 and 4 give the results of the calculation of the molecular composition and the value of $\mathcal{H}_0 + \log \frac{f_B}{f_{BH^+} f_{F^-}}$ for the hydrofluoric acid solutions studied, together with values for the acidity function $\mathcal{H}_0$ measured by the indicator method at 25° [9]. It can be seen from the data in Table 2 that the quantities $\mathcal{H}_0 + \log \frac{f_B}{f_{BH^+} f_{F^-}}$ and $\mathcal{H}_0$ coincide satisfactorily. This means that in the concentration range studied (up to 37 molal) the relationship $f_B / f_{BH^+} f_{F^-} = 1$ is valid.

LITERATURE CITED

[1] A. I. Shatenshtein. The Theory of Acids and Bases, 1949.*

[2] K. Elmore, I. D. Hatfield, C. M. Mason, and A. D. Jones, J. Am. Chem. Soc. 71, 2710 (1949).

[3] M. I. Vinnik, R. N. Kruglov, and N. M. Chirkov, Zhur. Fiz. Khim. 30, No. 4, 827 (1956).

[4] H. S. Gutowsky, and A. Saika, J. Chem. Phys. 21, 1688 (195).

[5] H. S. Gutowsky and C. J. Hoffman, J. Chem. Phys. 19, 1259 (1951); 20, 200 (1952).

[6] J. H. Simons, Fluorine Chemistry, N. Y. (1950).

*Original Russian pagination. See C.B. Translation.

[7] P. M. Borodin and F. I. Skripov, Fizich. Sborn. L'vovsk. Univ., No. 3 (8), 78 (1957).

[8] L. L. Dekabrun, Some Problems in Engineering Physics, No. 2, 85 (1957).

[9] R. P. Bell, K. N. Bascombe, and J. C. Mc Cowbrey, J. Chem. Soc. 1956, 1286.

Received October 22, 1958

THE INFLUENCE OF ADDED ALKALI METAL COMPOUNDS ON THE KINETICS OF THE REDUCTION OF ZINC SILICATE BY CARBON MONOXIDE

Corresponding Member AN SSSR D. M. Chizhikov and L. G. Berezkina

A. A. Baikov Institute of Metallurgy, USSR Academy of Sciences

In studies of the reduction of solid oxides by carbon it has been observed that the addition of compounds of the alkali metals has an accelerating effect on the process. Thus, D. N. Klushin and D. M. Chizhikov [1] have established that the addition of sodium carbonate has an accelerating influence on the reduction of zinc oxide by solid carbon. The reduction of zinc oxide takes place in two stages, the rate of the process being determined by the rate of the gasification process: $C + CO_2 = 2CO$. Workers in this field have attributed the observed acceleration to an increase in the reactivity of graphite toward gasification in the presence of added alkali metals. It is also possible, however, that these added materials have a direct effect on the reduction by the carbon monoxide. In this case the accelerqtion of the process may be due to an increase in the mobility of the particles in the reaction zone in the presence of the added materials, which facilitates the crystallochemical rearrangement of the lattice of the compound [2, 3].

The present work presents the results of a study of the kinetics of the reduction of zinc silicate $2ZnO \cdot SiO_2$ by carbon monoxide and of an examination of the effect on this process shown by the addition of the carbonates of potassium, sodium and lithium and also of sodium and calcium chlorides. It should be noted that the literature contains no data on the kinetics of the reduction of zinc silicate by carbon monoxide.

The zinc silicate was prepared by sintering purified quartz powder with zinc oxide at a temperature of 1380-1400°. The added materials were introduced by impregnation from aqueous solutions in quantities amounting to 7.5 mole % relative to the zinc silicate, which corresponds to concentrations of added materials in the mixture of from 2 to 5% by weight. The solid taken for reduction had a particle size of 200 mesh. The reduction was carried out in a vacuum assembly; the carbon monoxide was circulated continuously and the CO_2 produced in the reaction was frozen out using liquid nitrogen [4]. The course of the process was followed from the loss in weight of the original specimen which was weighed continuously on an electromagnetic balance. The readings were recorded and the temperature and pressure controlled automatically. Preliminary experiments showed that the degree of reduction is independent of the weight of the original sample taken.

Figure 1 gives data showing the influence of temperature on the kinetics of the reduction of zinc silicate by carbon monoxide. The rate of reduction becomes appreciable (3% per hour) at 1000°. Increase in temperature increases the rate of reduction considerably. Within the limits of the degree of reduction studied, the rate of the process is practically constant, and the kinetics of the reaction are given approximately by the linear equation $a = kt$. The apparent activation energy of the process amounts to 31 kcal/mole. The carbon monoxide pressure (within the range 50-400 mm mercury) has no influence on the degree of reduction of the zinc silicate.

Figure 2 gives data on the reduction of $2ZnO \cdot SiO_2$ with potassium carbonate added. It can be seen that in the presence of potassium carbonate the temperature at which the process starts is reduced considerably, while the degree of reduction of the zinc silicate is increased. 10% reduction takes place at 700° in 90 minutes, whereas when $2ZnO \cdot SiO_2$ is reduced without added material at 1000°, the degree of reduction after the same time

interval is only 5%. The apparent activation energy of the process, calculated from the rate constants of the equation $\alpha = 1 - \exp(kt^n)$, amounts to 17 kcal/mole. The rate of reduction of zinc silicate in the presence of potassium carbonate is increased considerably by increasing the pressure. Thus at 1000° and P_{CO} = 10 mm mercury, 9.5% zinc silicate is reduced in the first 10 minutes, at 50 mm 15.5% and at 200 mm 22%. At 200 and 400 mm mercury the kinetics of the process are given by a single curve, which characterizes the onset of adsorption saturation. Figure 3 gives comparative data showing the influence of a number of added materials on the rate and degree of reduction of $2ZnO \cdot SiO_2$ at 1000° and P_{CO} = 200 mm mercury. The rate of reduction of zinc silicate (at 10% reduction), when K_2CO_3 is added, is increased by a factor of 150; when Na_2CO_3 is added, by a factor of 25; when Li_2CO_3 is added, by a factor of 5; and when NaCl and $CaCl_2$ are added, by a factor of 1.5. The addition of potassium and sodium carbonates alters the kinetic characteristics of the reduction curves; the process starts at a maximum rate which decreases rapidly as the process continues.

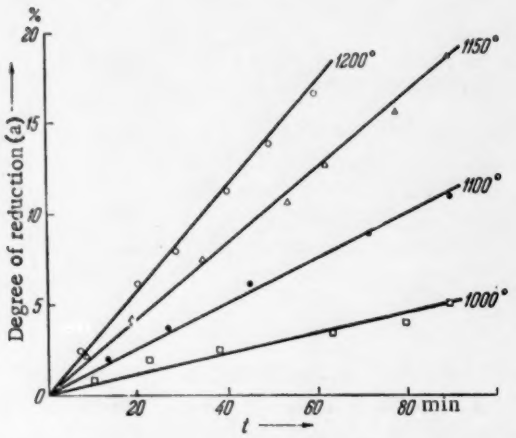

Fig. 1. Kinetics of the reduction of zinc silicate by carbon monoxide: a) degree of reduction, %; t) time, min.

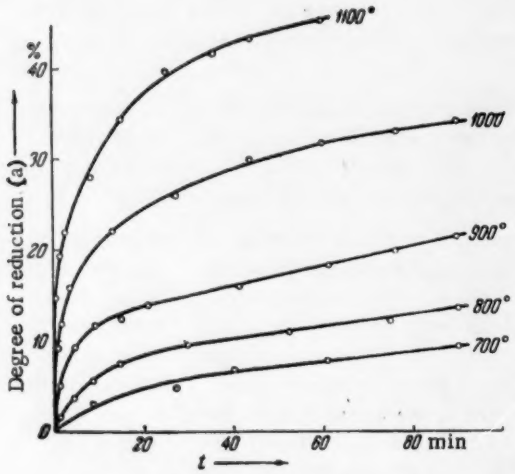

Fig. 2. Kinetics of the reduction of zinc silicate with potassium carbonate added, P_{CO} = 200 mm mercury: a) degree of reduction, %; t) time, min.

The cause and mechanism of the specific effect shown by the different added materials is possibly explained as follows. The added materials may undergo a number of changes in the course of the reduction process. Dissociation of the carbonates takes place at the temperatures of the experiment. The oxides of the alkali metals exhibit an appreciable volatility; in the vapor state they may be adsorbed on the surface of the silicate. The adsorption of the oxides on the reaction surface may possibly lead to the formation of lattice defects and the production of active centers for the reaction. The increase in the activity of the surface explains the positive influence of increase in the pressure on the process of silicate reduction in the presence of potassium carbonate. The electronic interaction between the adsorbed compounds and the ions of the surface layers of the lattice may lead to an increase in the surface mobility (migration) of the ions, which facilitates the crystallochemical changes taking place during the reduction [5].

The accelerating effect of added carbonates decreases along the series: potassium, sodium and lithium. The specific character of the effect of the added materials may be due to differences in the electronic interaction between the added material and the silicate lattice. The chemical bond energy in the alkali metal oxides, for example, increases from potassium to lithium, as is indirectly reflected by the increase in the heats and free energies of formation of the oxides. The heats of formation of the alkali metal oxides are: for K_2O 86.0, for Na_2O 102.0 and for Li_2O 142.3 kcal/mole. It is thus evidently possible that the electronic interaction between added potassium ion and the silicate lattice is greater than the corresponding interaction for sodium and lithium ions.

In the examination of the effect of added materials, it is necessary to take into account the fact that the oxides of potassium, sodium and lithium should react with zinc silicate at the temperature of the experiment. The accelerating effect of potassium and sodium carbonates is shown for the most part in the initial

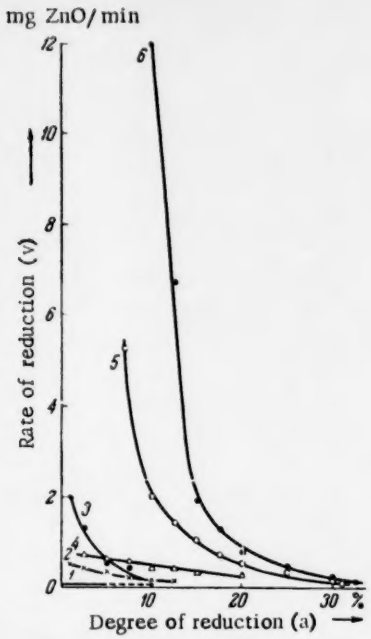

Fig. 3. The influence of added materials on the kinetics of the reduction of zinc silicate at 1000° and P_{CO} = 200 mm mercury: v) rate of reduction, mg ZnO/min; a) degree of reduction. 1) $2ZnO \cdot SiO_2$, 2) $2ZnO \cdot SiO_2 + NaCl$, 3) $2ZnO \cdot SiO_2 + CaCl_2$, 4) $2ZnO \cdot SiO_2 + Li_2CO_3$, 5) $2ZnO \cdot SiO_2 + Na_2CO_3$, 6) $2ZnO \cdot SiO_2 + K_2CO_3$.

stages of the reaction, after which the rate of the process decreases. This change in the nature of the curves with the passage of time may be due to the fact that the added materials become chemically bound. Thus when zinc silicate containing added potassium carbonate is ignited beforehand in an inert atmosphere, the increase in the rate of subsequent reduction of the silicate is much less pronounced.

The results obtained shown that it is possible to accelerate considerably the rate of indirect reduction by the addition of small quantities of alkali metal compounds, particularly sodium and potassium carbonates. The addition of these materials facilitates considerably the process of reduction, lowering the activation energy and the temperature at which the reaction starts. Some views have been put forward regarding the mechanism of the observed phenomena.

LITERATURE CITED

[1] D. N. Klushin and D. M. Chizhikov, Sborn. Tr.Gos. Inst. Tsvetn. Met. 8, 34 (1953).

[2] P. V. Gel'd, O. A. Esin and N. N. Serebrennikov, Tr. Ural'sk. Politekhn. Inst. 49, 61 (1954).

[3] N. V. Mukhin and V. V. Mikhailov, ibid., 49, 159 (1954).

[4] D. M. Chizhikov and G. G. Gvelesiani, Zav. Lab., No. 4 (1956).

[5] A. Rees, The Chemistry of the Defect Solid State, London, 1954.

Received November 5, 1958.

THE DETERMINATION OF THE INTERNAL STRESSES PRODUCED WHEN SOLID SURFACES ARE GLUED TO ONE ANOTHER

S. A. Shreiner and P. I. Zubov

L. Ya. Karpov Physicochemical Scientific Research Institute
Institute of Food Industry Technology, Leningrad

(Presented by Academician V. A. Kargin, August 16, 1958)

In our studies on the adhesive properties of gelatin solutions, we have established that the strength of adhesion is related to the conditions under which the layers of adhesive are produced. We have suggested that this relationship is determined by various internal (shrinkage) stresses, which reduce the strength of adhesion [1]. In this connection particular interest has been attached to methods for the quantitative estimation of the magnitude of the internal stresses.

V. A. Kargin and co-workers have recently shown [2] that when a layer of adhesive is formed on a flexible support, the internal stresses may be determined from the change in shape of the support. The stresses in transparent isotropic films produced on solid surfaces may be determined using an optical method [3] which enables the magnitude of the internal stresses to be estimated from the change in the optical properties of the films and from the magnitude of the resultant birefringence in particular.

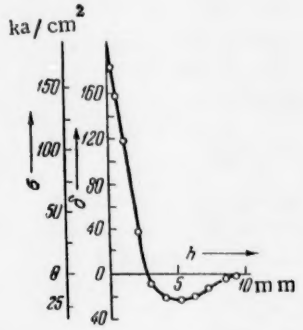

Fig. 1. The change in the path difference δ and in the internal stresses σ in the prism layers with change in the distance h of the layers from the face on which the film was produced; film thickness 0.22 mm, produced from 20% gelatin solution.

It is extremely difficult, however, to measure birefringence in nontransparent films. We have suggested that these difficulties might be overcome by using a support made of a transparent isotropic material with elastic properties. In this case the magnitude of the internal stresses in the films might be estimated from the change in the birefringence within the support, i.e., beyond the limits of the zone in which the layer of adhesive or adhesive film is produced. The present studies were arranged and carried out on the basis of this suggestion.

The supports used were rectangular glass prisms with dimensions 10 × 20 × 20 mm. The films were formed on the surface of the support by the evaporation of water from a 20% gelatin solution deposited on one of the faces of the prism. The birefringence in the thickness of the glass was measured using a polarizing microscope with rotating calcite KPK compensator. The magnitude of the internal stresses was determined from a displacement scale constructed on the basis of preliminary measurements of the path difference in the prisms under various loads between 10 and 120 kg / cm².

Preliminary experiments showed that when a gelatin film is formed on the surface of a glass prism a path difference is in fact produced in the thickness of the prism. It can be seen from Figure 1 that the path difference is not distributed regularly within the separate layers of the prism. The largest path difference is found, as might have been expected, in the layers lying next to the surface of the glass – film interface. As the distance

between the glass layer and the surface of the interface increases, the path difference decreases linearly and reaches zero at a distance h ≅ 3. When h is increased further, the curve becomes more complex in character.

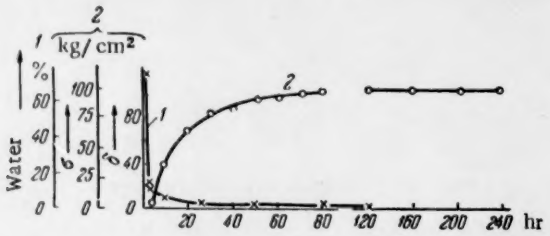

Fig. 2. The kinetics of drying (1) and the kinetics of the production of internal stresses σ and path difference δ (2) at the glass–gelatin interface; film produced from 20% gelatin solution by evaporation of the solvent.

From these data it may be concluded that by extrapolation of the path difference of h = 0 we may find the integral value of the birefringence (path difference) and consequently the magnitude of the internal stress in the support, which changes with change in the internal stress in the film.

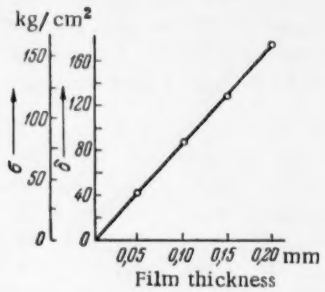

Fig. 3. The influence of film thickness on the path difference δ and on the internal stresses σ at the contact surface, produced during the formation of films 20% gelatin solution.

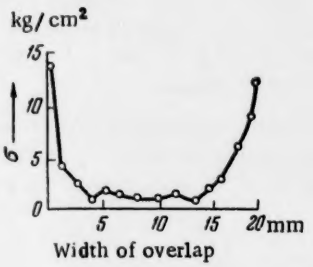

Fig. 4. Variation in the internal stresses σ with change in the width of overlap of specimens glued together with 20% gelatin solution.

Since the processes of growth and relaxation of the internal stresses in the adhesive layer and in the elastic transparent support are related symbatically to one another, measurement of the birefringence in the support may also be used to follow the change in the stresses within the growing films with change in the time of evaporation of the water (Figure 2), in the film thickness (Figure 3), in the width of the overlap of two glass surfaces stuck together (Figure 4), etc.

The present work thus presents a suggested method for the determination of the magnitude of the internal stresses in films formed on solid transparent isotropic supports; the method is based on the measurement of the birefringence beyond the limits of the zone in which the layer of adhesive is produced, and it has been shown that this method may be used to determine both the total magnitude of the internal (shrinkage) stresses and the kinetics of their growth.

We have to express our gratitude to Academician V. A. Kargin for a number of valuable observations made during discussion of the present work.

LITERATURE CITED

[1] S. A. Shreiner and P. L. Zubov, Koll. Zhurn. 5, 651 (1957).*

*Original Russian pagination. See C.B. Translation.

[2] M. L. Karyakina, V. A. Kargin, and T. L. Sogolova, Khim. Prom. 5, 265 (1957).

[3] A. V. Stepanov, Zhur. Tekh. Fiz. 2, 205 (1949).

Received August 6, 1958

GASEOUS INITIATION WITH OZONE IN THE OXIDATION OF ISODECANE AND ITS ASSOCIATED CHEMILUMINESCENCE

R. F. Vasil'ev, O. N. Karpukhin, V. Ya. Shlyapintokh and
Acad. Sci. USSR Corresponding Member N. M. Émanuél'
Institute of Physical Chemistry, Academy of Sciences of the USSR

The oxidation of hydrocarbons in the liquid phase represents a chain process with a degenerate branching of the chains [1]. A gradual accumulation of the branching agent (peroxide) in the system leads to a slow increase in the reaction rate. For this reason the stage of a rapid progress of reaction precedes, as a rule, the period of induction, lasting many hours in a number of cases. One of us had shown [2] that brief stimulations of the reaction at the very start of oxidation prove to be sufficient to shorten effectively the induction period. As initiating agents it is possible to use salt catalysts, chemically active gases and penetrating radiations [3].

It was observed that in a number of cases [3] the prolonged action of an initiator leads to negative results: to a reduction in the reaction rate and extent of conversion, the appearance of large amounts of secondary products in the system, etc. For these reasons it proved expedient to use gas initiators (nitrogen dioxide, ozone, chlorine, etc.), since the action of a gas initiator can be stopped when desired by simply terminating its addition to the system. Especially promising here is the use of ozone, since both a minimum amount of secondary products and the powerful action of this exceptionally active gas could be expected to derive from such use.

The gas initiation of the oxidation of a n-paraffin by means of ozone was studied in [4].

In this paper our objective was to study the isolated stage of initiation using ozone, i.e., to study those phenomena and processes that occur during the period of a brief exposure to the action of the initiator.

As study subject we selected isodecane (2, 7-dimethyloctane). Preliminary experiments had revealed that brief blowing of ozone through the system greatly accelerates reaction. The experiments were run at low temperature (from 26 to 90°) in order not to complicate the kinetic picture of the phenomena by secondary processes.*

In selecting the method of study we considered the fact that many reactions involving ozone are accompanied by chemiluminescence [5]. Since chemiluminescence arises due to the progress of elementary chemical processes in the system, a study of this phenomenon permits judging as to the reaction mechanism. We were able to register the appearance of a slight luminescence when oxygen, containing 2-3% of ozone, was bubbled at 20-90° through isodecane, contained in a glass oxidation cell. A FEU-19 photoamplifier served as the luminescence indicator. The photoelectric current was recorded using an EPPV-51 electron potentiometer with a high ohmic input.

A record of the change in the intensity of luminescence when ozone was blown continuously into isodecane at 55° is shown in Fig. 1. The intensity gradually increases, reaches a maximum in 2.5 hours, and then gradually decreases.

*The oxidation of isodecane proceeds quite rapidly at 110-120°.

It was established that termination of ozone addition at any stage of reaction leads to an immediate disappearance of luminescence. A rapid restoration of the previous intensity occurs when the addition of ozone is resumed. These results can be understood if it is assumed that luminescence arises in the reaction of ozone with the compound that, in turn, had previously been formed in the reaction of ozone with the hydrocarbon.

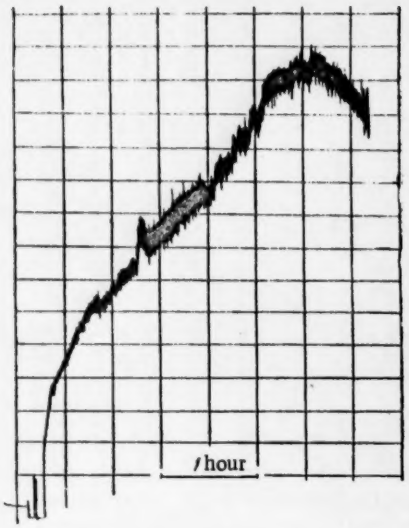

Fig. 1. Record of the photoelectric current of the photoamplifier when ozonized (2.5%) oxygen is bubbled continuously through isodecane at 55°.

The existence of an intensity extreme during the experiment indicates that the concentration of the hypothetical compound passes through a maximum, i.e., the accumulation rate of this compound coincides with the accumulation rate of the intermediate product in succeeding chemical reactions. The final reaction product, containing active oxygen, is formed at an accelerated rate at the start, which is also characteristic for the succeeding reactions (Fig. 2). Another possible reason for the autoacceleration is the branching action exerted by the products formed, leading to a progressive growth of the chain avalanche, which is not suitable, since in our experiments the temperature is slightly too low to permit chain growth.

Further proof of the intermediate character of the product obtained in the initial reaction of the

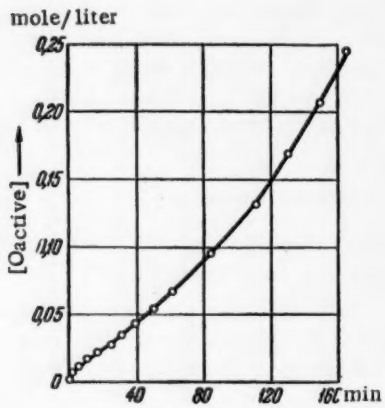

Fig. 2. Accumulation of active oxygen in the continuous ozonization of isodecane at 20°.

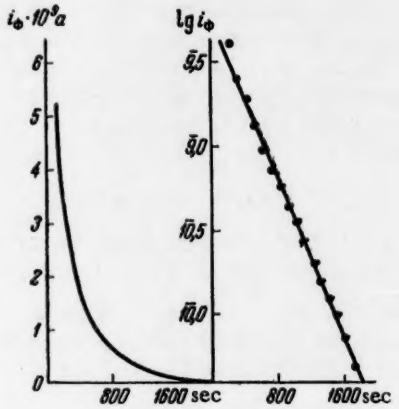

Fig. 3. Decomposition of the intermediate product, accompanied by luminescence, at 80°. Left – record of the photoelectric current. Right – semilogarithmic anamorphosis of the curve.

hydrocarbon with ozone was secured by us in the experiments run at elevated temperature. Isodecane, ozonized for 2-3 hours at room temperature, was rapidly heated to 80-85° in the absence of both oxygen and ozone. The photoamplifier registered a rapid blazing up of the luminescence and then its gradual diminution according to the monomolecular rule (Fig. 3) with constant $k = 2.5 \cdot 10^{15} e^{-29000/RT}$ sec^{-1}. Considering that the final reduction product – the hydroperoxide – does not decompose at the indicated temperatures, we ascribe this phenomenon to the thermal decomposition of the intermediate product.

As a result, the reaction of ozone with normal hydrocarbons at moderate temperatures represents a complex process, proceeding through the formation of a relatively stable intermediate compound.

LITERATURE CITED

[1] N. N. Semenov, Chain Reactions [in Russian], 1934.

[2] N. M. Émanuél', Proc. Acad. Sci. USSR 102, No. 3, 559 (1955).

[3] N. M. Émanuél', Bull. Acad. Sci. USSR, Div. Chem. Sci. 1957, 1298.*

[4] É. A. Blyumberg, V. G. Voronkov and N. M. Émanuél', Bull. Acad. Sci. USSR, Div. Chem. Sci. 1959, No. 1, 24.*

Received October 29, 1958

*Original Russian pagination. See C.B. Translation.

ROLE OF THE TUNNEL EFFECT IN THE KINETICS OF CHEMICAL REACTIONS AT LOW TEMPERATURES

V. I. Gol'danskii

P. N. Lebedev Physical Institute, Academy of Sciences of the USSR

(Presented by Academician V. N. Kondrat'ev, November 6, 1958)

Even in the studies of D. G. Bourgin and of S. Z. Roginskii and L. Rozenkevich [1], and also in a number of papers by R. Bell [2], the question of the possible role of the tunnel effect in chemical kinetics was raised. However, attempts to reveal experimentally such a role at temperatures close to room temperature failed to give well-defined results, while the region of extremely low temperatures, where the tunnel effect should be manifested more clearly, remained completely unstudied for a long time. Only recently has interest arisen in studying all of the possible chemical reactions that progress at low temperature, in which connection methods have been developed which make it possible to observe experimentally the progress of such reactions even at extremely slow rates (for example, the method of labeled atoms, that of paramagnetic resonance, etc.). In connection with this it seems expedient to list here the criteria that characterize the demarcation of the region of high temperatures, where the tunnel effect can be neglected, and the low-temperature region, where the role of the tunnel effect proves to be extremely important. It also seems desirable to discuss the problem of how strongly the temperature dependence of the reaction rate in the low-temperature region is influenced by the shape and width of the activation barrier and by the effective mass transferred via tunnel transition. An analysis of this problem will help in the future to establish the basic characteristics of activation barriers based on the experimental data obtained relative to the effect of temperature and the influence of the isotopic composition on the rate of chemical reaction in the low-temperature region.

The role of the tunnel effect in the progress of chemical reactions is determined by the interrelationship of three energy terms, and specifically: the energy of activation E_0, the energy of heat motion kT (T is the absolute temperature, and $k = 1.4 \times 10^{-16}$ erg/deg is the Boltzmann constant) and the "characteristic" energy of the system $\epsilon = \hbar^2/\mu d^2 = 1.11 \cdot 10^{-54}/\mu d^2$ erg (μ is the given mass, and $\underline{d}$ is the effective half-width of the activation barrier). We will introduce two dimensionless parameters, characterizing the ratios E_0, kT and ϵ: $\kappa = E_0/kT$ and $a = \pi \sqrt{2}\sqrt{E_0/\epsilon}$ (as a rule, $a \gg 1$). We further assume that the reacting particles show Maxwellian distribution in their rates of motion. Then the rate constant for the reactions in which the tunnel effect plays a role should be written in the form

$$K = \frac{2\sqrt{2\pi}\,R^2}{\sqrt{\mu}\,(kT)^{3/2}}\,(E_0)^2 \int_0^\infty y w(y)\, e^{-\kappa y}\, dy, \qquad (1)$$

where $y = E/E_0$; E is the energy of the relative motion of the particles; $R = r_1 + r_2$ is the sum of the radii of the reacting particles (for preciseness we will discuss the bimolecular reaction); and w(y) is the probability of tunnel permeability through the activation barrier ($y < 1$) or its passage over this barrier ($y > 1$).

As a simple and at the same time a quite general two-parametric expression for a symmetrical activation barrier we will adopt the following:

$$U(x) = \frac{E_0}{\mathrm{ch}^2(x/d)}, \qquad (2)$$

where $\underline{x}$ is a coordinate, read on both sides of the barrier center (shown by Curve 1 in Fig. 1).

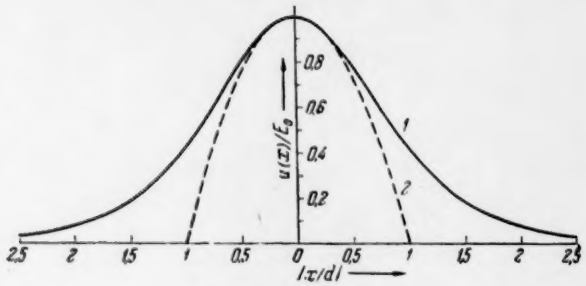

Fig. 1.

At small values of x/d equation (2) passes to the form obligatory for any symmetrical arch near the maximum of the parabolic function

$$U(x) \approx E_0\left(1 - \frac{x^2}{d^2}\right), \tag{3}$$

and in the future we will compare the results ensuing from equation (2) and those obtained in the extreme and clearly unreal case of a completely (clear up to x/d = 1) parabolic barrier (Curve 2 in Fig. 1). For both types of barriers (in accordance with (2) and (3)), with the accuracy up to the factor ranging from 1 to 2, it is possible to take $w(y > 1) = 1$ and to consider the rate constant as the sum of the ordinary Arrhenius constant

$$K_{\text{Arrhen}} = \frac{2\sqrt{2\pi}\,R^2}{\sqrt{\mu}\,(kT)^{3/2}} E_0^2 \int_1^\infty y e^{-\varkappa y}\,dy = \frac{2\sqrt{2\pi}\,R^2\sqrt{kT}}{\sqrt{\mu}}(1+\varkappa)e^{-\varkappa} \tag{4}$$

and the constant of the tunnel reaction

$$K_{\text{tunnel}} = \frac{2\sqrt{2\pi}\,R^2}{\sqrt{\mu}\,(kT)^{3/2}} E_0^2 \int_0^1 y w(y) e^{-\varkappa y}\,dy. \tag{5}$$

For a barrier described by (2) the probability of tunnel permeability is written [3] in the form

$$w(y) = \frac{\operatorname{sh}^2 a\sqrt{y}}{\operatorname{sh}^2 a\sqrt{y} + \operatorname{ch}^2\left[\frac{\pi}{2}\sqrt{4\frac{a^2}{\pi^2} - 1}\right]} \approx \frac{e^{2a\sqrt{y}}}{e^{2a\sqrt{y}} + e^{2a}} \tag{6}$$

(the last approximations are valid in the region $\sqrt{y} \gg 1/a$).

As a result, the subintegral function in expression (5) for K_{tunnel} has the form

$$f(y) \approx \frac{y e^{2a\sqrt{y}} e^{-\varkappa y}}{e^{2a\sqrt{y}} + e^{2a}} \approx \text{const} \cdot e^{2a\sqrt{y} - \varkappa y} \tag{7}$$

and converts to a maximum at

$$y = y_m \approx \left(\frac{a}{\varkappa}\right)^2 = 2\pi^2 \frac{kT}{\varepsilon}\frac{kT}{E_0}. \tag{8}$$

A substantial contribution by the tunnel effect to the total reaction rate is observed when the maximum of the function f(y) falls in the region of subbarrier energies ($y_m < 1$), i.e., in the given case when $\varkappa > a$.

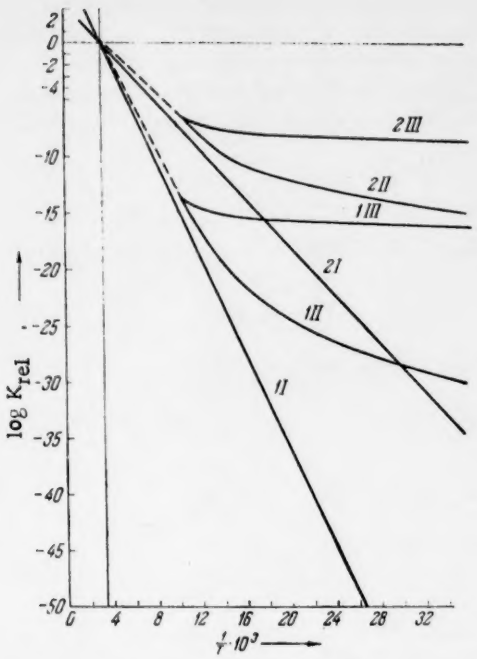

Fig. 2. 1) a = 50; 2) a = 25; I) Arrhenius rule; II) and III) taking the tunnel effect into account: II) barrier with shape $1/\mathrm{ch}^2(x/d)$, III) parabolic barrier.

In the case of a completely parabolic barrier [2] the probability of tunnel permeability is $w_1(y) = e^{-a(1-y)}$, while the subintegral function in (5) assumes the form

$$f_1(y) = ye^{-a}e^{(a-\varkappa)y}. \qquad (9)$$

It is evident that the condition $y_m = \frac{1}{\varkappa - a} < 1$, i.e., $\varkappa > a + 1$ corresponds now to the presence of a maximum for the subintegral function in the limits of the activation barrier. However, since $a \gg 1$, then in the case of a completely parabolic barrier the condition for a substantial contribution by the tunnel effect can be written as $\varkappa > a$. Consequently, the characteristic temperature T_q, below which the tunnel effect plays an important role, is determined, practically independent of the shape of the barrier, by the relationship

$$T_q = \frac{E_0}{ak} = \frac{V\overline{\varepsilon E_0}}{k\pi\sqrt{2}} = \frac{\hbar V\overline{E_0}}{k\pi d\sqrt{2\mu}}. \qquad (10)$$

For the value of the tunnel reaction constant in the region $T < T_q$, with barrier of type (2), we obtain by the transposition method

$$(K_{\text{tunnel}})_{T<T_q} \approx \frac{2\sqrt{2\pi}R^2\sqrt{kT_q}}{\sqrt{\mu}} 2\left(\frac{T}{T_q}\right)^2 a^{3/2} e^{-a} e^{-a(1-T/T_q)} \qquad (11)$$

i.e., instead of the usual linear (accurate up to the pre-exponent) function $\ln K = A - E/kT$, another function appears here: $(\ln K_{\text{tunnel}})_{T<T_q} = B + aT/T_q$. At $T = T_q$ in the given case $(K_{\text{tunnel}})_{T_q} \approx 2\sqrt{a}(K_{\text{Arrhenius}})_{T_q}$, while at $T \approx 3/2T_q$ both rate constants become equal, and in the region of higher temperatures the tunnel effect can be disregarded completely.

In the case of a parabolic barrier [2] in the region $T < T_q$

$$(K_{1\text{tunnel}})_{T<T_q} \approx \frac{2\sqrt{2\pi}R^2\sqrt{kT_q}}{\sqrt{\mu}} \frac{\sqrt{T/T_q}}{(1-T/T_q)^2} e^{-a} \times$$
$$\times \left\{1 - e^{-a(T/T_q-1)}\left[1 + a\left(\frac{T}{T_q} - 1\right)\right]\right\}, \qquad (12)$$

and at $\varkappa \gg a$, i.e., $T/T_q \ll 1$, the rate constant, with an accuracy up to the pre-exponential factor, ceases to depend on the temperature.

At $T \gtrsim T_q$ the expressions for the tunnel reaction constant in the two discussed cases of barrier shapes practically coincide.

To illustrate quantitatively the equations given above we have plotted in Fig. 2 the functions $\log K = f(1/T)$ in the temperature region 28-500° K (in which connection we took K = 1 at 300° K) for a = 50 and a = 25. As can be seen from (11) and (12) giving parameter a completely determines the nature of the dependence of K on T/T_q. For preciseness in Fig. 2 it is assumed that $T_q = 100°$ K; then $E_0 = 10{,}000$ cal/mole and $\epsilon = 5.6 \times 10^{-15}$ erg correspond to a = 50, and $E_0 = 5000$ cal/mole and $\epsilon = 1.12 \times 10^{-14}$ erg correspond to a = 25. At higher values of E_0 and ϵ the whole picture in Fig. 2 is shited toward higher temperatures.

In conclusion it should be emphasized that we did not discuss here the quite pronounced temperature fluctuations of the pre-exponent possible in the case of complex molecules. Experimental verification and use of the obtained equations to determine the shape and other characteristics (μ, d) of activation barriers is most conveniently done for specifically those reactions where the pre-exponent is abnormally large, and which consequently proceed at measurable speed even at very low temperatures. In the future a study of the tunnel effect at low temperatures should not be made for those cases where instead of a Maxwellian distribution the original system shows various quantum distributions of the energy.

LITERATURE CITED

[1] D. G. Bourgin, Proc. Natl. Acad. Sci., Washington, No. 15, 357 (1929); S. Z. Roginskii and L. Rozenkevich, Z. physik. Chem., Abt. B, 10, 47 (1930).

[2] R. Bell, Proc. Roy. Soc., A 139, 466 (1933); 148, 241 (1935); 158, 128 (1937).

[3] L. D. Landau and E. M. Lifshits, Quantum Mechanics [in Russian] (Moscow, 1948).

Received October 15, 1958

EFFECTIVE RADIUS OF THE ELECTRON IN CRYSTAL LATTICES

Acad. Sci. USSR Corresponding Member A. F. Kapustinskii

D. I. Mendeleev Institute of Chemical Technology (Moscow)

The dimensions of the electron were determined later and with less accuracy than either its charge or its mass, since the latter values have a greater constancy and possess greater importance in both physics and chemistry. It is well known [1] that the radius for the isolated electron is equal to 2.8×10^{-13} cm. This value is capable of showing great variation by changing the conditions. It shows a large increase when the electron enters into the composition of the atom. Thus, in the individual hydrogen atom [2] the distance between proton and electron is 5.3×10^{-9} cm, and since the radius of the proton can be taken equal to zero with an accuracy of 0.01 A, then the effective radius of the electron in the normal H atom is

$$\bar{r}_0 = 0{,}93 \text{ A}.$$

These dimensions increase still more on passing to crystal lattices. At the present time the values of ionic radii [3] and atomic radii [4] are known quite reliably, and specifically with an accuracy of up to 0.02 A. These data permit estimating the electron dimensions by means of three different methods, all leading to the same result.

1st Method. Since the negative hydrogen ion differs from neutral hydrogen in having two electrons instead of one, then it can be assumed that the difference in the dimensions of these particles will give the dimensions of one electron:

$$r_0 = \underset{(2\text{ electrons})}{r_{H^-}} - \underset{(1\text{ electron})}{r_{H^0}} = 1{,}54 \text{ A} - 0{,}78 \text{ A} = 0{,}76 \text{ A}.$$

2nd Method. Since the simplest positive metal ion, namely the lithium cation, contains two electrons, then substracting its radius from the radius of the neutral lithium atom, containing three electrons, we likewise arrive at an estimate of the dimensions of one electron:

$$r_0 = \underset{(3\text{ electrons})}{r_{Li^0}} - \underset{(2\text{ electrons})}{r_{Li^+}} = 1{,}57 \text{ A} - 0{,}78 \text{ A} = 0{,}79 \text{ A}.$$

3rd Method. Since in neutral hydrogen (it is understood, also in a crystal lattice) the radius of the proton, at least with an accuracy of up to 0.01 A, can be taken equal to zero [5], then the radius of the electron will be equal to the radius of neutral H:

$$r_0 = \underset{(1\text{ electron})}{r_{H^0}} = 0{,}78 \text{ A}.$$

Within the limits of generally accepted estimate error, all three methods give the same value (0.76; 0.79; 0.78 A) for the effective radii of the particles in the lattices of a solid, i.e.,

$$r_0 = 0{,}78 \pm 0{,}02 \text{ A}.$$

In more approximate calculations it is possible to take the effective radius of the electron as equal to 0.8 A.

This new constant can be used in the solution of various problems in both physics and physical chemistry.

Thus, it finds use when making a detailed examination of the model of the metallic state. It can be assumed that in the metallic state, at least for typical metallic lattices and for the elements that form noble-gas cations, the lattice is formed from free (external) electrons and a rigid skeleton of cations. In such case the electron can be regarded to be an independent partner and its dimensions can be discussed. Here, for each given metal, the radius of the electron should evidently be equal to the difference between the radius of the neutral particle and that of the cation. That such is actually the case is quite obvious from the data given in Table 1.

TABLE 1

Difference Between the Radius of the Metal and of the Cation, Taken Equal to the Radius of the Electron in the Lattice of the Metal (in A)

					Average by group
Li 0,7	Na 0,9	K 1,0	Rb 1,0	Cs 0,8	0,9
Be 0,8	Mg 0,8	Ca 0,8	Sr 0,8	Ba 0,8	0,8
B 0,8	Al 0,8	Sc 0,8	Y 0,8	La 0,6	0,8
C 0,6	Si 0,8	Ti 0,8	Zr 0,7	Ce 0,8	0,7
Average by periods	0,7	0,8	0,8	0,8	0,8

In Table 1, we have given the differences between the radii of the ions and the metals for all of the elements forming the noble-gas type of cations, for which the values of the ionic radii are known based on the V. M. Goldschmidt system [3] (not known for the B value calculated by G. B. Bokii [5]). The indicated values of the radii are taken from the review of B. F. Ormont [4]. Since the ionic radii of Goldschmidt relate to sixfold coordination, for the metals, with the exception of Sc, Y and La (for which radii are known only for a coordination unumber of 12), we have given the data for a coordination number of 8, since the correction for transition to a coordination number of 6 is small in this case. For completeness we have also included carbon (diamond) here, although it is not close to metals in its properties; naturally it is specifically for carbon that the greatest deviation from a regular sequence appears, as can be seen from the data in the table. Taking all of the above into consideration, we give all of the comparisons with an accuracy of not up to 0.02 A, but only up to 0.1 A.

We come to the conclusion that the dimensions of such an electron "coagulum" in the lattice of metals are actually constant and moreover are equal to the radius of the electron within the limits of permissible error. The presented data can be regarded both as supporting the model of the metallic state with free electrons and as additional argument benefiting the validity of our obtained estimate of the dimensions of the electron.

All of the above can be summarized in two statements: a) the effective radius of the electron is equal to 0.78 ± 0.02 A; and b) in metals, representing a system composed of cations of the noble-gas type and electrons, the constancy of the radius of the electron is maintained with an exactness of 0.1-0.2 A.

LITERATURE CITED

[1] H. Taylor and S. Glasstone, A Treatise on Physical Chemistry, 1, London, 1942.

[2] N. Lange, Handb. of Chemistry, USA, 1957.

[3] V. M. Goldschmidt, Crystal Chemistry [Russian translation] (Moscow, 1937).

[4] B. F. Ormont, Structure of Inorganic Compounds [in Russian] (Moscow—Leningrad, 1950).

[5] G. B. Bokoi, Crystallochemistry [in Russian] (1956).

Received November 4, 1958

THEORY OF STRAIN IN ORGANIC MOLECULES

A. I. Kitaigorodskii

Institute of Heteroorganic Compounds, Academy of Sciences of the USSR

(Presented by Academician M. I. Kabachnik, November 10, 1958)

1. In this paper we discuss the possibility of treating and predicting the strains and conformations (i.e., valence angles) that appear in cyclic organic molecules. The possibility of using an electrical model of the molecule for this purpose is highly problematical. In contrast, there is basis to assume that approaching the molecule as a mechanical system can be highly productive in this respect.

The concept of using a mechanical model to find the conformations existing in a molecule, provided the manner in which the atoms are linked in the molecule is known, consists in determining the minimum potential energy of the system of atoms. Since historically in organic chemistry the concept was created of certain "least" strained structures, then in judging as to the shapes of molecules an attempt was first made to estimate, and then reduce to a minimum the energy present in excess with respect to the unstrained molecule.

References to the isolated studies made up to now and lying within the scope of the concepts discussed here can be found in Westheimer [1]. The use of a mechanical model bears a very limited character in these studies, since reaction between atoms not bound by valence forces is considered only for those phenomena which in organic chemistry have received the designation of the ortho effect. A general discussion of the applicability of a mechanical model, and also a qualitative examination of the structure of organic molecules from the standpoint of such a model, can also be found in a paper [2] by the present author.

The potentialities of the mechanical model are analyzed in the present paper, and some of its applications are discussed.

2. Lying at the base of our discussion is the statement that the chemical bond determines the distances between atoms bound by valence forces and the "natural" angles between the directions of the bonds, while the conformation of the molecule is established by the tension interaction of the valence angles and by the repulsion of the atoms not bound by valence forces and found at a distance less than the sum of the intermolecular (van der Waals) radii. The attraction of atoms found at distances greater than the sum of the intermolecular radii is small and does not affect the conformation. Since both the tension of the angles and the repulsion are essentially weaker than valence forces, they cannot change the distances between atoms bound by valence forces.

As a result, it is postulated that the energy of the molecule is the sum of three components:

$$U = U_{\text{valence forces}} + U_{\text{angles}} + U_{\text{repulsion}}.$$

We will designate the strain energy of the molecule as the sum of the last two terms

$$U_{\text{strain}} = U_{\text{angles}} + U_{\text{repulsion}}.$$

We will mention that with such defintion all nonlinear molecules are strained, since in both benzene and cyclohexane, or in water and hydrogen sulfide, the atoms not bound by valence forces show repulsion, for they are found at distances that are less than equilibrium.

The conformation of a real molecule responds to the condition of a minimum strain

$$\frac{\partial U_{\text{strain}}}{\partial \epsilon_i} = 0,$$

where ϵ_i is the conformation parameters of the molecule.

Since the conformation parameters are varied within very narrow limits in seeking the minimum energy, it is always possible to represent not only the tension energy, but also the repulsion energy, as quadratic functions. Then the strain energy can be written in the form:

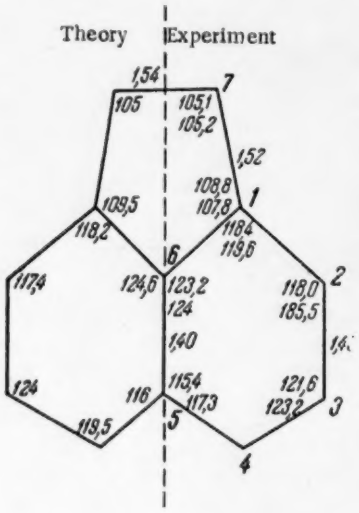

Fig. 1.

$$U_{\text{strain}} = \frac{1}{2}\sum k_i(\gamma_i - \gamma_{i0})^2 + \frac{1}{2}\sum K_i(d_{0i} - d_i)^2,$$

where γ_{i_0} is the "natural" angle, d_{i_0} is the equilibrium distance between the atoms not bound by valence forces, γ_i and d_i are respectively the angles and the distances in the real molecule (in aromatic systems the angles of the bonds out of plane are also included with the angles γ_i), and k and K are the coefficients of rigidity.

If n is the number of atoms in the molecule, and m is the number of bonds, then the number of independent parameters, determining the conformation, is equal to 3n−6−m (for a planar molecule it is 2n−3−m). Expressing d_i and γ_i through the independent parameters ϵ_i, it is always possible to represent the energy of the strain as $U_{\text{strain}} = U(\epsilon_i, \gamma_{i_0}, d_{i_0}, k, K)$.

Distributing U_{strain} in order by steps ϵ_i, we obtain as the condition for the system 3n−6−m having a minimum strain energy, equations of the type $\Sigma a_i \epsilon_i = c$, where a_i and c can be represented in the function of the values of the natural angles, the equilibrium intermolecular distances and the coefficients of rigidity (more accurately, the relationships of the rigidity coefficients to one of them).

In this manner it becomes possible to solve two problems: the direct problem – finding the conformation from known values of the rigidity, and the reverse – studying the coefficients of rigidity (and also, if there is any doubt here, the "normal" angles) based on accurate structural data.

3. The possibility of solving the direct problem is small at the present time due to absence of information on either the interaction potential of the atoms not bound by valence forces or the tension potential of the angle. For this reason it is all the more important to study the coefficients of rigidity on the basis of analyzing the structure of molecules, the geometry of which has been determined quite accurately.

Some idea as to the values of the strain energy derives from thermochemistry. However, it is naturally impossible to obtain from these data any information as to the energy components of the molecule, i.e., any information as to the tension energy or the steric repulsion.

It is customary to estimate the angle deformation energy as equal to $1/2k\delta^2$, where k is a coefficient, taken from the data on vibrational spectra, while δ is the deformation of the angle with respect to its "normal" value. Such an estimate is not justified. Actually, in the theory of molecular vibrations the energy is distributed in order around the equilibrium state. In the equilibrium state the energy is equal to zero, while δ is the angle of deviation from the equilibrium value (and not from the "normal"). In contrast, we are interested in the value of the strain energy of the equilibrium molecule. Further, the energy $1/2k\delta^2$ of the molecule in the vicinity of equilibrium is the sum of the corresponding changes in the tension energy of the angle and of steric interaction, and we are interested in the separate rigidities of both interactions.

As a result, information as to the interaction potentials can be obtained in only one manner – by analysis of the conformation of molecules with a quite accurately known geometry.

However, some simplifications can be assumed, at least in the initial studies. Examination of the structure of the simplest hydrides, and also that of methane derivatives, reveals that the tension coefficient of the angle changes but slightly in going from atom to atom. If it is assumed that in the limits of deformation up to 20° a quadratic representation of the energy is retained, then this means that $\underline{k}$ is a constant value.

The fact that organic substances show a similar compressibility and a narrow scattering of the equilibrium intermolecular distances in the crystal both suggest that the curves for the interaction of atoms not bound by valence forces are of a single type. Since the distances in molecules fail to show contractions essentially greater than $1/3 d_0$, the interaction curves should be more or less parallel.

In the initial stage of study it seems possible to speak of but one curve for the interaction of atoms not bound by valence forces, differing only in the abscissa of the minimum. The increase in the energy of steric repulsion rises more rapidly than by a quadratic rule. However, the distances change but slightly with variation in the strain energy and the quadratic approximation is fully justified. Consequently, we will use for the energy of steric repulsion the expression $1/2\ K\ (d_{0i} - d_i)^2$, where K in turn is a function of $\underline{d}$. Approximate calculations reveal that the ratio K/k varies in the limits 0.05–0.5 A^{-2}.

4. For many cyclic molecules, varying the conformation does not lead to changes in the energy of steric repulsion. Then the strain energy reduces to the tension energy of the angles. The rigidity coefficient $\underline{k}$ is reduced to the condition of a minimum, and calculation leads directly to the values of the angles, minimizing the energy.

To check the theory, we took acenaphthene as an example and made the appropriate calculations (Fig. 1). This molecule is essentially strained. Expansion of the external angles at atoms C_5 and C_1 due to repulsion by the carbon atoms assures these angles having only a small portion of the deformation. Consequently, with an accuracy sufficient for our purpose, it is possible to say for acenaphthene that $U_{strain} = U_{angles}$. Three independent parameters, which were taken as the deviations of the angles at C_6, C_1 and C_2 from 120°, determine the shape of the molecule, which possesses two planes of symmetry. The deformation of the CH_2 group does not have to be considered (see below), since the deviation of the angle at C_7 is a total of only 4°. The strain energy proves to be equal to $U = 6(2\epsilon_6 + 2\epsilon_1 + \epsilon_2 + 0.017)^2 + 6\epsilon_6^2 + 2\epsilon_1^2 + 2\epsilon_2^2 + 2(\epsilon_6 + 2\epsilon_1 + 2\epsilon_2 + 0.004)^2 + + 2(2\epsilon_6 + 3\epsilon_1 + 2\epsilon_2 + 0.012)^2 + 2(0.5\epsilon_6 + 0.038)^2 + 2(1.5\epsilon_6 - 0.30)^2 + 2(\epsilon_1 + 1.5\epsilon_6 - 0.30)^2$. The condition of a minimum gives $\epsilon_6 = 4.6°$, $\epsilon_1 = -1.8°$, $\epsilon_2 = -2.6°$. The excellent coincidence of calculation and experiment [3] is illustrated in Fig. 1, where the experimental values are given for two independent molecules.

5. The angles around an aliphatic carbon atom, connected to two H atoms and two C atoms, possess essential interest. Between the angles $\alpha = \angle CCC$, $\beta = \angle HCH$ and $\gamma = \angle HCC$ there exists a single bond – $\cos\gamma = \cos\frac{\alpha}{2}\cos\frac{\beta}{2}$. Having expressed the potential energy by means of independent parameters, which can be taken as the deviations of angles α and C from the tetrahedral value, and analyzing the conditions of a minimum, we come to the condition $\Delta\beta = -3/4\,\Delta\alpha$ and $\Delta\gamma = -1/16\,\Delta\alpha$, which is independent of the values of the rigidity ratio K/k. We also find that for any values of K/k, $\Delta\alpha > 0$. As a result, irrespective of the form of the interaction potentials of the angles, $\angle CCC$ has a value greater than tetrahedral, angle $\angle HCH$ has a value less than tetrahedral, while the angles $\angle HCC$ hardly retain a value of 109.5°. At K/k = = 0.15, we obtain $\Delta\alpha = 2.5°$.

In aliphatic compounds the angles $\angle CCC$ are increased to 112°. In our opinion, such an increase should always exist, independently of which compound the group enters. In particular, the angles around the carbon atoms in cyclohexane and the higher cycloalkanes should have similar values

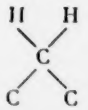

It seems of interest to make an analysis of the conditions of a minimum energy for all accurately determined structures, and also to institute a series of exact structural studies for the special purpose of determining

rigidity coefficients. It is wise to check the simple consequences of the theory, such, for example, as the contraction of the C_1 angle in the benzene ring of biphenyl.

LITERATURE CITED

[1] F. H. Westheimer, in Monograph "Steric Effects in Organic Chemistry" (1956).

[2] A. I. Kitaigorodskii, Bull. Acad. Sci. USSR, Phys. Ser. 15, 157 (1951); Organic Crystallochemistry [in Russian] (Izd. AN SSSR, 1955).

[3] H. W. Ehrlich, Acta Cryst. 10, 699 (1957).

Received November 4, 1958

THEORY OF THE HEAT-CHAIN PROPAGATION OF A FLAME WITH TWO ACTIVE CENTERS

L. A. Lovachev

Institute of Chemical Physics, Academy of Sciences of the USSR

(Presented by Academician V. N. Kondrat'ev, November 5, 1958)

The scheme for a reaction in which A and Б are the starting substances, C is the reaction product and P_1 and P_2 are active centers, is usually written in the form:

$$M + A \rightarrow 2P_1 + M, \quad \Phi_1 = h_{R1} R_1(T'); \tag{1}$$
$$P_1 + Б \rightarrow C + P_2, \quad Q_1 n_1 = h_1 F_1 n_1 = h_1 K_1(T')\, n_Б\, n_1; \tag{2}$$
$$P_2 + A \rightarrow C + P_1, \quad Q_2 n_2 = h_2 F_2 n_2 = h_2 K_2(T')\, n_A\, n_2; \tag{3}$$
$$2P_1 + M \rightarrow A + M, \quad X_1 n_1^2 = h_{W1} W_1(T')\, n_1^2. \tag{4}$$

On the right are given the expressions for the rates of heat evolution, where h_i is the heat effect of the reaction (cal/mole), n_1 and n_2 are the concentrations of the active centers P_1 and P_2 (mole/g of mixture), n_A, $n_Б$ and n_C are the concentrations of substances A, Б and C (mole/g of mixture), R_i is the rate of chain creation (mole/cu cm · sec), K_i and W_i are constants of the rate of reaction and T' is the temperature (° K). It is assumed that the diffusion coefficients of the starting substances D_A and $D_Б$ and of the product D_C are equal to the heat conductivity coefficient ($\lambda = c\rho\, D_A = c\rho\, D_Б = c\rho\, D_C$), and therefore $R = R(T')$ and $F_i = F_i(T')$.

The system of equations for a flat laminar flame under the assumed conditions and the reaction scheme reduce to three equations:

$$\lambda pp' - Bcp + Q_1 n_1 + Q_2 n_2 + X_1 n_1^2 + \Phi_1 = 0, \tag{5}$$
$$Dp^2 n_1'' - pn_1'(B - Dp') + F_2 n_2 - F_1 n_1 + R_1 - W_1 n_1^2 = 0, \tag{6}$$
$$Dp^2 n_2'' - pn_2'(B - Dp') + F_1 n_1 - F_2 n_2 = 0. \tag{7}$$

We will adopt the following designations: $\underline{x}$ is the coordinate (cm); $\underline{u}$ is the flow rate (cm/sec); ρ is the density (g/cu cm); λ is the heat conductivity of the mixture (cal/cm · sec · °C); $\underline{c}$ is the heat capacity (cal/g · °C); D_{p_1} and D_{p_2} are the diffusion coefficients of the active centers (sq cm/sec); $B = u\rho$; $D = \rho D_{p_1} = \rho D_{p_2}$; $T = T' - T_0'$; $p = dT/dx$; $p' = dp/dT$; $n_1' = dn_1/dT$; $n_1'' = d^2n_1/dT^2$; $n_2' = dn_2/dT$ and $n_2'' = d^2n_2/dT^2$. Index 0 refers to the initial state of the fresh mixture ($T' = T_0'$), index $\underline{g}$ refers to the state at the burning temperature ($T' = T_g'$) and index $\underline{m}$ refers to the state corresponding to the maximum value of the temperature gradient ($T' = T_m'$). The extreme values of the functions expressing the rates of chemical reactions are equal to zero [1], while the limiting conditions are equal to (5), (6) and (7), in accordance with [1].

Assuming at the start that $R_i = 0$ and $W_i = 0$, we will write, in accordance with [1], on the basis of (6) and (7), the concentration of the active centers at $T = T_m$ as:

$$n_{1m} = t_1 + (F_{2m} n_{2m} - F_{1m} n_{1m} - Bl_1 p_m) N, \tag{8}$$

$$n_{2m} = t_2 + (F_{1m} n_{1m} - F_{2m} n_{2m} - Bl_2 p_m) N, \tag{9}$$

$$n_m = n_{1m} + n_{2m} = t - Bl\, p_m N, \tag{10}$$

where $l_1 = \frac{n_{1g} - n_{10}}{T_g}$, $l_2 = \frac{n_{2g} - n_{20}}{T_g}$, $N = \frac{r}{2D_m p_m^2}$, $t_1 = n_{10} + l_1 T_m$, $t_2 = n_{20} + l_2 T_m$, $r = T_m(T_g - T_m)$, $l = l_1 + l_2$, $t = t_1 + t_2$ and $T_m = 0.5\, T_g$.

Equation (10) was obtained by combining (8) and (9). From (8) and (9) we find

$$n_{1m} = \frac{t_1 + F_{2m} N n_m - Bl_1 p_m N}{1 + (F_{1m} + F_{2m}) N}, \tag{11}$$

$$n_{2m} = \frac{t_2 + F_{1m} N n_m - Bl_2 p_m N}{1 + (F_{1m} + F_{2m}) N}. \tag{12}$$

Now from the total rate of heat evolution $Q_m n_m = Q_{1m} n_{1m} + Q_{2m} n_{2m}$, entering into (5), by substituting (11), (12) and (10), we obtain

$$Q_m = \frac{(l_1 Q_{1m} + l_2 Q_{2m}) + (Q_{1m} F_{2m} + Q_{2m} F_{1m}) Nl}{l(1 + F_{1m} N + F_{2m} N)}. \tag{13}$$

By finding n_m in (10) and Q_m in (13) the problem of the propagation of a flame with two active centers reduced to the solution that had been obtained [1, 2] for the simplified scheme of a chain reaction with one type of active center. This is confirmed by the realness of the simplified scheme. For the maximum temperature gradient $p_m = p_*$, according to [2], we obtain

$$2D_m p_m^2 = Q_m r L, \tag{14}$$

where $L = \frac{l}{c} \frac{(\varkappa - 2q)}{2q}$; $q = \frac{\mu_0}{\mu_m} \left(\frac{T_0'}{T_m'}\right)^{a+1}$ at $D_p \sim (T')^a$ and $\varkappa = \frac{cD_0}{\lambda_0}$.

Substituting (14) in (13), we find from the quadratic equation

$$Q_m = \frac{(LQ_l - F_m) \pm \sqrt{(LQ_l - F_m)^2 + 4LQ_F}}{2L},$$

where $Q_l = \frac{l_1 Q_{1m} + l_2 Q_{2m}}{l}$, $Q_F = Q_{1m} F_{2m} + Q_{2m} F_{1m}$ and $F_m = F_{1m} + F_{2m}$. (15)

Assuming that $LQ_l \ll F_m$ (it can be shown that this is always true), and decomposing the radical in (15) in sequence, we find

$$Q_m \simeq \frac{Q_F}{F_m} = (h_1 + h_2) \frac{F_{1m} F_{2m}}{F_{1m} + F_{2m}}. \tag{16}$$

Finally, in accordance with [2], for the propagation rate of the flame u_0 we obtain an equation that takes into consideration both the rates of chain creation ($R_1 \neq 0$) and the quadratic rupture of the chains ($W_1 \neq 0$):

$$u_0 = \varphi \xi \psi \frac{1}{\rho_0} \sqrt{\frac{n_g Q_m \rho_m D_{pm}}{2cT_g}}, \tag{17}$$

where $\varphi = 2\sqrt{\frac{2q}{\varkappa}\left(1 - \frac{2q}{\varkappa}\right)}$, $n_g = n_{1g} + n_{2g}$, $D_p = D_{p_1} = D_{p_2}$, while Q_m is determined either from (15) or from the approximate equation (16). Coefficients ξ and ψ, according to [1, 2] are determined by the equations

$$\xi = \left\{\frac{1}{2}\left[1 + \left(1 + \frac{16q\varkappa c\, T_g R_{1m}}{(\varkappa - 2q)^2 n_g^2 Q_m}\right)^{1/2}\right]\right\}^{1/2}, \tag{18}$$

$$\psi = \left(1 + \frac{qc\, T_g}{\varkappa Q_m}\, W_{1m}\right)^{-1/2} \tag{19}$$

Assuming, the same as in [1], that the distribution of the concentrations of P_1 and P_2 is determined by the values of terms at $T = T_m$, we obtain in accordance with (11) and (12) the dependence of the concentrations of P_1 and P_2 on the temperature:

$$n_1(T) = \frac{(2D_m p_m^2 l_1) T + (F_{2m} n_m - \eta l_1 p_m^2) T (T_g - T)}{2D_m p_m^2 + (F_{1m} + F_{2m}) T (T_g - T)}, \tag{20}$$

$$n_2(T) = \frac{(2D_m p_m^2 l_2) T + (F_{1m} n_m - \eta l_2 p_m^2) T (T_g - T)}{2D_m p_m^2 + (F_{1m} + F_{2m}) T (T_g - T)}, \tag{21}$$

where $n_m = \frac{n_g}{2}\left(1 - \frac{2q}{\varkappa}\right)$; $\eta = 4D_m q\, \frac{1}{\varkappa T_m}$; and p_m is found from (14).

Equations (15) or (16) and (10) make it possible to determine for the simplified scheme of a chain reaction [1, 3] the effective rate constant of continuing the chain and the value of the effective concentration of a single type of active center based on the data for a reaction scheme with two active centers.

From (16) it follows that the value Q_m, on which the rate of heat evolution in (17) depends, and consequently also the flame propagation rate, is determined basically by the least of the values F_{1m} or F_{2m}, is not dependent on n_{1g} and n_{2g} and on the individual heat effects, and is determined by the sum $(h_1 + h_2)$. The rate of heat evolution also depends on $n_g = n_{1g} + n_{2g}$, which will be mainly determined by the greatest of the concentrations of the two active centers at the burning temperature. The active center with the greatest concentration (mole/g) or proportionally greatest partial pressure at the burning temperature will be determining (leading) active center.

Equation (17) makes it possible to find the constants and activation energies of processes (2) and (3) from the experimental relationships between u_0 and T'_g in the case where, for example, in mixtures with excess substance Б $F_{1m} > F_{2m}$ (in the case it follows from (16) that $Q_m \cong (h_1 + h_2) F_{2m}$, and both constant K_2 and the energy of activation E_2 are determined), or in mixtures with excess A $F_{1m} < F_{2m}$ (here K_1 and E_1 are found). Having determined, for example, K_2 and E_2, it is possible to find K_1 and E_1 based on the relationship between u_0 and T'_g in mixtures with excess A.

When the constant and energy of activation of either process (2) or (3) are known, then the constant and energy of activation of the other process can be determined from the experimental relationship between u_0 and T'_g using equation (17) at any F_{1m} and F_{2m}.

For two cases of the chlorine-hydrogen flame we have calculated employing (17) the theoretical values of the flame propagation rates, which are given in Table 1 together with the corresponding experimental data taken from [4]. The rate constants were taken from [5]: $K_1 = 10^{13.9} \rho^2 \times \exp(-5500/RT')$, $K_2 = 10^{13.4} \rho^2 \exp(-2500/RT')$. The transfer coefficients were taken from [6]: $(D_{P_1})_0 = 0.19$ (Cl atom), $(D_{P_2})_0 = 1.04$ (H atom) and $\lambda_0 = 8.6 \times 10^{-5}$. The flame propagation rate is determined by the diffusion flow of the active centers, for which reason the value D_{P_m}, entering into (17), was calculated using the equation $D_{P_m} = (D_{P_{1m}} n_{1g} + D_{P_{2m}} n_{2g}) / (n_{1g} + n_{2g})$. A more accurate equation for D_{P_m} will be given in the next paper, in which solution at $D_{P_1} \neq D_{P_2}$ will be published.

Taking into consideration a comparison of the theoretical values of u_0, calculated from (17), with the results of a numerical integration of the original system of equations, given in [1], and also the agreement between the experimental and theoretical values given in Table 1, it must be concluded that a theoretical investigation of the flame propagation in systems, employing a reaction scheme similar to that given in the front of this paper, correctly describes the real process of such flame propagation.

The dependence of u_0 on the pressure and on the burning temperature T'_g are both essentially determined by the change in the concentrations of the active centers with pressure and with temperature [2]. Equation (17) makes it possible to estimate quantitatively the leading role of one of two active centers when their diffusion constants are the same. The concentrations of different active centers may depend differently on the pressure

TABLE 1

Experimental and Theoretical Values of the Propagation Rates (cm/sec) for Chlorine-Hydrogen Mixtures

Composition of burning mixture	$0.6H_2 + 0.4Cl_2$	$0.5H_2 + 0.5Cl_2$
Experimental data of Bartholomé [4]	405	350
From equation (17)	350	485

for a given mixture composition. The rate of change in the concentration of a given active center changes with change in the original composition of the mixture. For this reason decreasing the pressure can cause the determining (leading) role to pass from one active center to another, the concentration of which increases more rapidly with decrease in pressure. The slope of the angle in the graph where the experimental relationship is plotted in the coordinates log u_0 vs reciprocal temperature depends mainly on the heat of formation of the leading active center. For this reason if the experimental data are analyzed using equations obtained without taking the diffusion of the active centers into consideration, then instead of the energy of activation E some effective value $E_f = E + H_i$ will be found, where H_i is the effective heat, which depends on the composition of the mixture and is determined by the relationship of the proportionality $\sqrt{n_{ig}} \sim \exp(H_i / RT'_g)$.

The distribution of the concentrations of the active centers as a function of temperature is given by equations (20) and (21). If, for example, $n_{1g} > n_{2g}$, then the total concentration of active centers will be determined mainly by the diffusion of P_1, while the function $n(T) = n_1(T) + n_2(T)$ will have the shape of a curve, rising constantly from the initial concentration $n = n_0$ to the final $n = n_g$, greatest in value from the initial temperature to the burning temperature. The function $n_1(T)$ will be represented by a curve of the same character, while the curve of the function $n_2(T)$ will have a maximum between the initial temperature and the burning temperature, since at relatively small l_2 the value of the numerator in equation (21) will be determined mainly by the function $F_{1m} n_m T(T_g - T)$. With the reaction scheme adopted in the present paper, and real values of the chain-creation rates, the two curves $n_1(T)$ and $n_2(T)$ cannot simultaneously have maxima in the reaction zone.

On the basis of the above it is possible to obtain an equation for determining the rate of flame propagation in which the processes, both reverse and parallel to processes (2) and (3), and also the rate of creation and the rate of quadratic cleavage for the second active center, are taken into concentration.

LITERATURE CITED

[1] L. A. Lovachev, Proc. Acad. Sci. USSR 120, No. 6, 1287 (1958).*

[2] L. A. Lovachev, Proc. Acad. Sci. USSR 123, No. 3, 501 (1958).*

[3] D. B. Spalding, Phil Trans. Roy. Soc. London, A 249, No. 957, 1 (1956).

[4] E. Bartholomé, Zs. f. Elektrochem. 54, No. 3, 169 (1950).

[5] A. F. Trotman-Dickenson, Gas Kinetics, London, 1955, p. 182-186.

[6] K. Hellwig and R. C. Anderson, J. Am. Chem. Soc. 77, 232 (1955).

Received November 1, 1958

*Original Russian pagination. See C.B. Translation.

KINETIC ISOTOPIC EFFECT IN THE OXIDATION OF HYDROGEN ON PLATINUM

V. I. Popov and Acad. Sci. USSR Corresponding Member

S. Z. Roginskii

Institute of Chemical Physics, Academy of Sciences of the USSR

In homogeneous kinetics an investigation of the kinetic isotopic effects [1, 2] is extensively used to study the mechanism of chemical reactions. In heterogeneous catalysis such investigations were quite numerous in the last thirty years, but their results failed to exert any noticeable influence on the development of the theory of catalysis due to the contradictory nature and insufficient clearness in stating the problem. Individual papers employing modern methods of isotopic study have appeared in recent years [1, 3]. They contain interesting individual observations, but do not uncover paths for the broad use of the values of kinetic isotopic effects in the theory of catalysis. Meanwhile, it is easy to show that such measurements, closely linked with the measurement of other characteristics, can in principle offer essential information. In particular, with this method it can be hoped to determine the regimes of catalytic reactions, their stages, the nature of the bonds being either ruptured or formed in the controlling step, the structure of the transition complex, and also the adsorption and kinetic heterogeneity of the surface, etc. [1]. For this it is necessary to have first of all reliable measurements of the values of isotopic effects.

In this paper we discuss the results of measuring the kinetic isotopic effect in the oxidation of hydrogen on platinum in the presence of a large excess of hydrogen. The choice of this reaction was determined by the absence of secondary processes, the possibility of running the reaction in a broad temperature range, beginning with temperatures lying below 0°, the existence of a number of earlier studies from our laboratory, leading to the formulation of a scheme for the probable stages of the reaction [4], and also due to the description of some curious temperature anomalies in a number of old papers devoted to a study of the indicated reaction on platinum and palladium [5, 6].

EXPERIMENTAL

Principle of the method and description of the apparatus. The reaction was run under dynamic conditions using smooth platinum as the catalyst, which excluded the complications associated with porosity. The hydrogen stream with a high deuterium content, passing over the catalyst, was supplied constantly with oxygen in an amount equal to several percent of the stoichiometric. Only a certain portion of the total hydrogen present reacts when the oxygen is completely consumed. After removing the water formed, the unreacted hydrogen was quantitatively burned in an oxygen atmosphere. The isotopic composition of the starting hydrogen was calculated from the isotopic composition of the recuperate and of the water obtained in the catalytic oxidation. The value of the kinetic isotopic effect α was determined from the ratio of the concentrations of protium and deuterium in the water, formed as a result of catalytic reaction, and in the original hydrogen. The investigation was run in a completely sealed glass apparatus, a diagram of which is shown in Fig. 1.

The hydrogen and oxygen were obtained by the decomposition of water, rich in deuterium, in an electrolyzer with one cathode and two anodes, connected in parallel to the current source. The volume of the electrolyte (20% sodium hydroxide solution) was 650-700 ml. A rheostat was inserted in the circuit of the

small anode, making it possible to regulate the relative amounts of anodic current, and consequently the relative amounts of oxygen liberated at the two anodes. The oxygen from the small anode was used for the partial oxidation of hydrogen on platinum, while that from the larger anode was used to burn the unreacted hydrogen in a quartz burner. The flow rates of the gases were determined from the current strength.

The reactor was a U-shaped tube with a length of 120 cm and an internal diameter of 6.5 mm, enclosed in a jacket, through which water from a thermostat of the Heppler type was passed. A roll of platinum wire, 800 cm long and with a cross section of 0.2 mm (geometric surface 50 sq cm), was placed in the outlet portion of the tube reactor. In preliminary experiments a nichrome-constantan thermocouple was inserted directly in the reaction zone, but it proved that the temperature failed to change either at the start of reaction or during its progress, so consequently the insertion of the thermocouple into the reactor was omitted in subsequent experiments.

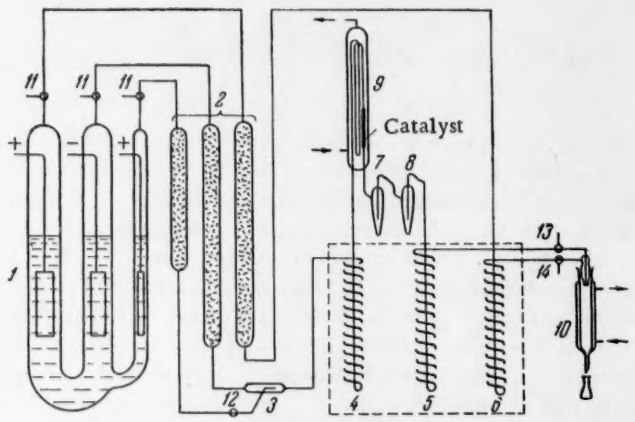

Fig. 1. Diagram of the apparatus for studying the kinetic isotopic effect in the oxidation of hydrogen on platinum. 1) electrolyzer; 2) columns with silica gel for drying the gases; 3) mixer; 4, 5, 6, 7, 8) traps, cooled with solid carbon dioxide; 9) reactor; 10) recuperator; 11, 12, 13, 14) stopcocks.

To freeze out the water formed in the catalytic oxidation of the hydrogen the reactor was connected in series to two traps, which made it possible to run the experiments with the removal of a single portion of water or with the removal of two successive portions. In the single experiments the water was frozen in trap 7, while in the double experiments it was frozen first in trap 8, with trap 7 heated to 160°, and then in trap 7. The unreacted hydrogen entered the recuperator, which was a quartz burner, connected by means of a ground-glass joint to a water condenser. In the single experiments the condensate from the recuperator was collected in a single receiver (test tube), while in the double experiments it was collected successively in two receivers.

Experimental operation. Prior to the start of experiment the electrolyzer was opened to the atmosphere by means of stopcocks 11, after which it was connected to the current source, and the electrode areas blown with a three-fold volume of the gases. At the same time the system was evacuated to a pressure of about 10^{-2} mm through the three-way stopcocks 13 and 14 (with stopcock 12 open), and the passage of water, heated to the experiment temperature, from the thermostat through the jacket of the reactor begun. Then the hydrogen line, as well as the "large" and "small" oxygen lines (up to stopcock 12), were filled respectively with hydrogen and oxygen from the electrolyzer. Experiment began with the admittance of oxygen from the "small" line through stopcock 12 and mixer 3 into the reactor, and for the case of unreacted hydrogen when the oxygen from the "large" line was admitted into recuperator 10.

In the present study the kinetic isotopic effect of hydrogen was measured at 95°. The space velocities of the hydrogen and oxygen, entering the reactor, were respectively 1.7 and 0.085 liter/hr. Complete consump-

tion of the oxygen corresponded to the oxidation of 0.1 of the introduced hydrogen. As a result, in the single experiments with operation for 4 hrs there was obtained 0.54 ml of water due to the catalytic oxidation of hydrogen and 5.4 ml due to oxidation in the recuperator. Both water portions were purified by the one-step "express-distillation" technique [7], and then analyzed by the drop method, the relative accuracy of which for our concentrations of deuterium (1.5-2.5 mole %) was ± 1% [7]. The isotopic composition of the original hydrogen was calculated from the isotopic composition of the two portions, and then the distribution coefficient was calculated.

TABLE 1

Expt. No.	Water portion	Catalytically oxidized hydrogen, % D_2O	Unreacted hydrogen (recuperator), %, D_2O	Original hydrogen (calc.), % D_2O	α
1	I	1,83	2,41	2,35	1,31
	II	1,72	2,22	2,17	1,28
2	I	1,56	2,05	2,00	1,31
3	I	1,56	2,12	2,06	1,35
	II	1,58	2,18	2,12	1,35
4	I	1,65	2,12	2,07	1,28

Experimental results and their discussion. The results of our experiments on the kinetic isotopic effect in the oxidation of hydrogen on platinum at 95° are given in Table 1. As can be seen from the data in the table, the water formed in the catalytic oxidation of hydrogen is enriched in protium. The values of the distribution coefficient α, calculated by means of the equation given below, in four experiments, of which two were double, varied within the relatively narrow limits of ± 0.04 from the average arithmetic value of $\alpha = 1.31$, i.e., $\Delta\alpha = \pm 3\%$.

If the reaction of substances, composed of two isotopic forms, is irreversible, and if the distorting influence of isotopic exchange is absent, then the reaction may be regarded as being two independent processes. In our case (with a small amount of deuterium in the hydrogen) this is simply

$$H_2 + {}^1/_2 O_2 = H_2O, \quad HD + {}^1/_2 O_2 = HDO.$$

Each of these processes includes hydrogen diffusion to the surface and the subsequent stages, which can begin with H_2 adsorption or with its reaction on colliding with the adsorbed oxygen, and are terminated by water desorption and its diffusion from the layer near the surface into the gas stream.

If external hydrogen diffusion controls the process then both reactions should proceed by a first-order mechanism:

$$\frac{d[H_2O]}{dt} = k_1([H_2] - [H_2O]), \qquad \frac{d[HDO]}{dt} = k_2([HD] - [HDO]).$$

Dividing individually the first kinetic equation by the second and integrating the result, we obtain

$$\frac{k_1}{k_2} = \frac{\ln(1 - f_1)}{\ln(1 - f_2)},$$

where $f_1 = [H_2O]/[H_2]$ and $f_2 = [HDO]/[HD]$ are the fractions of converted H_2 and HD, respectively.

The ratio of the constants $k_1/k_2 = D_1/D_2$ represents the sought kinetic effect or the distribution coefficient α when the process is controlled by the hydrogen diffusion.* Similar reasoning also holds if the process is controlled by the diffusion of the water, formed as the result of oxidation, from the surface layer of the catalyst into the gas stream.

In view of the known fact that the diffusion coefficient is inversely proportional to the square root of the mass of the diffusion molecules, the ratio of the constants k_1/k_2 in the case of hydrogen diffusion to the surface of the catalyst should be equal to $D_1/D_2 = \sqrt{m_{HD}/m_{H_2}}$, i.e., to 1.22, and in the case of the formed water molecules diffusion from the surface layer into the gas stream it should be equal to $D_1/D_2 = \sqrt{m_{HDO}/m_{H_2O}}$, i.e., to ≅ 1.03. Comparing these values with our obtained value $\alpha = 1.31$, which possibly is somewhat low

*D_1 and D_2 are the diffusion coefficients of the H_2 and HD molecules, respectively.

due to catalytic isotopic exchange between HD and H_2O (exerting an influence on the isotopic composition that is opposed to that of the kinetic isotopic effect), it must be concluded that the external diffusion of either hydrogen or water fails to occur in the controlling step.

The matter becomes much more complicated if the process of the catalytic oxidation of hydrogen is controlled by chemical or adsorption stages, since here the atoms of the catalyst surface become involved in the transition complexes, the thermodynamic effects of adsorption equilibria enter in hidden form, etc.

At low pressures the oxidation rate of H_2 on Pt and Pd is described by the equation $w = k \frac{[O_2]}{[H_2]^{1/2}}$, clearly including the hydrogen concentration [4]. At pressures close to atmospheric the reaction rate is proportional to the oxygen pressure and is practically independent of the hydrogen pressure [8, 9]. Apparently in our experiments the rate for the contact oxidation of hydrogen is controlled by stages, not including hydrogen directly (for example, chemisorption of O_2), or including hydrogen in a form that is not dependent on its concentration in the gas phase, for example, the hydrogen of the saturated adsorption layer on the active surface of the catalyst. However, this does not exclude the appearance of a hydrogen kinetic effect, since the fraction of O_2, O_2^- or O^-, reacting with the H_2 and HD molecules on the filled portions, depends on their specific content on the surface, i.e., on the concentration ratios in the gas phase with correction for the isotopic adsorption effect. In addition, the true kinetic isotopic effect in reacting O_2 (O_2^- or O^-) with H and D or with H_2 and HD must be taken into account.

Prior to obtaining direct measurements of the isotopic adsorption effect under catalyst conditions it is premature to speak more definitely on the character of the chemical stage in the contact oxidation of hydrogen, leading to the appearance of the observed separation of hydrogen isotopes. It is also necessary to determine the effect of change in catalyst activity on the value of α. Experiments with O^{16} and O^{18} and with hydrogen containing a high amount of deuterium, together with determining the temperature dependence of α, could help in defining both the nature of the chemical stage in the contact oxidation of hydrogen and of the transition complex more accurately.

LITERATURE CITED

[1] S. Z. Roginskii, Theoretical Principles in the Study of Chemical Reactions by Isotopic Methods [in Russian] (Izd. AN SSSR, 1956).

[2] Lars C. S. Melander, The Use of Nuclides in the Determination of Organic Reaction Mechanism, 1955.

[3] K. Wiberg, Chem. Rev. 55, 713 (1955).

[4] O. V. Krylov and S. Z. Roginskii, Proc. Acad. Sci. USSR 88, 293 (1953); Bull. Acad. Sci. USSR, Div. Chem. Sci, 1956, No. 2. *

[5] H. W. Melville, J. Chem. Soc., 1934, 1243.

[6] T. Tucholski, Zs. Phys. Chem. 40, 333 (1938).

[7] A. I. Shatenshtein, E. A. Yakovleva, et al., Isotopic Analysis of Water [in Russian] (Izd. An SSSR, 1957).

[8] G. K. Boreskov, M. G. Slin'ko and A. G. Filippova, Proc. Acad. Sci. USSR 92, No. 2, 353 (1953)

[9] C. N. Hinshelwood, J. Chem. Soc., 1929, 1727.

Received December 2, 1958

*See C.B. Translation.

THE CHARACTER AND ROLE OF INTERMEDIATE PRODUCTS IN THE RADIOLYTIC REDUCTION OF NITRATE

V. A. Sharpatyi, V. D. Orekhov and M. A. Proskurnin

L. Ya. Karpov Research Institute of Physical Chemistry

(Presented by Academician S. S. Medvedev, November 11, 1958)

It was mentioned in some studies [1, 2] that molecular oxygen, present in solution, exerts substantial influence on the radiolytic reduction of nitrate. The theory was expressed that the inhibiting action of molecular oxygen is associated with its reaction with the intermediate products of nitrate reduction of type HNO_3^-, and should be manifested even at exceedingly small O_2 concentrations. In addition, both the magnitude of γ-ray dosage and the solution temperature should have an effect on the reaction for the disproportionation of HNO_3^- ions (the second principal stage in the reduction of nitrate).

We investigated the relationship between the yield of nitrite and the magnitude of dosage in 1M nitrate solution and 1M NaOH in the dosage range of 0.04 to 1000 r/sec. The yield of nitrite in solutions saturated with air remains constant in the entire range of dosages studied and is equal to ~ 3 equiv / 100 ev (Fig. 1, 1). In the absence of oxygen (the solution was saturated with nitrogen), in the dosage range 0.5-1000 r/sec, the yield of nitrite is considerably higher (~ 8 equiv / 100 ev) (Fig. 1, 2). With an oxygen content of 2.5% in the gas mixture of oxygen and nitrogen over the solution $G_{NO_2^-}$ is directly proportional to the logarithm of the dosage (Fig. 1, 3).

These results can serve as indirect proof of the theory that the processes for the disproportionation of the ion of hydronitric acid and its oxidation by oxygen to nitrate ion are concurrent. At small dosage (0.04-0.5 r/sec) the average concentration of HNO_3^- in the solution volume is so small that an oxygen concentration of $0.5 \cdot 10^{-5}$ M is sufficient to enable the oxygen to compete with the process for the disproportionation of HNO_3 ions. At higher dosages (60-100 r/sec) it is necessary to have a higher O_2 concentration in solution for the reverse reaction $HNO_3^- + O_2 \rightarrow NO_3^- + HO_2$ to go. In the dosage range of 0.04 to 0.1 r/sec in 1M nitrate solution, saturated with nitrogen, the yield of nitrite rises to 10.5-11 equiv/100 ev (Fig. 1, 1), i.e., it reaches values that can correspond to the complete utilization of the products of the radiolyzed water molecules (the same as in the case of using coupled acceptors [1, 3]*).

To determine the role played by intermediate products in the process for the reduction of nitrate we ran a series of experiments in which the solutions were irradiated at various temperatures. As had been mentioned earlier, in the temperature range 20-90° the yield of nitrate does not change in solutions saturated with nitrogen [2, 3]. Apparently, such a change in temperature has little effect on the formation of the final product NO_3^- and NO_2^- based on the disproportionation reaction ($G_{NO_2^-} = 8$-8.5 equiv/100 ev). Irradiation of the solutions at lower temperatures (to − 25°) leads to a decrease in $G_{NO_2^-}$ to values of ~ 2.5 equiv /100 ev. **

*Under these conditions of irradiation the introduction of glycerol as a coupled acceptor of OH radicals does not change $G_{NO_2^-}$, which remains equal to 10.5-11 equiv/100 ev.

**The yield of nitrite was calculated on the assumption that the frozen solution represents a homogeneous mixture of ice and $NaNO_3$ crystals.

With further reduction in the solution temperature clear down to the temperature of liquid nitrogen $G_{NO_2^-}$ remains practically constant (Fig. 2, 1). In solutions containing oxygen (saturated with air) the dependence of the nitrite yield on the solution temperature has a somewhat different form (Fig. 2, 2). Here the reduction in yield begins at higher temperatures and is also conditioned by the reaction of O_2 with the intermediate products of nitrate reduction.

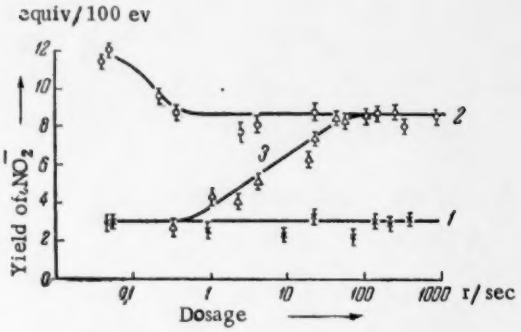

Fig. 1. Relationship between $G_{NO_2^-}$ and dosage with γ-rays (logarithmic scale): 1) solution saturated with air, 2) solution saturated with nitrogen, 3) solution saturated with a mixture of N_2 and O_2 gases, with 2.5% oxygen in the mixture over the solution.

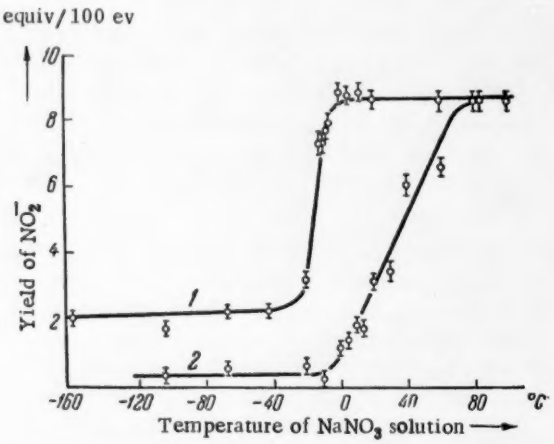

Fig. 2. Dependence of $G_{NO_2^-}$ on the solution temperature: 1) solution saturated with nitrogen, 2) with air.

To determine the exact values of $G_{NO_2^-}$ in frozen solutions it is necessary to know the mechanism for the transfer of absorbed energy and for the interaction of the formed radical products taking into consideration surface effects, since the eutectic represents a mixture of $NaNO_3$ and ice crystals [4].

The application of the electron paramagnetic resonance method to the system nitrate – water during irradiation with accelerated electrons made it possible to show in the temperature range of −196 to −70° a number of intermediate products of nitrate reduction and also atomic hydrogen.* It was observed that the intermediate radical products quickly disappear when the irradiation is terminated, and the disappearance is more rapid the higher the temperature of the frozen solution. In addition, it was revealed that frozen nitrate solutions evidently have a smaller amount of the radicals formed in frozen water present, which apparently react with the nitrate ions. From this, as a first approximation, we can assume that in the given case we are dealing with a homogeneous mixture of crystals, where ordinary radical reactions take place.

From what has been said it is possible to conclude, first, that the principal processes of nitrate reduction in frozen solutions occur prior to their thawing out for the purpose of analyzing them for the transformation products of the nitrate ion, which is not in agreement with the conclusions of certain authors [5]; second, together with the direct action of γ-radiation on NO_3^-, there occurs in frozen solutions, as had already been mentioned [1, 6], a radical reduction of the nitrate. In the future, using the electron paramagnetic resonance method it is proposed to make a more detailed study of the properties of the intermediate products found in this system.

The authors are deeply indebted to co-workers N. Ya. Buben, A. T. Koritskii, Yu. N. Molin and V. N. Shamshev of the Institute of Chemical Physics, Academy of Sciences of the USSR, for running a number of experiments in which an investigation of radicals was made using the electron paramagnetic resonance method during irradiation.

LITERATURE CITED

[1] V. A. Sharpatyi, V. D. Orekhov and M. A. Proshurnin, Monograph "Action of Ionizing Radiations on Inorganic and Organic Systems" [in Russian] (Izd. AN SSSR, 1958), p. 43.

*The concentration of H atoms was a thousand times less than the concentration of the intermediate radical radical products of nitrate reduction.

[2] M. A. Proskurnin, V. D. Orekhov, E. V. Barelko and A. I. Chernova, Monograph "Isotopes and Radiations in Chemistry" [in Russian] (Izd. AN SSSR, 1958), p. 119.

[3] V. A. Sharpatyi, V. D. Orekhov and M. A. Proskurnin, Monograph "Action of Ionizing Radiations on Inorganic and Organic Systems" [in Russian] (Izd. AN SSSR, 1958), p. 37.

[4] W. Althammer, Mathematical and Graphical Treatment of Salt Solutions [Russian translation] (1932), p. 10.

[5] Z. M. Bacq and P. Alexander, Fundamentals of Radiobiology, (London, 1955), p. 49.

[6] V. A. Sharpatyi, Trans. First All-Union Convention on Radiation Chemistry [in Russian] (Izd. AN SSSR, 1958), p. 112.

Received November 11, 1958

SIGNIFICANCE OF ABBREVIATIONS MOST FREQUENTLY ENCOUNTERED IN SOVIET CHEMICAL LITERATURE

Abbreviation (Transliterated)	Significance
FIAN	Phys. Inst. Acad. Sci. USSR
GIPKh	State Institute of Applied Chemistry
GIREDMET	State Rare Metals Scientific Research Institute
GITI	State Sci.-Tech. Press
GITTL	State Tech. and Theor. Lit. Press
GLAVKhIM	Main Administration of the Chemical Industry
GOI	State Optical Institute
GONTI	State United Sci.-Tech. Press
Goskhimizdat	State Chem. Press
GOST	All-Union State Standard
Gostoptekhizdat	State Scientific and Technical Publishing house of the Petroleum and Mineral Fuel Industry
GTTI	State Tech. and Theor. Lit. Press
IFKhA	Institute of Physicochemical Analysis
IL	Foreign Lit. Press
IOKhAN	Institute of Organic Chemistry of the Academy of Sciences of the USSR
IONKh	Institute of General and Inorganic Chemistry (N. S. Kurnakov)
IONKhAN	Institute of General and Inorganic Chemistry of the Academy of Sciences of the USSR
INBI	Institute of Biochemistry
IREA	Institute of Chemical Reagents
ISN (Izd. Sov. Nauk)	Soviet Science Press
IVKhTI	Ivanovo Chemical Engineering Institute
Izd. AN SSSR	Acad. Sci. USSR Press
Izd. MGU	Moscow State Univ. Press
KEIN	Colloid Electrochemical Institute
Khimizdat	Chemistry Press
LGU	Leningrad State University
LIM	Leningrad Institute of Metals
Metallurgizdat	Metallurgy Press
MITKhT	Moscow Institute of Fine Chemical Technology
OIYaI	Joint Institute of Nuclear Studies
OKhN	Division of Chemical Science
ONTI	United Sci.-Tech. Press
OTI	Division of Technical Information
OTN	Division of Technical Science
RIAN	Radium Institute, Academy of Sciences of the USSR
RZhKhim	Chemical Abstract Journal (USSR)
VKhO	All-Union Chemical Society (Mendeleev)
ZhFKh	Journal of Physical Chemistry (USSR)
ZhRKhO	Journal of the Russian Chemical Society

Note: Abbreviations not on this list and not explained in the translation have been transliterated no further information about their significance being available to us. – Publisher.